Space gravity spectroscopy

The sensitivity analysis of GPS-tracked satellite missions (case study CHAMP)

Doctoral thesis accepted by the
Faculty of Engineering and Surveying Science of the University of Stuttgart

Von der Fakultät für
Bauingenieur- und Vermessungswesen der Universität Stuttgart
zur Erlangung der Würde eines Doktor-Ingenieurs (Dr.-Ing.)
genehmigte Dissertation

submitted by - vorgelegt von

Christof Schäfer

Bruchsal

Main referee - Hauptberichter
Prof. Dr.-Ing.habil. Dr.tech.h.c.mult Dr.-Ing.E.h.mult Erik W. Grafarend, Stuttgart

Co-referees - Mitberichter
Prof. Dr.-Ing. Alfred Kleusberg, Stuttgart
Prof. Dr.-Ing. Reiner Rummel, Munich - München

Day of exam - Tag der Prüfung: 25.07.2000

Geodätisches Institut der Universität Stuttgart

October 13, 2000

Main referee - Hauptberichter

Prof. Dr.-Ing.habil. Dr.tech.h.c.mult Dr.-Ing.E.h.mult Erik W. Grafarend, Stuttgart

Co-referees - Mitberichter

Prof. Dr.-Ing. Alfred Kleusberg, Stuttgart
Prof. Dr.-Ing. Reiner Rummel, Munich - München

Day of exam - Tag der Prüfung: 25.07.2000

to my parents

Abstract:

The aim of a sensitivity analysis of a satellite's orbit is to determine the very parts of the Earth's gravitational field having the strongest effects on the orbit of an artificial satellite. Thus, the sensitivity analysis is an important prerequisite for the analysis of an orbit, that aims at the determination of gravity field values, as well as the planning and the optimisation of new satellite missions.

This thesis will present a method to perform a sensitivity analysis based on an analytical Fourier series analysis of the commonly used (surface) spherical harmonics series expansion for the representation of the Earth's gravitational field. By means of this spectrum the connection between the model coefficients and the frequencies in the field's representation is determined. The Fourier coefficients, which closely resemble the so-called lumped coefficients, are linear combinations of the weighted model's (surface) spherical harmonics series coefficients. The frequencies can also be found in the spectrum of the gravitational acceleration vectors acting on the satellite as well as in the perturbed orbit data along the orbit. A first detailed investigation into the spectrum along the orbit leads to information on the dominant frequencies; a second detailed investigation into the respective linear combinations (which form the dominant lumped coefficients) yields information on which (surface) spherical harmonics' coefficients have the strongest influence on the satellite's trajectory.

The dedicated gravity and magnetic field mission CHAMP, which is tracked by GPS, serves as an example for the method presented and to highlight special conditions that arise for sensitivity analyses of LEO missions. The determination of the gravitational acceleration vectors acting on CHAMP along the orbit from the GPS observables position and velocity is performed by means of a time-discrete Kalman filter for filtering and parameter estimation for nonlinear system's models.

Keywords: *High-low satellite-to-satellite tracking, Earth's gravitational field, Cartesian representation of the gravitational field, orbit sensitivity analysis, lumped coefficients, state space description of the system 'satellite trajectory', nonlinear filtering, time-discrete extended Kalman filter, parameter estimation, CHAMP*

Zusammenfassung:

Die Sensitivitätsanalyse einer Satellitenbahn dient der Bestimmung der Anteile des Gravitationsfelds der Erde, die die stärksten Auswirkungen auf die Bewegung des Satelliten haben. Damit ist sie Voraussetzung sowohl für eine Bahnanalyse mit dem Ziel der Bestimmung des Schwerefelds der Erde, als auch für die Planung und Optimierung neuer Missionen zur genaueren Untersuchung des Schwerefelds.

In dieser Arbeit wird eine auf einer analytischen Fourierdarstellung der heute üblichen Kugelflächenfunktions-darstellung des Erdschwerefelds basierende Methode zur Sensitivitätsanalyse vorgestellt. Durch dieses Spektrum wird der Zusammenhang zwischen den zu bestimmenden Modellkoeffizienten und den Frequenzen in der Darstellung des Gravitationsfelds ermittelt. Die Fourierkoeffizienten, die den sog. Lumped Coefficients sehr ähnlich sind, ergeben sich als Linearkombinationen der gewichteten Kugelflächenfunktionskoeffizienten des Erdschwere-feldmodells. Die Frequenzen finden sich in den gestörten Bahndaten, im wesentlichen den auf den Satelliten wirkenden Gravitationsbeschleunigungsvektoren, aber auch dem Bahnverlauf selbst wieder. Eine genaue Untersuchung des Spektrums entlang der Bahn liefert die dominanten Frequenzen; eine genaue Untersuchung der zugehörigen Lumped Coefficients liefert Informationen darüber, welche Gravitationsfeldkoeffizienten die stärksten Auswirkungen auf das Bahnverhalten des Satelliten haben.

Die Schwere- und Magnetfeldmission CHAMP, deren Bahn mittels GPS getrackt wird, dient als Beispiel für das vorgestellte Verfahren und zeigt gleichzeitig Besonderheiten auf, die bei der Sensitivitätsanalyse von tief-fliegenden Missionen (LEO-Missionen) zu erwarten sind. Die Bestimmung der entlang der Bahn auf CHAMP wirkenden Gravitationsbeschleunigungsvektoren aus den GPS-Beobachtungen Position und Geschwindigkeit erfolgt mit Hilfe eines zeitdiskreten Kalmanfilters zur Filterung und Parameterschätzung bei nichtlinearen Systemen.

Schlagworte: *High-low satellite-to-satellite tracking, Gravitationsfeld der Erde, Darstellung des Gravitations-felds in kartesischen Koordinaten, Sensitivitätsanalyse von Satellitenbahnen, Lumped Coefficients, Zustands-raumbeschreibung des Systems 'Satellitenbahn', nichtlineare Filterung, zeitdiskreter erweiterter Kalman-Filter, Parameterschätzung, CHAMP*

Résumé:

Le but d'une analyse de sensibilité d'orbite est de déterminer les parties du champ de gravitation de la terre, qui ont les effets les plus forts sur l'orbite d'un satellite artificiel. Ainsi, l'analyse de sensibilité est un préalable important à l'analyse d'une orbite pour la détermination du champ de gravitation aussi bien que pour la planification et l'optimisation des nouvelles missions.

Cette thèse présente une méthode d'analyse de sensibilité d'orbite basée sur une décomposition en série de Fourier analytique de la décomposition en harmoniques sphériques généralement utilisée pour la représentation

du champ de gravitation de la terre. Du spectre résulte une connexion entre les coefficients modèles et les fréquences déterminés dans la représentation de champ. Les coefficients de Fourier, qui ressemblent aux lumped coefficients, sont des combinaisons linéaires des coefficients de la décomposition en harmoniques du modèle. Les fréquences peuvent également être trouvées dans les vecteurs d'accélération de la gravitation, qui agissent sur le satellite, mais aussi bien dans les données perturbées de l'orbite. Une recherche détaillée sur le spectre rapporte les fréquences dominantes; une recherche détaillée sur les lumped coefficients respectivfs rapporte l'information suivante à savoir quels sont les coefficients du champ de gravitation qui ont l'influence la plus forte sur la trajectoire du satellite.

La mission CHAMP, développée pour la détermination du champ de gravitation aussi bien que du champ magnétique et de l'atmosphère, sert d'exemple à la méthode présentée et montre aussi les particularités d'une analyse de sensibilité d'orbite pour une mission de basse hauteur de vol (LEO). La détermination de l'accélération par la gravitation, qui dirige CHAMP, de sa position et sa vitesse, observées par GPS, est exécutée à l'aide d'un filtrage temps-discret de Kalman utilisée pour le filtrage et l'estimation des paramètres pour les modèles de système non linéaires.

Mots-clés: *dépistage haut-bas entre satellites, champ de gravitation, représentation cartésienne d'un modèle mathematique pour la gravitation, analyse de sensibilité d'orbite, lumped coefficients, modèle spatial d'état de système 'trajectoire d'un satellite', filtrage non linéaire, filtrage temps-discret de Kalman, estimation des paramètres, CHAMP*

Acknowledgments

Contents

List of important symbols and constants

geophysical and planetary parameters and constants:

G ...   gravitational constant $G = 6.673 \ (\pm 0.003) \ 10^{-11} \ m^3 kg^{-1} s^{-2}$,

GM ...   Earth centred gravitational constant $[m^3/s^2]$,

$M_\oplus$ ...   Earth's mass $[kg]$,

$R_\oplus$ ...   Earth's mean radius $[m]$,

$\boldsymbol{\omega}_\oplus$ ...   Earth's angular velocity vector $[rad \ s^{-1}]$.

vectors:

$\mathbf{x}(t)$ ...   three-dimensional geocentric position vector $[m]$,

$\dot{\mathbf{x}}(t)$ ...   three-dimensional velocity vector $[m/s]$,

$\ddot{\mathbf{x}}(t)$ ...   three-dimensional acceleration vector $[m/s^2]$.

Earth's gravitational field:

$U(\mathbf{x}(t), \mathbf{c})$ ...   Earth induced gravitational potential $[m^2/s^2]$,

$\mathbf{g}(\mathbf{x}(t), \mathbf{c})$ ...   Earth induced three-dimensional gravitational acceleration vector $[m/s^2]$,

$\underline{\mathbf{M}}(\mathbf{x}(t), \mathbf{c})$ ...   gravitational gradient tensor (Marussi-tensor),

$\mathbf{c}$ ...   vector of gravitational model's coefficients ((surface) spherical harmonics' coefficients) $c_k \in [\bar{c}_{ij}, \bar{s}_{ij}]$ $(0 \leq i \leq n_{max}, \ 0 \leq j \leq i, \ 1 \leq k \leq 1/2 \ (n_{max} + 1)(n_{max} + 2))$.

mathematical notation:

$a, \ e, \ldots$ ...   plain letters denote scalars,

$\mathbf{x}, \ \mathbf{y}, \ldots$ ...   bold letters denote vectors and first level tensors, respectively,

$\underline{\mathbf{M}}, \ \underline{\mathbf{P}}, \ldots$ ...   bold underlined capital letters denote matrices and second level tensors, respectively,

$\underline{\mathbf{E}}_{n \times n}$ ...   n-dimensional quadratic identity matrix,

$\mathbf{E} \{\mathbf{x}(t_{k+1})\}$ ...   denotes the first moment, the expectation, of a random variable,

$\widehat{\mathbf{x}}$ ...   denotes a predicted value for vector $\mathbf{x}$ (in contrast to the final or corrected value $\mathbf{x}$),

$\langle \ . \ , \ . \ \rangle$ ...   scalar product, inner product,

$[\ a \ ]$ ...   largest integer equal to or less than a.

abbreviations:

CoM   ...   a body's (satellite's) centre of mass,

CoG   ...   a body's (satellite's) centre of gravity,

hl-SST   ...   high-low satellite-to-satellite-tracking configuration (GPS-LEO configuration),

LEO   ...   low Earth orbiting satellite,

POD   ...   precise orbit determination,

SLR   ...   satellite laser ranging.

where no explicit numerical values are given, they depend on a chosen model; for an overview see e.g. Yoder (1995)

Chapter 1

Introduction

1-1   Description of the problem

For several decades already satellite missions provide a suitable means for the global determination of the long wavelength components of the Earth's gravitational field. Thus they play an important role in collecting gravitation induced data all over the planet, especially in areas where terrestrial observations are impossible due to various reasons (lack of observation infrastructure, ocean areas etc.).

Due to the dependency of the Earth's gravitational field on the distance between the sources (Earth's mass) and the body affected (satellite) increasing smoothing takes place the bigger the orbit height is. For very high orbits, the structure of the Earth's gravitational field will nearly be that of a central body (spherical and homogeneous). The consequence is that satellites usually 'see' a much smoother field structure than an observer on the surface of the Earth would detect by measurements. Classical satellite missions enabled a computation of gravitational model coefficients for the long wavelength part of the gravitational field especially. A resolution of global structures of an extension down to some thousand kilometres has thus been possible (table 1-1).

Future missions, that are due to launch during the next few years, are expected to provide high resolution data with respect to space as well as time. This improvement of the data on the gravitational field collected is achieved by four main improvements compared to classical missions.

- Mission orbit layout: The future missions will mainly be low Earth orbiting missions (LEO missions). This means, that the satellite will pass, due to its low orbit height (a few hundred kilometres), an area within the gravitational field in which there are still considerable inhomogeneities that are not yet smoothed out.

- Mission orbit height: The orbital height of forthcoming missions will vary considerably during the satellite's time of life. CHAMP for example will start its trajectory at an approximate height of about 450 km and it will decrease down to less than 350 km during the expected 5 years lifetime. Given a low solar flux maximum during the mission, CHAMP's orbit will even be lowered by an orbital manoeuvre, otherwise the lifetime would be much longer but also the probed area with respect to the radial direction would be much smaller. This height variation will provide a limited spatial data distribution instead of a distribution on the orbital surface only.

- Mission instrumentation / observables: Future satellite missions will all be equipped with GPS receivers and several other observation instruments depending on their main gravitational field observation method. For further details on specific missions see table 1-2.

- Mission tracking: The missions will usually be tracked by means of GPS receivers which allows to perform a precise orbit determination (POD) for the satellite having global coverage. Classical satellite tracking methods, like satellite laser ranging (SLR) for example, have the basic disadvantage of only providing tracking information where there is a ground station available.

With this data it is possible to enter a new field of accuracy and resolution in global gravitational field determination. The amount of data as well as the considerably higher resolution expected for the end product, the gravitational field model to be computed, aggravates a problem that has always been immanent when performing gravitational field determination.

In general nowadays, the gravitational field of a celestial body is described mathematically by means of a (surface) spherical harmonics series expansion. The mathematical connection between the satellite's orbital motion and the model coefficients describing the Earth's gravitational field is given by the satellite's equations of motion. These equations have to be solved for the unknown coefficients, which yields rather large systems of equations, that have to be inverted. This task requires special efforts. To reduce this efforts, a closer look should be taken at the satellite mission itself. Depending on the mission layout, only certain parts of the gravitational field

will have a visible influence on the observables. Vice versa, only these parts and the coefficients of the model, which stand for them, can be 'seen' in the observations. Thus the mission analysis only yields information on a specific set of coefficients of the Earth's gravitational field model. To be understood correctly, the other coefficients could also, in a solely mathematical way, be determined from position and velocity observations of this single mission. But the information gathered on these coefficients will not be as accurate as needed and can be determined much better by means of other missions with different layouts. To get an idea, which coefficients can be determined best from one specific mission's data, a so-called satellite orbit sensitivity analysis has to be performed. Following the same line of argumentation, the reverse process, the determination of the satellite's trajectory based on a given set of effects acting on it, the so-called *orbit synthesis* or *orbit prediction*, can be dealt with. Following the strict way of including all the gravitational effects on the satellite, the complete underlying gravitational model has to be evaluated which yields rather high computational efforts to be undertaken. This efforts could be reduced if the most important parts of the gravitational spectrum that act on the satellite to predict are known.

This thesis will focus on the problem of performing such a satellite orbit sensitivity analysis for a CHAMP-like ('**Cha**llenging **M**ini-Satellite **P**ayload for Geophysical Research and Application', for details refer to section 1-1-2 and annex C) satellite being tracked by means of GPS. For this mission both aims, the gravitational orbit analysis as well as the orbit prediction, will be focused.

	long	middle	short	very short
wavelength range	$20000 - 4000\ km$ $4000 - 1100\ km$	$1100 - 220\ km$	$220 - 20\ km$	$< 20\ km$
degree & order	$2 - 10$ $11 - 36$	$37 - 180$	$181 - 2000$	> 2001
number of coefficients $k = \frac{1}{2}\left(n_{max}+1\right)\left(n_{max}+2\right)$	$6 - 66$ $78 - 703$	$741 - 16471$	$16653 - 2003001$	> 2005003

table 1-1: Wavelength range representation of a (surface) spherical harmonics series expansion gravitational field model (following Reigber (1989) and Schäfer (1998a))

	instrumentation / observations	tracking POD	main mission purposes	launch expected
Ørsted	GPS, magnetometre	GPS	magnet., (POD)	02/23/1999
Sunsat	GPS, camera, SLR	GPS	photo., (POD)	02/23/1999
CHAMP	GPS, accelerometer	GPS	POD, occult., (altim.)	07/15/2000
SAC-C	GPS, altimeter	GPS	POD, occult., altim.	2000
JASON-1	GPS, altimeter, DORIS etc.	GPS, DORIS	POD, altim.	05/18/2000
VCL	GPS, laser altimeter	GPS	altim., (POD)	2000
GRACE	GPS, satellite-to-satellite ranging	GPS	POD, occult.	June 2001
ICESat	GPS, laser altimeter	GPS	altim., (POD)	2001
GPB	gyro, GPS	GPS	relativity	2001
GOCE	GPS, gradiometre	GPS	gradiometry	2004/2005

table 1-2: Future satellite missions tracked by GPS

(POD . . . **P**recise **O**rbit **D**etermination for gravitational sounding, occult. . . . GPS occultation observation for atmospheric sounding, magnet. . . . observation of the Earth's magnetic field, photo. . . . optical remote sensing, altim. . . . altimetry)

1-1.1   The term 'Space Gravity Spectroscopy'

One of the core issues of the methods presented in this thesis is the Fourier frequency representation of the gravitational values themselves as well as of the perturbations of orbital values caused by the gravitational effects. Thus, Fourier series representations of various kinds will be introduced. On the analytical part today's gravitational models based on (surface) spherical harmonics will be written in frequency representation. For the orbit values of the satellite mission, the gravitational acceleration vectors acting on the satellite will be decomposed into their frequencies by means of a fast Fourier transformation (FFT). Both computations will be performed along a supposed trajectory of the satellite. This will, generally speaking, lead to frequency representations of three-dimensional field values along a path through space. To describe this ansatz in a concise way, the term 'Space Gravity Spectroscopy' is used.

1-2   The GPS tracked satellite mission CHAMP

Champ is one of the first geodetic missions of a new generation of satellite mission concept, that will be tracked by an on-board GPS receiver for POD. Its main mission objectives are

- the determination of the gravitational field of the Earth with high resolution with respect to position as well as time,

- the determination of the Earth's magnetic field by means of the several on-board magnetometres,

- gathering atmospheric data by means of GPS occultation observations as well as measurements of the total electron content (TEC) of the ionosphere and

- testing a new method of passive GPS based altimetry on board a satellite.

The determination of the Earth's gravitational field will be based on the determination of a precise orbit of CHAMP by means of a GPS high-low satellite-to-satellite-tracking (hl-SST) configuration. Thus the observables will be full three-dimensional position and velocity vectors with respect to the World Geodetic System 1984 (WGS84), GPS' geocentric Earth-fixed Cartesian reference system. To be precise, all the so-called Earth-fixed reference systems presented throughout this thesis should be called *quasi*-Earth-fixed system, for their definition usually does not take into account the effects caused by polar motion (precession and nutation). All the systems are fixed with respect to a conventional rotation pole of the Earth at a certain reference date. Thus the definition of the third axis of the system, the rotational axis, usually differs from the instantaneous rotational axis of the Earth. In the following, the term Earth-fixed system will always denote quasi-Earth-fixed systems according to this definition.

A major topic for the determination of the gravitational accelerations on CHAMP from the observed trajectory is how to get rid of all the other perturbation effects that influence the satellite's motion besides Earth induced gravitation. These are mainly non-gravitational perturbing accelerations as well as effects of orbit manoeuvres. For the quantitative determination of the non-gravitational perturbations CHAMP carries an accelerometer at its centre of gravitation (CoG). By means of this, the effects of the non-gravitational forces can be measured and taken into account during the computation process. A somehow more severe problem is posed by the effects of orbit manoeuvres. Due to its shape (view figure 1-1 and annex C), CHAMP will tend to assume a position with its boom pointing radially away from the Earth. To avoid this and to keep CHAMP in a 'boom-ahead' orientation within a range of $\pm 2°$, the satellite carries thrusters. These thrusters will be fired in due time. Between the firings star cameras will determine the orientation of the satellite. Would the accelerometer be placed exactly at the CoG of the satellite and would the thrusters work properly, which means that only rotational accelerations would be transferred to the satellite, no effects would be seen by the accelerometer. In reality though, there will be also small translatory components within the acceleration vector. The accelerometer itself will not be positioned in the exact CoG of the satellite's body. Thus the attitude manoeuvres will have an influence on the acceleration values measured. This effect cannot be separated from the other, non-gravitational forces. To keep these effects as low as possible, which means smaller than the observable range of accelerations of the accelerometer, a maximum offset of 2 mm of the accelerometer off the CoG is allowed.

At the moment there are contradicting views on how often the thrusters will have to be set into action for attitude control and on the effects these attitude corrections will have on the accelerometer observations. Pessimistic expectations are based on firing intervals as short as several minutes and induced accelerations, that will exceed the accelerometer's range of measurement by far. This would mean, that the determination of the gravitational field would be forced to rely on a trajectory, that would be split off in a multitude of very short arcs, instead of taking into account long, nearly continuously observed arcs. In addition, including the non-gravitational effects into the computations will become more complicated, not to mention the effects these constant strain will have on the performance of the accelerometer itself. The final clarification will have to wait until the launch-and-early-orbit phase of CHAMP will be finished successfully and the first operational data is available.

Disregarding these open questions, a concept for an orbit sensitivity analysis based on CHAMP's observables, full three-dimensional position and velocity vectors from GPS, will be outlined in the next sections.
While this section mainly concentrated on the new possibilities for gravity field determination by means of data from the CHAMP mission and possible drawbacks, that may have to be faced, more technical information on the satellite itself, its instrumentation and mission layout as well as literature references can be found in annex C.

1-3   Existing methods for orbit sensitivity analysis

The analysis of the first satellite orbits being used for the determination of the gravitational field of the Earth mainly concentrated on the determination of perturbations, that were quite dominant in the spectrum of perturbations. These dominant effects are the so-called orbit resonances. If there is approximate commensurability between the mean motion $\bar{n}$ of the satellite and the angular velocity $\omega_\oplus$ of the Earth, resonance-like enforcements of the amplitude of periodic perturbation effects are caused. Based on respective principles from classical mechanics and using Kaula's perturbation theory (Kaula (1966)) it can be shown, that all non-zonal terms of order m of the Earth's gravitational field model (for further details on gravitational field models and especially the term 'order' refer to chapter 3) with

$$\bar{n} = 2\pi/\bar{T} \approx m\,\omega_\oplus \tag{1-1}$$

yield resonance effects. Commensurability is fulfilled, if $\bar{n} = 2\pi/\bar{T}$ and $\omega_\oplus$ form an integer valued ratio m. Looking for a geometrical interpretation of resonance, it is seen, that resonance comes up, if successive revolutions of the satellite are separated by an interval that corresponds to the wavelength belonging to the base function of the respective (surface) spherical harmonics coefficient causing the resonance effect. Thus the effects of that very perturbation add up with each passage of the satellite over the source of the perturbation. The computation of resonant frequencies of the orbit spectrum thus provides a good means for a first approximation of an orbit synthesis. Despite that, resonance is not that important for the future LEO missions. Due to their lower orbit height, the gravitational effects on the orbit will be much more detailed than for a high flying satellite. Thus a clear location of the resonant frequencies in the orbit spectrum will not be given. The difference in amplitude between the resonant parts and the other perturbations will not be that evident (Schwintzer (1999)). In addition to that the additional non-gravitational perturbations on the satellite become more and more important the lower the satellite orbits the Earth. Due to the dominant atmospheric perturbations (drag and lift) the satellite orbit will soon loose the state of resonance again. Thus the resonant effects are not able to add up over a long period of time and become evident.

---

table 1-3: Evaluation of existing sensitivity analysis methods

'resonance':   based on dominant parts of the orbit spectrum

$\ominus$ not really applicable for LEO mission layouts
$\otimes$ gives a rough idea on what to expect from the sensitivity analysis

'Kaula':   based on representation of disturbing potential in Kepler elements

$\oplus$ analytically derived formulae
$\ominus$ high analytical efforts necessary to derive formulae
$\ominus$ formulation based on Kepler elements (singularities, not in compliance with GPS)

'reference':   based on differences between reference orbit and orbit computed with perturbed coefficients

$\ominus$ high computing time requirements
$\ominus$ pre-information needed to reduce computing time requirements
$\otimes$ does not depend on parametrisation (Cartesian possible)

($\ominus$ ... disadvantage, $\oplus$ ... advantage, $\otimes$ ... neutral)

Following the line of reasoning of the classical lumped coefficient analysis for high flying satellites for gravitational analysis most sensitivity analysis methods are based on the assumption that it is sufficient to determine the

major dominant perturbations of the orbit and thus identifying the perturbations of which the describing parameters can be determined best from the orbit perturbation data.

There are mainly two different methods applied nowadays for the sensitivity analysis of gravity field satellite missions. The first one is based on the development of the Earth's gravitational effects with respect to Kepler elements, as proposed by Kaula (Kaula (1966)). This yields equations of sort 'acceleration equals function of Kepler elements (or a subset), co-ordinates of evaluation point, geophysical constants and (surface) spherical harmonics series coefficients'. The (surface) spherical harmonics coefficients appear multiplied with factors depending on the Kepler elements, or a subset of them, that depend on the mission's layout and can be interpreted as weights of influence. These weight factors provide an idea on the influence certain gravitational coefficients have on the satellite's orbit.

The second method is more numerically oriented. In a first step a reference orbit is computed based on a reference gravitational model, being of higher order usually. Starting from this model, certain coefficients are varied now one by one, all in the same way. For each varied model a new orbit computation is performed. The accumulated differences with respect to the reference orbit serve as a measure for the influence of the single coefficient on the satellite's orbit (Scheinert (1996)).

It is quite obvious, that the later method yields high numerical and computational efforts. These demands can only be reduced if additional information on the sensitivity of the orbit can be introduced. There, the question will be how to acquire this additional information. Despite the fact that the first method yields nice formulae, the efforts to derive these formulae are considerably high. A much more important problem is the fact that Kepler elements can create singularities for specific cases (compare section 2-2 on orbital elements). In addition the parametrisation of the orbit is not performed by means of Cartesian co-ordinates, as being derived from GPS code and/or phase measurements, which are canonical variables (see section 2-2.1 and Seeber (1989), section 3.1). The most important point is to avoid the possible singularities, thus any canonical system of description would suffice. Since the Cartesian co-ordinates are canonical and directly provided by the tracking system, they have been chosen.

1-4 Outline of the proposed orbit sensitivity analysis method

Mathematically the concept to be proposed in this thesis is based on a frequency representation of the observables - the components of the satellite's position and velocity vectors - as well as the Earth's gravitational field models. It will be shown, that a close connection between the Fourier series expansion coefficients computed by means of the frequency analysis of the gravitational field value and the (surface) spherical harmonics series coefficients of the gravitational field model can be found.

A coarse outline of the sensitivity analysis can be given as follows:

- Modelling of the Earth's gravitational acceleration vector by means of the (surface) spherical harmonics series expansion used in today's models for the gravitational field.

- Frequency analysis of the representation of the Earth's gravitational acceleration vector to find a connection between the Fourier coefficients and the (surface) spherical harmonics coefficients. The Fourier analysis will be carried out analytically along a fictitious trajectory represented in Cartesian co-ordinates provided by a satellite's GPS receivers.
  This frequency analysis of the gravitational vector expressed by means of a (surface) spherical harmonics model yields a formulation that closely resembles the representation by means of the so-called 'lumped coefficients' (for more details refer to section 1-5).

- Computation of the gravitational acceleration vector acting on the satellite at each point of time of observation from the observed position and velocity vectors.

- Frequency analysis of the computed gravitational acceleration vector. This analysis will be carried out numerically.

- Comparison of the obtained spectra leads to a selection of the very Fourier coefficients and (surface) spherical harmonics coefficients having the greatest effect on the satellite's trajectory. A suitable strategy for the comparison and the selection will have to be discussed with respect to the envisaged application of the results.

One of two key problems for the applicability of this method is to determine the gravitational vectors from the GPS observables position and velocity vector. To compute the gravitational vectors at each observation point at time t with position vector $\mathbf{x}(t)$ and velocity vector $\dot{\mathbf{x}}(t)$ given, a discrete Kalman filter method for nonlinear systems will be used. For the setup of this method several different approaches can be applied. The basis for the filter methods is a state-space model for the description of a satellite's trajectory and orbital motion. This model will be introduced on the basis of the determination of the satellite's motion and trajectory by means of a GPS

high-low satellite to satellite tracking (hl-SST) scenario. The observables are the complete satellite's position and velocity vectors as well as the resulting vector of all non-gravitational forces or accelerations respectively acting on the satellite. Thus the scenario corresponds to the future geodetic and geophysical low Earth orbiting (LEO) satellite mission CHAMP (see 1-2).

A vital point to be considered here is the representation of the gravitational field as main influence on the satellite's motion. Cartesian representations being derived from the well-known (surface) spherical harmonics series expansion of the gravitational potential, acceleration vector and gradient tensor are given.

The second key problem will be, as it has been mentioned already above, to find an applicable selection process for dealing with the gravitational model's and orbit data's spectra to determine the strongest influences on the satellite. It will be seen that this selection process depends on the task (orbit analysis or synthesis) to perform.
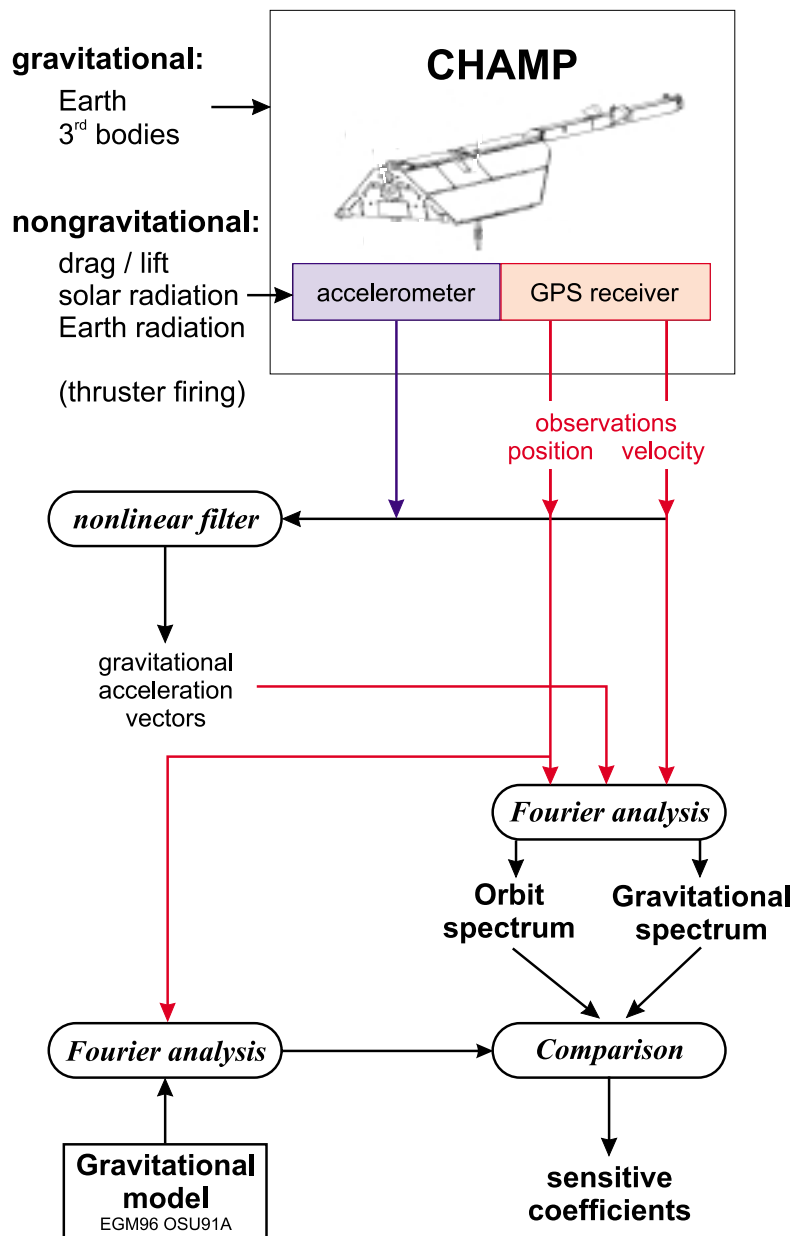

figure 1-1: Outline of the sensitivity analysis

1-5   Lumped coefficients representation of the gravitational field

The term 'lumped coefficient' was introduced by Klosko and Wagner in 1977 (Klosko and Wagner (1977)) and Klokočník in 1982 (Klokočník (1982)) to denote an infinite linear sum of weighted (surface) spherical harmonics

series expansion coefficients to form the Fourier coefficients of a perturbation with respect to a nominal value of some sort. Simply speaking the lumped coefficients are linear combinations of a particular order m of the fully normalized (surface) spherical harmonics coefficients $\bar{c}_{nm}$ and $\bar{s}_{nm}$ (Klokočník (1982)). From the physical point of view the addends of a lumped coefficient all produce the same phase and amplitude of orbit perturbation (Seeber (1989)). Thus the (surface) spherical harmonics coefficients $\bar{c}_{nm}$ and $\bar{s}_{nm}$ contributing to the same lumped coefficient are not separable from the analysis of only one specific satellite mission. Since the summation for the lumped coefficients depends on the layout of the satellite's trajectory (see the definition of lumped coefficients in Klokočník (1982), it shows the dependency on an inclination function) different satellite orbits have to be analysed.

Summarizing the rigorous definition drawn from Klosko and Wagner (1981) and Schrama (1986, 1991, 1992) a time dependant perturbation $\mathbf{f}(t)$, determined with respect to some nominal value can be written as a Fourier series expansion in the following way

$$\mathbf{f}(t) = \sum_{k=-\infty}^{+\infty} \sum_{m=0}^{+\infty} \left[\mathbf{A}_{km} \, \cos(\psi_{km}) + \mathbf{B}_{km} \, \sin(\psi_{km}) \right] \quad . \tag{1-2}$$

In the case of satellite orbit analysis $\mathbf{f}(t)$ will be some orbit related observations like orbit perturbations with respect to a nominal orbit (e.g. a $\bar{c}_{20}$ perturbed precessing Kepler ellipse), the disturbing potential itself acting on the satellite (Schrama (1992), Klosko and Wagner (1982)) or even observed values like gradiometre observations (Schrama (1991, 1992)), GPS satellite tracking observations and satellite-to-satellite-tracking (SST) observations (both in Schrama (1992), SST also in Wiejak et al. (1991)).

$$V \;=\; \frac{GM}{r} \sum_{n=2}^{\infty} \left(\frac{R}{r} \right)^n \sum_{m=0}^{n} \sum_{p=0}^{n} F_{nmp}(i) \sum_{q=-\infty}^{\infty} G_{npq}(e) \left[\begin{bmatrix} \bar{c}_{nm} \\ \bar{s}_{nm} \end{bmatrix} \cos\psi_{nmpq} + \begin{bmatrix} -\bar{s}_{nm} \\ \bar{c}_{nm} \end{bmatrix} \sin\psi_{nmpq} \right]_{n-m \; odd}^{n-m \; even} \tag{1-3}$$

Using e.g. the classical representation (1-3) of the perturbation potential along the orbit arc of a satellite by means of Kepler elements (Kaula (1966)) the angular argument ψ_{km} of the Fourier representation's sine and cosine terms is given as

$$\begin{aligned}
\psi_{lmpq} &= (l-2p)\,\omega + \underbrace{(l-2p+q)}_{=:\, k}\, M + m\,(\Omega - \theta) \\
\psi_{kmq} &= k\,\omega + k\,M + m\,(\Omega - \theta) - q\,\omega \quad ,
\end{aligned} \tag{1-4}$$

the respective frequency is obtained as

$$\dot{\psi}_{kmq} = \underbrace{k\,(\dot{\omega} + \dot{M}) + m\,(\dot{\Omega} - \dot{\theta})}_{=:\, \psi_{km0}} - q\,\dot{\omega} \quad . \tag{1-5}$$

In equations (1-4) and (1-5) l and m are degree and order of a (surface) spherical harmonics series expansion of a gravitational field value, p and q integer valued indices resulting from the eccentricity and inclination functions coming up with the gravitational potential's representation in Kepler elements (Kaula (1966)).

Equation (1-4) plays an important role for the determination of orbital resonance effects. Equation (1-5) already splits the frequency off into a high frequency part $\dot{\psi}_{km0}$ with m-daily, k-revolution and resonant period and secondary slow frequencies $-q\,\dot{\omega}$ with typical periods of 180 days (Schrama (1986) and (1992)).

Having a look at the linear perturbations of the Kepler elements and expanding them around the high frequencies yields the lumped coefficients as coefficients of a Fourier series expansion of each orbital (Kepler) element (Klosko and Wagner (1977, 1982))

$$E = E_0 + (Secular\ effects) \begin{bmatrix} C^{\star} \; \cos\psi_{km0} \\ S^{\star} \; \sin\psi_{km0} \end{bmatrix} \tag{1-6}$$

with $E \in [a, e, i, \omega, \Omega, M]$, the initial unperturbed value E_0 of the respective Kepler element and the lumped coefficients $C^{\star}$ and $S^{\star}$ being infinite sums linear with respect to the gravitational coefficients and themselves sine and cosine functions of the argument of perigee ω.

In the course of this thesis a somewhat different definition of the term lumped coefficient will be used, which slightly differs from the notion given above, although the resulting equations resemble each other. Lumped coefficients will stand for the Fourier coefficients of a frequency analysis of a gravitational field value along a satellite's trajectory. They are also linear with respect to the original gravitational coefficients, but are based on another angular argument. Details will be developed in chapter 3. Both definitions of lumped coefficients have similar key attributes which leads to the common naming:

- Lumped Coefficients are linear combinations of fully normalised (surface) spherical harmonics coefficients of a certain order m (Klokočník (1982)).

- From the physical point of view all addends of a lumped coefficient cause a perturbation of the same phase and amplitude (Seeber (1989)), thus each lumped coefficient corresponds a certain frequency and amplitude of a spectrum along an orbit.

- Usually the frequencies of neighbouring lumped coefficients do not overlap (non-overlapping condition with exceptions for zonal effects).

1-6   Structure of the thesis

Following this introduction chapter 2 will give an insight into a few important topics from satellite geodesy. Mainly the hierarchy of reference systems as well as the formulation of equations of motion for the satellite and the main sets of parameters for orbit representation will be presented. A special section is dedicated to the representation of the Earth's gravitational acceleration vector with respect to a space-fixed geocentric reference system as it will arise in the course of computation.

A detailed approach towards the mathematical representation of the Earth's gravitational field will be presented in chapter 3. Starting from the gravitational field equations and the standard (surface) spherical harmonics series representation in spherical co-ordinates with respect to an Earth-fixed geocentric reference system (as one possible solution for the field equations), a Cartesian representation will be derived, that will be well adapted to the reference system of the observables themselves. In addition to that and as a preparation for the sensitivity analysis itself Fourier series representations for both cases are given in chapter 4. The Fourier series expansions are set up considering two different approaches. On the one hand the series expansion will be performed along the parameter lines of the spherical co-ordinates, on the other hand along the trajectory of the satellite. These representations yield the so-called *lumped coefficients* providing a connection between the Fourier series' coefficients (frequency coefficients) and the (surface) spherical harmonics coefficients. Examples and numeric results are given for the EGM96 model.

As can be seen in figure 1-1, the analysis will be based on a comparison between the frequency spectra of a gravitational field model (lumped coefficients) and of the satellite's orbit or the gravitational acceleration acting on the satellite, respectively. Chapters 5 and 6 will present the basic modelling and the algorithm for the computation of gravitational field values from orbit data respectively. The main tool for the computation is a discrete Extended Kalman filter (dEKF), which determines gravitational acceleration vectors acting on the satellite from the GPS observations position and velocity. For applying a filtering technique the system 'Satellite Trajectory' has to be described by means of a state-space formulation. A problem oriented state-space description of the system satellite is given in chapter 5. Based on this model the dEKF is then set up in chapter 6. Using a standard extended Kalman filter for nonlinear systems can yield considerable errors mainly due to linearisations applied for the prediction of covariances. These errors will be discussed briefly and literature references for possible alternative methods of filtering the system will be given.

All these steps provide the input information and data for the sensitivity analysis itself, which is performed for a simulation of the CHAMP mission in chapter 7.

The main part will be concluded by a summary and some comments and further remarks in chapter 8.

The annexes give more detailed information on four subjects, mainly numerical methods, definitions and technical details. Annex A gives the mathematical definitions of the Legendre functions and their derivatives. Included are recursion formulae for the numerical evaluation. Based on the definitions of annex A scalar-, vector- and tensor-valued surface spherical harmonics will be introduced in annex B.

Annex C gives a few technical details on the German dedicated gravity field mission CHAMP, which is used throughout this thesis as an example. The numerical integration method for the computation of orbit data for CHAMP, an Adams-Moulton / Adams-Bashforth multistep method is presented in annex D. The second numerical integration method used in this thesis is a 6th order Runge-Kutta method also presented there.

Chapter 2

Selected fundamentals of satellite geodesy

2-1 Reference systems in satellite geodesy

For the computation of satellite trajectories the most important reference system is a (quasi-) inertial reference system. Following the hierarchical structure of reference systems given in Grafarend (1979) and (1999), a system like this is provided by the geocentric space-fixed Cartesian equatorial co-ordinate system $\mathbf{E}^\bullet$. The origin of $\mathbf{E}^\bullet$ is the CoM of the Earth, the z-axis is the rotational axis of the Earth. The x-axis is computed by the vector product of the Earth's rotational vector $\mathbf{\Omega}$ and the ecliptic normal vector $\mathbf{\Psi}$. By convention it points towards the equinox. The y-axis completes the system to be a right-handed Cartesian reference system. For most of the problems arising in satellite geodesy, equatorial space-fixed systems like $\mathbf{E}^\bullet$ provide a sufficient approximation to the required (quasi-) inertial reference system.
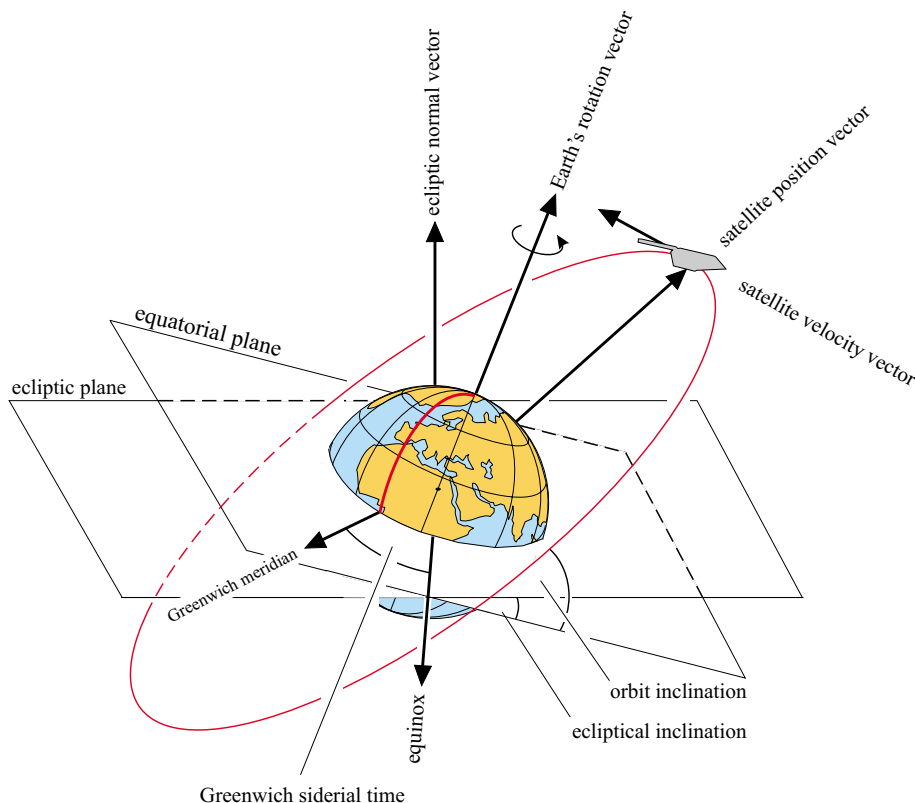
figure 2-1: Defining vectors

For the description of the Earth's gravitational field an Earth-fixed reference system is needed (see the remark on the strict naming of references systems on page 11 made with respect to WGS84). It is given by means of the geocentric Earth-fixed Cartesian equatorial system $\mathbf{F}^\bullet$. Its origin is also the CoM of the Earth, its z-axis points along the axis of rotation towards the Earth's pole of rotation. The x-axis points towards the intersection point of the equator and the zero (Greenwich) meridian at longitude $0°$. I.e., $\mathbf{F}_{1\bullet}$ is the projection of the gravity vector of Greenwich on to the equatorial plane (Grafarend (1979) p. 320, compare also table 2-2). The y-axis

again completes the system to a right-handed Cartesian system. This system rotates together with the Earth with angular velocity vector $\boldsymbol{\omega}_{\mathbf{E}^\star} = \boldsymbol{\omega}_{\oplus}$.

A further distinction within the two types of reference systems can be made with respect to the definition of the rotational pole and axis respectively. Since the rotational pole of the Earth is not fixed with respect to the Earth itself, it can either be considered at his actual position, resulting in a time-variant definition of the rotational axis, or its position at a certain point of time can be taken as basis for the definition. Systems based on the actual position of the pole are called true systems, systems based on the pole's position at a certain point of time are called conventional systems.

For the transformation between Earth- and space-fixed systems, depending of the respective definition of the poles of rotation, the effects of

- polar motion with angles of polar motion x, y,

- Earth rotation with rotation angle Greenwich sidereal time $\Theta_{Greenwich}$,

- precession with angles of precession ς, θ, z and

- nutation with nutation parameters $\Delta\psi, \Delta\varepsilon$

have to be taken into account. If neither the definition nor the movement of the pole's position are taken into account, the transformation results in a so-called **quasi**-Earth-fixed reference system (see also the comments on page 11) or **quasi**-space-fixed reference system. For the definition of the transformation parameters and the rotation matrices refer to Richter (1986) and (1994), pp. 42ff, or Moritz and Mueller (1988). A detailed summary of reference systems for satellite geodesy can also be found in Nagel (1976).

---

table 2-1: Space-fixed equatorial system $\mathbf{E}^\bullet$ - CIS

$$\mathbf{E}_{1\bullet} = \frac{\boldsymbol{\Psi} \times \boldsymbol{\Omega}}{\| \boldsymbol{\Psi} \times \boldsymbol{\Omega} \|}$$

$$\mathbf{E}_{2\bullet} = \mathbf{E}_{1\bullet} \times \mathbf{E}_{3\bullet}$$

$$\mathbf{E}_{3\bullet} = \frac{\boldsymbol{\Omega}}{\| \boldsymbol{\Omega} \|}$$

with :

$\boldsymbol{\Omega}$	...	Earth's vector of rotation,
$\boldsymbol{\Psi}$	...	ecliptic normal vector and
equinox	...	direction of line of intersection of equatorial and elliptical plane.

---
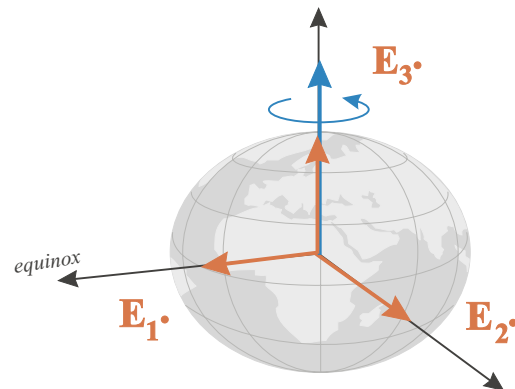
table 2-2: Earth-fixed equatorial system $\underline{\mathbf{F}}^\bullet$ - CTS

$$\mathbf{F}_{1\bullet} = \mathbf{F}_{2\bullet} \times \mathbf{F}_{3\bullet}$$

$$\mathbf{F}_{2\bullet} = \frac{\boldsymbol{\Omega} \times (-\boldsymbol{\Gamma}_{Greenwich})}{\| \boldsymbol{\Omega} \times (-\boldsymbol{\Gamma}_{Greenwich}) \|}$$

$$\mathbf{F}_{3\bullet} = \frac{\boldsymbol{\Omega}}{\| \boldsymbol{\Omega} \|} = \mathbf{E}_{3\bullet}$$

with :

$\boldsymbol{\Omega}$	...	Earth's rotational vector and
$-\boldsymbol{\Gamma}_{Greenwich}$	...	negative gravity vector at Greenwich.
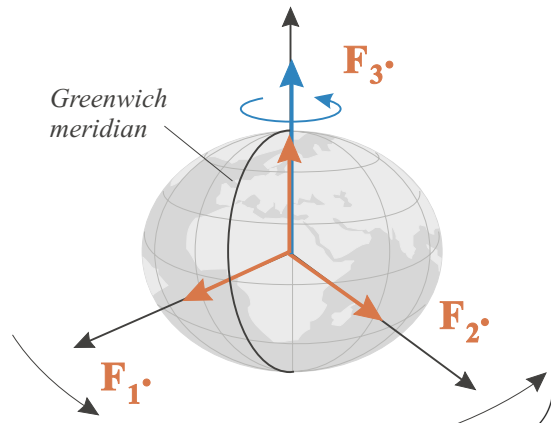
The necessary systems for the observation of the orbit of the satellite depend on the tracking method. Classical methods are usually Earth-bound and thus operate on terrestrial topocentric reference systems. Future satellite missions will be tracked by GPS in the first place (the GPS observations will only be supplemented by other, classical methods, e.g. SLR in case of CHAMP). These methods will be based on satellite-fixed reference systems of sorts, orbit related reference systems and GPS' reference system, respectively. Thus for classical methods (see table 2-3) one has to distinguish between

- a topocentric oriented reference system $\mathbf{E}^\star$ and

- a topocentric observation instrument fixed system $\mathbf{F}'$.

For GPS based tracking (see table 2-4) there are

- an orbit fixed reference system $\mathbf{B}^\star$ centred at the satellite's CoG and oriented with respect to the satellite's trajectory given by its position and velocity vector and

- a satellite fixed reference system $\mathbf{B}'$ related to the main axes of the space vehicle's body itself.

---

table 2-3: <u>Topocentric systems $\mathbf{E}^\star$ and $\mathbf{F}'$</u>

$$\mathbf{E}_{1^\star} = \mathbf{T} \qquad \mathbf{F}_{1'} = \mathbf{Z}$$

$$\mathbf{E}_{2^\star} = \mathbf{F}_{1^\star} \times \mathbf{F}_{3^\star} \qquad \mathbf{F}_{2'} = \mathbf{F}_{1'} \times \mathbf{F}_{3'}$$

$$\mathbf{E}_{3^\star} = \frac{-\mathbf{\Gamma}}{\|\mathbf{\Gamma}\|} \qquad \mathbf{F}_{3'} = \frac{-\mathbf{\Gamma}}{\|\mathbf{\Gamma}\|}$$

$$\mathbf{E}^\star = \underline{\mathbf{R}}_3(\Sigma)\,\mathbf{F}'$$

with :

$\mathbf{T}$	...	oriented direction (e.g. North),
$\mathbf{Z}$	...	zero direction of instrumental horizon,
Σ	...	orientation unknown.

---
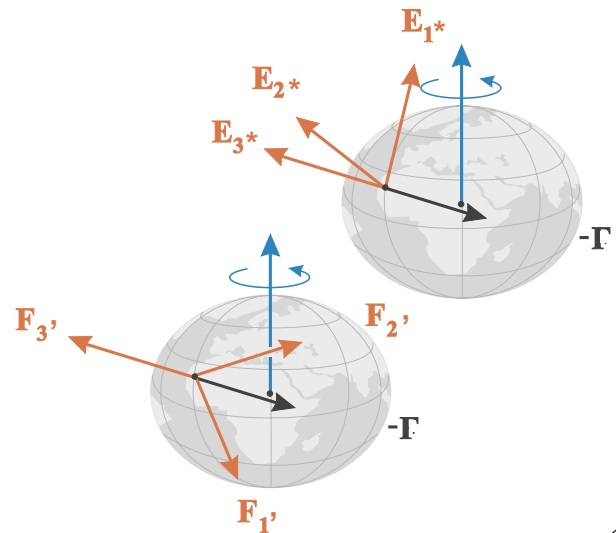
table 2-4: <u>Space vehicle systems $\mathbf{B}^\star$ and $\mathbf{B}'$</u>

SV-body system: *space vehicle fixed*

    $\mathbf{B}_{1'},\ \mathbf{B}_{2'},\ \mathbf{B}_{3'}$

SV-trajectory system: *orbit fixed*

    $\mathbf{B}_{1^\star}\ldots\ \mathbf{B}_{2^\star} \times \mathbf{B}_{3^\star}$
        'out of plane'

    $\mathbf{B}_{2^\star}\ldots$ direction of velocity
        'along track'

    $\mathbf{B}_{3^\star}\ldots$ direction of position
        'radial'
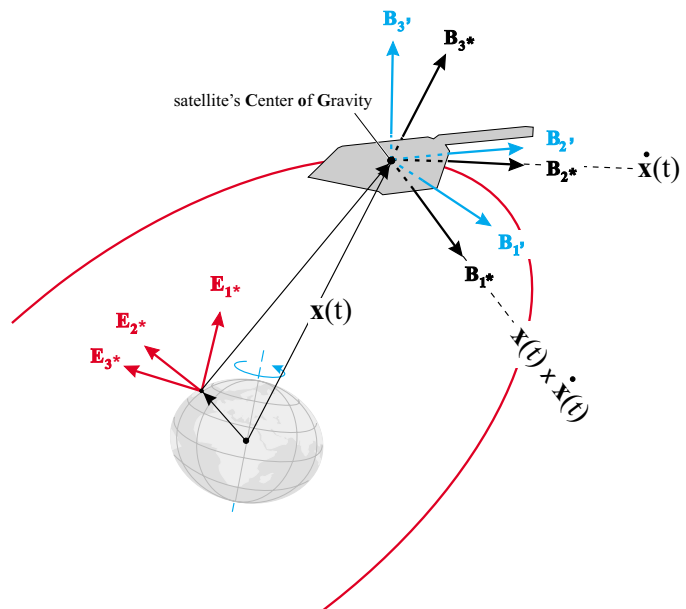
Figure 2-2 gives a concise overview over the main reference systems and examples for reference frames as implementations of these systems. The vectors on which the definitions of the various reference systems in tables 2-1, 2-2 and 2-3 are based, are shown in figure 2-1.
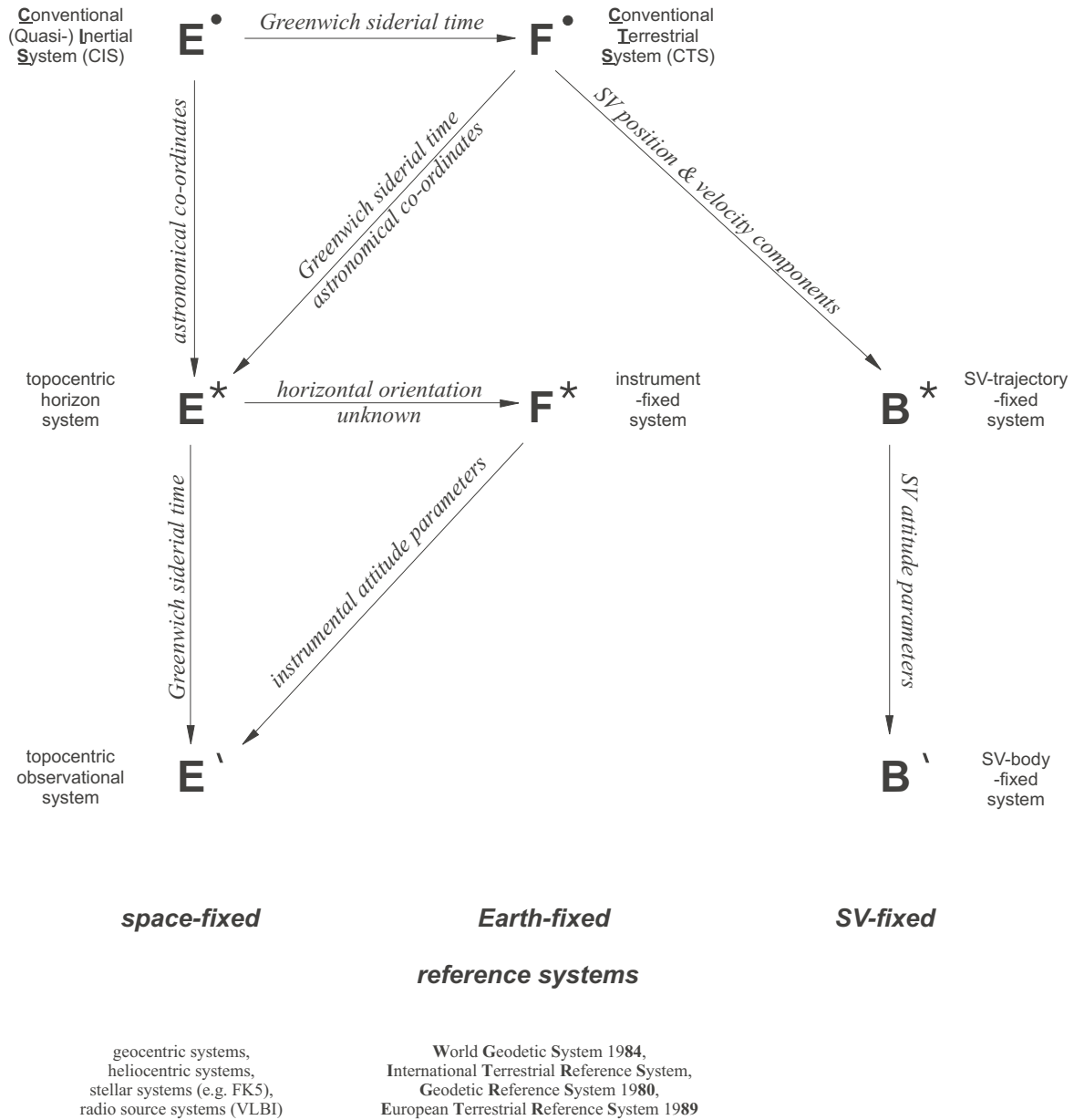
figure 2-2: Overview over reference systems and frames in satellite geodesy

2-2   Motion of satellites - General remarks

The trajectory of a satellite can be described mathematically by means of Newton's law of motion of point masses with respect to an inertial reference frame. The corresponding equation of motion (2-1) is a three-dimensional vectorial ordinary differential equation of order two depending on time t, position and velocity vector $\mathbf{x}(t)$ and $\dot{\mathbf{x}}(t)$, both depending on t themselves, and a set of geophysical and space vehicle related parameters $\mathbf{p}(t)$, partly depending on t (see list of perturbations table 2-5).

$$
\begin{aligned}
\ddot{\mathbf{x}}(t) &= \frac{1}{m}\,\mathbf{F}(t, \mathbf{x}(t), \dot{\mathbf{x}}(t), \mathbf{p}(t)) \\
&= \sum_{u=1}^{U} \ddot{\mathbf{x}}_u(t, \mathbf{x}(t), \dot{\mathbf{x}}(t), \mathbf{p}(t))
\end{aligned}
\tag{2-1}
$$

The vectorial force or acceleration term on the right side of equation (2-1) adds up all the effects influencing the satellite's motion. Most of the perturbations show an explicit time dependency due to time-variant parameters

or effects they stand for. Equation (2-2) gives the dependencies on $\mathbf{x}$ and $\dot{\mathbf{x}}$ more precisely. In addition each acceleration term usually depends on a specific set of parameters describing and modelling the geophysical effects that induce the very perturbation. Examples for that parameters are gravitational coefficients, parameters for atmospheric density models or reflexion indices of the satellite's surface.

$$
\begin{aligned}
\ddot{\mathbf{x}}(t) \quad = \quad & \mathbf{g}_\circ(\| \mathbf{x}(t) \|) && \text{spherical Earth,} \\
& + \mathbf{g}_{\text{non-sph.}}(\mathbf{x}(t)) && \text{non-spherical Earth,} \\
& + \ddot{\mathbf{x}}_{3^{rd} \text{ cel. bodies}}(t, \mathbf{x}(t)) && \text{sun, moon, planets,} \\
& + \ddot{\mathbf{x}}_{\text{tides}}^{\text{ocean}}(t, \mathbf{x}(t)) + \ddot{\mathbf{x}}_{\text{tides}}^{\text{solid}}(t, \mathbf{x}(t)) && \text{ocean and solid Earth tides,} \\
& + \ddot{\mathbf{x}}_{\text{drag}}(t, \mathbf{x}(t), \dot{\mathbf{x}}(t)) + \ddot{\mathbf{x}}_{\text{lift}}(t, \mathbf{x}(t), \dot{\mathbf{x}}(t)) && \text{aerodynamic effects,} \\
& + \ddot{\mathbf{x}}_{\text{solar rad.}}(t, \mathbf{x}(t)) + \ddot{\mathbf{x}}_{\text{Earth rad.}}(t, \mathbf{x}(t)) && \text{radiation effects,} \\
& + \ddot{\mathbf{x}}_{\text{ctrl.}}(t) && \text{orbit manoeuvres and attitude control.} \\
= \quad & \mathbf{g}_\circ(\| \mathbf{x}(t) \|) + \mathbf{g}_{\text{non-sph.}}(\mathbf{x}(t)) && \\
& + \ddot{\mathbf{x}}_{pert.}(\mathbf{x}(t), \dot{\mathbf{x}}(t), \mathbf{p}(t), t) &&
\end{aligned}
\tag{2-2}
$$

table 2-5: Main influences on satellite orbits and their parameters $\mathbf{p}(t)$

spherical Earth	geocentric gravitational constant GM	
	$\rightarrow$ *position of satellite*	
Earth's oblateness	geocentric gravitational constant GM, spherical harmonic's coefficient $\bar{c}_{2,0}$	
	$\rightarrow$ *position of satellite*	
non-spherical Earth, high order harmonics	geocentric gravitational constant GM, spherical harmonics' coefficients $\bar{c}_{n,m}$, $\bar{s}_{n,m}$ (except for $(0,0)$, $(2,0)$)	
	$\rightarrow$ *position of satellite*	
3rd celestial bodies	gravitational constant of i-th 3rd body GM_i, spherical harmonics model (if avail.)	
	$\rightarrow$ *position of satellite and 3rd bodies*	
ocean and solid Earth tides	Love numbers	*Pfister (1998)* Wahr (1995)
	$\rightarrow$ *position of satellite and 3rd bodies*	
atmospheric drag	atmospheric density (model), satellite's aerodynamic surface parameter	King-Hele (1987), *Krauss (1998)*
	$\rightarrow$ *satellite's attitude, position and velocity*	
atmospheric lift	atmospheric density (model), satellite's aerodynamic surface parameter	
	$\rightarrow$ *satellite's attitude, position and velocity*	
solar radiation pressure	solar flux, satellite's surface reflexion parameters	*Sayda (1997)*
	$\rightarrow$ *satellite's attitude and position*	
Earth albedo	solar flux, Earth's surface reflexion parameters, satellite's surface reflexion parameters	Knocke et al. (1987), Stephens et al. (1981), *Johannsen (1998)*
	$\rightarrow$ *satellite's attitude and position*	

There exists a wide range of publications dealing with the different perturbations on a satellite's orbit. Only a few examples shall be mentioned here. General overviews can be found especially in Escobal (1975), Capellari et al. (1976), Kaula (1966) or any other text book on satellite geodesy, e.g. Schneider (1988) or Seeber (1989). Feltens (1991) and Milani et al. (1987) specialize in the treatment of non-gravitational perturbations. Special literature on each perturbation effect can also be found. A selection is given in table 2-5. Literature references noted in italic style refer to overview theses prepared by students at the Geodetic Institute of the University of Stuttgart as a part of a long running project dealing with the modelling of orbit perturbations (Schäfer et al. (1998b)). They can be used for further literature reference.

As already mentioned, Newton's equations of motion only hold with respect to an inertial reference system. By definition the origin of an inertial reference system and the system's orientation are not affected by any accelerations, neither translational nor rotational. Thus directions of the axes of the inertial system are space-fixed within the $\Re^3$, the system's origin is either also fixed within $\Re^3$ or performs a non-accelerated movement. Seen by an observer fixed in a moving reference system, e.g. $\mathbf{F}^\bullet$, additional apparent forces have to be taken into account. The equation of motion then has the form of (2-3). When seen 'from outside', i.e. by an observer fixed in a (quasi-)inertial reference frame, e.g. $\mathbf{E}^\bullet$, except for the perturbing forces mentioned above, only the gravitational effects are acting on a satellite.

$$\ddot{\mathbf{x}}(t) = \underbrace{\ddot{\mathbf{x}}_0(t)}_{\substack{\text{translational} \\ \text{accel. of origin}}} + \ddot{\mathbf{x}}_{grav.}(t) + \underbrace{\omega(t) \times (\omega(t) \times \mathbf{x}(t))}_{\substack{\text{centrifugal} \\ \text{acceleration}}} + \underbrace{2\omega(t) \times \dot{\mathbf{x}}_{rel}(t)}_{\substack{\text{Coriolis} \\ \text{acceleration}}} + \underbrace{\dot{\omega}(t) \times \mathbf{x}(t)}_{\substack{\text{Euler} \\ \text{acceleration}}} + \ddot{\mathbf{x}}_{pert.}(t) \qquad (2\text{-}3)$$

The most important of these apparent effects is the centrifugal acceleration $\mathbf{x}_{centrif.}(\mathbf{x}(t), \omega_\oplus)$ pointing perpendicularly away from the axis of rotation of the system, which is the axis of rotation of the Earth. If the combined effects of the gravitational and centrifugal potentials are regarded, the field is called gravity field of the Earth in contrast to the gravitational field.

All the following considerations will be made on the basis of an observer fixed with respect to a quasi-inertial reference system $\mathbf{E}^\bullet$ with the geocentre as its origin, the Earth's axis of rotation as z-axis, the x-axis pointing towards the equinox and the y-axis completing the system to a right-handed Cartesian equatorial system. If seen from this reference system, the gravitational field of the Earth seems to be time variant, since it rotates together with the Earth. This would mean, that time variant representation coefficients (gravitational field representations and their coefficients will be presented in chapter 3) have to be introduced. To avoid this and to be able to use the standard gravitational potential models like OSU91A or lately EGM96, the gravitational effects are always computed within the Earth-fixed rotating reference system as shown in section 2-3.

---

table 2-6: Equations of motion - Orbit computation (orbit synthesis)

(with respect to an inertial reference system)

$$\ddot{\mathbf{x}}(t) = \frac{1}{m} \, \mathbf{F}(t, \mathbf{x}(t), \dot{\mathbf{x}}(t), \mathbf{p}(t)) \qquad (2\text{-}4)$$

with:

$\quad \mathbf{x}(t) \qquad\qquad\qquad \ldots \quad$ geocentric position vector,

$\quad m \qquad\qquad\qquad\quad\;\, \ldots \quad$ satellite's mass,

$\quad \mathbf{F}(t, \mathbf{x}(t), \dot{\mathbf{x}}(t), \mathbf{p}(t)) \quad \ldots \quad$ force vector depending on a set of parameters $\mathbf{p}(t)$ (see table 2-5)

and the initial values $\mathbf{x}(t_0) = \mathbf{x}_0$ and $\dot{\mathbf{x}}(t_0) = \dot{\mathbf{x}}_0$.

is equivalent to

$$\mathbf{x}(t) = \mathbf{x}_0 + \dot{\mathbf{x}}_0(t - t_0) + \frac{1}{m} \int_{t_0}^{t} (t - t') \, \mathbf{F}(t', \mathbf{x}(t'), \dot{\mathbf{x}}(t'), \mathbf{p}(t')) \, dt' \qquad (2\text{-}5)$$

As an equivalent to equation (2-1), an integral formulation of the equations of motion can be found. Tables 2-6 and 2-7 give the formulae for the case of an initial value formulation - which represents the case of orbit

computation (orbit synthesis) - and a boundary value problem formulation - which stands for the tasks of satellite orbit determination and orbit analysis. In literature different methods to solve this integral equations have been suggested. Since the method presented in the following will be based on the differential equation presentation (2-1) of the equation of motion, only literature references are given here without going into further detail. A very thorough treatment of the subject can be found in the works of the SFB78, a former special study group on satellite geodesy at Munich technical university, like Ilk (1972), Schneider (1968) and (1972a,b), Sigl et al. (1970) or more recently in Thalhammer (1995). The overall theory is developed in Roach (1968) and described in annex E.

---

table 2-7: Equations of motion - Orbit analysis

(*with respect to an inertial reference system*)

$$\ddot{\mathbf{x}}(t) = \frac{1}{m} \, \mathbf{F}(t, \mathbf{x}(t), \dot{\mathbf{x}}(t), \mathbf{p}(t)) \tag{2-6}$$

with:

$\mathbf{x}(t)$ ... geocentric position vector,
m ... satellite's mass,
$\mathbf{F}(t, \mathbf{x}(t), \dot{\mathbf{x}}(t), \mathbf{p}(t))$ ... force vector

and the boundary values $\mathbf{x}(t_0) = \mathbf{x}_0$ and $\mathbf{x}(t_n) = \mathbf{x}_n$.

is equivalent to

$$\mathbf{x}(t) = \frac{\mathbf{x}_n - \mathbf{x}_0}{t_n - t_0}(t - t_0) + \mathbf{x}_0 - \frac{(t_n - t_n)^2}{m} \int_{t_0}^{t_n} K(t, t') \, \mathbf{F}(t', \mathbf{x}(t'), \dot{\mathbf{x}}(t'), \mathbf{p}(t')) \, dt' \tag{2-7}$$

or with transformation of $[t_0, t_n]$ to $[0, 1]$

$$T = t_n - t_0 \tag{2-8}$$

$$\tau = \frac{t - t_0}{T} \quad \text{or} \quad \tau' = \frac{t' - t_0}{T} \tag{2-9}$$

$$\mathbf{x}(\tau) = (\mathbf{x}_n - \mathbf{x}_0)\tau + \mathbf{x}_0 - \frac{T^2}{m} \int_0^1 K(\tau, \tau') \, \mathbf{F}(\tau', \mathbf{x}(\tau'), \dot{\mathbf{x}}(\tau'), \mathbf{p}(\tau')) \, d\tau' \tag{2-10}$$

The integral's kernel is

$$K(t, t') = \begin{cases} (t' - t_0)(t_n - t) & \text{for} \quad t' \leq t \\ (t - t_0)(t_n - t') & \text{for} \quad t' \geq t \end{cases} \tag{2-11}$$

or

$$K(\tau, \tau') = \begin{cases} \tau'(1 - \tau) & \text{for} \quad \tau' \leq \tau \\ \tau(1 - \tau') & \text{for} \quad \tau' \geq \tau \end{cases} \tag{2-12}$$

It can be shown, that all these formulae, which originally are based on Newton's equation of motion for point masses only, can also be used to describe the motion of a satellite, which actually is not a point mass but an extended body (Schäfer (1997)). The, in general irregular, shape of the extended body of a satellite often causes an eigen-movement (for the case of non-attitude-stabilized satellites only). In most cases the satellites perform a rotation apart from their motion about a gravitating body. These rotations arise, if the distribution of mass within the satellite has different principle moments of inertia. In that case there exists a coupling between the satellite's eigen-rotation and its orbital movement. In general, neither a separation nor a linear superimposition of the rotation and the orbital movement are possible. The effect is called spin-orbit-coupling (Chauvineau and

Métris (1994)). The appearing coupling terms are of second order and can be estimated from the ratio

$$\frac{\text{discrete measure of the extended body}}{\text{characteristic distance of gravitating systems}} \overset{\text{e.g.}}{=} \frac{\text{diameter of satellite}}{\text{geocentric distance}} \tag{2-13}$$

For the spherical laser satellite GFZ-1 with diameter 21.5 cm and a mean geocentric distance of 6771 km this yields for example a magnitude of the coupling terms of $3.175 \cdot 10^{-8}$ (Schäfer (1997)).

A disconnection of the two components is possible if and only if the acting forces on the satellite solely depend on the position and the velocity of the extended body up to first order. Referring to the equations of motion, e.g. as given in (2-2), this condition usually holds. In this case two further conditions have to be fulfilled to allow a separation of the two effects: (1) The computations have to be performed with respect to an inertial system - which is always the case when Newton's equations of motion for point masses hold, since they require the same condition to be fulfilled - and (2) that the extended body can be regarded as a rigid system of mass points. A system of point masses is, by definition, called a rigid system, if the interactive forces between the individual mass elements compensate each other, i.e. the distances between the mass elements are constant. In addition to that, the interactive forces between the elements must not have an effect, neither translational nor rotational, on the motion of the system itself. Usually these conditions are fulfilled for a satellite's body. Thus a satellite in general can be referred to as a rigid system of mass elements and Newton's equations of motion hold. The motion of the system itself - the satellite's orbit - can be described by representing the trajectory of its CoG with respect to an inertial reference system.

$a,\ e$	shape of the orbital ellipse
$i,\ \Omega$	orientation of the orbital plane in space
ω	orientation of the orbital ellipse in the orbital plane
$\nu,\ M,\ E$	position of the satellite in the orbital ellipse
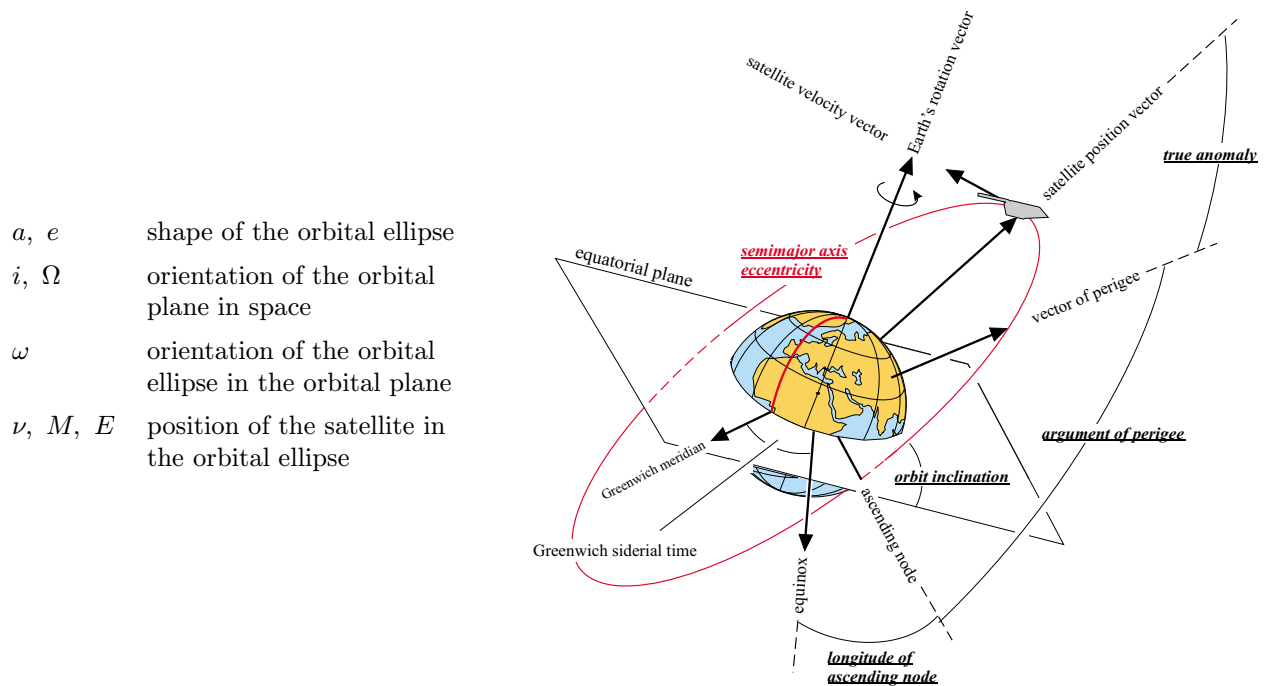
figure 2-3: Definition of the classical Kepler elements for orbit representation

Chauvineau and Métris (1994) give an estimate of the effects of spin-orbit-coupling. The results show, that spin-orbit-coupling has a considerable effect on the orbital motion of a satellite only if the satellite's dimension is around one-tenth of the orbital radius. In this case, it can even lead to chaotic orbital motion. This usually is not the case for Earth orbiting satellites. In the case of CHAMP spin-orbit-coupling does not have any effect, since CHAMP is attitude stabilized within a range of 2° with respect to its direction of motion and pointing towards Earth by means of the star sensor and thruster systems. Thus CHAMP is non-rotating.

2-2.1   Parametrisation of satellite orbits

To perform either of the tasks of orbit synthesis or orbit analysis, respectively, the equations of motion have to be solved. For the solution of a three-dimensional vectorial differential equation of order two $2 \cdot 3 = 6$ integration constants are required. Thus a satellite's trajectory is uniquely defined and described by six independent parameters. For that purpose, the classical Kepler elements for the description of a Kepler elliptic motion and, derived from the classical elements, the osculating Kepler variables for the description of arbitrary real perturbed orbits, are introduced. It has to be kept in mind that the original concept of the Kepler elements holds for ideal elliptic orbits and the anomalies $\nu,\ M,\ E$, which describe the position of the satellite within the space-fixed orbital ellipse (figure 2-3), are the only time-variant parameters in the set. These orbits only

occur for the undisturbed two body problem of one body orbiting another celestial body in its central field. Osculating Kepler variables however give a distinct set of parameters for each point of time, thus being all six time-dependent (this is also the reason for distinguishing between 'elements' and 'variables', following the usage of both terms in physics).

For orbits with eccentricity near zero or circular orbits (eccentricity $e \cong 0$) or orbits being or being near polar (inclination $i \cong 90°$) and geostationary orbits (inclination $i \cong 0°$) Kepler elements yield singularities in the dynamic's equations for the longitude of the ascending node $\dot{\Omega}$ (2-14), argument of perigee $\dot{\omega}$ (2-15) and the mean anomaly $\dot{M}$ (2-16).

$$\frac{d\Omega}{dt} = \frac{1}{na^2\sqrt{1-e^2}\sin i}\frac{\partial V}{\partial i} \tag{2-14}$$

$$\frac{dM}{dt} = n - \frac{1-e^2}{na^2 e}\frac{\partial V}{\partial e} - \frac{2}{na}\frac{\partial V}{\partial a} \tag{2-15}$$

$$\frac{d\omega}{dt} = -\frac{\cos i}{na^2\sqrt{1-e^2}\sin i}\frac{\partial V}{\partial i} + \frac{\sqrt{1-e^2}}{na^2 e}\frac{\partial V}{\partial e} \tag{2-16}$$

To avoid that, canonical elements like Hill (Chui and Mareyen (1992), Chui (1990) and (1997), Chui et al. (1997), Arfa-Kaboodvand (1997)), canonical spherical variables (Chui (1997), annex B) or KS (Kustaanheimo-Stiefel) elements (Stiefel and Scheifele (1971), You (1995)) can be used. These sets of elements and variables avoid the shortcomings of the Kepler elements but have to pay for that with not being as descriptive any more. The parameters that will be used in this thesis are Cartesian co-ordinates, which do not have singularities either and are provided derived from phase and/or code measurements by modern satellite tracking systems based on GPS receivers. The six Cartesian variables describing the satellite's trajectory are the three elements of each, the position and the velocity vector of the satellite, respectively, at each point of time of observation.

2-3 Transformation of vectors between space and Earth-fixed geocentric equatorial reference systems

The considerations of above's section imply, that the position of the satellite, at which the gravitational effects should be evaluated, has to be transformed from the space-fixed to the Earth-fixed reference frame first, then the gravitational potential or acceleration is computed and the result will be transformed back into the space-fixed system. The transformation parameters for that are the Greenwich sidereal time $\Theta_{Greenwich}$, which is the angle between the direction to equinox and the x-axis of the rotating Earth-fixed equatorial system, given in the equator plane, the parameters describing polar motion and the precession and nutation parameters. The transformation steps (Koop and Stelpstra (1989), Grafarend et al. (1990), Bettadpur et al. (1992)) are:

1. Transformation of the satellite position $\mathbf{x_{E\bullet}}(t)$ given with respect to a space-fixed system, e.g. $\mathbf{E^\bullet}$, to the Earth-fixed system $\mathbf{F^\bullet}$ by means of a rotation around the z-axis with rotation angle Greenwich sidereal time $\Theta_{Greenwich}$

$$\mathbf{x_{F\bullet}}(t) = \underline{\mathbf{R}}_3(\Theta_{Greenwich})\,\mathbf{x_{E\bullet}}(t) \tag{2-17}$$

yields a **quasi**-Earth-fixed system or

$$\mathbf{x_{F\bullet}}(t) = \underline{\mathbf{R}}_3(\Theta_{Greenwich})\,\underline{\mathbf{R}}(\text{polar motion})\,\underline{\mathbf{R}}((\text{precession \& nutation})\,\mathbf{x_{E\bullet}}(t), \tag{2-18}$$

an Earth-fixed system. If the position of the satellite is already given in an Earth-fixed reference system like GPS determined position vectors, this step is omitted.

2. Compute gravitational effects using a standard gravitational field model, e.g. the gravitational acceleration vector

$$\mathbf{g_{F\bullet}}(t) = f(\mathbf{x_{F\bullet}}(t), model)\quad. \tag{2-19}$$

3. Transformation of the result back to the space-fixed reference system

$$\mathbf{g_{E\bullet}}(t) = \underline{\mathbf{R}}_3^T(\Theta_{Greenwich})\,\mathbf{g_{F\bullet}}(t) \tag{2-20}$$

or

$$\mathbf{x_{F\bullet}}(t) = \underline{\mathbf{R}}_3^T(\Theta_{Greenwich})\,\underline{\mathbf{R}}^T(\text{polar motion})\,\underline{\mathbf{R}}^T(\text{precession \& nutation})\,\mathbf{x_{E\bullet}}(t) \tag{2-21}$$

respectively.

Chapter 3

Representation of the Earth's gravitational field

3-1 Introductory remarks

The gravitational attraction between two bodies is caused by the masses of the bodies themselves. The force or acceleration, respectively, acting between the gravitating bodies is described by means of Newton's law of gravitation for point masses. Like Newton's equations of motion for point masses, the gravitational law also holds for point masses only (see section 2-2). Since extended bodies can be decomposed into a countable infinite number of point masses adding up to the complete mass of the body, the law of gravitation can be applied to each single point mass of an extended body. Gravitational fields and their effects superimpose in an additive way. The complete gravitational effect between extended bodies can thus be determined by summation, i.e. integration over the contributions of the infinitesimal mass points.
Let one of the masses be a test mass of 1 kg, then, for each position in space within the gravitational field created by a gravitating body or, more generally speaking, mass distribution, a value for the gravitational effects can be given. This field can be described by means of various quantities:

- force of attraction on the test mass, caused by the gravitating mass distribution $[kg\ m\ s^{-2}]$, with direction and absolute value (vector-valued description),

- acceleration on the test mass, caused by the force of attraction mentioned above $[m\ s^{-2}]$, also in direction and absolute value (vector-valued description) and

- the so-called gravitational potential $[m^2\ s^{-2}]$ (scalar-valued description).

While the gravitational force and the acceleration are vector-valued quantities, the gravitational potential gives a scalar-valued description of the effects and strength of the gravitational field. The gravitational potential in a certain point can be defined as the work, that has to be performed against the gravitational field, to move a test mass of 1 kg from the position of the evaluation point to infinity. Thus, the gravitational potential decreases with increasing distance of the evaluation point from the source of the gravitational field. In the same way, the potential difference between two points in space can be defined as the work, that has to be performed to move the test mass mentioned from one point to the other.
The connections between the three gravitational quantities are given by (1) the fundamental equation of mechanics *force vector = mass times acceleration vector*, connecting gravitational force and acceleration vectors, and (2) the gradient operator, linking the gravitational potential and the acceleration vector being the gradient of the potential.
The mathematical description of the gravitational field of the Earth is based on the so-called Laplace-Poisson vectorial differential field equations (3-1). They describe the harmonic field outside the gravitating masses as sources of gravitation (Laplace equation), as well as the anharmonic field within gravitating masses (Poisson equation). The solution of the harmonic part, the Laplace equation, being the part of interest in satellite geodesy, can be found by a separation ansatz. This ansatz starts with an assumed representation of the gravitational potential of the Earth as a product of three separated equations (3-5) each depending on one component of position only. Introducing this assumption into the Laplace equation yields three ordinary differential equations with respect to the components of position (usually spherical co-ordinates), that have to be solved. The solution yields a (surface) spherical harmonics series expansion representation for the Earth's gravitational field (3-6). The base functions of this series expansion, the (surface) spherical harmonics, are based upon trigonometric functions as well as Legendre functions (for the corresponding definitions see annexes A and B). These functions have global support over a reference sphere.
The solution of the separation ansatz is not possible with respect to all sets of co-ordinates, but it is possible for

spherical co-ordinates as well as spheroidal co-ordinates (Ardalan (1996)) and a solution is possible in Cartesian co-ordinates (Moon and Spencer (1961)), too. An overview over the separation of different co-ordinate systems can be found in Moon and Spencer (1961).

---

table 3-1: <u>Earth's gravitational field equations and their solution</u>

Laplace-Poisson gravitational field equations:

$$\text{div grad } U(\mathbf{x}) = \begin{cases} 0 & \textbf{Laplace} \text{ equation} \quad harmonic \\ -4\pi\ g\ \rho(\mathbf{x}) & \textbf{Poisson} \text{ equation} \quad anharmonic \end{cases} \tag{3-1}$$

straight forward solution: Newton's integral over all gravitating masses

$$U(\mathbf{x}(r,\lambda,\phi)) \;=\; G \iiint\limits_{masses} \frac{\rho(\mathbf{x}')}{\parallel \mathbf{x}-\mathbf{x}' \parallel}\ d^3\mathbf{x}' \tag{3-2}$$

$$=\; G \int\limits_{\lambda'=0}^{2\pi} \int\limits_{\phi'=-\pi/2}^{+\pi/2} \int\limits_{r'=0}^{r(\lambda',\phi')} \frac{\rho(\lambda',\phi',r')}{\sqrt{r^2+r'^2-2rr'\cos\psi}}\ dr'\ d\phi'\ d\lambda' \tag{3-3}$$

$$=\; \underbrace{\frac{4\pi\ G}{r} \int\limits_{0}^{r} \rho(r')\ r'^2\ dr'}_{\substack{\text{masses } within \text{ the} \\ \text{spherical shell } r \text{ containing} \\ \text{the evaluation point}}} \;+\; \underbrace{4\pi\ G \int\limits_{r}^{R} \rho(r')\ r'\ dr'}_{\substack{\text{masses } outside \text{ the} \\ \text{spherical shell } r \text{ containing} \\ \text{the evaluation point}}} \tag{3-4}$$

remark: the simplified solution (3-4) of the Newton integral only holds for a **radially symmetric** geometry and density distribution of the gravitating masses.

separation ansatz in spherical co-ordinates $r,\ \lambda,\ \phi$:

$$U(\mathbf{x}(r,\lambda,\phi)) = R(r) \cdot \Lambda(\lambda) \cdot \Phi(\phi) \tag{3-5}$$

solution: (surface) spherical harmonics series expansion of the gravitational potential

$$U(\mathbf{x}(r,\lambda,\phi)) \;=\; \frac{GM}{r} \sum_{n=0}^{\infty} \left(\frac{R_\oplus}{r}\right)^n \sum_{m=0}^{n} (\bar{c}_{n,m}\ \cos(m\lambda) + \bar{s}_{n,m}\ \sin(m\lambda))\ \bar{P}_{n,m}(\sin\phi) \tag{3-6}$$

$$=\; \frac{GM}{R_\oplus} \sum_{n=0}^{\infty} \left(\frac{R_\oplus}{r}\right)^{n+1} \sum_{m=0}^{n} (\bar{c}_{n,m}\ \cos(m\lambda) + \bar{s}_{n,m}\ \sin(m\lambda))\ \bar{P}_{n,m}(\sin\phi) \tag{3-7}$$

with :

λ, ϕ, r	...	spherical co-ordinates of evaluation point $[°,°,m]$,
ψ	...	angle between position vector of evaluation point and of integration point,
GM	...	geocentric gravitational constant $[m^3/s^2]$,
$R_\oplus$	...	mean radius of the Earth (Bjerhammar sphere) $[m]$,
$\bar{P}_{n,m}(\sin\phi)$	...	fully normalized Legendre function of degree n and order m $[-]$ and
$\bar{c}_{n,m}, \bar{s}_{n,m}$	...	series expansion coefficients, gravitational model's coefficients $[-]$.

Detailed information on how to choose the upper summation limit, i.e. the maximum degree & order of the series expansion, can be found in subsection 4-4.1, page 48, of the following chapter.

The (surface) spherical harmonics series expansion provides one possible solution of the gravitational field equations. Another very well-known possibility to describe the gravitational potential mathematically is the so-called Newton integral (3-2) as summation over all infinitesimal mass elements of the body, i.e. the whole mass of the body. For each mass element Newton's law of gravitational attraction of point masses holds. Applying summation, i.e. integration in the case of infinitesimal small mass elements, the gravitational effect of the whole

body can be determined. Since the computability of the Newton integral depends on a variety of different simplifying assumptions and absolutely requires some knowledge on the density distribution in the Earth's interior, it is not relevant in satellite geodesy and thus only mentioned for completeness. But besides from choosing a completely different method to solve the field equations, it is also possible to turn to a different set of base functions. This aims at the very heart of the current discussion on the representation of the gravitational field.

3-1.1   Current discussion and the requirements for satellite geodesy

within the already mentioned The physical structure of the Earth's gravitational field is that of a field, that is mainly governed by the effects caused by a reference body modelling the Earth. That means, that the major part of the gravitational effects within the Earth's field is caused by a spherical model Earth. The field structure of this main part is that of a central field with spherical equipotential surfaces and straight radial field (plumb-) lines. The share of the central field in the total gravitational field is about 95% (a quantitative estimation is possible by means of the degree variances; the percentage value can be computed as quotient of the degree variance of degree and order 0 and the degree variances of the complete model, usually degree and order 360). In the (surface) spherical harmonics series expansions the term of degree 0 denotes this central field part. The second largest part is caused by oblation effects, modelled by the $\bar{c}_{2,0}$ coefficient of the series expansion. Features of short wavelengths make up a very small part of the Earth's total gravitational field, but contain the information on details in its structure, i.e. the very important information on the inhomogeneities. Having global support, the (surface) spherical harmonics provide a sort of endless periodic oscillation over their reference sphere. Thus they exactly depict the frequencies contained in the gravitational field of the Earth. What is not at all represented, is the location of certain detailed perturbations or inhomogeneities, respectively. I.e. that the source of a certain perturbation, causing a defined detail in the structure of the field, cannot be located. This effect is due to an uncertainty principle (Freeden (1999)). According to this principle, the product of localisation in the spatial domain and frequency localisation is bounded from below by a constant. Advantages on either side can only be achieved by a deterioration of the other. Thus, having high frequency localisation, the (surface) spherical harmonics have poor localisation in the spatial domain. This attribute is presented in the left side of figure 3-1. This property is uncritical as long as only global features, like the long- and medium-wavelength features, of the Earth's gravitational field are to be described. As soon as detailed information on inhomogeneities is to be represented, the position of a certain perturbation is also of interest. The best space localisation is provided by the Dirac pulse, illustrated in the right part of figure 3-1. It can be clearly seen, that the function $\sin(x/\epsilon) / (\pi x)$ approximating the Dirac pulse for $\epsilon \to 0$ provides decreasing frequency localisation with increasing space localisation (top down).
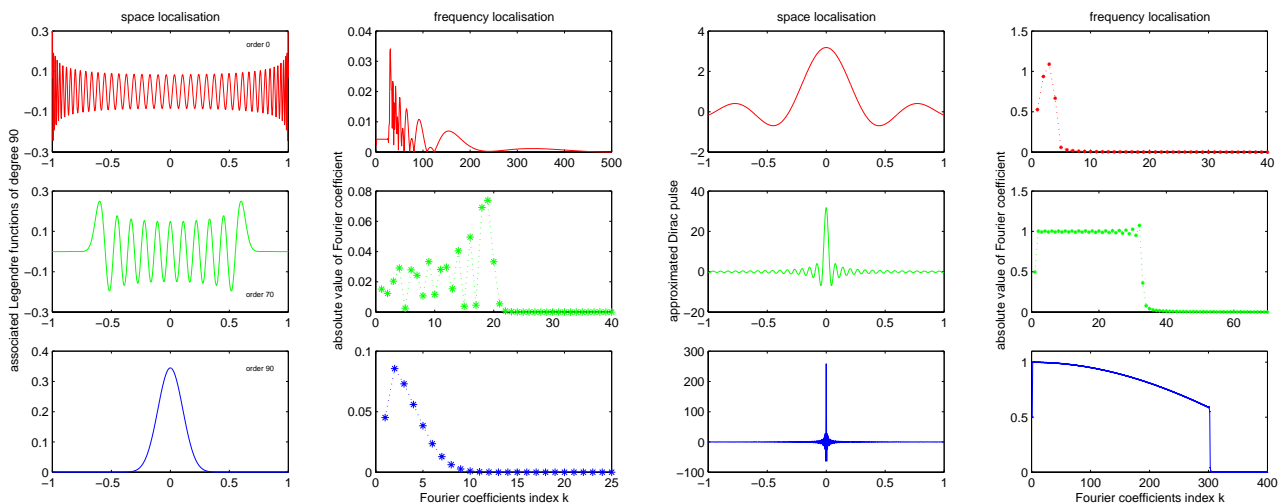
figure 3-1: Space and frequency localisation of normalized associated Legendre functions (*left*) and an approximated Dirac pulse (*right*)

A good example to show the differences between localisation in the spatial domain and frequency localisation is to have a look at what happens if new data is introduced to improve an existing gravitational field model. Let the Earth's gravitational field be modelled by means of a (surface) spherical harmonics series expansion and by means of some space localising only model (for a detailed example, the so-called wavelets, see next paragraph). The first has global support with high frequency localisation but poor localisation in the spatial domain, the latter local support with high localisation in the spatial domain but poor frequency localisation. Let the new data to be introduced be a local density anomaly. For the (surface) spherical harmonics model this

new information requires that the complete model is computed once again. In general, a lot of the coefficients will change. From the re-determined model the position, at which this anomaly caused the perturbation of the field, will not be recoverable. The frequency of this perturbation however will be clearly visible in the frequency spectrum of the gravitational field. For the space localising only model the introduction of the new data only requires a change in the existing model at the very position the anomaly is located. Vice versa the position of the anomaly will be detectable from the model again.

A set of base functions having high localisation in the spatial domain brought into discussion recently are wavelets. In contrast to (surface) spherical harmonics, wavelets provide a very high localisation in the spatial domain. Thus they are well suited to model details, but, following the uncertainty principle, the frequency location will be rather poor.

For the application in geodesy with special focus on satellite geodesy the current discussion tries to find a suitable course to pursue to find the best model. Whereas the (surface) spherical harmonics are the classical approach and the fundamental literature is well known, wavelets and their application in geodesy are a rather recent topic. Especially the works of the geomathematics group at the university of Kaiserslautern deal with the application of wavelets in geodesy. Bayer et al. (1998), Freeden (1999) and Freeden et al. (1995), (1997) and (1998) provide details on that method.

To decide on one of the possibilities of mathematical modelling of the Earth's gravitational field, a closer look has to be taken at today's data situation as well as the requirements of satellite geodesy in the case of this thesis. The requirements a mathematical model has to fulfil mainly depend on the data that is available for the setting up of an Earth gravitational field model. Recently, the sets of available gravitational field data have changed considerably or are due to change in the near future. Especially quality, reliability, coverage and resolution of the data have been improved. Until today, mainly terrestrial data has been available in the 'rich' countries, that could afford extensive measurement campaigns. The coverage was dominated by large gaps, e.g. poorer countries, but also in areas where terrestrial measurements were difficult or impossible to perform, like oceans and polar regions. The main bulk of globaly available gravitational data was satellite data. It's coverage also showed lots of gaps, caused by the orbits of the satellites itself, e.g. polar gaps due to small inclinations, and the fact that observation and tracking methods have been ground-based so far (e.g. SLR). All this yields a rather coarse resolution of the gravitational field (degree and order 360 of a (surface) spherical harmonics series expansion stands for a resolution of 100 km at the equator). In addition, satellites only 'see' the long wavelength parts of the gravitational field's spectrum. I.e. they are mainly influenced by the smooth global features in the field, an effect, that is increased by the damping of the field's finer structures with growing distance from the sources, i.e. growing height of flight. Thus this data yields a very smooth representation of the field up to degree and order 60-80. More detailed field representations are not necessary, since in the past, the available data did not contain any detailed information on the gravitational field, except for the few areas with terrestrial data available. For these areas regional or even local models could be applied.

Today, the situation changed and is still considerably changing. More dense terrestrial data and new satellite missions, especially LEO missions, provide a more detailed insight into the structure of the gravitational field of the Earth. Even local and regional details can be detected now more or less globaly. In consequence, models are needed that are capable of representing these details. Base functions with local support, like wavelets coming up on the field of gravitation models, provide a thorough means to represent these details. Despite the considerable increase in detailed information on the Earth's gravitational field, it is a fact that there are mostly long wavelength features making up the whole field. These can be excellently represented by models based on global base functions. Especially for satellites orbiting the Earth in a certain height above the surface, local details are smoothed away to some extent. Thus, depending on its height, a satellite will mainly 'see' long wavelength features. The consequence is, that models like (surface) spherical harmonics series expansions provide a suitable means for representing the gravitational field in satellite geodesy. This statement may not hold for the upcoming LEO missions and will definitely not hold for all geodetic observation campaigns performed on the surface of the Earth. There, local and regional details will well be 'seen' and their effects have to be dealt with. But again the main part of the gravitational field will be dominated by the long wavelength features. Due to that, models based on locally supported base functions only do not seem to be the ideal solution. The same is true for models of solely global support. The best way to set up a model of the gravitational field for these purposes will be, what has been proposed recently: a combination of a part of the model being based on globaly supported base functions and for the details a part being based on locally supported ones (Freeden and Windheuser (1997)). The globaly supported part, e.g. a spherical harmonics series expansion up to degree and order 360, will be augmented by the locally supported part, e.g. using the wavelet method, in and only in the areas where more detailed information on the field is available. In the first place this will be the continents, where terrestrial gravity measurements are performed, but may in the future also be areas, that are covered by a LEO satellite. These models are not yet available and, in addition, would not be improved in their locally supported part by means of existing satellite missions.

This thesis will restrict itself to the available models for the gravitational field of the Earth, since the aim of the examined LEO satellite mission CHAMP, that will serve as an example, is mainly to improve these existing

models. The only existing models at the moment are models based on (surface) spherical harmonics series expansions. The (surface) spherical harmonics, definitions see annex B, have global support. Mere wavelet models until now have only been computed using existing (surface) spherical harmonics models like EGM96 or, before that, OSU91A. Thus they cannot contain any further local or regional details of the field's structure yet. There are also no combination models existing so far, as already has been stated.

In this and in the following chapter the description of the Earth's gravitational field based on two sets of base functions will be presented: (Surface) spherical harmonics and Fourier base functions. The Fourier representation will be derived based on the standard (surface) spherical harmonics representation and will then further be applied for the sensitivity analysis method (see overview in figure 1-1).

As far as not stated differently all used co-ordinates will be given with respect to a geocentric Earth-fixed equatorial reference system.

---

table 3-2: Transformation from spherical to Cartesian co-ordinates

Spherical → Cartesian:

$$\begin{pmatrix} x \\ y \\ z \end{pmatrix} = r \begin{pmatrix} \cos\phi \ \cos\lambda \\ \cos\phi \ \sin\lambda \\ \sin\phi \end{pmatrix} \tag{3-8}$$

$$r = \sqrt{x^2 + y^2 + z^2} \tag{3-9}$$

$$\begin{aligned} \sin\phi &= \frac{z}{\sqrt{x^2 + y^2 + z^2}} & \cos\phi &= (1 - \frac{z^2}{x^2 + y^2 + z^2})^{1/2} \\ \sin\lambda &= \frac{y}{\sqrt{x^2 + y^2}} & \cos\lambda &= \frac{x}{\sqrt{x^2 + y^2}} \end{aligned} \tag{3-10}$$

Inversion of Moivre's formulae:

$$\cos(m\lambda) = \cos^{-m}\phi \sum_{i=0}^{[m/2]} (-1)^i \begin{pmatrix} m \\ 2i \end{pmatrix} \left(\frac{x}{r}\right)^{m-2i} \left(\frac{y}{r}\right)^{2i} \tag{3-11}$$

$$\sin(m\lambda) = \cos^{-m}\phi \sum_{i=0}^{[(m-1)/2]} (-1)^i \begin{pmatrix} m \\ 2i+1 \end{pmatrix} \left(\frac{x}{r}\right)^{m-(2i+1)} \left(\frac{y}{r}\right)^{2i+1} \tag{3-12}$$

with the upper summation bounds $[m/2]$ and $[(m-1)/2]$ being the largest integers equal to or less than $m/2$ and $(m-1)/2$ respectively (the same result has been derived independently in Grafarend et al. (1998)).

Fully normalized Legendre functions according to their definition in annex A:

$$\bar{P}_{n,m}(\sin\phi) = \bar{n}_{n,m} \ \cos^m\phi \sum_{k=0}^{[(n-m)/2]} b_{n,m,k} \left(\frac{z}{r}\right)^{n-m-2k} \quad , \tag{3-13}$$

with the upper summation bound $[(n-m)/2]$ being the integer $(n-m)/2$ or $(n-m-1)/2$ respectively, too.

Surface spherical harmonics according to their definition in annex B:

$e_{n,m}(\lambda, \phi) =$

$$\begin{cases} \bar{n}_{n,m} \sum_{i=0}^{[\frac{m}{2}]} \sum_{k=0}^{[\frac{(n-m)}{2}]} (-1)^i \ b_{n,m,k} \begin{pmatrix} m \\ 2i \end{pmatrix} \left(\frac{x}{r}\right)^{m-2i} \left(\frac{y}{r}\right)^{2i} \left(\frac{z}{r}\right)^{n-m-2k} & (m \geq 0) \\[4ex] \bar{n}_{n,|m|} \sum_{i=0}^{[\frac{|(m-1)|}{2}]} \sum_{k=0}^{[\frac{n-|m|}{2}]} (-1)^i \ b_{n,|m|,k} \begin{pmatrix} |\,m\,| \\ 2i+1 \end{pmatrix} \left(\frac{x}{r}\right)^{|m|-(2i+1)} \left(\frac{y}{r}\right)^{2i+1} \left(\frac{z}{r}\right)^{n-|m|-2k} & (m < 0) \end{cases}$$

$$\tag{3-14}$$

with upper summation bounds as above.

3-1.2 Cartesian versus spherical representation of gravitational field values

It has been shown in the previous subsection, that the representation providing a description being closest to the real gravitational field of the Earth comes from the separation ansatz. Since the gravitational field is inhomogeneous, caused by an inhomogeneous surface and interior of the Earth, this solution will naturally yield some series expansion representation. The well known (surface) spherical harmonics series expansion is based on functions that are primarily defined on the surface of a unit sphere (see the definitions of the (surface) spherical harmonics in annex B). The natural choice for an appropriate set of co-ordinates for this description leads to geocentric Earth-fixed spherical co-ordinates longitude $0 \leq \lambda \leq 2\pi$, latitude $-\pi/2 \leq \phi \leq +\pi/2$ or polar distance $0 \leq \theta \leq \pi$ and radius r, the geocentric distance. The co-ordinates are chosen to be Earth-fixed since the gravitational field, caused by the masses of the Earth, will rotate together with the body.
In the following sections the representation of the gravitational field values is given using geocentric Earth-fixed spherical co-ordinates, but also geocentric Cartesian Earth-fixed co-ordinates x, y, z. The reason for that is to be found in the description of the satellites' orbits. In section 2-2 it has been shown, why it is useful to apply Cartesian co-ordinates to represent a satellite's orbit:

- to avoid singularities that may arise if using classical Kepler elements,

- to take advantage of directly using Cartesian co-ordinates that are provided by the upcoming GPS-tracked satellite missions.

It has to be pointed out, that the Cartesian representation presented in this thesis differs considerably from what is understood by this term in literature. Cartesian representations of the gravitational field, as they are presented e.g. in Kleusberg (1983), annex A2, Jarosch (1984) or before that for the directional derivatives of the potential in Hotine (1969), are based on a set of completely new, or better, different Cartesian base functions. The aim of this thesis is to perform an orbit sensitivity analysis for the purpose of determining these (surface) spherical harmonics coefficients which can be expected to be determined more accurately from a certain mission. Thus it will always refer to existing gravitational field models like EGM96 (table 3-4) or others. These models are all based on the (surface) spherical harmonics solution of the separation ansatz (3-6). Due to that, the Cartesian representation of the gravitational field given in this thesis is a transformation of the existing (surface) spherical harmonics series expansion from spherical to Cartesian co-ordinates. Using newly defined Cartesian base functions for the series would lead to expansion coefficients that also differ from the definition of the coefficients in the existing models. Although a connection between the 'spherical coefficients' and the 'Cartesian coefficients' may be found, the transformation approach is more appropriate.

3-2 Description of the gravitational potential

Representing the Earth by a model ellipsoid of revolution with semimajor axis $R_\oplus$ and geocentric gravitational constant GM, the gravitational field in the exterior of this Earth model can be described by the well-known (surface) spherical harmonics series expansion (3-6) in spherical co-ordinates with respect to an Earth fixed geocentric Cartesian equatorial reference system. Using geocentric spherical co-ordinates, this representation is the basis for current gravitational field models like OSU91A and more recently EGM96 which are presented in tables 3-3 and 3-4. Using the relations (3-8) - (3-13) the series expansion of the gravitational potential can be transformed from spherical co-ordinates r, ϕ, λ to Cartesian co-ordinates x, y, z with respect to an Earth-fixed geocentric Cartesian equatorial reference system.

$$U(x,y,z) \;=\; GM \sum_{n=0}^{\infty} R_\oplus^n \sum_{m=0}^{n} \bar{n}_{n,m} \sum_{k=0}^{[(n-m)/2]} b_{n,m,k}\, z^{n-m-2k}\, (x^2+y^2+z^2)^{k-n-1/2} \tag{3-15}$$

$$\cdot \left[\bar{c}_{n,m} \sum_{i=0}^{[m/2]} (-1)^i \begin{pmatrix} m \\ 2i \end{pmatrix} x^{m-2i}\, y^{2i} + \bar{s}_{n,m} \sum_{i=0}^{[(m-1)/2]} (-1)^i \begin{pmatrix} m \\ 2i+1 \end{pmatrix} x^{m-2i-1}\, y^{2i+1} \right]$$

Brackets $[(n-m)/2]$, $[m/2]$ and $[(m-1)/2]$ denote the largest integer being equal to or less than $(n-m)/2$, $m/2$ and $(m-1)/2$, respectively.

table 3-3: Earth's gravitational model OSU91A
(Rapp et al. (1991))

$$U(r, \phi, \lambda) = \frac{GM}{r} \left[1 + \sum_{n=2}^{360} \left(\frac{a}{r}\right)^n \sum_{m=0}^{n} (\bar{c}_{n,m} \ \cos(m\lambda) + \bar{s}_{n,m} \ \sin(m\lambda)) \ \bar{P}_{n,m}(\sin \phi) \right] \qquad (3\text{-}16)$$

with:

geocentric gravitational constant $GM = 3986004.415 \ 10^8 \ m^3 \ s^{-2}$
semimajor axis of the model Earth $a = 6378137.000 \ m$

r, ϕ, λ ...   spherical co-ordinates geocentric distance, latitude and longitude of the evaluation point,

$\bar{P}_{n,m}$ ...   fully-normalised Legendre functions (see annex A)

$$\bar{P}_{n,m}(\sin \phi) = P_{n,m}(\sin \phi) \begin{cases} (2 \ n + 1)^{1/2} & (m = 0) \\[2mm] [\ 2 \ (2 \ n + 1) \ \dfrac{(n-m)!}{(n+m)!} \ ]^{1/2} & (m \neq 0) \end{cases}$$

$P_{n,m}$ ...   Legendre functions (see annex A)

$$P_{n,m}(t) = \frac{1}{2^n \ n!} \ (1 - t^2)^{m/2} \ \frac{d^{n+m}}{dt^{n+m}} \ (t^2 - 1)^n \quad (\ |t| = |\sin \phi| \leq 1 \ , \ 0 \leq |m| \leq n \ ) \ ,$$

$\bar{c}_{n,m}, \bar{s}_{n,m}$ ...   fully-normalised unit-free spherical harmonic coefficients.
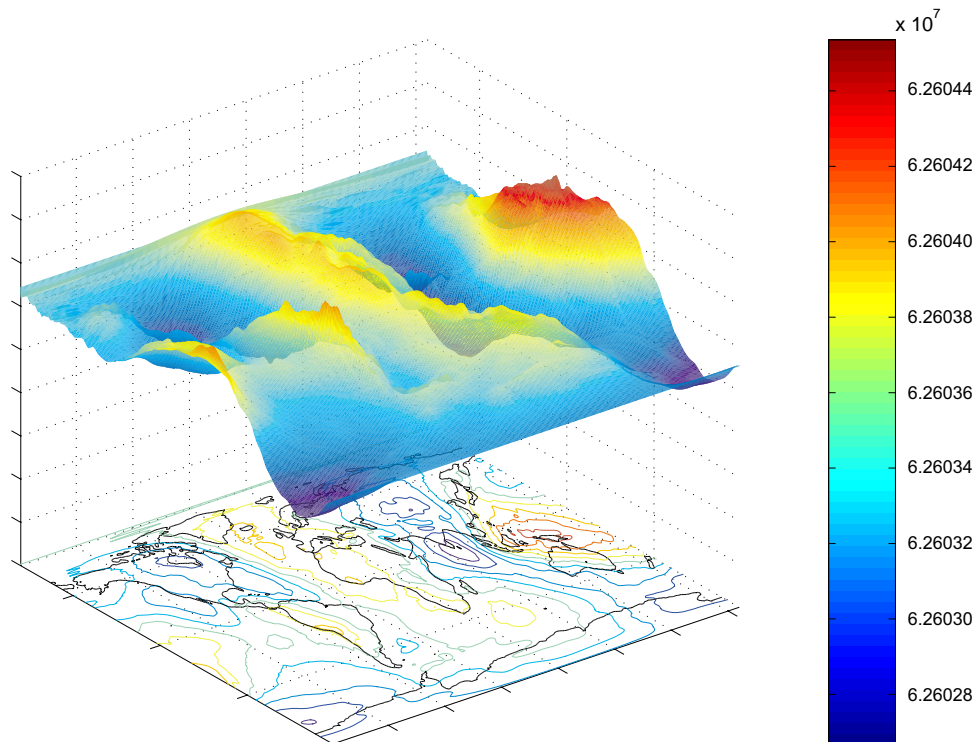
figure 3-2: Gravitational potential up to degree & order 75 from the OSU91A model without $\bar{c}_{2,0}$ part
(omitted for better readability) on the surface of a reference Earth with $r = 6371 \ km$
(see figure 3-4 for the differences between OSU91A and EGM96 (table 3-4))

table 3-4: Earth's gravitational model EGM96
(Lemoine et al. (1998))

$$U(r, \theta, \lambda) = \frac{GM}{r} \left[1 + \sum_{n=2}^{360} \left(\frac{a}{r}\right)^n \sum_{m=-n}^{n} c_{n,m} \, Y_{n,m}(\theta, \lambda) \right] \tag{3-17}$$

with:

geocentric gravitational constant $GM = 3986004.415 \; 10^8 \; \dfrac{m^3}{s^2}$
semimajor axis of the modell Earth $a = 6378136.3 \; m$

r, θ, λ ... spherical co-ordinates geocentric distance, polar distance and longitude of the evaluation point,

$Y_{n,m}$ ... surface spherical harmonics (see annex B)

$$Y_n^m(\lambda, \phi) = \left\{ \begin{array}{c} \cos(m\lambda) \\ \sin(m\lambda) \end{array} \right\} P_{n,m}(\sin \phi) \;,$$

$P_{n,m}$ ... Legendre functions (see annex A)

$$P_{n,m}(t) = \frac{1}{2^n \, n!} \, (1 - t^2)^{m/2} \, \frac{d^{n+m}}{dt^{n+m}} \, (t^2 - 1)^n \quad (\; |t| = |\sin \phi| \leq 1 \;,\; 0 \leq |m| \leq n \;) \;,$$

$c_{n,m}$ ... unit-free spherical harmonic coefficients.

web address: *http://cddisa.gsfc.nasa.gov/926/egm96/egm96.html*

This is the official EGM96 website by the **G**oddard **S**pace **F**light **C**enter, the **N**ational **I**magery and **M**apping **A**gency and the Ohio State University (address valid at September 22, 2000). The data of the model as well as additional information on how the coefficients were determined can be found there.
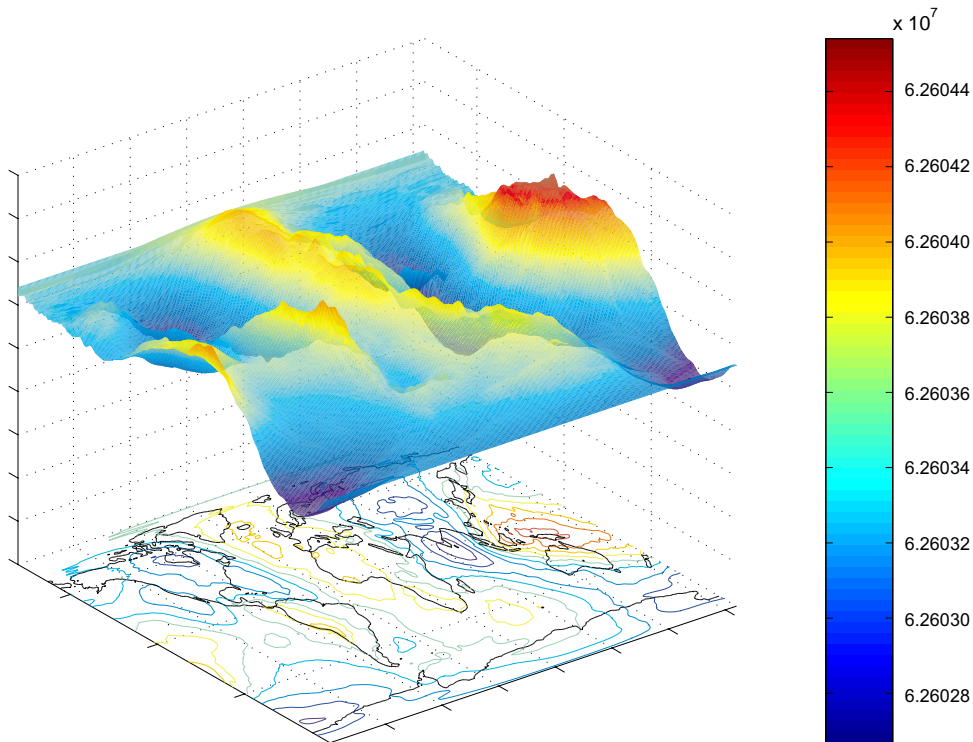
figure 3-3: Gravitational potential up to degree & order 75 from the EGM96 model without $\bar{c}_{2,0}$ part (omitted for better readability) on the surface of a reference Earth with $r = 6371 \; km$
(see figure 3-4 for the differences between OSU91A (table 3-3) and EGM96)
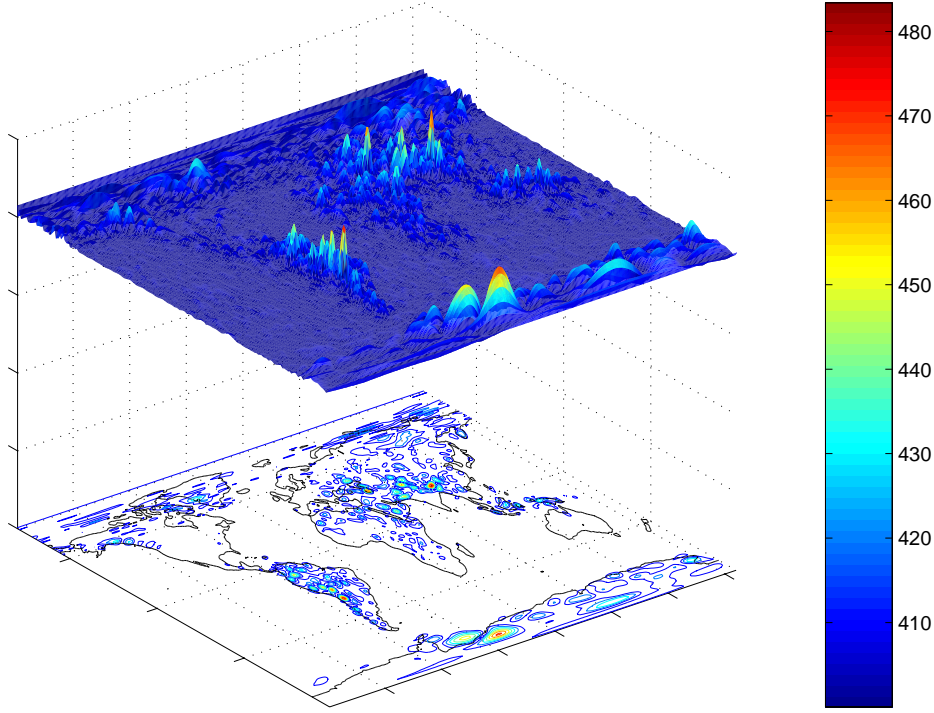
figure 3-4: Absolute values of the differences of the gravitational potential up to degree & order 75 computed from the EGM96 and the OSU91A model without $\bar{c}_{2,0}$ part (omitted for better readability) on the surface of a reference Earth with $r = 6371\ km$

(see tables 3-4 and 3-3 for the descriptions of the models)

3-3   The gradient operator and the computation of the gravitational vector field

The gravitational vector field is computed by means of the gradient operator applied to the gravitational potential. In spherical co-ordinates (3-18) and in Cartesian co-ordinates (3-19) respectively the gradient operator is defined as the first order derivative of a scalar field in direction of the main change of the scalar field value.

---

table 3-5: Gradient operator in **_spherical_** and **_Cartesian_** co-ordinates

$$\mathbf{g}(\lambda, \phi, r) = grad\ U(\lambda, \phi, r) = \frac{\partial U}{\partial r}\ \mathbf{e}_r + \frac{1}{r}\ \frac{\partial U}{\partial \phi}\ \mathbf{e}_\phi + \frac{1}{r\ \cos\phi}\ \frac{\partial U}{\partial \lambda}\ \mathbf{e}_\lambda \qquad (3\text{-}18)$$

$$\mathbf{g}(x, y, z) = grad\ U(x, y, z) = \frac{\partial U}{\partial x}\ \mathbf{e}_x + \frac{\partial U}{\partial y}\ \mathbf{e}_y + \frac{\partial U}{\partial z}\ \mathbf{e}_z \qquad (3\text{-}19)$$

For its computation the first-order partial derivatives of the gravitational potential with respect to the co-ordinates are needed.

$$\frac{\partial U}{\partial \lambda} = \frac{GM}{r} \sum_{n=0}^{\infty} \left(\frac{R_\oplus}{r}\right)^n \sum_{m=0}^{n} m\ (-\bar{c}_{n,m}\ \sin(m\lambda) + \bar{s}_{n,m}\ \cos(m\lambda))\ \bar{P}_{n,m}(\sin\phi) \qquad (3\text{-}20)$$

$$\frac{\partial U}{\partial \phi} = \frac{GM}{r} \sum_{n=0}^{\infty} \left(\frac{R_\oplus}{r}\right)^n \sum_{m=0}^{n} (\bar{c}_{n,m}\ \cos(m\lambda) + \bar{s}_{n,m}\ \sin(m\lambda))\ \frac{\partial \bar{P}_{n,m}(\sin\phi)}{\partial \phi} \qquad (3\text{-}21)$$

$$\frac{\partial U}{\partial r} = -\frac{GM}{r^2} \sum_{n=0}^{\infty} (n+1) \left(\frac{R_\oplus}{r}\right)^n \sum_{m=0}^{n} (\bar{c}_{n,m}\ \cos(m\lambda) + \bar{s}_{n,m}\ \sin(m\lambda))\ \bar{P}_{n,m}(\sin\phi) \qquad (3\text{-}22)$$

Thus applying the gradient operator in its appropriate form to the gravitational potential (3-6) and (3-15) yields the gravitational acceleration vector in spherical (3-30) and Cartesian co-ordinates (3-35) respectively with respect to an Earth-fixed geocentric Cartesian equatorial reference frame.

$$
\mathbf{g}(\lambda, \phi, r) = \frac{GM}{r^2} \sum_{n=0}^{\infty} \left(\frac{R_\oplus}{r}\right)^n \sum_{m=0}^{n} [\ (\bar{c}_{n,m} \ \cos(m\lambda) + \bar{s}_{n,m} \ \sin(m\lambda)) \tag{3-23}
$$

$$
(-(n+1)\ \bar{P}_{n,m}(\sin\phi)\ \mathbf{e}_r + \frac{\partial \bar{P}_{n,m}(\sin\phi)}{\partial\phi}\ \mathbf{e}_\phi)
$$

$$
+ \frac{1}{\cos\phi}\ (-\bar{c}_{n,m}\ \sin(m\lambda) + \bar{s}_{n,m}\ \cos(m\lambda))\ \bar{P}_{n,m}(\sin\phi)\ \mathbf{e}_\lambda]
$$

Using the definitions (B-5), (B-7) and (B-8) of the vector-valued spherical harmonics the gravitational vector can also be expressed as in (3-32).

$$
\frac{\partial U}{\partial x} = GM \sum_{n=0}^{\infty} R_\oplus^n \sum_{m=0}^{n} \bar{n}_{n,m} \sum_{k=0}^{[(n-m)/2]} b_{n,m,k}\ z^{n-m-2k}\ r^{2k-2n-1}
$$

$$
\left[\bar{c}_{n,m} \sum_{i=0}^{[m/2]} (-1)^i \binom{m}{2i} y^{2i} \left((m-2i)\ x^{m-2i-1} + (2k-2n-1)\ x^{m-2i+1}\ r^{-2}\right) \right. \tag{3-24}
$$

$$
\left. + \bar{s}_{n,m} \sum_{i=0}^{[(m-1)/2]} (-1)^i \binom{m}{2i+1} y^{2i+1} \left((m-2i-1)\ x^{m-2i-2} + (2k-2n-1)\ x^{m-2i}\ r^{-2}\right) \right]
$$

$$
\frac{\partial U}{\partial y} = GM \sum_{n=0}^{\infty} R_\oplus^n \sum_{m=0}^{n} \bar{n}_{n,m} \sum_{k=0}^{[(n-m)/2]} b_{n,m,k}\ z^{n-m-2k}\ r^{2k-2n-1}
$$

$$
\left[\bar{c}_{n,m} \sum_{i=0}^{[m/2]} (-1)^i \binom{m}{2i} x^{m-2i} \left(2i\ y^{2i-1} + (2k-2n-1)\ y^{2i+1}\ r^{-2}\right) \right. \tag{3-25}
$$

$$
\left. + \bar{s}_{n,m} \sum_{i=0}^{[(m-1)/2]} (-1)^i \binom{m}{2i+1} x^{m-2i-1} \left((2i+1)\ y^{2i} + (2k-2n-1)\ y^{2i+2}\ r^{-2}\right) \right]
$$

$$
\frac{\partial U}{\partial z} = GM \sum_{n=0}^{\infty} R_\oplus^n \sum_{m=0}^{n} \bar{n}_{n,m} \sum_{k=0}^{[(n-m)/2]} \left[(n-m-2k) + (2k-2n-1)\ z^2 r^{-2}\right] b_{n,m,k}\ z^{n-m-2k-1}\ r^{2k-2n-1}
$$

$$
\left[\bar{c}_{n,m} \sum_{i=0}^{[m/2]} (-1)^i \binom{m}{2i} x^{m-2i}\ y^{2i} + \bar{s}_{n,m} \sum_{i=0}^{[(m-1)/2]} (-1)^i \binom{m}{2i+1} x^{m-2i-1}\ y^{2i+1} \right] \tag{3-26}
$$

The gradient operator in Cartesian co-ordinates yields with the geocentric distance $r = \sqrt{x^2 + y^2 + z^2}$

$$
\mathbf{g}(x,y,z) = GM \sum_{n=0}^{\infty} R^n \sum_{m=0}^{n} \bar{n}_{n,m} \sum_{k=0}^{[(n-m)/2]} b_{n,m,k}\ z^{n-m-2k}\ r^{2k-2n-1} \tag{3-27}
$$

$$
[\bar{c}_{n,m} \sum_{i=0}^{[m/2]} (-1)^i \binom{m}{2i}
$$

$$
\{ y^{2i} \left((m-2i)\ x^{m-2i-1} + (2k-2n-1)\ x^{m-2i+1}\ r^{-2}\right)\ \mathbf{e}_x
$$

$$
+ x^{m-2i} \left(2i\ y^{2i-1} + (2k-2n-1)\ y^{2i+1}\ r^{-2}\right)\ \mathbf{e}_y
$$

$$
+ x^{m-2i}\ y^{2i}\ z^{-1} \left[(n-m-2k) + (2k-2n-1)\ z^2\ r^{-2}\right]\ \mathbf{e}_z \}
$$

$$
+ \bar{s}_{n,m} \sum_{i=0}^{[(m-1)/2]} (-1)^i \binom{m}{2i+1}
$$

$$
\{ y^{2i+1} \left((m-2i-1)\ x^{m-2i-2} + (2k-2n-1)\ x^{m-2i}\ r^{-2}\right)\ \mathbf{e}_x
$$

$$
+ x^{m-2i-1} \left((2i+1)\ y^{2i} + (2k-2n-1)\ y^{2i+2}\ r^{-2}\right)\ \mathbf{e}_y
$$

$$
+ x^{m-2i-1}\ y^{2i+1}\ z^{-1} \left[(n-m-2k) + (2k-2n-1)\ z^2\ r^{-2}\right]\ \mathbf{e}_z \}]\quad .
$$

table 3-6: Spherical harmonics series expansion in *spherical* co-ordinates

gravitational potential $[m^2/s^2]$:

$$U(\lambda, \phi, r) = \frac{GM}{r} \sum_{n=0}^{\infty} \left(\frac{R_\oplus}{r}\right)^n \sum_{m=0}^{n} (\ \bar{c}_{n,m}\ \cos(m\lambda) + \bar{s}_{n,m}\ \sin(m\lambda)\ ) \ \bar{P}_{n,m}(\sin\phi) \quad (3\text{-}28)$$

$$= \frac{GM}{R_\oplus} \sum_{n=0}^{\infty} \left(\frac{R_\oplus}{r}\right)^{n+1} \sum_{m=-n}^{+n} \left\{ \begin{array}{c} \bar{c}_{n,m} \\ \bar{s}_{n,|m|} \end{array} \right\} e_{n,m}(\lambda, \phi) \quad (3\text{-}29)$$

gravitational acceleration vector $[m/s^2]$:

$$\mathbf{g}(\lambda, \phi, r) = \frac{GM}{r^2} \sum_{n=0}^{\infty} \left(\frac{R_\oplus}{r}\right)^n \sum_{m=0}^{n} [\ (\ \bar{c}_{n,m}\ \cos(m\lambda) + \bar{s}_{n,m}\ \sin(m\lambda)\ ) \quad (3\text{-}30)$$

$$(-(n+1)\ \bar{P}_{n,m}(\sin\phi)\ \mathbf{e}_r + \frac{\partial \bar{P}_{n,m}(\sin\phi)}{\partial\phi}\ \mathbf{e}_\phi)$$

$$+ \frac{m}{\cos\phi}\ (-\bar{c}_{n,m}\ \sin(m\lambda) + \bar{s}_{n,m}\ \cos(m\lambda))\ \bar{P}_{n,m}(\sin\phi)\ \mathbf{e}_\lambda\ ]$$

$$= \frac{GM}{r^2} \sum_{n=0}^{\infty} \left(\frac{R_\oplus}{r}\right)^n \sum_{m=-n}^{+n} \left\{ \begin{array}{c} \bar{c}_{n,m} \\ \bar{s}_{n,|m|} \end{array} \right\} [\ -(n+1)\ e_{n,m}(\lambda, \phi)\ \mathbf{e}_r \quad (3\text{-}31)$$

$$+ \frac{\partial e_{n,m}(\lambda, \phi)}{\partial\phi}\ \mathbf{e}_\phi + \frac{1}{\cos\phi}\ \frac{\partial e_{n,m}(\lambda, \phi)}{\partial\lambda}\ \mathbf{e}_\lambda\ ]$$

$$= \frac{GM}{R_\oplus^2} \sum_{n=0}^{\infty} \left(\frac{R_\oplus}{r}\right)^{n+2} \sum_{m=-n}^{+n} \left\{ \begin{array}{c} \bar{c}_{n,m} \\ \bar{s}_{n,|m|} \end{array} \right\} [\ -(n+1)\ \mathbf{R}_{n,m}(\lambda, \phi) \quad (3\text{-}32)$$

$$+ \sqrt{n(n+1)}\ \mathbf{S}_{n,m}(\lambda, \phi)\ ]$$

gravitational force vector $[kg\ m/s^2]$:

$$\mathbf{F}(\lambda, \phi, r) = m_{Sat.}\ \mathbf{g}(\lambda, \phi, r) \quad (3\text{-}33)$$

with :

λ, ϕ, r ...   spherical co-ordinates of evaluation point $[°,°\,, m]$,

GM ...   geocentric gravitational constant $[m^3/s^2]$,

$R_\oplus$ ...   mean radius of the Earth (Bjerhammar sphere) $[m]$,

$\bar{P}_{n,m}(\sin\phi)$ ...   fully normalized Legendre function of degree n and order m $[-]$,

$e_{n,m}(\lambda, \phi)$ ...   scalar-valued spherical surface harmonics (definition see annex B)

$$e_{n,m}(\lambda, \phi) = \left\{ \begin{array}{c} \cos m\lambda \\ \sin |\,m\,|\,\lambda \end{array} \right\} \bar{P}_{n,|m|}(\sin\phi) \qquad \left\{ \begin{array}{l} \text{for } m \geq 0 \\ \text{for } m < 0 \end{array} \right.,$$

$\mathbf{R}_{n,m}(\lambda, \phi)$ ...   radial vector-valued spherical surface harmonics (definition see annex B)

$$\mathbf{R}_{n,m}(\lambda, \phi) = e_{n,m}(\lambda, \phi)\ \mathbf{e}_r\ ,$$

$\mathbf{S}_{n,m}(\lambda, \phi)$ ...   sectorial vector-valued spherical surface harmonics (definition see annex B)

$$\mathbf{S}_{n,m}(\lambda, \phi) = \frac{1}{\sqrt{n(n+1)}} \left(\frac{1}{\cos\phi}\ \frac{\partial}{\partial\lambda} e_{n,m}(\lambda, \phi)\ \mathbf{e}_\lambda + \frac{\partial}{\partial\phi} e_{n,m}(\lambda, \phi)\ \mathbf{e}_\phi \right) \text{ and}$$

$\bar{c}_{n,m}, \bar{s}_{n,m}$ ...   series expansion coefficients, gravitational model's coefficients $[-]$.

table 3-7: Spherical harmonics series expansion in *Cartesian* co-ordinates

general remark: The Cartesian representation of the gravitational potential of the Earth presented here is achieved by transformation of the classical spherical harmonics representation in spherical co-ordinates to Cartesian co-ordinates. The base functions remain the same as do the series coefficients. For details refer to subsection 3-1.2, page 31

gravitational potential $\left[m^2/s^2\right]$:

$$
U(x,y,z) = GM \sum_{n=0}^{\infty} R_{\oplus}^n \sum_{m=0}^{n} \bar{n}_{n,m} \sum_{k=0}^{[(n-m)/2]} b_{n,m,k}\, z^{n-m-2k}\, r^{2k-2n-1}
$$

$$
\left[\bar{c}_{n,m} \sum_{i=0}^{[m/2]} (-1)^i \begin{pmatrix} m \\ 2i \end{pmatrix} x^{m-2i}\, y^{2i} \right. \tag{3-34}
$$

$$
\left. + \bar{s}_{n,m} \sum_{i=0}^{[(m-1)/2]} (-1)^i \begin{pmatrix} m \\ 2i+1 \end{pmatrix} x^{m-(2i+1)}\, y^{2i+1} \right]
$$

gravitational acceleration vector $\left[m/s^2\right]$:

$$
\mathbf{g}(x,y,z) = GM \sum_{n=0}^{\infty} R_{\oplus}^n \sum_{m=0}^{n} \bar{n}_{n,m} \sum_{k=0}^{[(n-m)/2]} b_{n,m,k}\, z^{n-m-2k}\, r^{2k-2n-1} \tag{3-35}
$$

$$
[\, \bar{c}_{n,m} \sum_{i=0}^{[m/2]} (-1)^i \begin{pmatrix} m \\ 2i \end{pmatrix}
$$

$$
\left\{ y^{2i} \left((m-2i)\, x^{m-2i-1} + (2k-2n-1)\, x^{m-2i+1}\, r^{-2} \right)\, \mathbf{e}_x \right.
$$

$$
+ x^{m-2i} \left(2i\, y^{2i-1} + (2k-2n-1)\, y^{2i+1}\, r^{-2} \right)\, \mathbf{e}_y
$$

$$
\left. + x^{m-2i}\, y^{2i}\, z^{-1} \left[(n-m-2k) + (2k-2n-1)\, z^2\, r^{-2} \right]\, \mathbf{e}_z \right\}
$$

$$
+ \bar{s}_{n,m} \sum_{i=0}^{[(m-1)/2]} (-1)^i \begin{pmatrix} m \\ 2i+1 \end{pmatrix}
$$

$$
\left\{ y^{2i+1} \left((m-2i-1)\, x^{m-2i-2} + (2k-2n-1)\, x^{m-2i}\, r^{-2} \right)\, \mathbf{e}_x \right.
$$

$$
+ x^{m-2i-1} \left((2i+1)\, y^{2i} + (2k-2n-1)\, y^{2i+2}\, r^{-2} \right)\, \mathbf{e}_y
$$

$$
\left. + x^{m-2i-1}\, y^{2i+1}\, z^{-1} \left[(n-m-2k) + (2k-2n-1)\, z^2\, r^{-2} \right]\, \mathbf{e}_z \right\}]
$$

gravitational force vector $\left[kg\, m/s^2\right]$:

$$
\mathbf{F}(x,y,z) = m_{Sat.}\, \mathbf{g}(x,y,z) \tag{3-36}
$$

with :

x,y,z ...   spherical co-ordinates of evaluation point $[m]$,

r ...   geocentric distance of evaluation point

$$r = \sqrt{x^2 + y^2 + z^2}\ [m]\ ,$$

GM ...   geocentric gravitational constant $\left[m^3/s^2\right]$,

$R_{\oplus}$ ...   mean radius of the Earth (Bjerhammar sphere) $[m]$,

$\bar{c}_{n,m}, \bar{s}_{n,m}$ ...   series expansion coefficients, gravitational model's coefficients $[-]$,

$\bar{n}_{n,m}$ ...   normalization factor for $\bar{P}_{n,m}(\sin\phi)$

$$\bar{P}_{n,m}(t) = \bar{n}_{n,m}\, P_{n,m}(t)$$

with $\bar{n}_{n,m} = 2^{-n} \left[(2 - \delta_{0,m})\, (2\, n+1)\, \dfrac{(n-m)!}{(n+m)!} \right]^{1/2}$,

$$b_{n,m,k} = (-1)^k\, \frac{(2\, n - 2\, k)!}{k!\,(n-k)!\,(n-m-2\,k)!}\quad .$$

3-4 Gravitational gradient

The gravitational gradient is computed by applying the gradient operator once again to the components of the gravitational acceleration vector. This results in a tensor of second order. Using index notation it can be written as

$$\mathbf{M} = M_{i,j} \; \mathbf{e}_i \otimes \mathbf{e}_j \tag{3-37}$$

with the $M_{i,j}$ being the components of the gradient operator applied once to the gravitational acceleration vector or two times to the gravitational potential respectively.

$$\mathbf{M} = grad\,(\mathbf{\Gamma}) = grad\,(grad\,U) \tag{3-38}$$

In spherical co-ordinates the components $M_{i,j}(\lambda, \phi, r)$ are

$$M_{r,r} = \frac{\partial^2}{\partial r^2}U(\lambda, \phi, r) = \frac{GM}{r^3}\sum_{n=0}^{\infty}(n+1)(n+2)\left(\frac{R_\oplus}{r}\right)^n\sum_{m=-n}^{+n}\bar{k}_{n,m}\,e_{n,m}(\lambda, \phi)$$

$$M_{r,\phi} = \frac{1}{r}\frac{\partial^2}{\partial\phi\partial r}U(\lambda, \phi, r) = -\frac{GM}{r^3}\sum_{n=0}^{\infty}(n+1)\left(\frac{R_\oplus}{r}\right)^n\sum_{m=-n}^{+n}\bar{k}_{n,m}\,\frac{\partial e_{n,m}(\lambda, \phi)}{\partial\phi}$$

$$M_{r,\lambda} = \frac{1}{r\cos\phi}\frac{\partial^2}{\partial\lambda\partial r}U(\lambda, \phi, r) = -\frac{GM}{r^3\cos\phi}\sum_{n=0}^{\infty}(n+1)\left(\frac{R_\oplus}{r}\right)^n\sum_{m=-n}^{+n}\bar{k}_{n,m}\,\frac{\partial e_{n,m}(\lambda, \phi)}{\partial\lambda}$$

$$M_{\phi,r} = \frac{\partial}{\partial r}\left(\frac{1}{r}\frac{\partial}{\partial\phi}U(\lambda, \phi, r)\right) = -\frac{GM}{r^3}\sum_{n=0}^{\infty}(n+2)\left(\frac{R_\oplus}{r}\right)^n\sum_{m=-n}^{+n}\bar{k}_{n,m}\,\frac{\partial e_{n,m}(\lambda, \phi)}{\partial\phi}$$

$$M_{\phi,\phi} = \frac{1}{r^2}\frac{\partial^2}{\partial\phi^2}U(\lambda, \phi, r) = \frac{GM}{r^3}\sum_{n=0}^{\infty}\left(\frac{R_\oplus}{r}\right)^n\sum_{m=-n}^{+n}\bar{k}_{n,m}\,\frac{\partial^2 e_{n,m}(\lambda, \phi)}{\partial\phi^2}$$

$$M_{\phi,\lambda} = \frac{1}{r^2\cos\phi}\frac{\partial^2}{\partial\lambda\partial\phi}U(\lambda, \phi, r) = \frac{GM}{r^3\cos\phi}\sum_{n=0}^{\infty}\left(\frac{R_\oplus}{r}\right)^n\sum_{m=-n}^{+n}\bar{k}_{n,m}\,\frac{\partial^2 e_{n,m}(\lambda, \phi)}{\partial\lambda\partial\phi}$$

$$M_{\lambda,r} = \frac{\partial}{\partial r}\left(\frac{1}{r\cos\phi}\frac{\partial}{\partial\lambda}U(\lambda, \phi, r)\right) = -\frac{GM}{r^3\cos\phi}\sum_{n=0}^{\infty}(n+2)\left(\frac{R}{r}\right)^n\sum_{m=-n}^{+n}\bar{k}_{n,m}\,\frac{\partial e_{n,m}(\lambda, \phi)}{\partial\lambda}$$

$$M_{\lambda,\phi} = \frac{1}{r^2}\frac{\partial}{\partial\phi}\left(\frac{1}{\cos\phi}\frac{\partial}{\partial\lambda}U(\lambda, \phi, r)\right) = -\frac{GM}{r^3 cos^2\phi}\sum_{n=0}^{\infty}\left(\frac{R_\oplus}{r}\right)^n\sum_{m=-n}^{+n}\bar{k}_{n,m}\,(\sin\phi\frac{\partial e_{n,m}(\lambda, \phi)}{\partial\lambda}$$
$$+\cos\phi\frac{\partial^2 e_{n,m}(\lambda, \phi)}{\partial\lambda\partial\phi})$$

$$M_{\lambda,\lambda} = \frac{1}{r^2\cos^2\phi}\frac{\partial^2}{\partial\lambda^2}U(\lambda, \phi, r) = \frac{GM}{r^3\cos^2\phi}\sum_{n=0}^{\infty}\left(\frac{R_\oplus}{r}\right)^n\sum_{m=-n}^{+n}\bar{k}_{n,m}\,\frac{\partial^2 e_{n,m}(\lambda, \phi)}{\partial\lambda^2}$$

$$\tag{3-39}$$

and the abbreviations for the spherical harmonics series coefficients

$$\bar{k}_{n,m} = \left\{ \begin{array}{ll} \cos m\lambda & \text{for } m \geq 0 \\ \sin|m|\lambda & \text{for } m < 0 \end{array} \right\} \quad . \tag{3-40}$$

Using Cartesian co-ordinates yields

$$\underline{\mathbf{M}}(x, y, z) = \begin{bmatrix} \dfrac{\partial^2}{\partial x^2}U(x, y, z) & \dfrac{\partial^2}{\partial x\partial y}U(x, y, z) & \dfrac{\partial^2}{\partial x\partial z}U(x, y, z) \\[2ex] & \dfrac{\partial^2}{\partial y^2}U(x, y, z) & \dfrac{\partial^2}{\partial y\partial z}U(x, y, z) \\[2ex] \text{sym.} & & \dfrac{\partial^2}{\partial z^2}U(x, y, z) \end{bmatrix} \quad . \tag{3-41}$$

For the second order derivatives of the gravitational potential with respect to to Cartesian co-ordinates x, y, z only the derivatives with respect to x are given as an example.

$$\frac{\partial'\mathbf{g}}{\partial x} = \begin{pmatrix} \partial^2 U/\partial x^2 \\ \partial^2 U/\partial y\partial x \\ \partial^2 U/\partial z\partial x \end{pmatrix}$$

$$
= \ GM \ \sum_{n=0}^{\infty} R_{\oplus}^{n} \ \sum_{m=0}^{n} \ \bar{n}_{n,m} \ \sum_{k=0}^{[(n-m)/2]} \ b_{n,m,k} \ z^{n-m-2k} \ r^{2k-2n-1} \tag{3-42}
$$

$$
\begin{bmatrix}
\bar{c}_{n,m} \sum_{i=0}^{[m/2]} (-1)^{i} \ x^{m-2i} y^{2i} \begin{pmatrix} m \\ 2i \end{pmatrix}
\begin{Bmatrix}
\begin{array}{l}
(m-2i)(2k-2n-1)r^{-2} \\
+ \ (m-2i)(m-2i-1)x^{-2} \\
+ \ (2k-2n-1)(2k-2n-3)x^{2}r^{-4} \\
+ \ (m-2i+1)(2k-2n-1)r^{-2} \\
\\
2i(2k-2n-1)xy^{-1}r^{-2} \\
+ \ 2i(m-2i)x^{-1}y^{-1} \\
+ \ (2k-2n-1)(2k-2n-3)xyr^{-4} \\
+ \ (m-2i)(2k-2n-1)x^{-1}yr^{-2} \\
\\
(n-2k-m)(2k-2n-1)xz^{-1}r^{-2} \\
+ \ (n-2k-m)(m-2i)x^{-1}z^{-1} \\
+ \ (2k-2n-1)(2k-2n-3)xz^{-1}r^{-4} \\
+ \ (m-2i)(2k-2n-1)x^{-1}z^{-1}r^{-2}
\end{array}
\end{Bmatrix}
\\
\\
+\bar{s}_{n,m} \sum_{i=0}^{[(m-1)/2]} (-1)^{i} \ x^{m-2i}y^{2i} \begin{pmatrix} m \\ 2i+1 \end{pmatrix}
\begin{Bmatrix}
\begin{array}{l}
(m-2i-1)(2k-2n-1)x^{-1}yr^{-2} \\
+ \ (m-2i-1)(m-2i-2)x^{-3}y \\
+ \ (2k-2n-1)(2k-2n-3)xyr^{-4} \\
+ \ (m-2i)(2k-2n-1)x^{-1}yr^{-2} \\
\\
(2i+1)(2k-2n-1)r^{-2} \\
+ \ (2i+1)(m-2i-1)x^{-2} \\
+ \ (2k-2n-1)(2k-2n-3)y^{2}r^{-4} \\
+ \ (m-2i-1)(2k-2n-1)x^{-2}y^{2}r^{-2} \\
\\
(n-2k-m)(2k-2n-1)yz^{-1}r^{-2} \\
+ \ (n-2k-m)(m-2i-1)x^{-2}yz^{-1} \\
+ \ (2k-2n-1)(2k-2n-3)yz^{-1}r^{-4} \\
+ \ (m-2i-1)(2k-2n-1)x^{-2}yz^{-1}r^{-2}
\end{array}
\end{Bmatrix}
\end{bmatrix}
$$

Chapter 4

Fourier frequency analysis of the Earth's gravitational field

Since (surface) spherical harmonics as functions on a sphere provide a close analogy to trigonometric functions as base functions along one axis, the (surface) spherical harmonics representation of the Earth's gravitational field clearly includes information on frequencies and wavelengths of the gravitational field. In section 3-1.1, especially figure 3-1 on page 28, it has been shown, that the (surface) spherical harmonics have high frequency localisation. The aim of the representation of the gravitational potential and acceleration vector by means of a multi-dimensional Fourier series is to detect the frequencies or wavelengths respectively, that are included within the field and to try to relate their Fourier coefficients to the (surface) spherical harmonics coefficients of the series expansions presented in the previous chapter. For that purpose, two different approaches of setting up a Fourier series expansion based on the (surface) spherical harmonics series expansion of the gravitational field are presented here: A Fourier series expansion following the parameter lines of the spherical co-ordinates, i.e. meridians and circles of constant latitude, and a Fourier series expansion in spherical and Cartesian co-ordinates following a supposed trajectory of a satellite around the Earth.

---

table 4-1: <u>Fourier series representation of a periodic scalar-valued function</u>

variable x with period length $T = t_N - t_0$

transformation to variable $\bar{x}$ with period length 2π

$$\frac{\bar{x}}{x} = \frac{2\pi}{t_N - t_0} \quad \Leftrightarrow \quad \bar{x} = \frac{2\pi x}{t_N - t_0} \tag{4-1}$$

$$f(\bar{x}) = \frac{a_0}{2} + \sum_{\bar{k}=1}^{\infty} \left(a_{\bar{k}} \cos \bar{k}\bar{x} + b_{\bar{k}} \sin \bar{k}\bar{x} \right) \quad \Leftrightarrow \quad f(x) = \frac{a_0}{2} + \sum_{\bar{k}=1}^{\infty} \left(a_{\bar{k}} \cos \frac{2\pi\bar{k}\,x}{t_N - t_0} + b_{\bar{k}} \sin \frac{2\pi\bar{k}\,x}{t_N - t_0} \right) \tag{4-2}$$

with the Fourier coefficients $\left(\bar{k} = 1, 2, \ldots \right)$

$$a_0 = \frac{2}{t_N - t_0} \int_{t_0}^{t_N} f(x')\; dx' \tag{4-3}$$

$$a_{\bar{k}} = \frac{2}{t_N - t_0} \int_{t_0}^{t_N} f(x')\; \cos \frac{2\pi\bar{k}}{t_N - t_0}\; x'\; dx' \qquad b_{\bar{k}} = \frac{2}{t_N - t_0} \int_{t_0}^{t_N} f(x')\; \sin \frac{2\pi\bar{k}}{t_N - t_0}\; x'\; dx' \tag{4-4}$$

a spectral representation is given by

$$f(x) = \frac{a_0}{2} + \sum_{\bar{k}=1}^{\infty} A_{\bar{k}}\; \sin\left(\frac{2\pi\bar{k}}{t_N - t_0} + \phi_{\bar{k}}\right) \tag{4-5}$$

with   *amplitude spectrum* $A_{\bar{k}} = \sqrt{a_{\bar{k}}^2 + b_{\bar{k}}^2}$ and   *phase spectrum* $\tan \phi_{\bar{k}} = a_{\bar{k}}/b_{\bar{k}}$

4-1 Fourier representation of a periodic function

A Fourier series expansion is applicable to 2π periodic functions. Considering the gravitational field of the Earth along a satellite's trajectory it is clearly seen that $2 - \pi$ periodicity does not hold. During one revolution of the satellite about the Earth the gravitational field rotates together with the Earth. For CHAMP e.g. the duration of one revolution is about 94 minutes which lets the field rotate about $23.5°$. In addition the real orbit of a satellite is neither plane nor closed nor elliptical nor space-fixed. Thus even for the orbital data $2 - \pi$ periodicity is not given. What remains is the possibility to consider the complete orbit arc to be analysed as one period and to transform the variable and the period to the interval 2π.

Consider a function $f(x)$ periodic on an interval $t_0 \le x \le t_N$ with length $T = t_N - t_0$. To be represented by a Fourier series expansion the variable x has to be transformed from the original period interval to 2π. The base functions of a Fourier expansion are sine and cosine functions of integer multiples of the transformed 2π periodic variable $\bar{x}$ (table 4-1 and by analogy for vector-valued functions table 4-2).

Disregarding temporal variations, e.g. tidal effects and movements of masses in the interior of the Earth, the gravitational field of the Earth is periodic. After completing one closed way around the Earth the computation yields the same gravitational field value at the same evaluation point again. This statement naturally holds for an arbitrary closed trajectory around the Earth as well as for a trajectory following a parameter line. Expressed in spherical co-ordinates the period length with respect to longitude $0 \le \lambda \le 2\pi$ as well as latitude $-\pi/2 \le \phi \le +\pi/2$ is $l_\lambda = l_\phi = 2\pi$. Respective statements hold for the use of Cartesian parameters x, y and z. For the Fourier representation of functions given by a time series of discrete functional values refer to subsection 4-4.1. For the case of a time-discrete vector-valued signal refer to tables 4-6, 4-7 and 4-8.

---

table 4-2: Fourier series representation of a periodic vector-valued function

$$\text{interval length} \quad T = t_n - t_0$$

$$\mathbf{f}(x(t), y(t), z(t)) = \frac{a_0}{2} + \sum_{\bar{k}=1}^{\infty} \left(\mathbf{a}_{\bar{k}} \cos \frac{2\pi \bar{k} t}{t_n - t_0} + \mathbf{b}_{\bar{k}} \sin \frac{2\pi \bar{k} t}{t_n - t_0} \right) \tag{4-6}$$

with the Fourier coefficients $\left(\bar{k} = 1, 2, \dots \right)$

$$\mathbf{a}_0 = \frac{2}{T} \int_{t_0}^{t_n} \mathbf{f}(x(t'), y(t'), z(t')) \, dt' \tag{4-7}$$

$$\mathbf{a}_{\bar{k}} = \frac{2}{T} \int_{t_0}^{t_n} \mathbf{f}(x(t'), y(t'), z(t')) \, \cos \frac{2\pi \bar{k} t'}{t_n - t_0} \, dt' \qquad \mathbf{b}_{\bar{k}} = \frac{2}{T} \int_{t_0}^{t_n} \mathbf{f}(x(t'), y(t'), z(t')) \, \sin \frac{2\pi \bar{k} t'}{t_n - t_0} \, dt'$$

$$\tag{4-8}$$

In the following sections two cases of Fourier series representation of gravitational values of the Earth will be presented. First a scalar-valued Fourier series representation of the gravitational potential will be given. There, advantage is taken of the potential's representation in spherical co-ordinates depending, strictly speaking, on trigonometric functionals of the angular parameters longitude λ and latitude ϕ. Thus a rather straight forward way of constructing a Fourier representation along the parameter lines of longitude and latitude can be followed. The second approach will be based on the spherical as well as Cartesian representation of the Earth's gravitational acceleration vector. It will lead to a vector-valued Fourier representation along the trajectory of a satellite. In all cases special emphasis is put on finding a connection between the Fourier series expansion's coefficients and the original (surface) spherical harmonics series expansion's coefficients.

4-2 Fourier representation along parameter lines

Following (3-28) the gravitational potential of the Earth can be written as

$$U(\lambda, \phi, r) = \frac{GM}{r} \sum_{n=0}^{\infty} \left(\frac{R_\oplus}{r} \right)^n \sum_{m=0}^{n} \left(\bar{c}_{n,m} \, \cos(m\lambda) + \bar{s}_{n,m} \, \sin(m\lambda) \right) \bar{P}_{n,m}(\sin \phi) \tag{4-9}$$

with spherical longitude $0 \leq \lambda \leq 2\pi$ and spherical latitude $-\pi/2 \leq \phi \leq +\pi/2$. This equation can be transformed into

$$U(\lambda, \phi, r) = \sum_{m=0}^{\infty} \sum_{n=m}^{\infty} \left(\underbrace{\frac{GM}{r} \left(\frac{R_{\oplus}}{r}\right)^n \bar{c}_{n,m} \bar{P}_{n,m}(\sin\phi) \ \cos m\lambda}_{=:a_{n,m}} + \underbrace{\frac{GM}{r} \left(\frac{R_{\oplus}}{r}\right)^n \bar{s}_{n,m} \bar{P}_{n,m}(\sin\phi) \ \sin m\lambda}_{=:b_{n,m}} \right).$$

(4-10)

Reordering the summations yields a one-dimensional Fourier series expansion of the gravitational potential depending on the spherical longitude λ, i.e. an expansion following a line of constant latitude (parallel).

To find a Fourier series expansion representation of the Earth's gravitational potential along a meridian, a circle of constant longitude, the fully normalized Legendre functions' dependency on latitude ϕ has to be taken into account. Thus the Legendre functions have to be written in terms of polynomials in $\sin k\phi$ and $\cos k\phi$. Following Colombo (1981) and annex A, equation (A-6), yields

$$P_{n,m}(\sin\phi) = \frac{1}{2^n} \cos^m \phi \sum_{k=0}^{[(n-m)/2]} a_{k,n,m} \ \sin^{(n-m-2k)} \phi$$

(4-11)

with the upper summation bound being an integer $(n-m)/2$ or $(n-m-1)/2$ and the factor

$$a_{k,n,m} = (-1)^k \frac{(2n-2k)!}{k! \ (n-k)! \ (n-m-2k)!}.$$

Using the normalization factor from annex A, (A-13), the fully normalized Legendre functions yield

$$\begin{aligned}
\bar{P}_{n,m}(\sin\phi) &= \frac{1}{2^n} \ [(2-\delta_{0,m}) \ (2n+1) \frac{(n-m)!}{(n+m)!}]^{1/2} \ \cos^m \phi \sum_{k=0}^{[(n-m)/2]} a_{k,n,m} \ \sin^{(n-m-2k)} \phi \\
&= \cos^m \phi \sum_{k=0}^{[(n-m)/2]} \bar{a}_{k,n,m} \ \sin^{(n-m-2k)} \phi \\
&= \sum_{k=0}^{[(n-m)/2]} \bar{a}_{k,n,m} \ \cos^m \phi \ \sin^{(n-m-2k)} \phi
\end{aligned}$$

(4-12)

with coefficients

$$\bar{a}_{k,n,m} = \frac{(-1)^k}{2^n} \ [(2-\delta_{0,m}) \ (2n+1) \frac{(n-m)!}{(n+m)!}]^{1/2} \frac{(2n-2k)!}{k! \ (n-k)! \ n-m-2k)!}.$$

(4-13)

Having a closer look at the powers of $\sin\phi$ and $\cos\phi$ it is quite obvious that

- $\cos^m(-\phi) = \cos^m(+\phi)$ is an even function for all m,

- $\sin^{n-m-2k}(-\phi) = (-1)^{n-m-2k} \sin^{n-m-2k}(+\phi)$ is an even function for $(n-m)$ even and an odd function for $(n-m)$ odd,

- the product $\cos^m \phi \ \sin^{(n-m-2k)} \phi$ is an even function for $(n-m)$ even (products of even functions only yield even functions) and an odd function if $(n-m)$ odd ('mixed' products of 2 factors always yield odd functions).

The Fourier representation of even functions only consists of cosine addends, for odd functions only sine addends are used. Thus, in equation (4-14) the Legendre functions' Fourier representation can either be written as a sum over cosine or sine addends, depending on whether $(n-m)$ is even or odd. The maximum degree of the Fourier series expansion results as $max(m, n-m-2k)$. This yields $max(m, n-m-2k) = n$ since $m \leq n$ and $min(n) = min(k) = 0$. Thus there will only be terms having the degree of the Legendre function as maximum factor of the latitude ϕ (Sneeuw (1996), Bronstein and Semedjajew (1989)).

$$\bar{P}_{n,m}(\sin\phi) = \sum_{k=0}^{[(n-m)/2]} \bar{a}_k(n,m) \sum_{p=0}^{n} d_{k,p,n,m} \begin{cases} \cos(p\phi) & \text{for } (n-m) \text{ even} \\ \sin(p\phi) & \text{for } (n-m) \text{ odd} \end{cases}$$

(4-14)

table 4-3: Fourier representation of the Earth's gravitational potential along a parallel ϕ

(using spherical co-ordinates)

$$U(\lambda, \phi\, r) = A_0 + \sum_{m=1}^{\infty} \left[A_m \, \cos m\lambda + B_m \, \sin m\lambda \right] \tag{4-15}$$

with Fourier coefficients

$$A_0 = \sum_{n=0}^{\infty} a_{n,0} \;=\; \sum_{n=0}^{\infty} \frac{GM}{r} \left(\frac{R_\oplus}{r} \right)^n \bar{c}_{n,0} \, \bar{P}_{n,0}(\sin\phi) \tag{4-16}$$

$$\left[\begin{array}{c} A_m \\ B_m \end{array} \right] = \sum_{n=m}^{\infty} \left[\begin{array}{c} a_{n,m} \\ b_{n,m} \end{array} \right] \;=\; \sum_{n=m}^{\infty} \frac{GM}{r} \left(\frac{R_\oplus}{r} \right)^n \left[\begin{array}{c} \bar{c}_{n,m} \\ \bar{s}_{n,m} \end{array} \right] \bar{P}_{n,m}(\sin\phi) \tag{4-17}$$

and

λ, ϕ, r ...   spherical co-ordinates of evaluation point $[^o, ^o, m]$,

GM ...   geocentric gravitational constant $[m^3/s^2]$,

$R_\oplus$ ...   semimajor axis of Earth's reference ellipsoid $[m]$,

$\bar{c}_{n,m}, \bar{s}_{n,m}$ ...   spherical harmonics series expansion coefficients $[-]$.

The Fourier coefficients of a periodic function $f(x)$ of period length $2l$ over $-l \le x \le +l$ are obtained as

$$a_k = \frac{1}{l} \int_{-l}^{+l} f(x) \left\{ \begin{array}{c} \cos \\ \sin \end{array} \right\} \left(\frac{k\pi x}{l} \right) dx \quad . \tag{4-18}$$

Thus

$$d_{k,p,n,m} = \frac{2}{\pi} \int_{-\pi/2}^{+\pi/2} \cos^m \phi \, \sin^{n-m-2k} \phi \left\{ \begin{array}{c} \cos \\ \sin \end{array} \right\} \left(\frac{p\phi}{2} \right) d\phi \tag{4-19}$$

and

$$\bar{d}_{p,n,m} \;=\; \sum_{k=0}^{[(n-m)/2]} \bar{a}_{k,n,m} \, d_{k,p,n,m} \tag{4-20}$$

$$=\; \frac{2}{\pi} \sum_{k=0}^{[(n-m)/2]} \bar{a}_{k,n,m} \int_{-\pi/2}^{+\pi/2} \cos^m \phi \, \sin^{n-m-2k} \phi \left\{ \begin{array}{c} \cos \\ \sin \end{array} \right\} \left(\frac{p\phi}{2} \right) d\phi \quad . \tag{4-21}$$

The Fourier representation of the fully normalized Legendre functions is

$$\bar{P}_{n,m}(\sin\phi) = \frac{2}{\pi} \bar{d}_{p,n,m}^{\left\{ \begin{smallmatrix} \cos \\ \sin \end{smallmatrix} \right\}} \left\{ \begin{array}{ll} \cos p\phi & \text{for } n-m \text{ even} \\ \sin p\phi & \text{for } n-m \text{ odd} \end{array} \right. \quad . \tag{4-22}$$

Introducing these results into table 4-3 yields

$$A_0 \;=\; \sum_{p=0}^{\infty} \underbrace{\frac{2}{\pi} \frac{GM}{r} \sum_{n=p}^{\infty} \left(\frac{R}{r} \right)^n \bar{c}_{n,0} \, \bar{d}_{p,n,0}^{\left\{ \begin{smallmatrix} \cos \\ \sin \end{smallmatrix} \right\}}}_{=: \bar{e}_{p,0}^{\bar{c}}} \left\{ \begin{array}{ll} \cos p\phi & \text{for } n-m \text{ even} \\ \sin p\phi & \text{for } n-m \text{ odd} \end{array} \right. \tag{4-23}$$

$$A_m \;=\; \sum_{p=0}^{\infty} \underbrace{\frac{2}{\pi} \frac{GM}{r} \sum_{n=p}^{\infty} \left(\frac{R}{r} \right)^n \bar{c}_{n,m} \, \bar{d}_{p,n,m}^{\left\{ \begin{smallmatrix} \cos \\ \sin \end{smallmatrix} \right\}}}_{=: \bar{e}_{p,m}^{\bar{c}}} \left\{ \begin{array}{ll} \cos p\phi & \text{for } n-m \text{ even} \\ \sin p\phi & \text{for } n-m \text{ odd} \end{array} \right. \tag{4-24}$$

$$B_m \;=\; \sum_{p=0}^{\infty} \underbrace{\frac{2}{\pi} \frac{GM}{r} \sum_{n=p}^{\infty} \left(\frac{R}{r} \right)^n \bar{s}_{n,m} \, \bar{d}_{p,n,m}^{\left\{ \begin{smallmatrix} \cos \\ \sin \end{smallmatrix} \right\}}}_{=: \bar{e}_{p,m}^{\bar{s}}} \left\{ \begin{array}{ll} \cos p\phi & \text{for } n-m \text{ even} \\ \sin p\phi & \text{for } n-m \text{ odd} \end{array} \right. \quad . \tag{4-25}$$

This yields a one-dimensional Fourier representation of the gravitational potential following a meridian $\lambda = const.$, table 4-4, as well as a two-dimensional Fourier representation of the gravitational potential, table 4-5. For the computation of the Fourier coefficients $\bar{d}_{p,n,m}$ of the series expansion of the Legendre functions refer to Sneeuw (1996) and for a more detailed treatment to Ricardi and Burrows (1972). Efficient recursive formulae can be found in Hofsommer and Potters (1960).

This representation resembles the so-called lumped coefficient representation of the perturbing potential in dynamic satellite geodesy, that has been introduced in section 1-5. The Fourier coefficients (4-23) to (4-25) as well as their combinations in table 4-5 with the coefficients (4-16) and (4-17), that result in a two-dimensional Fourier representation, are linear combinations of the (surface) spherical harmonics series expansion's coefficients $\bar{c}_{n,m}$ and $\bar{s}_{n,m}$ multiplied with weights. The weights depend on the orbit of the satellite.

---

table 4-4: Fourier representation of the Earth's gravitational potential along a meridian λ

*(using **spherical co-ordinates**)*

$$U(\lambda, \phi\, r) = \sum_{p=0}^{\infty} \bar{A}_p \begin{cases} \cos p\phi & \text{for } (n-m) \text{ even} \\ \sin p\phi & \text{for } (n-m) \text{ odd} \end{cases} \tag{4-26}$$

with :

$$\bar{A}_p = \sum_{m=0}^{\infty} \left(\bar{e}_{p,m}^{\bar{c}}\ \cos m\lambda + \bar{e}_{p,m}^{\bar{s}}\ \sin m\lambda \right)$$

$$\bar{e}_{p,m}^{\bar{c}} = \frac{2}{\pi}\ \frac{GM}{r}\ \sum_{n=p}^{\infty} \left(\frac{R_{\oplus}}{r} \right)^n\ \bar{c}_{n,m}\ \bar{d}_{p,n,m}^{\{\begin{smallmatrix}\cos\\\sin\end{smallmatrix}\}} \qquad \bar{e}_{p,m}^{\bar{s}} = \frac{2}{\pi}\ \frac{GM}{r}\ \sum_{n=p}^{\infty} \left(\frac{R_{\oplus}}{r} \right)^n\ \bar{s}_{n,m}\ \bar{d}_{p,n,m}^{\{\begin{smallmatrix}\cos\\\sin\end{smallmatrix}\}}$$

$$\bar{d}_{p,n,m}^{\{\begin{smallmatrix}\cos\\\sin\end{smallmatrix}\}} = \frac{2}{\pi} \sum_{k=0}^{(n-m)/2} \bar{a}_{k,n,m} \int_{-\pi/2}^{+\pi/2} \cos^m \phi\ \sin^{n-m-2k} \phi \begin{Bmatrix} \cos \\ \sin \end{Bmatrix} \left(\frac{p\phi}{2} \right) d\phi$$

λ, ϕ, r ...   spherical co-ordinates of evaluation point $[^o, {}^o, m]$,

GM ...   geocentric gravitational constant $[m^3/s^3]$,

$R_{\oplus}$ ...   semimajor axis of Earth's reference ellipsoid $[m]$,

$\bar{c}_{n,m}, \bar{s}_{n,m}$ ...   spherical harmonics series expansion coefficients $[-]$,

$\bar{d}_{n,m,k,p}^{\{\begin{smallmatrix}\cos\\\sin\end{smallmatrix}\}}$ ...   Fourier expansion coefficients for an expansion of the Legendre functions $[-]$.

---

table 4-5: Two-dimensional Fourier representation of the Earth's gravitational potential

*(using **spherical co-ordinates**)*

$$U(\lambda, \phi\, r) = \sum_{m=0}^{\infty} \sum_{p=0}^{\infty} \left[\bar{e}_{p,m}^{\bar{c}}\ \cos m\lambda + \bar{e}_{p,m}^{\bar{s}}\ \sin m\lambda \right] \begin{cases} \cos p\phi & \text{for } (n-m) \text{ even} \\ \sin p\phi & \text{for } (n-m) \text{ odd} \end{cases} \tag{4-27}$$

with :

$$\bar{e}_{p,m}^{\bar{c}} = \frac{2}{\pi}\ \frac{GM}{r}\ \sum_{n=p}^{\infty} \left(\frac{R_{\oplus}}{r} \right)^n\ \bar{c}_{n,m}\ \bar{d}_{p,n,m}^{\{\begin{smallmatrix}\cos\\\sin\end{smallmatrix}\}} \qquad \bar{e}_{p,m}^{\bar{s}} = \frac{2}{\pi}\ \frac{GM}{r}\ \sum_{n=p}^{\infty} \left(\frac{R_{\oplus}}{r} \right)^n\ \bar{s}_{n,m}\ \bar{d}_{p,n,m}^{\{\begin{smallmatrix}\cos\\\sin\end{smallmatrix}\}}$$

$$\bar{d}_{p,n,m}^{\{\begin{smallmatrix}\cos\\\sin\end{smallmatrix}\}} = \frac{2}{\pi} \sum_{k=0}^{(n-m)/2} \bar{a}_{k,n,m} \int_{-\pi/2}^{+\pi/2} \cos^m \phi\ \sin^{n-m-2k} \phi \begin{Bmatrix} \cos \\ \sin \end{Bmatrix} \left(\frac{p\phi}{2} \right) d\phi$$

(explanation of variables see table 4-4 above)

table 4-6:
Fourier representation of the Earth's gravitational acceleration vector following the satellite's trajectory
*(using **spherical co-ordinates** wrt. an Earth-fixed geocentric system)*

$$\text{period length} \quad T = t_n - t_0$$

$$\mathbf{g}(r(t), \lambda(t), \phi(t)) = \frac{GM}{r^2} \sum_{n=0}^{\infty} \left(\frac{R_\oplus}{r}\right)^n \sum_{m=0}^{n}$$

$$[\ \bar{c}_{n,m}\ \underbrace{[\cos(m\lambda)\ (-(n+1)\ \bar{P}_{n,m}(\sin\phi)\ \mathbf{e}_r + \frac{\partial \bar{P}_{n,m}(\sin\phi)}{\partial\phi}\ \mathbf{e}_\phi) - \sin(m\lambda)\ \frac{m}{\cos\phi}\ \bar{P}_{n,m}(\sin\phi)\ \mathbf{e}_\lambda]}_{=:\ \mathbf{C}(r(t), \lambda(t), \phi(t))}$$

$$+\ \bar{s}_{n,m}\ \underbrace{[\sin(m\lambda)\ (-(n+1)\ \bar{P}_{n,m}(\sin\phi)\ \mathbf{e}_r + \frac{\partial \bar{P}_{n,m}(\sin\phi)}{\partial\phi}\ \mathbf{e}_\phi) + \cos(m\lambda)\ \frac{m}{\cos\phi}\ \bar{P}_{n,m}(\sin\phi)\ \mathbf{e}_\lambda]}_{=:\ \mathbf{S}(r(t), \lambda(t), \phi(t))}\ ]$$

$$= \frac{\mathbf{a}_0}{2} + \sum_{\bar{k}=1}^{\infty} \left(\mathbf{a}_{\bar{k}}\ \cos\frac{2\bar{k}\pi t}{t_n - t_0} + \mathbf{b}_{\bar{k}}\ \sin\frac{2\bar{k}\pi t}{t_n - t_0} \right)$$

with Fourier coefficients $(\bar{k} = 1, 2, \ldots)$:

$$\mathbf{a}_0\ =\ \frac{2}{t_n - t_0} \int_{t_0}^{t_n} \mathbf{g}(r(t), \lambda(t), \phi(t))\ dt = \sum_{n=0}^{\infty} \sum_{m=0}^{n} \bar{c}_{n,m}\ \left(\frac{2GM}{t_n - t_0}\ R_\oplus^n \int_{t_0}^{t_n} \frac{\mathbf{C}(r(t'), \lambda(t'), \phi(t'))}{r(t')^{n+2}}\ dt' \right)$$

$$+\ \bar{s}_{n,m}\ \left(\frac{2GM}{t_n - t_0}\ R_\oplus^n \int_{t_0}^{t_n} \frac{\mathbf{S}(r(t'), \lambda(t'), \phi(t'))}{r(t')^{n+2}}\ dt' \right)$$

$$\mathbf{a}_{\bar{k}}\ =\ \frac{2}{t_n - t_0} \int_{t_0}^{t_n} \mathbf{g}(r(t'), \lambda(t'), \phi(t'))\ \cos\frac{2\bar{k}\pi t'}{t_n - t_0}\ dt'$$

$$= \sum_{n=0}^{\infty} \sum_{m=0}^{n} \bar{c}_{n,m}\ \left(\frac{2GM}{t_n - t_0}\ R_\oplus^n \int_{t_0}^{t_n} \frac{\mathbf{C}(r(t'), \lambda(t'), \phi(t'))}{r(t')^{n+2}}\ \cos\frac{2\bar{k}\pi t'}{t_n - t_0}\ dt' \right)$$

$$+\ \bar{s}_{n,m}\ \left(\frac{2GM}{t_n - t_0}\ R_\oplus^n \int_{t_0}^{t_n} \frac{\mathbf{S}(r(t'), \lambda(t'), \phi(t'))}{r(t')^{n+2}}\ \cos\frac{2\bar{k}\pi t'}{t_n - t_0}\ dt' \right)$$

$$\mathbf{b}_{\bar{k}}\ =\ \frac{2}{t_n - t_0} \int_{t_0}^{t_n} \mathbf{g}(r(t), \lambda(t), \phi(t))\ \sin\frac{2\bar{k}\pi t}{t_n - t_0}\ dt$$

$$= \sum_{n=0}^{\infty} \sum_{m=0}^{n} \bar{c}_{n,m}\ \left(\frac{2GM}{t_n - t_0}\ R_\oplus^n \int_{t_0}^{t_n} \frac{\mathbf{C}(r(t'), \lambda(t'), \phi(t'))}{r(t')^{n+2}}\ \sin\frac{2\bar{k}\pi t'}{t_n - t_0}\ dt' \right)$$

$$+\ \bar{s}_{n,m}\ \left(\frac{2GM}{t_n - t_0}\ R_\oplus^n \int_{t_0}^{t_n} \frac{\mathbf{S}(r(t'), \lambda(t'), \phi(t'))}{r(t')^{n+2}}\ \sin\frac{2\bar{k}\pi t'}{t_n - t_0}\ dt' \right)$$

t_0 ... starting point of time of orbit arc to be analysed,
t_n ... end point of time of orbit arc to be analysed.
(index n must not be mistaken for the degree n of the (surface) spherical harmonics functions)

4-3   Fourier representation along a satellite's trajectory

The basic aim of the computations of the previous section was to find a Fourier representation of the gravitational potential along the parameter lines of the spherical co-ordinates longitude λ and latitude ϕ, i.e. along the meridians and parallels. These computations yield a representation of the gravitational potential as a 2π-periodic function in spherical co-ordinates. For the following analysis of a satellite's trajectory by means of its frequency spectrum, a Fourier series expansion of the gravitational potential and the gravitational acceleration vector along the trajectory is needed. As has already been stated at the beginning of this thesis the computations will be based mainly on Cartesian co-ordinates as parameters for the description of the satellite's orbit. Thus, in the following, a Fourier representation of the components of the gravitational acceleration vector will be presented based on the description of the gravitational field using Cartesian co-ordinates (tables 4-7 and 4-8). For completeness and better understanding table 4-6 gives the Fourier representation based on spherical co-ordinates for the description of the satellite's orbit.

---

table 4-7:

Fourier representation of the Earth's gravitational acceleration vector following the satellite's trajectory

*(using **Cartesian co-ordinates** wrt. an Earth-fixed geocentric system)*

period length $T = t_n - t_0$

$$\mathbf{g}(x(t), y(t), z(t)) = \frac{\mathbf{a}_0}{2} + \sum_{\bar{k}=1}^{\infty} \left(\mathbf{a}_{\bar{k}} \ \cos \frac{2\pi \bar{k} t}{t_n - t_0} + \mathbf{b}_{\bar{k}} \ \sin \frac{2\pi \bar{k} t}{t_n - t_0} \right) \tag{4-28}$$

with Fourier coefficients $(\bar{k} = 1, 2, \ldots)$:

$$\mathbf{a}_0 = \frac{2}{t_n - t_0} \int_{t_0}^{t_n} \mathbf{g}(x(t'), y(t'), z(t')) \ dt' \tag{4-29}$$

$$\mathbf{a}_{\bar{k}} = \frac{2}{t_n - t_0} \int_{t_0}^{t_n} \mathbf{g}(x(t'), y(t'), z(t')) \ \cos \frac{2\pi \bar{k} t'}{t_n - t_0} \ dt' \qquad \mathbf{b}_{\bar{k}} = \frac{2}{t_n - t_0} \int_{t_0}^{t_n} \mathbf{g}(x(t'), y(t'), z(t')) \ \sin \frac{2\pi \bar{k} t'}{t_n - t_0} \ dt'$$

$$\tag{4-30}$$

for a time-discrete gravitational signal $\mathbf{g}$ of length $T = N \cdot dt$ sampled N times at t_i, $(i = 0, .., N - 1)$ with constant time spacing dt (the upper summation limit $N/2$ stems from the sampling theorem, see page 48)

$$\mathbf{g}(x(t), y(t), z(t)) \approx \frac{\mathbf{a}_0}{2} + \sum_{\bar{k}=1}^{N/2} \left(\mathbf{a}_{\bar{k}} \ \cos \frac{2\pi \bar{k} t}{t_n - t_0} + \mathbf{b}_{\bar{k}} \ \sin \frac{2\pi \bar{k} t}{t_n - t_0} \right) \tag{4-31}$$

t_0 $\ldots$ starting point of time of orbit arc to be analysed,

t_n $\ldots$ end point of time of orbit arc to be analysed.

(index n must not be mistaken for the degree n of the (surface) spherical harmonics functions)

The relation between the Fourier coefficients and the (surface) spherical harmonics series expansion's coefficients of the gravitational model can be formulated in matrix notation as follows.

$$
\begin{bmatrix} \mathbf{a}_0 \\ \mathbf{a}_1 \\ \vdots \\ \mathbf{a}_{N/2} \\ \mathbf{b}_1 \\ \vdots \\ \mathbf{b}_{N/2} \end{bmatrix} =
\begin{bmatrix}
\mathbf{a}_{\mathbf{0},0,0}^{\bar{c}} & \mathbf{a}_{\mathbf{0},1,0}^{\bar{c}} & \cdots & \mathbf{a}_{\mathbf{0},N,N}^{\bar{c}} & \mathbf{a}_{\mathbf{0},1,1}^{\bar{s}} & \mathbf{a}_{\mathbf{0},2,1}^{\bar{s}} & \cdots & \mathbf{a}_{\mathbf{0},N,N}^{\bar{s}} \\
\mathbf{a}_{\mathbf{1},0,0}^{\bar{c}} & \mathbf{a}_{\mathbf{1},1,0}^{\bar{c}} & \cdots & \mathbf{a}_{\mathbf{1},N,N}^{\bar{c}} & \mathbf{a}_{\mathbf{1},1,1}^{\bar{s}} & \mathbf{a}_{\mathbf{1},2,1}^{\bar{s}} & \cdots & \mathbf{a}_{\mathbf{1},N,N}^{\bar{s}} \\
\vdots & \vdots & & \vdots & \vdots & \vdots & & \vdots \\
\mathbf{a}_{\mathbf{N/2},0,0}^{\bar{c}} & \mathbf{a}_{\mathbf{N/2},1,0}^{\bar{c}} & \cdots & \mathbf{a}_{\mathbf{N/2},N,N}^{\bar{c}} & \mathbf{a}_{\mathbf{N/2},1,1}^{\bar{s}} & \mathbf{a}_{\mathbf{N/2},2,1}^{\bar{s}} & \cdots & \mathbf{a}_{\mathbf{N/2},N,N}^{\bar{s}} \\
\mathbf{b}_{\mathbf{1},0,0}^{\bar{c}} & \mathbf{b}_{\mathbf{1},1,0}^{\bar{c}} & \cdots & \mathbf{b}_{\mathbf{1},N,N}^{\bar{c}} & \mathbf{b}_{\mathbf{1},1,1}^{\bar{s}} & \mathbf{b}_{\mathbf{1},2,1}^{\bar{s}} & \cdots & \mathbf{b}_{\mathbf{1},N,N}^{\bar{s}} \\
\vdots & \vdots & & \vdots & \vdots & \vdots & & \vdots \\
\mathbf{b}_{\mathbf{N/2},0,0}^{\bar{c}} & \mathbf{b}_{\mathbf{N/2},1,0}^{\bar{c}} & \cdots & \mathbf{b}_{\mathbf{N/2},N,N}^{\bar{c}} & \mathbf{b}_{\mathbf{N/2},1,1}^{\bar{s}} & \mathbf{b}_{\mathbf{N/2},2,1}^{\bar{s}} & \cdots & \mathbf{b}_{\mathbf{N/2},N,N}^{\bar{s}}
\end{bmatrix}
\begin{bmatrix} \bar{c}_{0,0} \\ \bar{c}_{1,0} \\ \vdots \\ \bar{c}_{N,N} \\ \\ \bar{s}_{1,1} \\ \bar{s}_{2,1} \\ \vdots \\ \bar{s}_{N,N} \end{bmatrix}
$$

$$\tag{4-32}$$

Using $\mathbf{a}^{Fourier}$ for the $((N+1)\times 1)$-dimensional vector of the Fourier coefficients, $\mathbf{c}^{GravMod}$ for the $((N+1)^2 \times 1)$-dimensional vector containing the gravitational model's (surface) spherical harmonics coefficients and $\underline{\mathbf{A}}$ for the matrix having as elements the weights of the (surface) spherical harmonics coefficients within the linear combination of the corresponding Fourier / lumped coefficient, (4-32) yields

$$\mathbf{a}^{Fourier}_{((N+1)\times 1)} \quad = \quad \underline{\mathbf{A}}_{((N+1)\times(N+1)^2)} \quad \mathbf{c}^{GravMod}_{((N+1)^2 \times 1)} \quad . \tag{4-33}$$

A closer look at this matrix equation and especially at the so-called weight matrix $\underline{\mathbf{A}}$ will be taken in chapter 7 in connection with the sensitivity analysis of CHAMP orbit arcs.

---

table 4-8: <u>Fourier coefficients for **table** 4-7</u>

$$\mathbf{a}_0 = \frac{2\,GM}{t_n - t_0} \sum_{n=0}^{\infty} R_{\oplus}^n \sum_{m=0}^{n} \bar{n}_{n,m} \left[\mathbf{a}_{\mathbf{0},n,m}^{\bar{c}}\, \bar{c}_{n,m} + \mathbf{a}_{\mathbf{0},n,m}^{\bar{s}}\, \bar{s}_{n,m} \right] \tag{4-34}$$

$$\mathbf{a}_{\bar{k}} = \frac{2\,GM}{t_n - t_0} \sum_{n=0}^{\infty} R_{\oplus}^n \sum_{m=0}^{n} \bar{n}_{n,m} \left[\mathbf{a}_{\mathbf{k},n,m}^{\bar{c}}\, \bar{c}_{n,m} + \mathbf{a}_{\mathbf{k},n,m}^{\bar{s}}\, \bar{s}_{n,m} \right] \tag{4-35}$$

$$\mathbf{b}_{\bar{k}} = \frac{2\,GM}{t_n - t_0} \sum_{n=0}^{\infty} R_{\oplus}^n \sum_{m=0}^{n} \bar{n}_{n,m} \left[\mathbf{b}_{\mathbf{k},n,m}^{\bar{c}}\, \bar{c}_{n,m} + \mathbf{b}_{\mathbf{k},n,m}^{\bar{s}}\, \bar{s}_{n,m} \right] \tag{4-36}$$

with

$$\mathbf{a}_{\mathbf{0},n,m}^{\bar{c}} = \sum_{k=0}^{[(n-m)/2]} b_{n,m,k} \int_{t_0}^{t_n} z^{n-m-2k} r^{2k-2n-1} \sum_{i=0}^{[m/2]} (-1)^i \binom{m}{2i} \mathbf{g}^I(x(t),y(t),z(t))\ dt$$

$$\mathbf{a}_{\mathbf{0},n,m}^{\bar{s}} = \sum_{k=0}^{[(n-m)/2]} b_{n,m,k} \int_{t_0}^{t_n} z^{n-m-2k} r^{2k-2n-1} \sum_{i=0}^{[(m-1)/2]} (-1)^i \binom{m}{2i+1} \mathbf{g}^{II}(x(t),y(t),z(t))\ dt$$

$$\mathbf{a}_{\mathbf{k},n,m}^{\bar{c}} = \sum_{k=0}^{[(n-m)/2]} b_{n,m,k} \int_{t_0}^{t_n} z^{n-m-2k} r^{2k-2n-1} \cos\frac{2\bar{k}\pi t}{t_n - t_0} \sum_{i=0}^{[m/2]} (-1)^i \binom{m}{2i} \mathbf{g}^I(x(t),y(t),z(t))\ dt$$

$$\mathbf{a}_{\mathbf{k},n,m}^{\bar{s}} = \sum_{k=0}^{[(n-m)/2]} b_{n,m,k} \int_{t_0}^{t_n} z^{n-m-2k} r^{2k-2n-1} \cos\frac{2\bar{k}\pi t}{t_n - t_0} \sum_{i=0}^{[(m-1)/2]} (-1)^i \binom{m}{2i+1} \mathbf{g}^{II}(x(t),y(t),z(t))\ dt$$

$$\mathbf{b}_{\mathbf{k},n,m}^{\bar{c}} = \sum_{k=0}^{[(n-m)/2]} b_{n,m,k} \int_{t_0}^{t_n} z^{n-m-2k} r^{2k-2n-1} \sin\frac{2\bar{k}\pi t}{t_n - t_0} \sum_{i=0}^{[m/2]} (-1)^i \binom{m}{2i} \mathbf{g}^I(x(t),y(t),z(t))\ dt$$

$$\mathbf{b}_{\mathbf{k},n,m}^{\bar{s}} = \sum_{k=0}^{[(n-m)/2]} b_{n,m,k} \int_{t_0}^{t_n} z^{n-m-2k} r^{2k-2n-1} \sin\frac{2\bar{k}\pi t}{t_n - t_0} \sum_{i=0}^{[(m-1)/2]} (-1)^i \binom{m}{2i+1} \mathbf{g}^{II}(x(t),y(t),z(t))\ dt$$

and (also view **table 3-7**)

$$\mathbf{g}^I(x(t),y(t),z(t)) = y^{2i}\left((m-2i)\,x^{m-2i-1} + (2k-2n-1)\,x^{m-2i+1}\,r^{-2}\right)\ \mathbf{e}_x$$
$$+ x^{m-2i}\left(2i\,y^{2i-1} + (2k-2n-1)\,y^{2i+1}\,r^{-2}\right)\ \mathbf{e}_y$$
$$+ x^{m-2i}\,y^{2i}\,z^{-1}\left[(n-m-2k) + (2k-2n-1)\,z^2\,r^{-2}\right]\ \mathbf{e}_z$$

$$\mathbf{g}^{II}(x(t),y(t),z(t)) = y^{2i+1}\left((m-2i-1)\,x^{m-2i-2} + (2k-2n-1)\,x^{m-2i}\,r^{-2}\right)\ \mathbf{e}_x$$
$$+ x^{m-2i-1}\left((2i+1)\,y^{2i} + (2k-2n-1)\,y^{2i+2}\,r^{-2}\right)\ \mathbf{e}_y$$
$$+ x^{m-2i-1}\,y^{2i+1}\,z^{-1}\left[(n-m-2k) + (2k-2n-1)\,z^2\,r^{-2}\right]\ \mathbf{e}_z$$

4-4   Fourier representation for spherical harmonics models - case study EGM96

In the following subsections an analysis of an existing gravitational model will be performed based on a supposed typical trajectory of the CHAMP mission (compare with figure 7-1). The NASA GSFC (**G**oddard **S**pace **F**light **C**enter (USA)) and NIMA (**N**ational **I**magery and **M**apping **A**gency (USA)) joint geopotential model **E**arth **G**ravity **M**odel 96 (EGM96) has been chosen because it represents the state of the art of global gravitation modelling. The number of Fourier coefficients that have to be computed depends on the resolution given by the original model. A valuation computation to find the necessary connection between the resolution of the Fourier series and the resolution of the (surface) spherical harmonics model will be presented in the following subsection.

4-4.1   Evaluating the resolution of a Fourier representation

For the sampling of an arbitrary signal the Shannon or sampling theorem holds: To recover all periods (and frequencies respectively) of a signal down to a certain period length λ_{min}, it is necessary to sample the signal at least two times per period, i.e. with $\lambda_{min}/2$. To reconstruct the original signal from the sampled data it is essential to know about the signal's behaviour. It has to be a sine or cosine function. Thus the sampling theorem can easily be applied to Fourier representations of more complicated signals. The period length of a Fourier series' addend is easily computed from its index.

The Fourier series representation of the Earth-induced gravitational acceleration vector based on an N-point time series of sampled values is

$$\mathbf{g}(x(t_i), y(t_i), z(t_i)) = \frac{\mathbf{a}_0}{2} + \sum_{\bar{k}=1}^{N/2} \left(\mathbf{a}_{\bar{k}} \ \cos \frac{2\bar{k}\pi t_i}{t_n - t_0} + \mathbf{b}_{\bar{k}} \ \sin \frac{2\bar{k}\pi t_i}{t_n - t_0} \right) \tag{4-37}$$

with $0 \leq i \leq N$ which leads to

$$\frac{2\pi}{t_n - t_0} \bar{k}t_i = \omega_0 \bar{k}t_i = \omega_{\bar{k}} t_i \qquad \Longleftrightarrow \qquad f_{\bar{k}} = \bar{k} f_0 = \frac{\bar{k}}{t_n - t_0} \qquad [Hz] \tag{4-38}$$

for the frequency corresponding to a certain Fourier index $\bar{k}$. From that the period length is computed as

$$p_{\bar{k}} = \frac{1}{f_{\bar{k}}} \qquad [s] \ . \tag{4-39}$$

Referring to the equations in tables 3-7, 4-7 and 4-8 the following dimensions of the summations can be given.

- The number of weights $\mathbf{a}_{\mathbf{k},n,m}^{\bar{c}}$, $\mathbf{a}_{\mathbf{k},n,m}^{\bar{s}}$ $(\bar{k} = 0, 1, \ldots, K)$ and $\mathbf{b}_{\mathbf{k},n,m}^{\bar{c}}$, $\mathbf{b}_{\mathbf{k},n,m}^{\bar{s}}$ $(\bar{k} = 1, \ldots, K)$ for the spherical harmonics coefficients in the summation equations (4-34)-(4-36) for the Fourier coefficients is

$$2 \ N/2 + 1 = N + 1$$

  with each coefficient itself being a vector of three components.

- A (surface) spherical harmonics series expansion up to degree and order $n_{\max}$ consists of

$$2 \ \frac{1}{2} \ \sum_{i=0}^{n_{\max}} (i + 1) = (n_{max} + 1) \ (n_{max} + 2)$$

  addends. For degree and order 0 the sine terms of the (surface) spherical harmonics do not exist, thus the $\bar{s}_{n,0}$ need not be determined. This yields a total number of addends

$$(n_{max} + 1) \ (n_{max} + 2) - (n_{max} + 1) = (n_{max} + 1)^2 \ .$$

From this the whole number of unknown weights, that are to be computed, goes up to $3 \ (N + 1) \ (n_{max} + 1)^2$ (counted component-wise).

The resolution of a (surface) spherical harmonics' series expansion of the Earth's gravitational field can easily be estimated approximately by revisiting the definition and geometry of the (surface) spherical harmonics (see annex B). Sectoral harmonics, having the same degree and order values, divide the sphere's surface into $2 \ n$ - two times the degree - sectors. This yields $2 \ n$ intersections with the equator and compartments of $2\pi \ R_\oplus/(2 \ n)$ width. Following the sampling theorem, the period length of a sine or cosine wave can be detected by at

least two sampling points results as $2 \cdot (2\pi \, R_\oplus/(2 \, n)) = 2\pi \, R_\oplus \, / \, n$. This yields the following estimation at the Earth's surface as well as CHAMP's orbital level.

Wavelength $d_\oplus$ of a detectable detail at the Earth's surface $\quad d_\oplus \quad = \quad \dfrac{2\pi \, R_\oplus}{n} \qquad [m]$

corresponding wavelength at orbital level $\qquad d_{sat.} \quad = \quad \dfrac{R_\oplus + h_{sat.}}{R_\oplus} \, d_\oplus \qquad [m]$

corresponding flight time of satellite $\qquad t_{sat.} \quad = \quad \dfrac{d_{sat.}}{\bar{v}_{sat.}} \qquad [s]$

frequency $\qquad f_{\bar{k}} \quad = \quad \dfrac{1}{t_{sat.}} \qquad [Hz] \qquad$ and

the maximum Fourier index $\bar{k}$ to capture detail $d_{sat.}$ $\qquad \bar{k} \quad = \quad f_{\bar{k}}/t_0 = f_{\bar{k}} \, (t_n - t_0) \quad [-] \, .$

Small n denotes the maximum degree of the underlying (surface) spherical harmonics expansion.
The following table 4-9 shows the sampling rates for some specific cases. All the cases are based on an assumed CHAMP mission with a mean velocity of the satellite of $\bar{v} = 7\,633 \, m/s$. The columns of table 4-9 give

- column 1 *maximum degree*: gives the upper limit of the gravitational series expansion used,

- column 2 *model*: gives some exemplary models for the related maximum degree. The respective literature references for the models are for the **GPM98x** models Wenzel (1998a) and (1998b), for **OSU91A** Rapp et al. (1991), for **EGM96** Lemoine et al. (1996), for **OSU81** Rapp (1981), for **JGM3** Tapley et al. (1996), for **GRIM4x** Schwintzer et al. (1992) and (1997), for **GRIM3x** Reigber (1983a) and (1983b) and for **GEMx** Lerch et al. (1972) and (1974). A complete list of (surface) spherical harmonics models can be found in Wenzel (1998b),

- column 3 *minimum details resolved*: gives the size of the minimum details that can be resolved using this expansion on the surface of the Earth (values in brackets refer to a mean orbit level of 400 km of CHAMP),

- column 4 *time*: gives the time the satellite needs to run through an appropriate compartment based on a mean velocity of $\bar{v} = 7\,633 \, m/s$ for CHAMP,

- column 5 *frequency*: gives the respective frequency and from this

- column 6 $\bar{k}_{max}$: gives the necessary number of Fourier coefficients to compute depending on the length of the orbit arc $T = N \, dt$ in $[s]$ (values stand for $T = 45000 \, s \approx 12.5 \, h$ chosen as an example).

max. degree	model	min. details resolved [km]	time [s]	frequency [Hz]	$\bar{k}_{max.}$
1800	GPM98A/B	22.24 (23.56)	3.10	0.32295	14533
720	GPM98ar/br/cr	55.60 (59.09)	7.74	0.12918	5814
360	OSU91A, EGM96	111.19 (118.18)	15.48	0.00646	2907
180	OSU81	222.39 (236.35)	30.96	0.03229	1454
120		333.58 (354.53)	46.45	0.02153	969
100		400.30 (425.43)	55.74	0.01794	808
90		444.78 (472.70)	61.93	0.01615	727
80		500.38 (531.79)	69.67	0.01435	646
70	JGM3	571.86 (607.76)	79.62	0.01256	566
60		667.17 (709.06)	92.89	0.01076	485
50	GRIM4c2/s2	800.60 (850.87)	114.72	0.00897	404
36	GRIM3/3b/311	1111.95 (1181.76)	154.82	0.00646	291
12	GEM3/5	3335.85 (3545.29)	464.47	0.00215	97

table 4-9: Resolution of (surface) spherical harmonics series expansions

Table 4-9 presents an interesting result. Columns five and six show, that given a certain frequency $f_{\bar{k}}$, the number of necessary Fourier coefficients can be determined by the relation $\bar{k} = f_{\bar{k}} \cdot T$. This relation naturally depends on the period length T of the signal in which $f_{\bar{k}}$ is to be detected. For the period length $T = N \cdot dt$ holds, which shows that either the number of sampling points or the time step width can be treated as a parameter

free to chose more or less freely within the limitations of the Shannon's theorem. Considering satellite orbits the period length T will usually be determined by the length of the orbit arc to be analysed, since only for the special case of ideal Kepler elliptic orbits (ideal case of unperturbed two-body problem) a periodic behaviour in the strict sense is given.

4-4.2   Fourier analysis of the (surface) spherical harmonics

It would be tempting to follow the line of argumentation presented in the previous chapter for two reasons. First of all, it provokes the idea to select an ideal number of sampling points or time step width respectively for the representation of a satellite orbit computed from a (surface) spherical harmonics based gravitational field model up to some degree and order. It is quite obvious that the selected time step width must not be mistaken for the time step width that is necessary for any numerical integration method to perform the orbit synthesis. Second, the equations of table 4-8 are infinite sums of products of the (surface) spherical harmonics coefficients $\bar{c}_{n,m}$ and $\bar{s}_{n,m}$ and their weights. A reduction of the number of addends in these summation equations would be desirable. For that the frequency spectrum of the (surface) spherical harmonics is investigated more closely. Zonal harmonics having order $m = 0$ divide the sphere by means of n parallels (circles of constant latitude) into $n + 1$ zones where the harmonics either run above or below the surface of the sphere. From the same degree and order $n = m$ the sectoral harmonics are obtained. They divide the sphere into $2n$ sectors by means of $2n$ meridians. The general case of $n \neq m \neq 0$ yields the tesseral harmonics and divides the sphere along the meridians and lines of constant latitude into a chessboard pattern of $4m$ spherical triangles and $2m\,(n - m - 1)$ spherical squares. Considering an ideal polar orbit for the tesseral case would yield an estimated wavelength on the level of the surface of the sphere of radius $R_\oplus$ (figure 4-1) of

$$\lambda = 4\pi\ R_\oplus/(n - m + 1)\ . \tag{4-40}$$

This approach provides an idealistic view suggesting a somehow 'one-to-one' connection between Fourier frequencies and (surface) spherical harmonics, which in practice does not exist. In reality the weights $\mathbf{a}^{\bar{c}}_{\mathbf{k},n,m}$, $\mathbf{a}^{\bar{s}}_{\mathbf{k},n,m}$, $\mathbf{b}^{\bar{c}}_{\mathbf{k},n,m}$ and $\mathbf{b}^{\bar{s}}_{\mathbf{k},n,m}$ depend on the orbital inclination and height and in general a (surface) spherical harmonic influences all frequencies. As an example, figure 4-2 shows the result of a Fast Fourier Transformation of the values of the tesseral (surface) spherical harmonic $Y_{12,2}$ computed along one revolution of the sample CHAMP orbit in chapter 7 (table 7-1). It can be clearly seen, that the (surface) spherical harmonic and hence its coefficient contributes to all the frequencies (see also figure 3-1). The desired 'one-to-one' connection does not exist. Small or even vanishing frequencies in the spectrum would be completely accidental. Consequently the infinite sums cannot be reduced by selecting the frequencies and the corresponding Fourier coefficients. In the following subsection examples for these infinite sums, the lumped coefficients, for the geopotential model **E**arth **G**ravity **M**odel **96** (EGM96) are given.
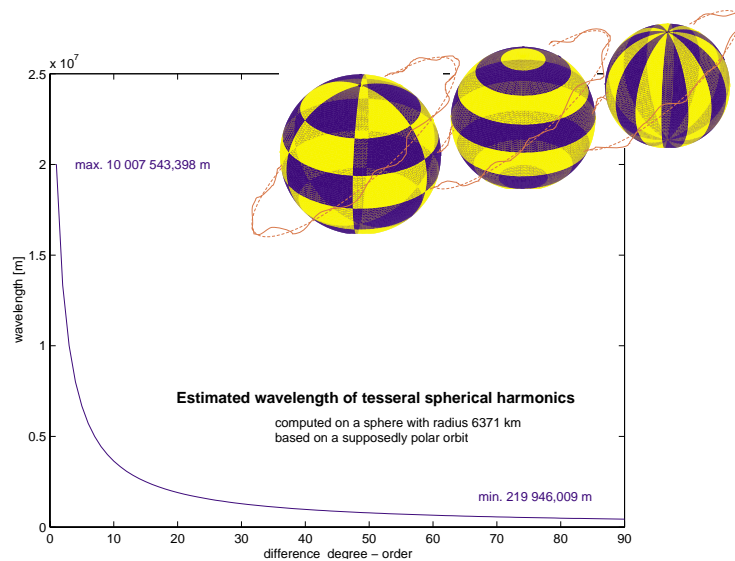

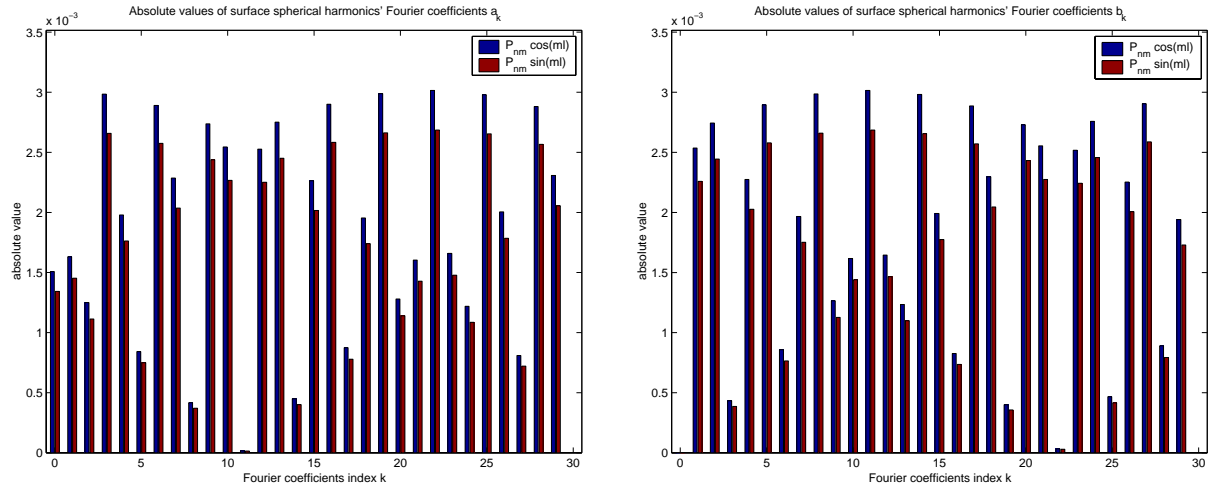**figure 4-1**: Idealized Fourier analysis of tesseral (surface) spherical harmonics

figure 4-2: Fourier frequency analysis of the tesseral (surface) spherical harmonic $Y_{12,2}$ along a CHAMP orbit (orbit height about 400 km)

4-4.3 Earth Gravity Model EGM96

The following figures represent the products of the weights $\mathbf{a}^{\bar{c}}_{\mathbf{k},n,m}$, $\mathbf{a}^{\bar{s}}_{\mathbf{k},n,m}$, $\mathbf{b}^{\bar{c}}_{\mathbf{k},n,m}$ and $\mathbf{b}^{\bar{s}}_{\mathbf{k},n,m}$ with the spherical harmonics series expansion's coefficients $\bar{c}_{n,m}$ and $\bar{s}_{n,m}$ which form the lumped coefficients (see equations in table 4-4). A simulated CHAMP orbit with length of three revolutions computed from EGM96 up to degree and order 36 is used.

A Fourier analysis of the gravitational data yields the frequency spectrum shown in table 4-10 (the columns of the table are explained in the text on page 77, the Fourier frequency analysis is addressed in more detail in chapter 7). The Fourier coefficients and their frequency and period are sorted in descending order with respect to the size of the contribution each coefficient has to the signal power of the complete signal.

index	p [sec/rev.]		f [rev./sec]	% of complete signal power (cumulative)	
4	$5.120000000 10^3$	(0d 1h 25m 20s)	$1.953125000 10^{-4}$	33.646592	(33.6465917)
3	$6.826666667 10^3$	(0d 1h 53m 47s)	$1.464843750 10^{-4}$	24.056733	(57.7033245)
5	$4.096000000 10^3$	(0d 1h 08m 16s)	$2.441406250 10^{-4}$	10.309814	(68.0131384)
7	$2.925714286 10^3$	(0d 0h 48m 46s)	$3.417968750 10^{-4}$	10.050616	(78.0637549)
6	$3.413333333 10^3$	(0d 0h 56m 53s)	$2.929687500 10^{-4}$	7.129118	(85.1928731)
2	$1.024000000 10^4$	(0d 2h 50m 40s)	$9.765625000 10^{-5}$	5.024030	(90.2169034)
1	$2.048000000 10^4$	(0d 5h 41m 20s)	$4.882812500 10^{-5}$	2.476193	(92.6930962)
8	$2.560000000 10^3$	(0d 0h 42m 40s)	$3.906250000 10^{-4}$	1.962202	(94.6552977)
15	$1.365333333 10^3$	(0d 0h 22m 45s)	$7.324218750 10^{-4}$	0.628291	(95.2835889)
10	$2.048000000 10^3$	(0d 0h 34m 08s)	$4.882812500 10^{-4}$	0.533623	(95.8172116)
9	$2.275555556 10^3$	(0d 0h 37m 56s)	$4.394531250 10^{-4}$	0.492955	(96.3101670)
11	$1.861818182 10^3$	(0d 0h 31m 02s)	$5.371093750 10^{-4}$	0.439310	(96.7494769)
14	$1.462857143 10^3$	(0d 0h 24m 23s)	$6.835937500 10^{-4}$	0.361838	(97.1113147)
18	$1.137777778 10^3$	(0d 0h 18m 58s)	$8.789062500 10^{-4}$	0.236821	(97.3481358)
16	$1.280000000 10^3$	(0d 0h 21m 20s)	$7.812500000 10^{-4}$	0.206206	(97.5543419)
19	$1.077894737 10^3$	(0d 0h 17m 58s)	$9.277343750 10^{-4}$	0.205177	(97.7595185)
21	$9.752380952 10^2$	(0d 0h 16m 15s)	$1.025390625 10^{-3}$	0.180141	(97.9396591)
29	$7.062068966 10^2$	(0d 0h 11m 46s)	$1.416015625 10^{-3}$	0.165579	(98.1052383)
20	$1.024000000 10^3$	(0d 0h 17m 04s)	$9.765625000 10^{-4}$	0.162297	(98.2675355)
12	$1.706666667 10^3$	(0d 0h 28m 27s)	$5.859375000 10^{-4}$	0.138613	(98.4061488)
22	$9.309090909 10^2$	(0d 0h 15m 31s)	$1.074218750 10^{-3}$	0.131770	(98.5379189)
25	$8.192000000 10^2$	(0d 0h 13m 39s)	$1.220703125 10^{-3}$	0.127367	(98.6652862)
17	$1.204705882 10^3$	(0d 0h 20m 05s)	$8.300781250 10^{-4}$	0.115560	(98.7808462)
26	$7.876923077 10^2$	(0d 0h 13m 08s)	$1.269531250 10^{-3}$	0.101234	(98.8820805)
23	$8.904347826 10^2$	(0d 0h 14m 50s)	$1.123046875 10^{-3}$	0.088480	(98.9705603)
13	$1.575384615 10^3$	(0d 0h 26m 15s)	$6.347656250 10^{-4}$	0.078151	(99.0487110)

table 4-10: Fourier coefficients for gravitational acceleration on CHAMP (EGM96 up to degree & order 36, Kepler and $\bar{c}_{2,0}$ term removed) in descending order with respect to their signal power.
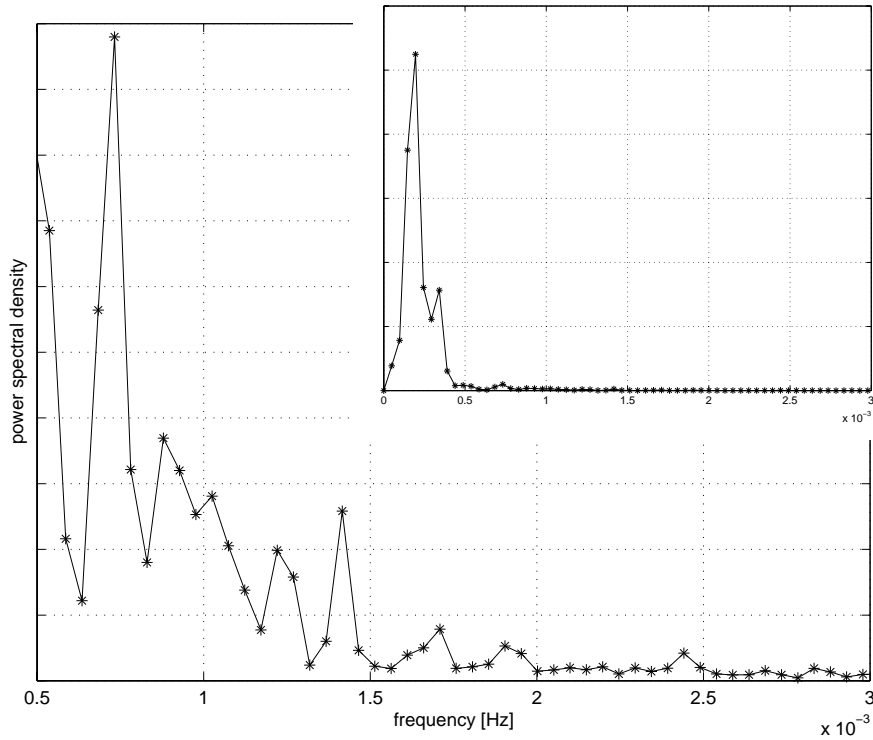
figure 4-3: Power spectral density for gravitational acceleration on CHAMP from EGM96 up to degree & order 36, Kepler and $\bar{c}_{2,0}$ term removed.
(complete graph on the right side on top, details in the major graph)

Computing the lumped coefficients, i.e. the addends of the infinite sum which are the (surface) spherical harmonics coefficients multiplied by their weights, yields the result presented in table 4-11. There the degree and order of the most important addends are given in descending order with respect to the contribution they provide for the lumped coefficient $\mathbf{a}_4$ (respective results are found for $\mathbf{b}_4$ but not given here due to reasons of space). To make this contribution more evident, table 4-11 contains a column '%' which gives the percentage of contribution of the respective summand to the analyzed lumped coefficient.

degree	order	value	%	degree	order	value	%
4	3	$1.975293 \ 10^{-1}$	9.2022832	4	2	$2.079682 \ 10^{-1}$	14.4110485
3	1	$1.862439 \ 10^{-1}$	8.6765270	6	2	$1.312948 \ 10^{-1}$	9.0980076
5	2	$1.694134 \ 10^{-1}$	7.8924483	2	2	$1.021144 \ 10^{-1}$	7.0759680
3	2	$1.569792 \ 10^{-1}$	7.3131770	3	3	$6.690810 \ 10^{-2}$	4.6363623
2	2	$1.377532 \ 10^{-1}$	6.4174976	6	5	$6.541546 \ 10^{-2}$	4.5329307
4	1	$1.264535 \ 10^{-1}$	5.8910801	6	4	$4.740452 \ 10^{-2}$	3.2848722
4	0	$1.169653 \ 10^{-1}$	5.4490546	4	1	$3.940021 \ 10^{-2}$	2.7302175
4	2	$6.978625 \ 10^{-2}$	3.2511262	5	2	$3.757803 \ 10^{-2}$	2.6039502
5	3	$6.692600 \ 10^{-2}$	3.1178760	4	4	$2.795277 \ 10^{-2}$	1.9369729
3	0	$5.810022 \ 10^{-2}$	2.7067102	8	3	$2.456005 \ 10^{-2}$	1.7018763
7	4	$3.882297 \ 10^{-2}$	1.8086424	8	6	$2.428554 \ 10^{-2}$	1.6828539
6	0	$3.689605 \ 10^{-2}$	1.7188731	7	3	$2.423791 \ 10^{-2}$	1.6795535
7	1	$2.560004 \ 10^{-2}$	1.1926269	7	4	$2.002051 \ 10^{-2}$	1.3873108
9	3	$2.478850 \ 10^{-2}$	1.1548199	5	5	$1.990402 \ 10^{-2}$	1.3792390
3	3	$2.223207 \ 10^{-2}$	1.0357236	3	2	$1.924907 \ 10^{-2}$	1.3338543
10	2	$2.131168 \ 10^{-2}$	0.9928454	10	3	$1.864822 \ 10^{-2}$	1.2922185
8	4	$2.040375 \ 10^{-2}$	0.9505477	6	6	$1.587093 \ 10^{-2}$	1.0997678
5	4	$1.830928 \ 10^{-2}$	0.8529727	5	1	$1.413440 \ 10^{-2}$	0.9794357
8	2	$1.586057 \ 10^{-2}$	0.7388949	11	3	$1.306712 \ 10^{-2}$	0.9054797
10	4	$1.488673 \ 10^{-2}$	0.6935267	8	5	$1.136823 \ 10^{-2}$	0.7877559

table 4-11: Lumped coefficient $\mathbf{a}_4$
(the three columns on the left refer to $\bar{c}_{n,m}$, the three on the right to $\bar{s}_{n,m}$).
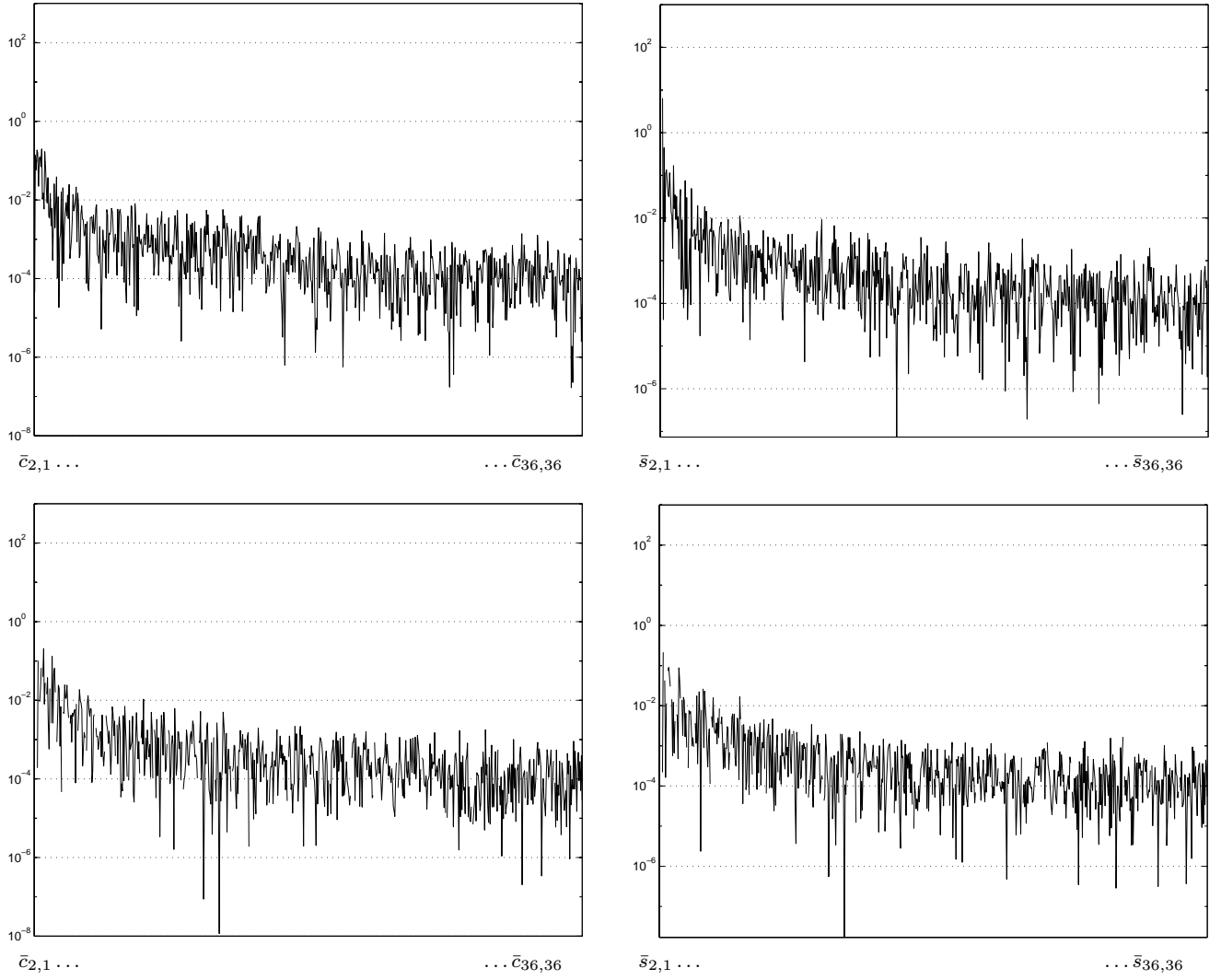
figure 4-4: Contribution of the addends for $\bar{c}_{n,m}$ (left column) and $\bar{s}_{n,m}$ (right column) to the lumped coefficients $\mathbf{a}_4$ (top line) and $\mathbf{b}_4$ (bottom line).
(explanation of axes' values see text)

Figure 4-4 gives a graphical representation of the composition of the lumped coefficients $\mathbf{a}_4$ and $\mathbf{b}_4$. On the x-axis the combinations of degree and order for the respective (surface) spherical harmonics gravitational coefficients $\bar{c}_{n,m}$ (left column of figures) and $\bar{s}_{n,m}$ (right column of figures) are given in the order $(2,1)$, $(2,2)$, $(3,0)$, $(3,1)$, $\ldots$, $(36,36)$ (the parts for $(0,0)$ and $(2,0)$ have been removed in order to obtain the perturbations). The y-axis gives the value of

$$2\,GM \cdot (t_n - t_0)^{-1} \cdot R_\oplus^n \cdot \bar{n}_{n,m} \cdot \bar{c}_{n,m} \cdot \| \mathbf{a}_{\mathbf{k=4},n,m}^{\bar{c}} \| \quad ,$$
$$2\,GM \cdot (t_n - t_0)^{-1} \cdot R_\oplus^n \cdot \bar{n}_{n,m} \cdot \bar{s}_{n,m} \cdot \| \mathbf{a}_{\mathbf{k=4},n,m}^{\bar{s}} \| \quad ,$$
$$2\,GM \cdot (t_n - t_0)^{-1} \cdot R_\oplus^n \cdot \bar{n}_{n,m} \cdot \bar{c}_{n,m} \cdot \| \mathbf{b}_{\mathbf{k=4},n,m}^{\bar{c}} \| \quad \text{and}$$
$$2\,GM \cdot (t_n - t_0)^{-1} \cdot R_\oplus^n \cdot \bar{n}_{n,m} \cdot \bar{s}_{n,m} \cdot \| \mathbf{b}_{\mathbf{k=4},n,m}^{\bar{s}} \|$$

according to table 4-8 in logarithmic scaling. FIELD

Chapter 5

State space description of the system satellite

5-1 A general state space description for a nonlinear system and its temporal behaviour

There are several ways to describe the temporal behaviour of a system, one of which is the state space description method. The state of a system at a certain point of time t_k is described by a vector containing at least the number of parameters necessary to uniquely represent the system. These elements are called the states or state components of the system, the vector consisting of the state components is called state space vector.

In principle the state space vector originally contains the state components for the purpose of describing and estimating the temporal behaviour of the system only, but it can also be extended for the purpose of parameter estimation. Parameters, that are not essential for the unique description of the system at a certain point of time, can be included into the state vector. Estimation and filtering methods, e.g. a Kalman filter, can then provide not only a temporal estimate (prediction) of the essential state components but also of the additional parameters, if an observability condition holds which will be explained in more detail in the following.

5-1.1 Setting up of a general state space description

A very general formulation of an extended state space vector for a nonlinear time-variant system is given by (5-1).

$$\mathbf{x}(t) = [\ \underbrace{\mathbf{x}_e(t, \mathbf{p}_1(t), \mathbf{p}_2)}_{\text{'essential' states}} \ \ | \ \ \underbrace{\mathbf{p}_1(t) \qquad \mathbf{p}_2}_{\substack{\text{additional parameters} \\ \text{time-variable} \quad \text{time-invariant}}} \ \ ]^T \tag{5-1}$$

$\mathbf{x}_e(t, \mathbf{p}_1(t), \mathbf{p}_2)$ contains the essential components for the description of the system. Since a system is usually described mathematically by means of a set of differential equations, $\mathbf{x}_e(t, \mathbf{p}_1(t), \mathbf{p}_2)$ will have as many components as constants of integration are needed for this system of differential equations (see section 2-2 for an example). $\mathbf{p}_1(t)$ and $\mathbf{p}_2$ are vectors of parameters to extend the state vector. They are split off into two sets of parameters: time-dependent and time-invariant, respectively. Usually the state components will depend on the parameters in some way.

Considering a certain state $\mathbf{x}(t_k)$ of a given nonlinear system at point of time t_k, a prediction of the system's state at a following point of time t_{k+1} can be made. For that, the temporal behaviour of the system has to be determined, which means to compute the first order derivative of the system's state with respect to time

$$\dot{\mathbf{x}}(t, \mathbf{p}_1(t), \dot{\mathbf{p}}_1(t), \mathbf{p}_2) = \left[\ \dot{\mathbf{x}}_e(t, \mathbf{p}_1(t), \mathbf{p}_2) + \frac{\partial \dot{\mathbf{x}}_1(t, \mathbf{p}_1(t), \mathbf{p}_2)}{\partial \mathbf{p}_1(t)} \dot{\mathbf{p}}_1(t) \ \ | \ \ \dot{\mathbf{p}}_1(t) \quad \mathbf{0} \ \right]^T \ . \tag{5-2}$$

Let the state vector and its elements be stochastic variables. An estimate for the state of the system at point of time t_k is achieved by an integral equation (throughout the whole chapter the notation of Schaffrin (1991) and (1992) will be used)

$$\widehat{\mathbf{x}}(t_{k+1}) = \mathbf{x}(t_k, \mathbf{p}_1(t_k), \mathbf{p}_2) + \int\limits_{t_k}^{t_{k+1}} \dot{\mathbf{x}}(t', \mathbf{p}_1(t'), \dot{\mathbf{p}}_1(t'), \mathbf{p}_2) \, dt' \tag{5-3}$$

which can be solved by applying a suitable numerical integration technique. This is necessary because the nonlinearity of the system means, that there is no closed analytical solution.

In the following, a state space description will be developed which describes the movement of an artificial satellite orbiting the Earth on its trajectory.

5-1.2 Evaluation of a state space model - Observability analysis

A state space model has to fulfil certain conditions to provide a suitable basis for the analysis of the temporal behaviour of a system.

- Observability holds if and only if the state of a dynamic system is uniquely determinable from its given model for the system's temporal dynamics and the input and output time series (Grewal and Andrews (1993)). If observability holds for all states over a certain time interval during which the system has been observed, the system is called completely observable (Bramer and Stiffling (1985)) and the initial values of the filtering process can be uniquely determined from input (sometimes also called system's control), output (observations) and system's model. The mathematical formulation of a system's observability analysis will be presented in detail in the following.

- Controllability holds if the initial state $\mathbf{x}(t_0)$ can be transformed into an arbitrary state $\mathbf{x}(t_i)$ by means of a valid system input (Grewal and Andrews (1993)). Since the systems presented in this thesis for application in satellite geodesy do not take into account any input or control values (external forces on the satellite like e.g. attitude control manoeuvres or general propulsion forces could be introduced as inputs but are not considered here), controllability plays a minor role.

As stated above, observability requires that the states of the system over a certain interval of observations are uniquely determinable from the observations, the control input and the given system's model. This means that a system of equations has to be built from the state components' dynamics' equations, the observation equation and its temporal derivatives, that allows a unique determination of the states. Linearly dependent equations in this system mean, that there are some state components that are not determinable; these are denoted as unobservable. Only linear combinations of these state components are determinable.

This analytical observability analysis method can be performed up to rather high order of the system (Schrick (1977)), but the necessary efforts will clearly increase with each additional state component. From a certain order on the efforts will be too high to perform the analytical method and a numerical algorithm has to be applied.

For linear systems a numerical method to determine whether a system is observable or not can be found in literature, e.g. Grewal and Andrews (1993). As necessary as well as sufficient condition for the observability of a linear system equation (5-4) has to be fulfilled.

$$\text{rank } \underline{\mathbf{Q}} = \text{rank } \begin{bmatrix} \underline{\mathbf{H}}_0 & \underline{\mathbf{F}}_0\underline{\mathbf{H}}_1 & \underline{\mathbf{F}}_0\underline{\mathbf{F}}_1\underline{\mathbf{H}}_2 & \cdots & \underline{\mathbf{F}}_0\underline{\mathbf{F}}_1\ldots\underline{\mathbf{F}}_{N-1}\underline{\mathbf{H}}_N \end{bmatrix} = \dim(\mathbf{x}) \tag{5-4}$$

$\underline{\mathbf{F}}_i$ denotes the process model's transition matrix, $\underline{\mathbf{H}}_i$ the observation model's transition matrix both at point of time $t_i \in [t_0 \ldots t_N]$, the interval of observation, with $i \in [0 \ldots N]$. $\underline{\mathbf{Q}}$ denotes the system's covariance.
In the following section three state space descriptions for the system 'satellite trajectory - orbit analysis' will be presented together with an analytical observability analysis.

5-2 System 'satellite trajectory'

As pointed out in section 2-2 the satellite's state at a specific point of time is described by the six variables of its position and velocity vector being the constants of integration for the solution of the second-order vectorial equations of motion. This yields six essential state elements. Thus the equations

extended state vector: $\qquad \mathbf{x}(t) \quad = \quad [\ \mathbf{x}_e(t, \mathbf{p}_1(t), \mathbf{p}_2) \quad \mathbf{p}_1(t) \quad \mathbf{p}_2\ ]^T$

extended states' dynamics: $\qquad \dot{\mathbf{x}}(t) \quad = \quad \left[\ \left(\dot{\mathbf{x}}_e(t, \mathbf{p}_1(t), \mathbf{p}_2) + \dfrac{\partial \dot{\mathbf{x}}_e(t, \mathbf{p}_1(t), \mathbf{p}_2)}{\partial \mathbf{p}_1(t)}\ \dot{\mathbf{p}}_1(t) \right) \quad \dot{\mathbf{p}}_1(t) \quad \mathbf{0}\ \right]^T$

state and parameter prediction: $\quad \widehat{\mathbf{x}}(t_{k+1}) \quad = \quad \mathbf{x}(t_k) + \int\limits_{t_k}^{t_{k+1}} \dot{\mathbf{x}}(t', \mathbf{p}_1(t'), \dot{\mathbf{p}}_1(t'), \mathbf{p}_2)\ dt'$

describe the system by means of a six-dimensional vector $\mathbf{x}_e$ built from the position and the velocity vector of the satellite. The parameter vectors $\mathbf{p}_1(t)$ and $\mathbf{p}_2$ contain additional parameters influencing the satellite's trajectory. Time-variant effects are gravitational accelerations or time-varying geophysical parameters (solar flux, atmospheric density, ...) e.g.. Time-invariant parameters are constants of nature or gravitational model coefficients (spherical harmonics' coefficients). A detailed list on time dependency is given in table 6-4 on page 70.

In the following three examples for extended state space descriptions of a satellite system are given, one for each of the cases 'time-variant parameters only', 'time-invariant-parameters only'and a combined general case, derived from the first two.

5-2.1 State space description for determination of gravitational acceleration vectors - case of time variant parameters

The gravitational vector, which is to be determined, is a three-dimensional time dependent vector, although the time dependency is not a direct one. Instead of $\mathbf{g}(t)$ the acceleration vector should rather be denoted by $\mathbf{g}(\mathbf{x}_1(t))$. The time dependency is an indirect one by means of the dependency on the position vector (the evaluation point of the gravitation so to speak). Thus, the proposed extended state space description for a satellite's state at a certain point of time t is represented by means of its nine-dimensional state space vector (5-5).

$$\mathbf{x}(t) = [\ \underbrace{(x(t), y(t), z(t))}_{\text{position } \mathbf{x_1}(t)}\ \underbrace{(\dot{x}(t), \dot{y}(t), \dot{z}(t))}_{\text{velocity } \mathbf{x_2}(t)}\ \underbrace{(g_x(t), g_y(t), g_z(t))}_{\text{grav. acc. } \mathbf{g}(t)}\ ]^T \tag{5-5}$$

All elements of the satellite's state vector are given in Cartesian co-ordinates with respect to the same reference system, a three-dimensional geocentric Cartesian equatorial system, e.g. WGS84, GPS' reference system.

---

table 5-1: State-space description of system satellite

estimation of <u>time-variant</u> parameters: gravitational acceleration vector

ext. state vector: $\mathbf{x}(t)\quad = \quad [\ \mathbf{x_1}(t), \mathbf{x_2}(t),\ \mathbf{g}(t)\ ]^T$

ext. states' dynamics: $\dot{\mathbf{x}}(t)\quad = \quad \begin{bmatrix} \mathbf{x}_2(t) \\ \mathbf{g}(t) + \underbrace{(\mathbf{a}_{3.cb}(\mathbf{x}(t), t) + \mathbf{a}_{non-gr.}(\mathbf{x}(t), t))}_{=:\mathbf{a}_{pert.}(\mathbf{x}(t), t)} \\ \underline{\mathbf{M}}(t)\ \mathbf{x}_2(t) \end{bmatrix}$ (5-6)

prediction: $\widehat{\mathbf{x}}(t_{k+1})\quad = \quad \mathbf{x}(t_k) + \int\limits_{t_k}^{t_{k+1}} \begin{bmatrix} \mathbf{x}_2(t') \\ \mathbf{g}(t') + \mathbf{a}_{pert.}(\mathbf{x}(t'), t') \\ \underline{\mathbf{M}}(\mathbf{x}_1(t'))\ \mathbf{x}_2(t') \end{bmatrix}\ dt'$

with

$\mathbf{g}(.)$ ...   gravitational acceleration vector,

$\underline{\mathbf{M}}(.)$ ...   gravitational gradient $\dfrac{\partial \mathbf{g}(\mathbf{x}_1(t), \mathbf{c})}{\partial \mathbf{x}_1(t)}$,

$\mathbf{a}_{3.cb}(.)$ ...   direct and indirect gravitational effects of other celestial bodies
                            (*moon, sun, planets*),

$\mathbf{a}_{non-gr.}(.)$ ...   non-gravitational effects on the satellite's orbit
                            (*atmospheric drag and lift, solar and Earth radiation pressure, orbit manoeuvres*).

The equations of the state components' dynamics describe the variation of the state vector's components with time and thus they are formulated as ordinary first order differential equations. The first order derivative of the satellite's position with respect to time yields its velocity, the derivative of the velocity the resulting vector of all accelerations acting on the satellite. The first order derivative with respect to time t of the gravitational vector yields

$$\frac{\partial \mathbf{g}(\mathbf{x}_1(t))}{\partial t} = \frac{\partial \mathbf{g}(\mathbf{x}_1(t))}{\partial \mathbf{x}_1(t)}\ \frac{d\mathbf{x}_1(t)}{dt} = \underline{\mathbf{M}}(\mathbf{x}_1(t))\ \mathbf{x}_2(t)\quad , \tag{5-7}$$

the matrix product of the gravitational gradient with the velocity of the satellite.
This yields the following ordinary vector-valued first-order differential equation for the state components' dy-

namics.

$$\dot{\mathbf{x}}(t) = \begin{bmatrix} \mathbf{x}_2(t) \\ \mathbf{g}(t) + \mathbf{a}_{3.cb}(\mathbf{x}_1(t), t) + \mathbf{a}_{non-gr.}(\mathbf{x}_1(t), \mathbf{x}_2(t), t) \\ \underline{\mathbf{M}}(\mathbf{x}_1(t)) \, \mathbf{x}_2(t) \end{bmatrix} \tag{5-8}$$

It should be kept in mind that the velocity's derivative contains all accelerations acting on the satellite, gravitational as well as non-gravitational. It represents Newton's equation of motion (2-1) being a sum of all acting acceleration vectors. For more details refer to chapter 2.

Thus the satellite state components' dynamics are given in (5-8) for the very general case of an arbitrarily perturbed orbit. The non-gravitational accelerations $\mathbf{a}_{non-gr.}(t)$ are considered to be measured by means of an accelerometer system as already mentioned earlier for CHAMP. They are available as a time series and their first-order derivative with respect to time t can be considered to be zero. The perturbing accelerations of third celestial bodies $\mathbf{a}_{3.cb}(\mathbf{x}_1(t), t)$, for simplicity, are treated in the same way. Its values can be computed by means of an appropriate model.

For further consideration and simulation and testing of the presented method it is assumed throughout the rest of this thesis that only gravitational effects are affecting the satellite's orbit. Thus the system's description simplifies to (5-6). Nevertheless for the sake of completeness the equations for the state space descriptions discussed here will be given in a way showing non-gravitational and tidal influences also.

---

table 5-2: State-space description of system satellite

estimation of time-invariant parameters: gravitational expansion coefficients

ext. state vector: $\quad \mathbf{x}(t) \quad = \quad [\, \mathbf{x_1}(t), \mathbf{x_2}(t), \, \mathbf{c} \,]^T$

ext. states' dynamics: $\quad \dot{\mathbf{x}}(t) \quad = \quad \begin{bmatrix} \mathbf{x}_2(t) \\ \mathbf{g}(t, \mathbf{c}) + (\mathbf{a}_{3.cb}(t) + \mathbf{a}_{non-gr.}(t)) \\ \mathbf{0} \end{bmatrix}$ $\tag{5-9}$

prediction: $\quad \widehat{\mathbf{x}}(t_{k+1}) \quad = \quad \mathbf{x}(t_k) + \int\limits_{t_k}^{t_{k+1}} \begin{bmatrix} \mathbf{x}_2(t') \\ \mathbf{g}(t', \mathbf{c}) + (\mathbf{a}_{3.cb}(t') + \mathbf{a}_{non-gr.}(t')) \\ \mathbf{0} \end{bmatrix} \, dt'$

with

$\mathbf{g}(.)$ ... gravitational acceleration vector,

$\mathbf{c}$ ... gravitational series expansion coefficients to be determined,

$\mathbf{a}_{3.cb}(t)$ ... direct and indirect gravitational effects of other celestial bodies (*moon, sun, planets*),

$\mathbf{a}_{non-gr.}(t)$... non-gravitational effects on the satellite's orbit (*atmospheric drag and lift, solar and Earth radiation pressure, orbit manoeuvres*).

5-2.2 State space description for determination of gravitational coefficients - case of time invariant parameters

The gravitational coefficients are the time invariant coefficients of the spherical harmonics series expansion of the Earth's gravitational field.

$$\mathbf{x}(t) = [\, \underbrace{(x(t), y(t), z(t))}_{\text{position } \mathbf{x_1}(t)} \quad \underbrace{(\dot{x}(t), \dot{y}(t), \dot{z}(t))}_{\text{velocity } \mathbf{x_2}(t)} \quad \underbrace{(c_1, c_2, \ldots, c_c)}_{\text{grav. coeff. } \mathbf{c}} \,]^T \tag{5-10}$$

This time the extended state vector is of dimension $(6 + c \times 1)$ with c denoting the number of gravitational coefficients to be determined. The state components' dynamics are

$$\dot{\mathbf{x}}(t) = \begin{bmatrix} \mathbf{x}_2(t) \\ \mathbf{g}(\mathbf{x}_1(t), \mathbf{c}) + \mathbf{a}_{3.cb}(\mathbf{x}_1(t), t) + \mathbf{a}_{non-gr.}(\mathbf{x}_1(t), \mathbf{x}_2(t), t) \\ \mathbf{0} \end{bmatrix} \qquad (5\text{-}11)$$

Note that the gravitational acceleration vector, the first order temporal derivative of the state velocity, depends on the parameter vector $\mathbf{c}$. The velocity's derivative contains all accelerations acting on the satellite.

---

table 5-3: State-space description of system satellite

*estimation of <u>time-variant</u> and <u>time-**in**variant</u> parameters:*
gravitational acceleration vectors and spherical harmonics series' expansion coefficients

ext. state vector: $\mathbf{x}(t) \quad = \quad [\, \mathbf{x_1}(t), \mathbf{x_2}(t),\ \mathbf{g}(t, \mathbf{c}),\ \mathbf{c}\,]^T$

ext. states' dynamics: $\dot{\mathbf{x}}(t) \quad = \quad \begin{bmatrix} \mathbf{x}_2(t) \\ \mathbf{g}(t, \mathbf{c}) + \underbrace{\left(\mathbf{a}_{3.cb}(\mathbf{x}(t), t) + \mathbf{a}_{non-gr.}(\mathbf{x}(t), t)\right)}_{=:\mathbf{a}_{pert.}(\mathbf{x}(t), t)} \\ \underline{\mathbf{M}}(\mathbf{x}_1(t), \mathbf{c})\ \mathbf{x}_2(t) \\ \mathbf{0} \end{bmatrix} \qquad (5\text{-}12)$

prediction: $\widehat{\mathbf{x}}(t_{k+1}) \quad = \quad \mathbf{x}(t_k) + \displaystyle\int_{t_k}^{t_{k+1}} \begin{bmatrix} \mathbf{x}_2(t') \\ \mathbf{g}(t', \mathbf{c}) + \mathbf{a}_{pert.}(\mathbf{x}(t'), t') \\ \underline{\mathbf{M}}(\mathbf{x}_1(t), \mathbf{c})\ \mathbf{x}_2(t) \\ \mathbf{0} \end{bmatrix} dt'$

with

$\mathbf{g}(.)$ ...   gravitational acceleration vector,

$\mathbf{c}$ ...   gravitational series expansion coefficients to be determined,

$\underline{\mathbf{M}}(.)$ ...   gravitational gradient $\dfrac{\partial \mathbf{g}(\mathbf{x}_1(t), \mathbf{c})}{\partial \mathbf{x}_1(t)}$,

$\mathbf{a}_{3.cb}(.)$ ...   direct and indirect gravitational effects of other celestial bodies
                                        (*moon, sun, planets*),

$\mathbf{a}_{non-gr.}(.)$ ...   non-gravitational effects on the satellite's orbit
                                        (*atmospheric drag and lift, solar and Earth radiation pressure, orbit manoeuvres*).

5-2.3   State space description for a combined model

This subsection gives a combined general model containing time variant and time invariant parameters. It is a combination of the previous two examples and thus aims at the determination of both gravitational acceleration vectors and gravitational series expansion coefficients. The extended state space vector has a general form following (5-1) and is of dimension $(9 + c \times 1)$.

$$\mathbf{x}(t) = [\, \underbrace{(x(t), y(t), z(t))}_{\text{position } \mathbf{x_1}(t)}\ \ \underbrace{(\dot{x}(t), \dot{y}(t), \dot{z}(t))}_{\text{velocity } \mathbf{x_2}(t)}\ \ \underbrace{(g_x(t), g_y(t), g_z(t))}_{\text{grav. acc. } \mathbf{g}(t)}\ \ \underbrace{(c_1, c_2, \ldots, c_c)}_{\text{grav. coeff. } \mathbf{c}}\,]^T \qquad (5\text{-}13)$$

For the sake of readability, (5-13) contains only the time dependency of the elements of the state space vector. However, for the computation of the state components' dynamics model a more detailed description of the

dependencies, as it is given in (5-14), is necessary to compute the correct derivatives.

$$
\begin{aligned}
\text{position:} \quad & \mathbf{x}_1(t) \\
\text{velocity:} \quad & \mathbf{x}_2(t) \quad = \quad \dot{\mathbf{x}}_1(t) \\
\text{gravitational acceleration:} \quad & \mathbf{g}(\mathbf{x}_1(t), \mathbf{c}) \quad = \quad \ddot{\mathbf{x}}_1(t, \mathbf{c}) \\
\text{gravitational coefficients:} \quad & \mathbf{c}
\end{aligned}
\tag{5-14}
$$

Thus, the states' dynamics are

$$
\dot{\mathbf{x}}(t) = \begin{bmatrix}
\mathbf{x}_2(t) \\
\mathbf{g}(t, \mathbf{c}) + \mathbf{a}_{3.cb}(\mathbf{x}_1(t), t) + \mathbf{a}_{non-gr.}(\mathbf{x}_1(t), \mathbf{x}_2(t), t) \\
\underline{\mathbf{M}}(\mathbf{x}_{1(t)}, \mathbf{c})\, \mathbf{x}_2(t) \\
\mathbf{0}
\end{bmatrix} .
\tag{5-15}
$$

Note that the gravitational acceleration vector, which is the first order temporal derivative of the state velocity as well as the gravitational gradient $\underline{\mathbf{M}}$, which is the spatial derivative of the gravitational acceleration vector, depends on the parameter vector $\mathbf{c}$. The velocity's derivative again contains all accelerations acting on the satellite.

5-3 Observing the system 'satellite trajectory'

As stated in the introductory section of the thesis, future satellite missions like CHAMP will be tracked by GPS receivers which provide the trajectory of the satellite in full three-dimensional position and velocity vectors with respect to GPS' reference system WGS84, an Earth fixed geocentric Cartesian equatorial system. Both vectors are derived from the GPS receiver's original observables pseudoranges for the real-time navigation solution and/or phase observations for the post-processing precise orbit determination (POD). Thus the vector of observations can be written as a six-dimensional vector

$$
\mathbf{z}(t) = [\underbrace{x(t) \quad y(t) \quad z(t)}_{\text{position } \mathbf{z_1}(t)} \quad \underbrace{\dot{x}(t) \quad \dot{y}(t) \quad \dot{z}(t)}_{\text{velocity } \mathbf{z_2}(t)}]^T .
\tag{5-16}
$$

Representing the connection between observations and states, the measurement model of a satellite tracked by GPS is linear with respect to the observations and can be written in matrix form as

$$
\mathbf{z}(t) = \begin{bmatrix}
\mathbf{E}_{3\times3} & \mathbf{0}_{3\times3} & \mathbf{0}_{3\times d} \\
\mathbf{0}_{3\times3} & \mathbf{E}_{3\times3} & \mathbf{0}_{3\times d}
\end{bmatrix} \mathbf{x}(t) = \underline{\mathbf{H}}\, \mathbf{x}(t) ,
\tag{5-17}
$$

where d denoting the dimension of the parameter vectors augmenting the essential states (dimension of $\mathbf{p_1}(t)$ and $\mathbf{p_2}$ together).

However, the simple structure of the observation's transition matrix $\underline{\mathbf{H}}$ results from the special case of linear observation equations for GPS and this way of state space description. In general, for nonlinear systems, the observation model will also be nonlinear.

Either by means of an error analysis of the observations or by means of reasonable values adopted from experience or the GPS receiver's calibration the covariance matrix of the observations $\underline{\mathbf{R}}$ can be set up.

5-3.1 Observability analysis

Following the general description of an analysis method for observability of a system and its state space description in subsection 5-1.2, the observability of the three state space descriptions presented for the trajectory of a satellite can be investigated. First a system of equations containing the state components' dynamics and observation equations has to be built. This system then is extended by the temporal derivatives of the observation equation, in order to find enough linearly independent equations to compute the state components position $\mathbf{x}_1(t)$, velocity $\mathbf{x}_2(t)$, gravitational acceleration $\mathbf{g}(t, \mathbf{c})$ and gravitational model coefficients $\mathbf{c}$ from the observations $\mathbf{z}_1(t)$ and $\mathbf{z}_2(t)$. The resulting system of equations can be seen in table 5-4.

It is quite obvious that the state components position $\mathbf{x}_1(t)$ and velocity $\mathbf{x}_2(t)$ are observable, since they are observed directly and the connection between them and the observation components is given by the observation equations. Thus, to prove observability it suffices to show that the remaining two state components can also be uniquely determined from the observations.

For the determination of the gravitational acceleration vector $\mathbf{g}(t, \mathbf{c})$ the system (5-18) of three linearly independent equations can be set up, which proves that $\mathbf{g}(t, \mathbf{c})$ is also observable in addition to the two indispensable components position and velocity of the state vector.

$$
\begin{aligned}
\mathbf{x}_1(t) &= \mathbf{z}_1(t) \\
\mathbf{x}_2(t) &= \mathbf{z}_2(t) \\
\mathbf{g}(t, \mathbf{c}) &= \dot{\mathbf{z}}_2(t)
\end{aligned}
\tag{5-18}
$$

When investigating the observability of the gravitational model's (surface) spherical harmonics' coefficients, the general statement that from one satellite mission only linear combinations of gravitational coefficients can be determined is nicely proven. The system of equations cannot be extended in a way that allows a unique determination of each single coefficient. Only combinations of gravitational field coefficients can be computed from the equations (5-19).

$$
\begin{aligned}
\dot{\mathbf{g}}(\mathbf{x}_1(t), \mathbf{c}) &= \underline{\mathbf{M}}(\mathbf{x}_1(t), \mathbf{c})\, \mathbf{x}_2(t) \\
\ddot{\mathbf{z}}_2(t) &= \underline{\mathbf{M}}(\mathbf{x}_1(t), \mathbf{c})\, \mathbf{x}_2(t) \\
\mathbf{z}_1^{(3)}(t) &= \underline{\mathbf{M}}(\mathbf{x}_1(t), \mathbf{c})\, \mathbf{x}_2(t) \\
\mathbf{z}_2^{(3)}(t) &= \mathbf{x}_2(t)\, \frac{\partial}{\partial \mathbf{x}_1(t)} \underline{\mathbf{M}}(\mathbf{x}_1(t), \mathbf{c})\, \mathbf{x}_2(t) + \underline{\mathbf{M}}(\mathbf{x}_1(t), \mathbf{c})\, \mathbf{g}(t, \mathbf{c})
\end{aligned}
\tag{5-19}
$$

A mere mathematical possibility of the determination of all the coefficients from one satellite mission does in fact exist - in this sense, the given system is observable - but the accuracies of the determination will not be sufficient for most cases. Only a combination of data from different missions with different layout will yield a satisfying result.

$\dot{\mathbf{x}}_1(t) = \mathbf{x}_2(t)$	state components' dynamics
$\dot{\mathbf{x}}_2(t) = \mathbf{g}(t, \mathbf{c})$	
$\dot{\mathbf{g}}(t, \mathbf{c}) = \dot{\mathbf{g}}(\mathbf{x}_1(t), \mathbf{c}) = \underline{\mathbf{M}}(\mathbf{x}_1(t), \mathbf{c})\, \mathbf{x}_2(t)$	
$\dot{\mathbf{c}} = \mathbf{0}$	

$\mathbf{z}_1(t) = \mathbf{x}_1(t)$	observation equations
$\mathbf{z}_2(t) = \mathbf{x}_2(t)$	

$\dot{\mathbf{z}}_1(t) = \mathbf{x}_2(t)$	temporal derivatives of
$\dot{\mathbf{z}}_2(t) = \mathbf{g}(t, \mathbf{c})$	the observation equations
$\ddot{\mathbf{z}}_1(t) = \mathbf{g}(t, \mathbf{c})$	
$\ddot{\mathbf{z}}_2(t) = \underline{\mathbf{M}}(\mathbf{x}_1(t), \mathbf{c})\, \mathbf{x}_2(t)$	
$\mathbf{z}_1^{(3)}(t) = \underline{\mathbf{M}}(\mathbf{x}_1(t), \mathbf{c})\, \mathbf{x}_2(t)$	
$\mathbf{z}_2^{(3)}(t) = \mathbf{x}_2(t)\, \dfrac{\partial}{\partial \mathbf{x}_1(t)} \underline{\mathbf{M}}(\mathbf{x}_1(t), \mathbf{c})\, \mathbf{x}_2(t) + \underline{\mathbf{M}}(\mathbf{x}_1(t), \mathbf{c})\, \mathbf{g}(t, \mathbf{c})$	

table 5-4: System of equations to test observability of the system 'Satellite Trajectory'

In the following chapter for the estimation of gravitational acceleration vectors that act on a satellite the state space description for time variant parameters from table 5-1 is used. The observability of this description for the estimation of the gravitational acceleration vectors has been shown above by means of the analytical approach.

Chapter 6

Estimation of gravitational acceleration vectors from given orbit data

'*The Kalman filter is a set of mathematical equations that provides an efficient computational (recursive) solution of the least-squares method. The filter is very powerful in several aspects: it supports estimations of past, present and even future states, and it can do so even when the precise nature of the modelled system is unknown.*'

Welch, Bishop (1996)

6-1 The problem

As a result of tracking a satellite using GPS, full three-dimensional position and velocity vectors with respect to the WGS84 are available. To be able to compute information on the gravitational field of the Earth from this data, it is necessary to determine the gravitational effects causing the satellite's movements. Thus for example, the gravitational acceleration vectors acting on the satellite at each point of time of observation have to be computed based on the position and velocity measurements of GPS.

In this chapter a way is presented to compute gravitational information in the form of gravitational acceleration vectors acting on the satellite from time series of three-dimensional position and velocity vectors using a Kalman filter method. First the basic idea and principles of Kalman filtering are concisely introduced. Based on these algorithms and the state space descriptions given in chapter 5 as well as the results of the observability analysis performed in section 5-1.2 and analytically in section 5-3.1, a Kalman filter method for the solution of the problem will be set up.

6-2 Purpose and principle of Kalman filtering

The original Kalman filter was published by R.E. Kalman in 1960 (Kalman (1960)) as a recursive solution to the linear filtering problem of discrete data. The classical Kalman filter is a linear procedure based on the method of least squares, that enables a prediction of the past, current and future states of a system as well as a set of additional parameters. Thus it is a vital tool for prediction, analysis and control purposes. Based on a time series of perturbed observations (system's output) and control and steering effects on the system (system's input or system's control respectively), the Kalman filter takes into account a priori knowledge of the dynamic behaviour of the system as well as a priori stochastic information on the initial states, the system's noise and the observation and control noise. Based on that data he provides a sequential solution for the estimation problem of a linear dynamic system. It is statistically optimal with respect to any quadratic function of error estimation (Grewal and Andrews (1993)). While the Kalman filter deals with discrete data, the so-called Kalman-Bucy filter is designed for continuous systems. The development of the filtering equations in the linear case can be found in any text book on Kalman filter, e.g. Grewal and Andrews (1993), G. and J. Minkler (1993), Chui and Chen (1989), Schrick (1977) or Brammer and Siffling (1985).

The main algorithm of the Kalman filter is split off into several major steps. First, a state space model for the system's behaviour has to be set up. This is usually done by means of a set of first order differential equations with respect to time which describes the temporal change in the state variables of the system. This model will not be exact due to modelling errors and effects either not precisely known or too complex to be modelled accurately. Remember from the introducing quotation that the system need not be known exactly. The model is described mathematically by the state transition equation (6-1). The only available information about the system is a time series of observations of either the state variables or a subset of them, or of functionals of the state variables, or a combination of all. For general systems a time series of input signals, e.g. control

and steering commands, but also external effects on the system's behaviour, is known or can be modelled. In the case of the system satellite orbit such external and steering effects could for example be orbit manoeuvres, but also further external perturbations. For the investigations of this thesis, such effects will not be taken into account.

The connection between the observations and the state vector is formulated by means of the measurement model (6-2). As far as the observation of functionals is concerned, this second model will also be inaccurate. To account for the uncertainties in the two models additive noise vectors for both the state transition as well as the observation model are introduced. Both vectors are assumed to be white noise.

In the following the main outline of the Kalman filter algorithm will be described. As for notation, in adjustment theory $\underline{\mathbf{P}}(t_k)$ usually denotes the weight matrix, being the inverse of the covariance matrix, which is denoted by $\underline{\mathbf{C}}_{\mathbf{x}}(t_k)$. The general notation in filtering theory (e.g. refer to Grewal and Andrews (1993), G. and J. Minkler (1993)) differs by using $\underline{\mathbf{P}}(t_k)$ for the covariance matrix itself. In this thesis the notation of the Kalman filtering theory will be used to keep up compatibility with the existing literature.

---

table 6-1: State space model - basic equations

time discrete *state transition equation*:

$$\mathbf{x}(t_{k+1}) = \mathbf{F}(\mathbf{x}(t_k), t_k) + \mathbf{w}(t_k) \tag{6-1}$$

$\mathbf{F}(\cdot, \cdot)$	...	process model,
$\mathbf{x}(t_k)$	...	stochastic state vector of the system at point of time t_k,
$\mathbf{w}(t_k)$	...	stochastic process noise vector.

time discrete *observation equation*:

$$\mathbf{z}(t_{k+1}) = \mathbf{H}(\mathbf{x}(t_{k+1}), t_{k+1}) + \mathbf{v}(t_{k+1}) \tag{6-2}$$

$\mathbf{H}(\cdot, \cdot)$	...	observation model,
$\mathbf{z}(t_{k+1})$	...	stochastic vector of observations at point of time t_{k+1},
$\mathbf{x}(t_{k+1})$	...	stochastic state vector of the system at point of time t_{k+1},
$\mathbf{v}(t_k)$	...	additive stochastic measurement noise vector.

additive white noise vectors:

$$
\begin{aligned}
E[\mathbf{w}] = E[\mathbf{v}] &= \mathbf{0} \\
E[\mathbf{w}(\mathbf{t_i})\,\mathbf{w}(\mathbf{t_j})^T] &= \delta_{ij}\,\underline{\mathbf{Q}} \\
E[\mathbf{v}(\mathbf{t_i})\,\mathbf{v}(\mathbf{t_j})^T] &= \delta_{ij}\,\underline{\mathbf{R}} \\
E[\mathbf{w}(\mathbf{t_i})\,\mathbf{v}(\mathbf{t_j})^T] &= \underline{\mathbf{0}}
\end{aligned}
$$

remark:
Since all vectors in eqns. (6-1) and (6-2) are stochastic vectors, the state transition and the observation equations both give the first order moments (expectation) of the predicted state and the observation vector, respectively. Thus they should be denoted as

$$\mathbf{E}\{\mathbf{x}(t_{k+1})\} = \mathbf{F}(\mathbf{E}\{\mathbf{x}(t_k)\}, t_k) \tag{6-3}$$

$$\mathbf{E}\{\mathbf{z}(t_{k+1})\} = \mathbf{H}(\mathbf{E}\{\mathbf{x}(t_{k+1})\}, t_{k+1}) \tag{6-4}$$

The notation in (6-1) and (6-2) will serve as an abbreviation in the further course of this thesis, that should always be understood in the sense of (6-3) and (6-4).

Starting with the known state $\mathbf{x}(t_k)$ and its covariance matrix $\underline{\mathbf{P}}_{\mathbf{x}}(t_k)$ at point of time t_k the prediction step of the Kalman filter computes an a priori estimate $\widehat{\mathbf{x}}^{(-)}(t_{k+1})$ for the state of the system and its covariance $\widehat{\underline{\mathbf{P}}}_{\mathbf{x}}^{(-)}(t_{k+1})$ at point of time t_{k+1} using the system dynamics model. Due to the model's inaccuracies, this prediction will not be exact. If there exists an observation made at t_{k+1}, the predicted state will be introduced to the measurement model to compute a predicted a priori measurement $\widehat{\mathbf{z}}^{(-)}(t_{k+1})$. This naturally will differ from the observation made in reality. In the following correction step of the filter, the so-called Kalman gain $\underline{\mathbf{G}}(t_{k+1})$ can be determined from the differences of the predicted and actually performed observations and the

measurement noise. This gain is used for a correction of the predicted states in such a way that the real and the predicted observations based on the predicted states match better in some sense. A more detailed definition of 'better in some sense' will be given below. For this correction the statistical properties of the states and observations are taken into account to find a somehow best solution. Thus modelling errors are considered and removed in a way the system matches the real observations and their accuracies.
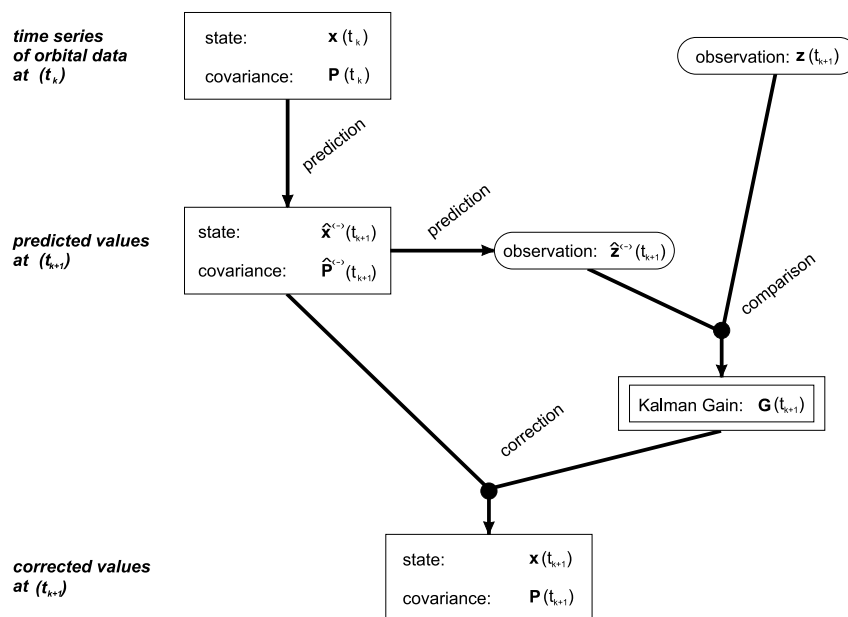

figure 6-1: Principle of Kalman filter

Let only mean and (co-)variance of a distribution be given and let in addition be assumed that the distribution is Gaussian, then the Kalman filter as an application of a linear operator to a Gaussian distribution yields another Gaussian distribution again. It can be shown, that the Kalman filter provides a best estimate of state and covariance of a system. This statement only holds for linear operators. 'Best' stands for a solution of the temporal system's prediction problem provided by the Kalman filter, where each state component has minimum variance of estimation error

$$\boldsymbol{\sigma}^2_{\mathbf{x}(t_{k+1})-\widehat{\mathbf{x}}(t_{k+1})} \longrightarrow min. \tag{6-5}$$

Note that neither the observations have to be direct observations of the system's states, nor all state variables have to be observed in some way or the other. This means that it is also possible to include additional parameters or unknown functionals of the parameters into the system's state vector. These additional values will not be observed directly, but they will be corrected together with the directly or indirectly measured values as long as the observability conditions of section 5-1.2 and 5-3.1 are fulfilled.

Thus the Kalman filter is an appropriate means for parameter estimation for complicated models. An example of the application of this quality of the filter is the system's description of the system satellite given in chapter 5. There the necessary number of independent state variables to describe the system is six, as we have seen in the introduction 2-2. Nevertheless the state vector is augmented by the components of the gravitational acceleration vector. This additional three components are not observed directly but in an indirect way by observing the other six state components, being position and velocity vector of the satellite. The connection between the observed essential state components and the additional parameters to be estimated is given by the system of observation equations and their derivatives with respect to time. By means of the Kalman filter algorithm the gravitational acceleration's components will also be estimated in the same corrected way as will be the observed state variables. This provides an efficient possibility of analysing an observed satellite trajectory's arc.

Only a very small number of real world problems can be modelled using linear state transition or observation equations. Thus one of the main requirements for the application of the classical Kalman filter is rarely satisfied. To apply the Kalman filtering methods to nonlinear problems, a linearisation process is a way to compute the predicted values, especially the predicted covariance.

For linearising a general nonlinear system's model two different approaches (see e.g. Schrick (1977), section XX, for further details) can be taken. Both consist of a Taylor series based linearisation process around (1) a nominal trajectory being known a priori, or (2) around the momentary estimation of the state vector. The first method of linearising around a known nominal trajectory requires a priori knowledge of the temporal behaviour of the state vector, which, to avoid high estimation errors, has to match the reality rather closely.

table 6-2: <u>Time-discrete Extended Kalman filter</u>

nonlinear dynamic model

$$\mathbf{x}(t_k) = \mathbf{F}(\mathbf{x}(t_{k-1}), t_{k-1}) + \mathbf{w}(t_{k-1}) \tag{6-6}$$

with system's noise

$$\mathbf{w}(t_k) \sim N(0, \underline{\mathbf{Q}}(t_k)) \tag{6-7}$$

and system's covariance matrix $\underline{\mathbf{Q}}(t_k)$

nonlinear measurement model

$$\mathbf{z}(t_k) = \mathbf{H}(\mathbf{x}(t_k), t_k) + \mathbf{v}(t_k) \tag{6-8}$$

with measurement's noise

$$\mathbf{v}(t_k) \sim N(0, \underline{\mathbf{R}}(t_k)) \tag{6-9}$$

and observations' covariance matrix $\underline{\mathbf{R}}(t_k)$

––––––––––––––––––––––––––––––––––-

prediction step
　　state prediction

$$\widehat{\mathbf{x}}^{(-)}(t_{k+1}) = \mathbf{F}(\mathbf{x}(t_k), t_k) \tag{6-10}$$

measurement prediction

$$\widehat{\mathbf{z}}^{(-)}(t_{k+1}) = \mathbf{H}(\widehat{\mathbf{x}}^{(-)}(t_{k+1}), t_{k+1}) \tag{6-11}$$

covariance prediction

$$\widehat{\underline{\mathbf{P}}}_{\mathbf{x}}^{(-)}(t_{k+1}) = \underline{\boldsymbol{\Phi}} \, \underline{\mathbf{P}}_{\mathbf{x}}(t_k) \, \underline{\boldsymbol{\Phi}}^T + \underline{\mathbf{Q}}(t_k) \tag{6-12}$$

with system dynamic's Jacobian at state's predicition

$$\underline{\boldsymbol{\Phi}} = \frac{\partial \mathbf{F}(\mathbf{x}(t_k), t_k)}{\partial \mathbf{x}} \Big|_{\mathbf{x} = \widehat{\mathbf{x}}^{(-)}(t_{k+1})} \tag{6-13}$$

––––––––––––––––––––––––––––––––––-

correction step
　　state correction

$$\mathbf{x}(t_{k+1}) = \widehat{\mathbf{x}}^{(-)}(t_{k+1}) + \underline{\mathbf{G}}(t_{k+1}) \, (\mathbf{z}(t_{k+1}) - \widehat{\mathbf{z}}^{(-)}(t_{k+1})) \tag{6-14}$$

covariance correction

$$\underline{\mathbf{P}}_{\mathbf{x}}(t_{k+1}) = \left(\underline{\mathbf{E}}_{\{dim(\underline{\mathbf{P}}_{\mathbf{x}})\}} - \underline{\mathbf{G}}(t_{k+1}) \, \underline{\mathbf{H}}(t_{k+1}) \right) \widehat{\underline{\mathbf{P}}}_{\mathbf{x}}^{(-)}(t_{k+1}) \tag{6-15}$$

with the so-called Kalman gain

$$\underline{\mathbf{G}}(t_{k+1}) = \widehat{\underline{\mathbf{P}}}_{\mathbf{x}}^{(-)}(t_{k+1}) \, \underline{\mathbf{H}}^T(t_{k+1}) \tag{6-16}$$
$$\cdot \left[\underline{\mathbf{H}}(t_{k+1}) \, \widehat{\underline{\mathbf{P}}}_{\mathbf{x}}^{(-)}(t_{k+1}) \, \underline{\mathbf{H}}^T(t_{k+1}) + \underline{\mathbf{R}}(t_{k+1}) \right]^{-1}$$

and the observation model's Jacobian at state's predicition

$$\underline{\mathbf{H}} = \frac{\partial \mathbf{H}(\mathbf{x}(t_k), t_k)}{\partial \mathbf{x}} \Big|_{\mathbf{x} = \widehat{\mathbf{x}}^{(-)}(t_{k+1})} \tag{6-17}$$

Thinking of the application for satellite orbit analysis, a nominal trajectory could be based on either an elliptic Kepler orbit caused by a homogeneous central field or a $\bar{c}_{2,0}$-perturbed orbit. Here trajectory does not mean the satellite's orbital position only, but the time series of the complete state vector. When analysing long orbit arcs the differences between the real orbit and the nominal orbit will be considerably high. Due to that, the method of linearisation around a nominal orbit proves not to be applicable. The second method of linearising around the momentary estimation directly leads to the Extended Kalman Filter (EKF).

6-3 The extended Kalman filter for nonlinear systems

While the original Kalman filter aims at solving problems based on linear process models the extended Kalman filter was set up to extend the methods of the linear case to nonlinear problems. It is used if either the system's state transition equation (6-1) or the observation equation (6-2) or both are nonlinear. Table 6-2 gives a summary of the formulae for the time discrete case of the EKF, the so-called discrete Extended Kalman filter (dEKF), based on the principles of the linear case. The explicit formulae for the case of a linear system's and measurement model can be found e.g. in Welch and Bishop (1996) or any other of the text books already referred to above. The Kalman filter formulae derived for the linear problem work linearly with respect to the observations but do not require the model equations themselves to be linear.

The system's state is predicted using the original nonlinear model while for the propagation of the covariance a linearisation is made. Assuming the size of the errors is small a Taylor series can be set up for the model (6-6) about the previously estimated state $\mathbf{x}(t_{k-1})$. Neglecting terms of second and higher order yields prediction formulae (6-12) for the covariance similar to the results of the general law of error propagation.

The formulae of the discrete Extended Kalman filter (dEKF) summarized in table 6-2 are intended to give a general overview over the principle steps of a Kalman filtering process. For the prediction as well as for the correction process several different methods some of which will be presented in the following sections are applicable. Which one to choose from this different methods highly depends on the system model used.

6-3.1 Prediction methods

State vector prediction

For the prediction of the state of a system the following integral equation must be solved:

$$\mathbf{x}(t_{k+1}) = \mathbf{F}(t, x(t_k)) = \mathbf{x}(t_k) + \int\limits_{t_k}^{t_{k+1}} \mathbf{f}(t', x(t_k)) \; dt' \quad . \tag{6-18}$$

For most real-world problems equation (6-18) will be highly nonlinear. It will probably not be possible to find a closed solution for the integral over the system's dynamics with respect to time in most cases. On the other hand using the observations of several state's components as given by the measurement model

$$\mathbf{z}(t_k) = \mathbf{H}(\mathbf{x}(t_k), t_k) + \mathbf{v}(t_k) \tag{6-19}$$

the state $\mathbf{x}(t_k)$ is known - at least an estimate for $\mathbf{x}(t_k)$ is known from the previous filtering step which is assumed to be reasonably close to the real state - and the integral equation can be solved by numerical integration. For that several of the well known integration methods can be used. In the following some of these methods are presented in a concise way. The question which method to choose mainly depends on the system. If the system's behaviour is rather smooth without any sudden or strong changes, a rather simple method of numerical integration will do. This holds so much the more as it has always to be kept in mind that the aim of the correction step in Kalman filtering is to account for errors made with the prediction due to modelling inaccuracies and also errors caused by the prediction method itself. These errors are eliminated to a certain extend by comparing the predicted with the observed state and finding a solution optimal in the sense of equation (6-5) when considering the accuracy of both. Thus the efforts for implementing a sophisticated numerical integration method should not be exaggerated.

The easiest way to get a state vector prediction is to use any sort of difference quotient. The shortcoming of this prediction method is the relative coarseness of approximation of the real system. Thus it is only applicable for observation series with relatively short time step length between the measurements. The general formulation of a forward difference quotient, in equation (6-20), and central difference quotient, in equation (6-21), is given.

$$\mathbf{x}(t_{k+1}) = \mathbf{x}(t_k) + \dot{\mathbf{x}}(t_k) \underbrace{(t_{k+1} - t_k)}_{=:\; dt} = \mathbf{F}^{\star}(\mathbf{x}(t_k), t_k, t_{k+1}) \tag{6-20}$$

$$\mathbf{x}(t_{k+1}) = \mathbf{x}(t_{k-1}) + \dot{\mathbf{x}}(t_k) \underbrace{(t_{k+1} - t_{k-1})}_{=:\; 2\; dt} = \mathbf{F}^{\star\star}(\mathbf{x}(t_k), t_{k-1}, t_k, t_{k+1}) \tag{6-21}$$

More sophisticated numerical integration techniques, like e.g. Runge-Kutta methods, can also be used to perform the state's prediction (see annex D for two examples of numerical integration methods). In the following the 6th order Runge-Kutta method will be used.

$$\mathbf{x}(t_{k+1}) = \mathbf{x}(t_k) + \frac{t_{k+1} - t_k}{336} \left(14\ \mathbf{K}_1 + 35\ \mathbf{K}_4 + 162\ \mathbf{K}_5 + 125\ \mathbf{K}_6\right) \tag{6-22}$$

where

$$\mathbf{K}_1 = \mathbf{f}\left(t_k, \mathbf{x}(t_k)\right)$$

$$\mathbf{K}_2 = \mathbf{f}\left(t_k + \frac{t_{k+1} - t_k}{2}, \mathbf{x}(t_k) + \frac{t_{k+1} - t_k}{2}\ \mathbf{K}_1\right)$$

$$\mathbf{K}_3 = \mathbf{f}\left(t_k + \frac{t_{k+1} - t_k}{2}, \mathbf{x}(t_k) + \frac{t_{k+1} - t_k}{2}\ \mathbf{K}_2\right)$$

$$\mathbf{K}_4 = \mathbf{f}\left(t_k + (t_{k+1} - t_k), \mathbf{x}(t_k) + (t_{k+1} - t_k)\ \mathbf{K}_3\right)$$

$$\mathbf{K}_5 = \mathbf{f}\left(t_k + \frac{2}{3}\ (t_{k+1} - t_k), \mathbf{x}(t_k) + \frac{t_{k+1} - t_k}{27}\ \left(7\ \mathbf{K}_1 + 10\ \mathbf{K}_2 + \mathbf{K}_4\right)\right)$$

$$\mathbf{K}_6 = \mathbf{f}\left(t_k + \frac{1}{5}\ (t_{k+1} - t_k), \mathbf{x}(t_k) + \frac{t_{k+1} - t_k}{625}\ \left(28\ \mathbf{K}_1 - 125\ \mathbf{K}_2 + 546\ \mathbf{K}_3 + 54\ \mathbf{K}_4 - 378\ \mathbf{K}_5\right)\right)\quad .$$

State covariance prediction

The prediction of the state's covariance matrix is a point that also strongly influences the decision of which integration method to choose. As stated in section 6-3 the covariance prediction is performed by applying the general law of error propagation to the state prediction formulae. The more complicated these formulae are, the more complicated and costly the computation of the covariance prediction will be. The first order error formula for covariance prediction, the so-called general law of error propagation, also given in table 6-2 is

$$\widehat{\mathbf{P}}_{\mathbf{x}}^{(-)}(t_{k+1}) = \underline{\mathbf{\Phi}}\ \underline{\mathbf{P}}_{\mathbf{x}}(t_k)\ \underline{\mathbf{\Phi}}^T + \underline{\mathbf{Q}}(t_k) \tag{6-23}$$

where $\underline{\mathbf{\Phi}}$ stands for the system dynamic's Jacobian at the state's prediction

$$\underline{\mathbf{\Phi}} = \frac{\partial \left(\mathbf{x}(t_k) + \int\limits_{t_k}^{t_{k+1}} \mathbf{f}(t', x(t_k))\ dt'\right)}{\partial \mathbf{x}}\Big|_{\mathbf{x} = \widehat{\mathbf{x}}^{(-)}(t_{k+1})}\quad . \tag{6-24}$$

From this procedure serious problems may arise for highly nonlinear systems. This will be covered in more detail in section 6-3.2.

Applying the general form of the law of error propagation to the difference quotient methods of state prediction, (6-20) and (6-21) presented above, yields prediction formulae for the state's covariance matrix $\underline{\mathbf{P}}_{\mathbf{x}}(t_k)$. The non-errorfree variables in equations (6-20) and (6-21) are the states $\mathbf{x}(t_k)$ and for (6-21) also $\mathbf{x}(t_{k-1})$. Their first-order derivatives $\dot{\mathbf{x}}(t_k)$ depend on the states. Thus the first-order derivatives of the state prediction equations for point of time t_{k+1} with respect to the states at the preceding point of time t_k and t_{k-1} yield

$$\frac{\partial}{\partial \mathbf{x}(t_k)} \mathbf{F}^{\star}(\mathbf{x}(t_k), t_k, t_{k+1}) = \underline{\mathbf{E}}_{(dim(\mathbf{x})x dim(\mathbf{x}))} + \frac{\partial}{\partial \mathbf{x}(t_k)} \dot{\mathbf{x}}(t_k)\ (t_{k+1} - t_k) \tag{6-25}$$

and

$$\frac{\partial}{\partial \mathbf{x}(t_k)} \mathbf{F}^{\star\star}(\mathbf{x}(t_k), t_k, t_{k+1}) = \frac{\partial}{\partial \mathbf{x}(t_k)} \dot{\mathbf{x}}(t_k)\ (t_{k+1} - t_{k-1})$$

$$\frac{\partial}{\partial \mathbf{x}(t_{k-1})} \mathbf{F}^{\star\star}(\mathbf{x}(t_k), t_k, t_{k+1}) = \underline{\mathbf{E}}_{(dim(\mathbf{x}) \times dim(\mathbf{x}))}\quad . \tag{6-26}$$

Following this example, the next section sets up a time-discrete EKF for the solution of the nonlinear problem of computing gravitational acceleration vectors from given position and velocity vectors of a satellite will presented. For the prediction a 6th order Runge-Kutta-method will be used.

6-3.2   Problems and shortcomings of the dEKF

When referring to the literature on the field of tracking and control there is a general consensus that the EKF is not an optimal method to solve and predict the behaviour of nonlinear systems. Despite the fact that it is

widely used, experience seems to have shown, that it is difficult to be tuned as well as to be implemented. Even worse, it only works reliably for nonlinear systems that are very near to linearity with respect to time (Julier and Uhlmann (1994b)).

The extended Kalman filter's purpose is to allow for an application of the formulae of the Kalman filter for linear systems even in the case of nonlinear systems. As already stated above, the Kalman filter provides a best estimate for the states as well as their covariance. In this sense it is optimal. Despite the fact, that the Extended Kalman filter uses the same formulae, it is usually non-optimal for nonlinear systems. The reason for that is, that the estimates of states, covariance and observations are all based on the assumption that the errors introduced by the linearisation are small. A good numerical example showing that the linearisation for the extended Kalman filter produces a non-optimal result can be found in Julier and Uhlmann (1996).

The linearisation is based on a cut-off Fourier series expansion of the state prediction formula.

State prediction:

$$\widehat{\mathbf{x}}(t_{k+1}) \quad = \quad \mathbf{x}(t_k) + \int_{t_k}^{t_{k+1}} \mathbf{f}(t', x(t_k)) \, dt' \tag{6-27}$$

$$\stackrel{\text{diff. quot.}}{\approx} \quad \mathbf{x}(t_k) + \dot{\mathbf{x}}(t_k) \, (t_{k+1} - t_k) \quad =: \quad \mathbf{F}(t, \mathbf{x}(t), \dot{\mathbf{x}}(t)) \tag{6-28}$$

Taylor series expansion about $\mathbf{x}(t_k)$ *and linearisation:*

$$\widehat{\mathbf{x}}(t_{k+1}) \quad \stackrel{\text{TAYLOR}}{=} \quad \mathbf{F}(t_k, \mathbf{x}(t_k), \dot{\mathbf{x}}(t_k)) + \frac{\partial}{\partial \mathbf{x}} \mathbf{F}(\cdot) \mid_{\mathbf{x}(t) = \mathbf{x}(t_k)} \, (\mathbf{x}(t) - \mathbf{x}(t_k))$$
$$+ \frac{1}{2!} \frac{\partial^2}{\partial \mathbf{x}^2} \mathbf{F}(\cdot) \mid_{\mathbf{x}(t) = \mathbf{x}(t_k)} \, (\mathbf{x}(t) - \mathbf{x}(t_k))^2 + \dots \tag{6-29}$$

$$= \quad \widehat{\mathbf{x}}(t_k) + \frac{\partial}{\partial \mathbf{x}} \widehat{\mathbf{x}}(t) \mid_{t=t_k} \, (\widehat{\mathbf{x}}(t_{k+1}) - \widehat{\mathbf{x}}(t))$$
$$+ \frac{1}{2!} \frac{\partial^2}{\partial \mathbf{x}^2} \widehat{\mathbf{x}}(t) \mid_{t=t_k} \, (\widehat{\mathbf{x}}(t_{k+1}) - \widehat{\mathbf{x}}(t))^2 + \dots \tag{6-30}$$

$$\stackrel{\text{lin.}}{\approx} \quad \widehat{\mathbf{x}}(t_k) + \frac{\partial}{\partial \mathbf{x}} \widehat{\mathbf{x}}(t) \mid_{t=t_k} \, (\widehat{\mathbf{x}}(t_{k+1}) - \widehat{\mathbf{x}}(t)) \tag{6-31}$$

Jacobian:

$$\underline{\boldsymbol{\Phi}} \mid_{\mathbf{x}(t_k)} = \widehat{\mathbf{x}}(t_k) + \frac{\partial}{\partial \mathbf{x}} \widehat{\mathbf{x}}(t) \mid_{t=t_k} \, (\widehat{\mathbf{x}}(t_{k+1}) - \widehat{\mathbf{x}}(t)) \tag{6-32}$$

General law of error propagation:

$$\widehat{\underline{\mathbf{P}}}_{\mathbf{x}}^{(-)}(t_{k+1}) = \underline{\boldsymbol{\Phi}} \mid_{\mathbf{x}(t_k)} \, \underline{\mathbf{P}}_{\mathbf{x}}(t_k) \, \underline{\boldsymbol{\Phi}}^T \mid_{\mathbf{x}(t_k)} \tag{6-33}$$

An rough estimate for the minimum linearisation error can be obtained from the quadratic term of the Fourier series (6-31), that is the first and presumably highest term to be neglected. Using a simple forward difference quotient for the prediction of the system's state with time (6-20) the related derivatives will have the form

$$\frac{\partial}{\partial \mathbf{x}} \widehat{\mathbf{x}}(t) \mid_{t=t_k} \quad = \quad \underbrace{\frac{\partial}{\partial \mathbf{x}} \widehat{\mathbf{x}}(t)}_{= \, \mathbf{E}} + (t_{k+1} - t_k) \frac{\partial}{\partial \mathbf{x}} \dot{\mathbf{x}}(t) \mid_{t=t_k} \tag{6-34}$$

$$\frac{\partial^2}{\partial \mathbf{x}^2} \widehat{\mathbf{x}}(t) \mid_{t=t_k} \quad = \quad (t_{k+1} - t_k) \frac{\partial^2}{\partial \mathbf{x}^2} \dot{\mathbf{x}}(t) \mid_{t=t_k} \quad . \tag{6-35}$$

The estimate for the linearisation error will then be

$$\epsilon_{min.} \quad \approx \quad \frac{t_{k+1} - t_k}{2} \frac{\partial^2}{\partial \mathbf{x}^2} \dot{\mathbf{x}}(t) \mid_{t=t_k} \, (\widehat{\mathbf{x}}(t_{k+1}) - \widehat{\mathbf{x}}(t))^2 \quad . \tag{6-36}$$

6-4   Time-discrete EKF methods for the determination of gravitational effects

In the following a time-discrete extended Kalman filter (dEKF) method is presented for the computation of the gravitational acceleration vector acting on a satellite orbiting the Earth based on the state space descriptions introduced in chapter 5. The observed data being the basis for this computation are full three-dimensional position and velocity vectors given with respect to a space fixed geocentric equatorial Cartesian reference system. Only the forces caused by the Earth's gravitational field will be considered.
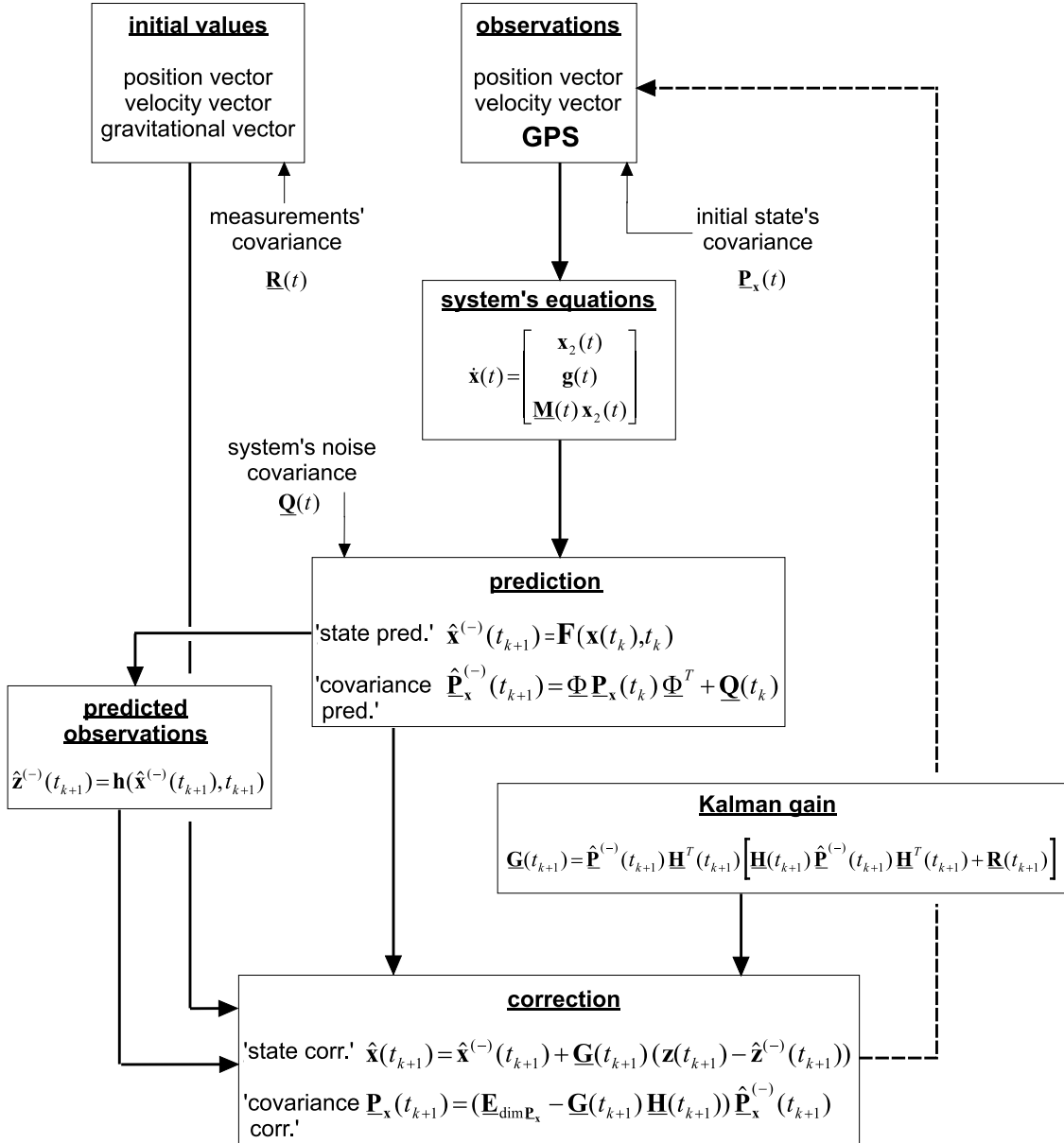
figure 6-2: dEKF's flowchart

The state vector of the satellite is of dimension 9:

$$\mathbf{x}(t_k) = [\ \underbrace{x(t_k), y(t_k), z(t_k)}_{\text{position } \mathbf{x}_1(t_k)}\ ,\ \underbrace{\dot{x}(t_k), \dot{y}(t_k), \dot{z}(t)_k}_{\text{velocity } \mathbf{x}_2(t_k)}\ ,\ \underbrace{g_x(t_k), g_y(t_k), g_z(t_k)}_{\text{grav. acc. } \mathbf{g}(t_k)}\ ]^T \quad . \tag{6-37}$$

The first order derivative of the state vector with respect to time t yields the satellite system's dynamics

$$\mathbf{f}(t, \mathbf{x}(t_k)) := \dot{\mathbf{x}}(t_k) = \begin{bmatrix} \mathbf{x}_2(t_k) \\ \mathbf{g}(t_k) \\ \underline{\mathbf{M}}(t_k)\ \mathbf{x}_2(t_k) \end{bmatrix} \quad . \tag{6-38}$$

For the prediction of the state at point of time t_{k+1} we have to solve the following equation.

$$\mathbf{x}(t_{k+1}) = \mathbf{x}(t_k) + \int_{t_k}^{t_{k+1}} \begin{bmatrix} \mathbf{x}_2(t') \\ \mathbf{g}(t') \\ \underline{\mathbf{M}}(t')\, \mathbf{x}_2(t') \end{bmatrix} dt' \tag{6-39}$$

To solve this equation the 6th order Runge-Kutta method given in (6-22) and (6-23) is used. Keep in mind that the first parameter t of the function $\mathbf{f}(t, \mathbf{x}(t))$ stands for explicit time dependencies in the system dynamics. If considering only gravitational effects of the Earth by use of a standard gravitational model these effects are time invariant with respect to the Earth fixed geocentric equatorial reference system. An explicit time dependency arises if the model would be formulated and computed with respect to a space fixed reference system (see also chapter 3 on page 26). There, the gravitational field appears to be time variant, because it is rotating together with the Earth. This effect is accounted for by a transformation of the satellite's position vector from the space to the Earth fixed system before evaluating the gravitational model and a transformation back of the values computed as shown in the diagram of table 6-3. An explicit time dependency will arise if other perturbing effects are considered that do not solely depend on the satellite's position and velocity. Table 6-4 gives a short overview of the main perturbing effects and the quantities they are influenced by. Thus for the case presented here an explicit time dependency does not have to be taken into account. In this special case the formulae for the 6th order Runge-Kutta method simplify in the following way

$$\mathbf{K}_1(\mathbf{x}(t_k)) = \begin{bmatrix} \mathbf{x}_2(t_k) \\ \mathbf{g}(t_k) \\ \underline{\mathbf{M}}(t_k)\, \mathbf{x}_2(t_k) \end{bmatrix} \tag{6-40}$$

$$\mathbf{K}_2(\mathbf{x}(t_k)) = \begin{bmatrix} \mathbf{x}_2(t_k) + \dfrac{t_{k+1} - t_k}{2}\, \mathbf{x}_2(t_k) \\ \mathbf{g}(t_k) + \dfrac{t_{k+1} - t_k}{2}\, \mathbf{g}(t_k) \\ \underline{\mathbf{M}}(t_k)\, \mathbf{x}_2(t_k) + \dfrac{t_{k+1} - t_k}{2}\, \underline{\mathbf{M}}(t_k)\, \mathbf{x}_2(t_k) \end{bmatrix} = \begin{bmatrix} \mathbf{x}_2(t_k) \\ \mathbf{g}(t_k) \\ \underline{\mathbf{M}}(t_k)\, \mathbf{x}_2(t_k) \end{bmatrix} (1 + \dfrac{t_{k+1} - t_k}{2}) \tag{6-41}$$

$$\mathbf{K}_3(\mathbf{x}(t_k)) = \quad etc.\ by\ analogy$$

which leads to

$$\mathbf{x}(t_{k+1}) = \mathbf{x}(t_k) + \underbrace{\left(15837 + \frac{85847}{54}\, dt + 9991\, dt^2 + \frac{3297}{4}\, dt^3 - 2\, dt^4 \right)}_{=:\ \tau} \begin{bmatrix} \mathbf{x}_2(t_k) \\ \mathbf{g}(t_k) \\ \underline{\mathbf{M}}(t_k)\, \mathbf{x}_2(t_k) \end{bmatrix} \tag{6-42}$$

For the prediction of the covariance by means of the general law of error propagation the first order partial derivatives of the system's model equations with respect to the inaccurate state components are needed.

$$\begin{array}{llll}
\dfrac{\partial \mathbf{x}_2(t)}{\partial \mathbf{x}_1} = \underline{\mathbf{0}}_{3\times3} & \dfrac{\partial \mathbf{g}(t)}{\partial \mathbf{x}_1} = \tau\, \underline{\mathbf{M}}_{3\times3}(t) & \dfrac{\partial\, (\underline{\mathbf{M}}(t)\, \mathbf{x}_2(t))}{\partial \mathbf{x}_1} = \tau\, \mathbf{x}_2(t)\, \dfrac{\partial \underline{\mathbf{M}}(t)}{\partial \mathbf{x}_1} & \\[3mm]
\dfrac{\partial \mathbf{x}_2(t)}{\partial \mathbf{x}_2} = \tau\, \underline{\mathbf{E}}_{3\times3} & \dfrac{\partial \mathbf{g}(t)}{\partial \mathbf{x}_2} = \underline{\mathbf{0}}_{3\times3} & \dfrac{\partial\, (\underline{\mathbf{M}}(t)\, \mathbf{x}_2(t))}{\partial \mathbf{x}_2} = \tau\, \underline{\mathbf{M}}(t) & \tag{6-43} \\[3mm]
\dfrac{\partial \mathbf{x}_2(t)}{\partial \mathbf{g}} = \underline{\mathbf{0}}_{3\times3} & \dfrac{\partial \mathbf{g}(t)}{\partial \mathbf{g}} = \tau\, \underline{\mathbf{E}}_{3\times3} & \dfrac{\partial\, (\underline{\mathbf{M}}(t)\, \mathbf{x}_2(t))}{\partial \mathbf{g}} = \underline{\mathbf{0}}_{3\times3} &
\end{array}$$

These partial derivatives form the system dynamic's Jacobian with respect to the state's components.

$$\underline{\boldsymbol{\Phi}} = \underline{\mathbf{E}}_{9\times9} + \begin{bmatrix} \dfrac{\partial \mathbf{x}_2(t)}{\partial \mathbf{x}_1} & \dfrac{\partial \mathbf{x}_2(t)}{\partial \mathbf{x}_2} & \dfrac{\partial \mathbf{x}_2(t)}{\partial \mathbf{g}} \\[3mm] \dfrac{\partial \mathbf{g}(t)}{\partial \mathbf{x}_1} & \dfrac{\partial \mathbf{g}(t)}{\partial \mathbf{x}_2} & \dfrac{\partial \mathbf{g}(t)}{\partial \mathbf{g}} \\[3mm] \dfrac{\partial\, (\underline{\mathbf{M}}(t)\, \mathbf{x}_2(t))}{\partial \mathbf{x}_1} & \dfrac{\partial\, (\underline{\mathbf{M}}(t)\, \mathbf{x}_2(t))}{\partial \mathbf{x}_2} & \dfrac{\partial\, (\underline{\mathbf{M}}(t)\, \mathbf{x}_2(t))}{\partial \mathbf{g}} \end{bmatrix} \tag{6-44}$$

table 6-3: <u>Computation of gravitational effects</u>

For the transformation between Earth-fixed and space-fixed systems only the Greenwich sidereal time, i.e. the effect of the Earth's rotation, is considered here. For a detailed treatment of the transformation problem refer to section 2-3.

X, Y, Z satellite's position   *space-fixed system*

$\downarrow$ $[x \ y \ z]^T = \underline{\mathbf{R}}_3(\Theta_{Greenwich}) \ [X \ Y \ Z]^T$

x, y, z satellite's position   *Earth-fixed system*

$\downarrow$ eqns. (3-23), (3-27) and (3-38), (3-41)

$\mathbf{g}_{x,y,z}, \underline{\mathbf{M}}_{x,y,z}$ gravitational quantities   *Earth-fixed system*

$\downarrow$ $\mathbf{g}_{X,Y,Z} = \underline{\mathbf{R}}_3(\Theta_{Greenwich})^T \ \mathbf{g}_{x,y,z}$

$\mathbf{g}_{X,Y,Z}, \underline{\mathbf{M}}_{X,Y,Z}$ gravitational quantities   *space-fixed system,*

('system' in this table always stands for geocentric Cartesian equatorial reference system)

table 6-4: <u>Time dependencies of perturbation effects</u>

dependency on position and/or velocity vector of satellite only

- gravitational effects of the Earth (if considered with respect to an Earth-fixed geocentric equatorial system),

- aerodynamic effects lift and drag (if time independent rotational symmetric atmospheric density models are used).

dependency on position and/or velocity vector <u>and</u> time

- gravitational effects of the Earth (if considered with respect to a space-fixed geocentric equatorial system),

- gravitational effects of other celestial bodies and tides of Earth and oceans,

- aerodynamic effects lift and drag (if time dependent non-rotational symmetric atmospheric density models are used and/or the atmosphere is not considered to rotate together with the Earth),

- solar and Earth radiation effects.

The measurement model has the form given in equation (5-17). For the computation of the Kalman gain the Jacobian of the measurement model's equations with respect to time is needed. Since the observation equations of the measurement model are linear for the special case of a GPS tracked mission, the structure of $\underline{\mathbf{H}}$ is quite simple.

$$\underline{\mathbf{H}} = \begin{bmatrix} \underline{\mathbf{E}}_{3\times 3} & \underline{\mathbf{0}}_{3\times 3} & \underline{\mathbf{0}}_{3\times 3} \\ \underline{\mathbf{0}}_{3\times 3} & \underline{\mathbf{E}}_{3\times 3} & \underline{\mathbf{0}}_{3\times 3} \end{bmatrix} \tag{6-45}$$

table 6-5: <u>dEKF for determination of gravitational acceleration vector</u>

(*Special case: Earth's gravitational effects only*)

state space vector

$$\mathbf{x}(t_k) = [\ \underbrace{x(t_k), y(t_k), z(t_k)}_{\text{position}}\ ,\ \underbrace{\dot{x}(t_k), \dot{y}(t_k), \dot{z}(t)_k}_{\text{velocity}}\ ,\ \underbrace{g_x(t_k), g_y(t_k), g_z(t_k)}_{\text{grav. acc.}}\ ]^T \qquad (6\text{-}46)$$

state prediction (based on 6th order Runge-Kutta method)

$$\mathbf{x}(t_{k+1}) = \mathbf{x}(t_k) + \left(15837 + \frac{85847}{54}\ dt + 9991\ dt^2 + \frac{3297}{4}\ dt^3 - 2\ dt^4\right) \begin{bmatrix} \mathbf{x}_2(t_k) \\ \mathbf{g}(t_k) \\ \underline{\mathbf{M}}(t_k)\ \mathbf{x}_2(t_k) \end{bmatrix} \qquad (6\text{-}47)$$

system dynamic's Jacobian

$$\underline{\mathbf{\Phi}} = \begin{bmatrix} \underline{\mathbf{E}}_{3\times3} & \tau\ \underline{\mathbf{E}}_{3\times3} & \underline{\mathbf{0}}_{3\times3} \\[2mm] \tau\ \underline{\mathbf{M}}_{3\times3}(t) & \underline{\mathbf{E}}_{3\times3} & \tau\ \underline{\mathbf{E}}_{3\times3} \\[2mm] (\tau\ \mathbf{x}_2(t)\ \frac{\partial \underline{\mathbf{M}}(t)}{\partial \mathbf{x}_1(t)})_{3\times3} & \tau\ \underline{\mathbf{M}}_{3\times3}(t) & \underline{\mathbf{E}}_{3\times3} \end{bmatrix} \qquad (6\text{-}48)$$

system's covariance prediction

$$\widehat{\underline{\mathbf{P}}}_{\mathbf{x}}^{(-)}(t_{k+1}) = \underline{\mathbf{\Phi}}\ |_{\mathbf{x}(t_k)}\ \underline{\mathbf{P}}_{\mathbf{x}}(t_k)\ \underline{\mathbf{\Phi}}^T\ |_{\mathbf{x}(t_k)} + \mathbf{Q}(t_k) \qquad (6\text{-}49)$$

with

$$\begin{aligned} \underline{\mathbf{Q}}(.) &\quad \dots \quad \text{process noise covariance matrix,} \\ \underline{\mathbf{E}}_{n\times n} &\quad \dots \quad \text{n times n unit matrix,} \\ \underline{\mathbf{M}}(.) &\quad \dots \quad \text{gravitational gradient tensor (see chapter 3).} \end{aligned}$$

$$\tau = \left(15837 + \frac{85847}{54}\ dt + 9991\ dt^2 + \frac{3297}{4}\ dt^3 - 2\ dt^4\right)$$

6-4.1 Results of the dEKF method

Using the discrete extended Kalman filter method presented above in table 6-5, the gravitational acceleration vectors for an 12,5 h (45000 s) long orbit arc have been determined. For the orbit arc a simulated CHAMP scenario has been used. CHAMP will be tracked by GPS receivers, thus a time series of complete three-dimensional position and velocity vectors with respect to the quasi-Earth-fixed geocentric equatorial Cartesian reference system WGS84 will be available. The expected time step length is 10 s. Considering a mean velocity of about 7 km/s, this yields a step width of about 70 km. The simulated CHAMP orbit is created by numerical integration of the satellite's equations of motion (2-1) taking into account gravitational effects on the satellite by means of the EGM96 model up to degree and order 90. Numerical integration was performed by means of a 12th-order Adams-Moulton / Adams-Bashford multistep method (annex D). As for control, the gravitational acceleration vectors themselves are computed together with the numerical integration evaluating the EGM96 model up to degree and order 90 also.

The figures 6-3 and 6-5 show the differences between the norm of the precomputed position, velocity and gravitational acceleration vectors and the results of the prediction step of the filter and the final filtering result, respectively. Since the prediction of the gravitational acceleration vector is based on a spherical harmonics gravitational field model taking into account the term of degree zero and $\bar{c}_{2,0}$ only, the filter needs a certain but very short time to adjust to the control values. This can be clearly seen in the plots of the RMS values. For the other figures 6-3 and 6-5 the first 2 states have been omitted to guarantee better representation of the data.

This is also true for figure 6-6 presenting the RMS values for the components of the three vectors forming the satellite's state vector.
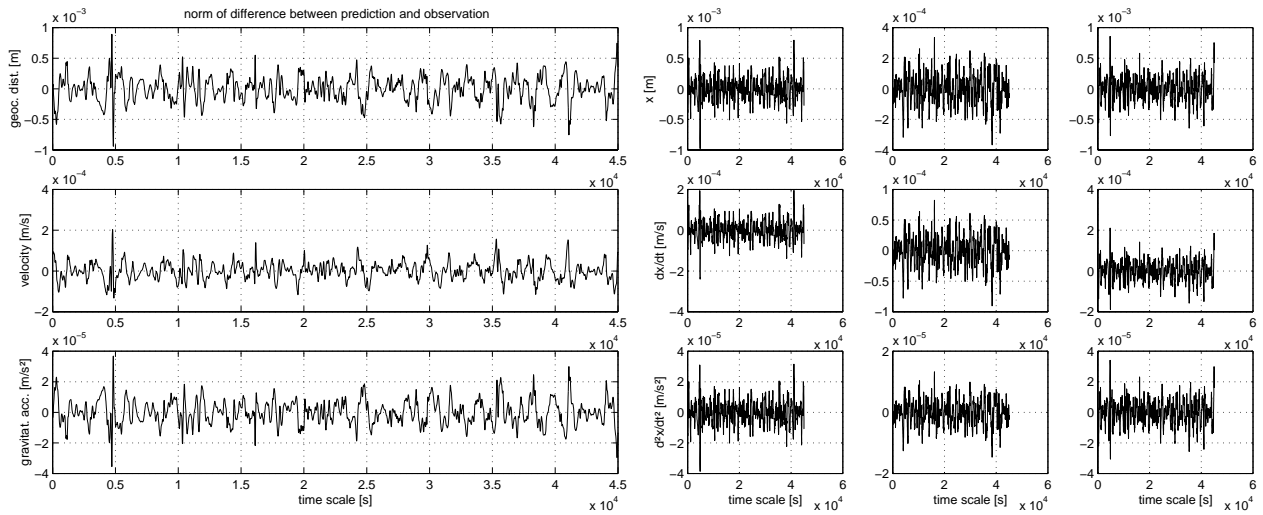
figure 6-3: Differences between __prediction__ step results of filter (6-46)...(6-48) and control values
(*left*: norm of vectors, *right*: components)
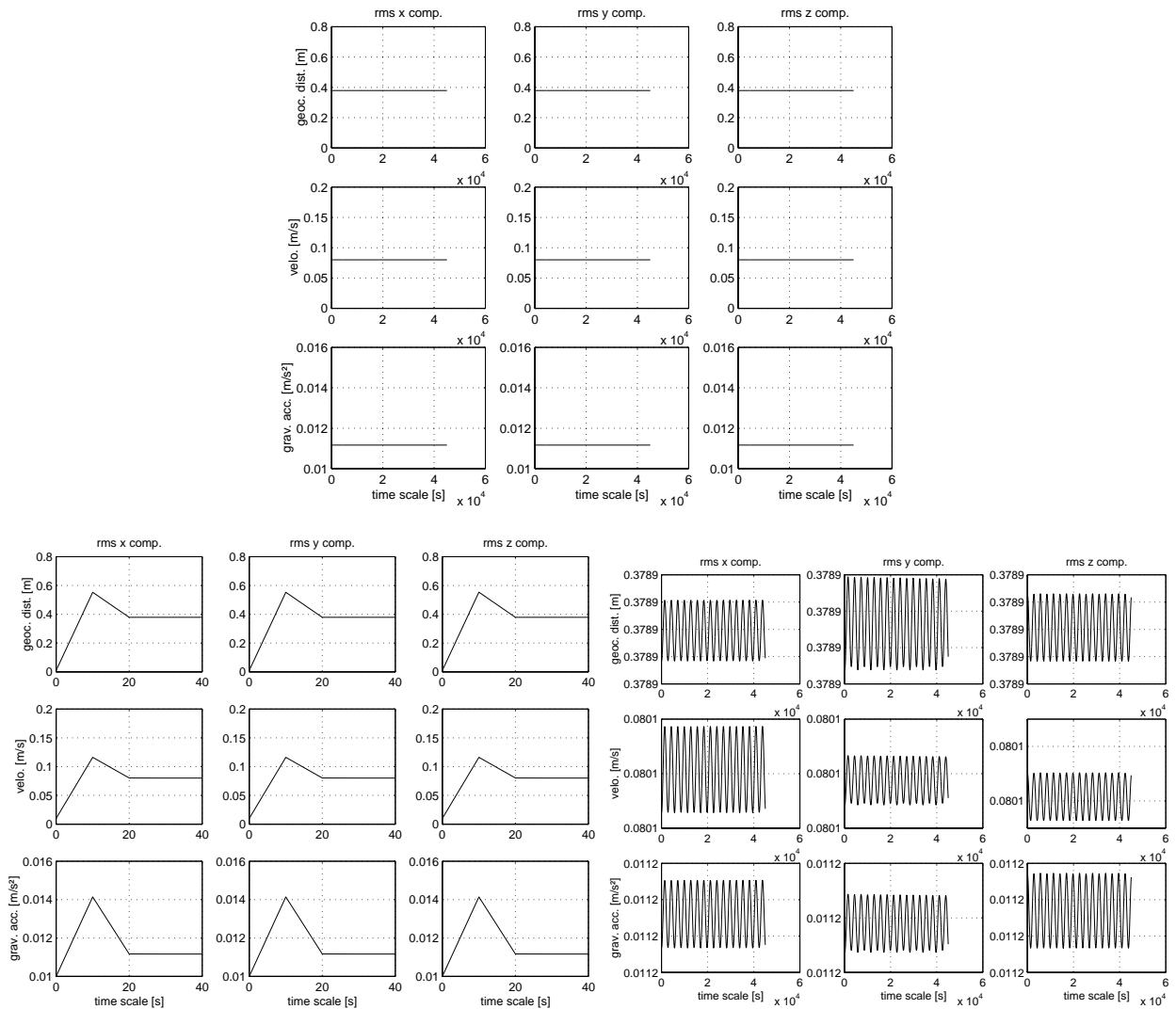
figure 6-4: RMS of __prediction__ step results
(*up*: complete view, *lower left*: states 1 to 5, *lower right*: states 5 up)
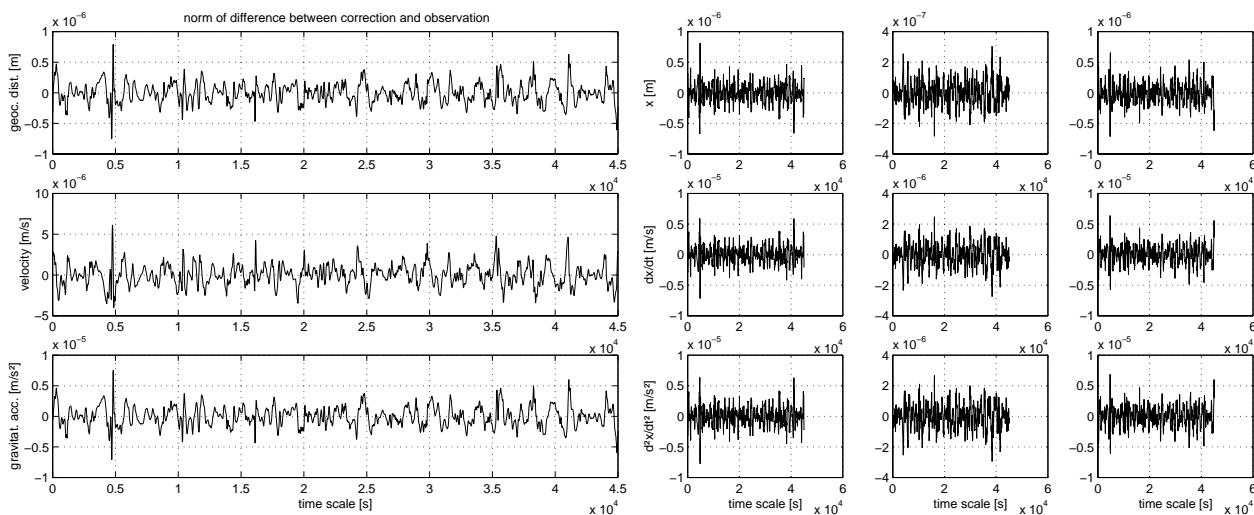
figure 6-5: Differences between **final** (correction step) results of filter (6-14)...(6-17) and control values
(*left*: norm of vectors, *right*: components)
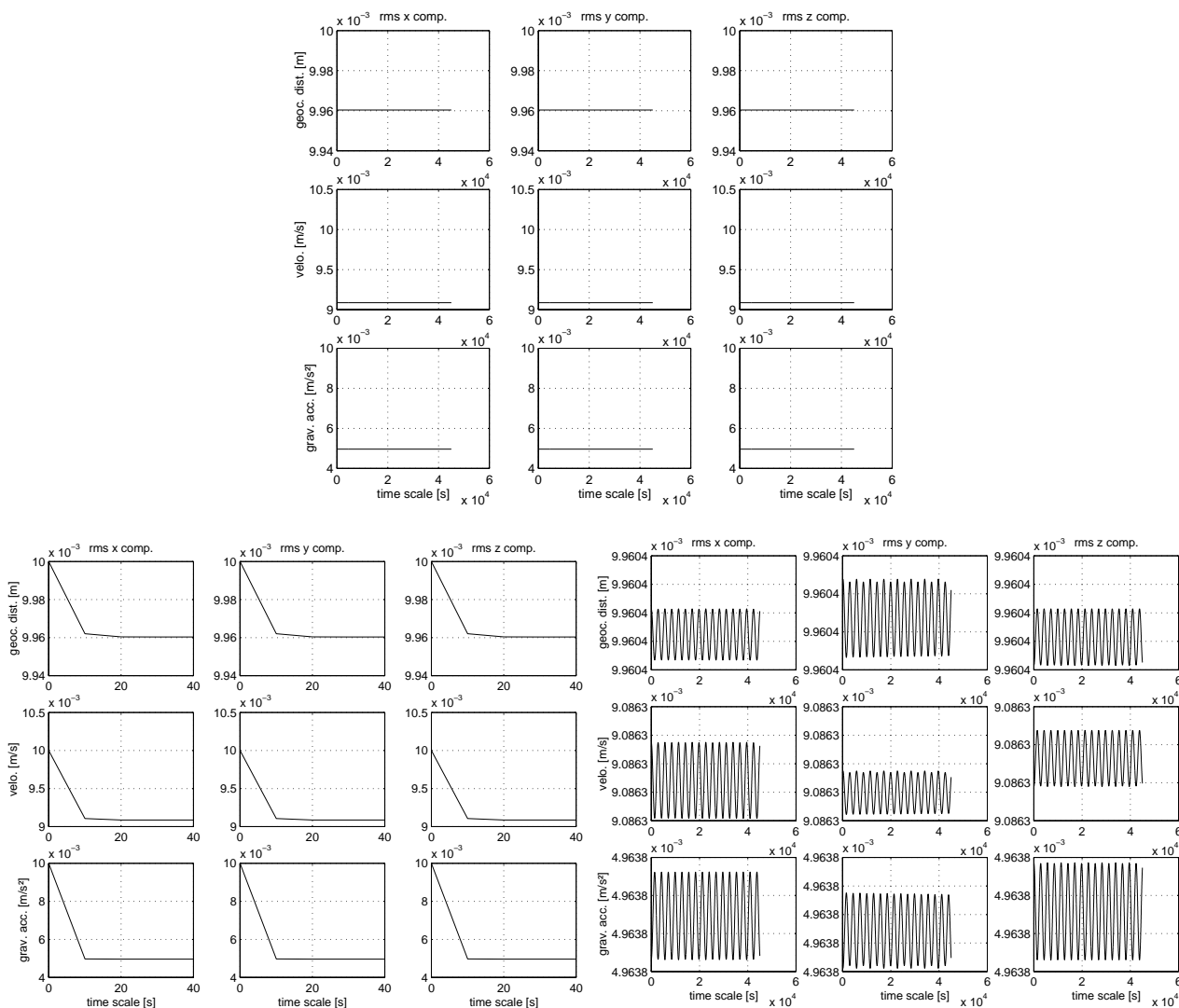
figure 6-6: RMS of **final** (correction step) results
(*up*: complete view, *lower left*: states 1 to 5, *lower right*: states 5 up)

ORBIT DATA

Chapter 7

Spectral analysis of the CHAMP mission

In this chapter the spectral analysis for a sample orbit of the CHAMP mission will be performed. The outline of the spectral analysis method has already been presented in the introductory chapter. A point that has not yet been referred to in the previous chapters is how to define an appropriate selection criterion for the selection of the major influences on the satellite's orbit which is to be analyzed. This important question will be addressed in detail in the respective sections 7-4 and 7-3.

table 7-1: CHAMP $200'000\ s\ (=\ 2^d\ 7^h\ 33^{mn}\ 20^s)$ orbit scenario

initial state vector with respect to WGS84:

$$[\ \underbrace{-113.604674 \cdot 10^3,\ 339.528581 \cdot 10^3,\ 6831.624647 \cdot 10^3}_{\text{position [m]}}\ \underbrace{-7.238785 \cdot 10^3,\ -2.422064 \cdot 10^3,\ 0.000000}_{\text{velocity [m/s]}}\ ]$$

or in Keplerian elements

$$\text{a} = 6841\ km,\ \text{i} = 87°,\ \text{e} = 0,\ \text{RAAN} = 18°30',\ \omega = 90°,\ \text{M} = \text{E} = \nu = 0°$$
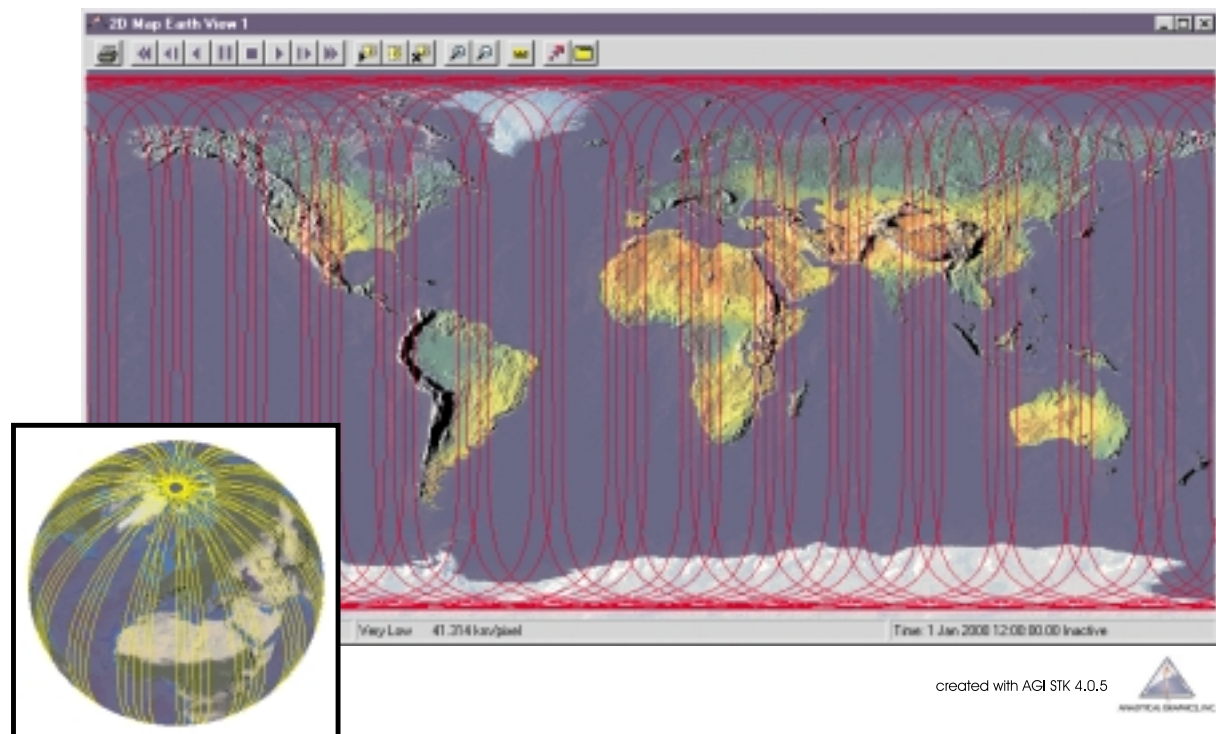
figure 7-1: Simulated CHAMP orbit and polar gap

As already hinted at before, the spectral analysis method can serve for two main purposes: the orbit sensitivity analysis on the one hand and, on the other hand, it can provide a means to simplify the orbit computation for certain tasks. 'Simplify' has to be understood with respect to computational efforts and efforts necessary to represent and/or store the orbital information in a way that enables a fast and effective reconstruction.

The simulated trajectory of the satellite CHAMP consists of 29 revolutions. This is a length of orbit arc of $1^d \ 21^h \ 30^{mn} \ 40^s$) which equals $16384 (= 2^{14})$ observations à $10 \ s$ observation step length. The length of the arc has been chosen as a power of 2 in order to take advantage of the higher accuracy of the standard fast Fourier transformation (FFT) methods.

- **1st step**: orbit simulation, computation of orbital position and velocity vectors with respect to the WGS84 by means of a 12th order Adams-Moulton/Adams-Bashforth multistep numerical integration method (see annex D) for integration of the satellite's equation of motion.

- **2nd step**: computation of gravitational acceleration vectors from the orbit data by means of a nonlinear discrete extended Kalman filter method (see chapter 6). By subtraction of the gravitational values of a reference orbit, e.g. a Kepler or a precessing Kepler orbit, the perturbations are obtained.

- **3rd step**: componentwise Fourier frequency analysis of the orbit data by means of a fast Fourier transformation (FFT).

- **4th step**: selection of the frequencies with respect to an appropriate selection criterion which will be presented in detail in the following. The most important frequencies influencing and perturbing the orbit are found here.

- **5th step**: computation of the lumped coefficients for the selected frequencies (see chapter 4, especially section 4-3).

- **6th step**: selection of the (surface) spherical harmonics which have the strongest influence in the lumped coefficients as possible candidates for the orbit analysis. This second selection criterion will also be defined in the following.

7-1   1st step: Computation of orbit data

By application of numerical integration methods the equation of motion (2-1) of the satellite, being a vector valued second order ordinary differential equation with respect to time, can be solved to predict the satellite's trajectory. The numerical integration method applied in this case is a 12th order Adams-Moulton/Adams-Bashforth multistep method (annex D). Test computations of the implementation showed a good behaviour of the integration error. A simple Kepler orbit, that has to be a closed ellipse, fulfils that condition with a maximum error of a position component of $4 \cdot 10^{-4} \ m$ after 35 revolutions computed. The complete results for these tests can be seen in figure 7-2 for 35 revolutions and the numerical integration methods 12th order Adams-Moulton/Adams-Bashforth multistep and 6th order Runge-Kutta.
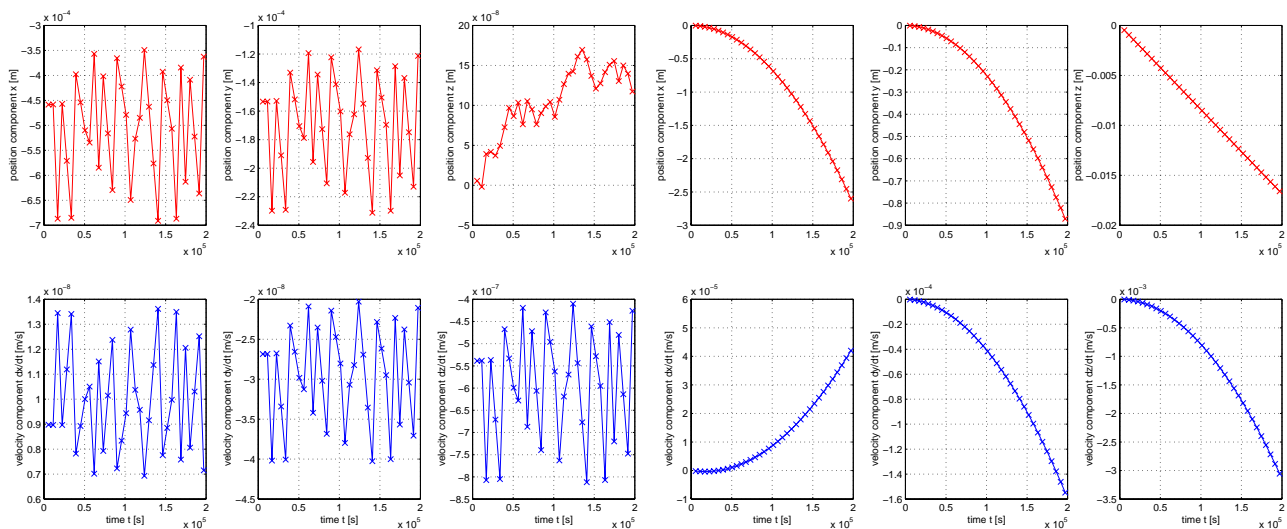
figure 7-2: Orbital closing error due to numerical integration method for an ideal Kepler ellipse and 35 revolutions plotted componentwise for position (top line) and velocity (bottom line)
(*6 fig. on the left*: 12th order Adams-Moulton / Adams-Bashforth, *6 fig. on the right*: 6th order Runge-Kutta)
Note that the scale of the y axes is not uniform to guarantee better readability

For a detailed discussion of the application of either of these methods refer to Sanz-Serna (1992), also especially the references given in that paper.

The initial values underlying the simulated CHAMP orbit to be generated as well as a graphical representation of the orbit's footprint are given in table 7-1.

7-2   2nd step: Determination of gravitational acceleration vectors

The determination of gravitational acceleration vectors from the satellite's position and velocity vectors' data will be performed by means of the discrete Extended Kalman filter method dEKF presented in section 6-4.
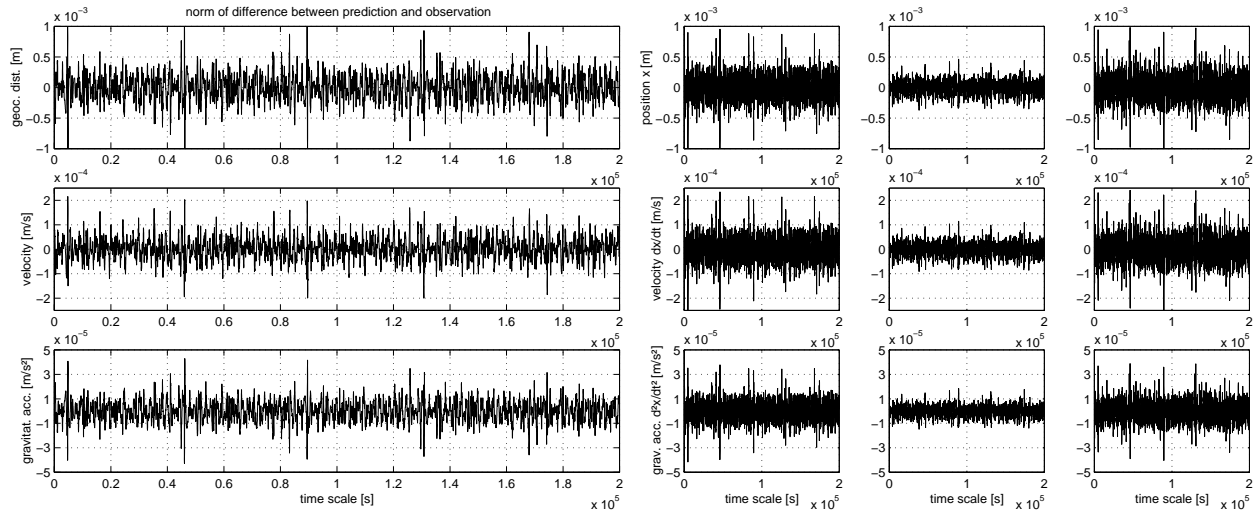
figure 7-3: Differences between **prediction** step results of filter (6-46)...(6-48) and control values (*left*: norm of vectors, *right*: components)
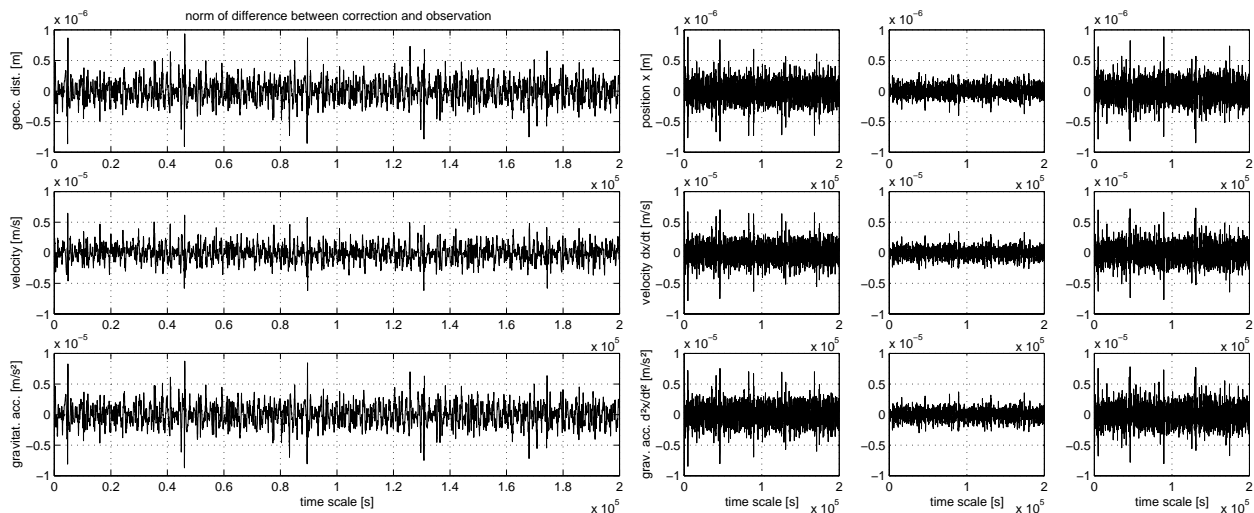
figure 7-4: Differences between **final** (correction step) results of filter (6-14)...(6-17) and control values (*left*: norm of vectors, *right*: components)

7-3   3rd to 6th step: Spectral analysis for approximate orbit synthesis

To detect the frequencies within the orbital and gravitational signal a Fourier transformation is applied to the components of the orbital data vectors. The following tables and figures show the spectral analysis' results for the simulated CHAMP orbit. First the spectral analysis of the position data for orbit approximation is presented, the spectral analysis of gravitational acceleration data for orbit sensitivity analysis follows.

7-3.1 Fourier analysis of orbital position data

The satellite's position vector for the complete sample trajectory is the basis for the Fourier analysis for the purpose of orbit synthesis based on reduced information on the orbit. Table 7-2 gives the Fourier coefficients in descending order with respect to their part of the complete signal power. The listing is broken off as soon as 99.999% of the signal power are reached. The index column gives the respective Fourier coefficient's index, the 1st and 2nd column give the period length in seconds and divided into days-hours-minutes-seconds, the 3rd column gives the respective frequency, the 4th column the percentage of total signal power for each coefficient and for the 5th column these percentage values are accumulated.

index	p [sec/rev.]		f [rev./sec]	% of complete signal power (cumulative)	
29	$5.649655172 \ 10^3$	(0d 01h 34m 10s)	$1.770019531 \ 10^{-4}$	99.987982	(99.9879823)
28	$5.851428571 \ 10^3$	(0d 01h 37m 31s)	$1.708984375 \ 10^{-4}$	0.003677	(99.9916597)
30	$5.461333333 \ 10^3$	(0d 01h 31m 01s)	$1.831054688 \ 10^{-4}$	0.003565	(99.9952245)
27	$6.068148148 \ 10^3$	(0d 01h 41m 08s)	$1.647949219 \ 10^{-4}$	0.000919	(99.9961434)
31	$5.285161290 \ 10^3$	(0d 01h 28m 05s)	$1.892089844 \ 10^{-4}$	0.000898	(99.9970414)
26	$6.301538462 \ 10^3$	(0d 01h 45m 02s)	$1.586914063 \ 10^{-4}$	0.000410	(99.9974516)
32	$5.120000000 \ 10^3$	(0d 01h 25m 20s)	$1.953125000 \ 10^{-4}$	0.000400	(99.9978520)
25	$6.553600000 \ 10^3$	(0d 01h 49m 14s)	$1.525878906 \ 10^{-4}$	0.000224	(99.9980764)
33	$4.964848485 \ 10^3$	(0d 01h 22m 45s)	$2.014160156 \ 10^{-4}$	0.000220	(99.9982959)
24	$6.826666667 \ 10^3$	(0d 01h 53m 47s)	$1.464843750 \ 10^{-4}$	0.000147	(99.9984433)
34	$4.818823529 \ 10^3$	(0d 01h 20m 19s)	$2.075195312 \ 10^{-4}$	0.000143	(99.9985862)
58	$2.824827586 \ 10^3$	(0d 00h 47m 05s)	$3.540039062 \ 10^{-4}$	0.000130	(99.9987163)
23	$7.123478261 \ 10^3$	(0d 01h 58m 43s)	$1.403808594 \ 10^{-4}$	0.000103	(99.9988194)
35	$4.681142857 \ 10^3$	(0d 01h 18m 01s)	$2.136230469 \ 10^{-4}$	0.000099	(99.9989188)
22	$7.447272727 \ 10^3$	(0d 02h 04m 07s)	$1.342773438 \ 10^{-4}$	0.000076	(99.9989952)
36	$4.551111111 \ 10^3$	(0d 01h 15m 51s)	$2.197265625 \ 10^{-4}$	0.000073	(99.9990684)

table 7-2: Fourier coefficients for a perturbed CHAMP orbit (EGM96 up to degree & order 90) in descending order with respect to their signal power (explanation of columns see text)

7-3.2 Results for orbit synthesis

Considering the results of the orbital data's frequency analysis the idea is to reduce the computational efforts for orbit synthesis by determining the most important frequencies of the position data of the orbit. The orbit will then be presented by a small set of coefficients containing a certain percentage of the complete signal (= time series of position vectors) power sufficient for the needed accuracy of the approximation.

Consider the case that an orbit of a satellite is to be computed based on any (surface) spherical harmonics series expansion gravitational model up to a certain degree and order. The evaluation of the whole model at each evaluation point of time needs rather high computational time efforts. This efforts can be reduced if, instead of the gravitational model itself, only the set of major perturbing frequencies acting on the satellite is used. These major frequencies will be taken into account for an orbit synthesis based on an inverse fast Fourier transform (IFFT). This will naturally yield an approximation of the satellite's real trajectory only, but if the approximation is sufficiently close to the real world and the predicted orbit arc is sufficiently short, it will be an effective substitute for the costly exact and strict computation. The definition of 'being close to the real world' will depend on the purpose for which the orbit prediction is performed.

For the selection of the major frequencies from all frequencies a Fourier analysis of a satellite's position data yields, a suitable selection criterion has to be found. The signal power already mentioned is a suitable selection criterion. The Fourier frequencies and their respective coefficients can be selected with respect to their contribution to the complete signal power. Applying this selection criterion to the CHAMP orbit different levels of adoption of the approximate orbit to the real orbit are reached and presented in table 7-3. The last column gives the number of seconds that have to be cut off at the beginning and the end of the arc to avoid the boundary effects, which can be clearly seen in figure 7-5 and reach the order of magnitude of the level of accuracy given in the previous column.

It can be seen that 99% of the complete signal power is reached by using 2 Fourier coefficients out of $n/2$, 99.99% by using 3 and so forth. Using the inverse fast Fourier transform (IFFT) an orbit synthesis can be performed using only the Fourier coefficients to reach a certain percentage of the whole signal power. Figure 7-5 shows the differences of the radial component between the approximating orbit that has been determined by an IFFT and the given 'original' orbit used as input for the Fourier analysis. The different levels of approximation from table 7-3 are presented beginning from the top with an approximation level of 99.9% of the signal power taken

into account down to 100% of the complete signal power. For the last case, the differences theoretically have to vanish. What can be seen in the graph are residual effects resulting from the numerical method itself.

% of complete signal power	number of coefficients	approx. error	cut-off
99.900000	2 of 8192	$4 \cdot 10^4 \ m$	0
99.990000	3 of 8192	$5 \cdot 10^3 \ m$	0
99.999000	17 of 8192	$5 \cdot 10^3 \ m$	2900
99.999900	79 of 8192	$2 \cdot 10^3 \ m$	3000
99.999990	674 of 8192	$500 \ m$	4000
99.999999	4763 of 8192	$50 \ m$	5000
100.000000	8192 of 8192	$5 \cdot 10^{-8} m$	0

table 7-3: Adoption levels and error order for an approximate orbit synthesis
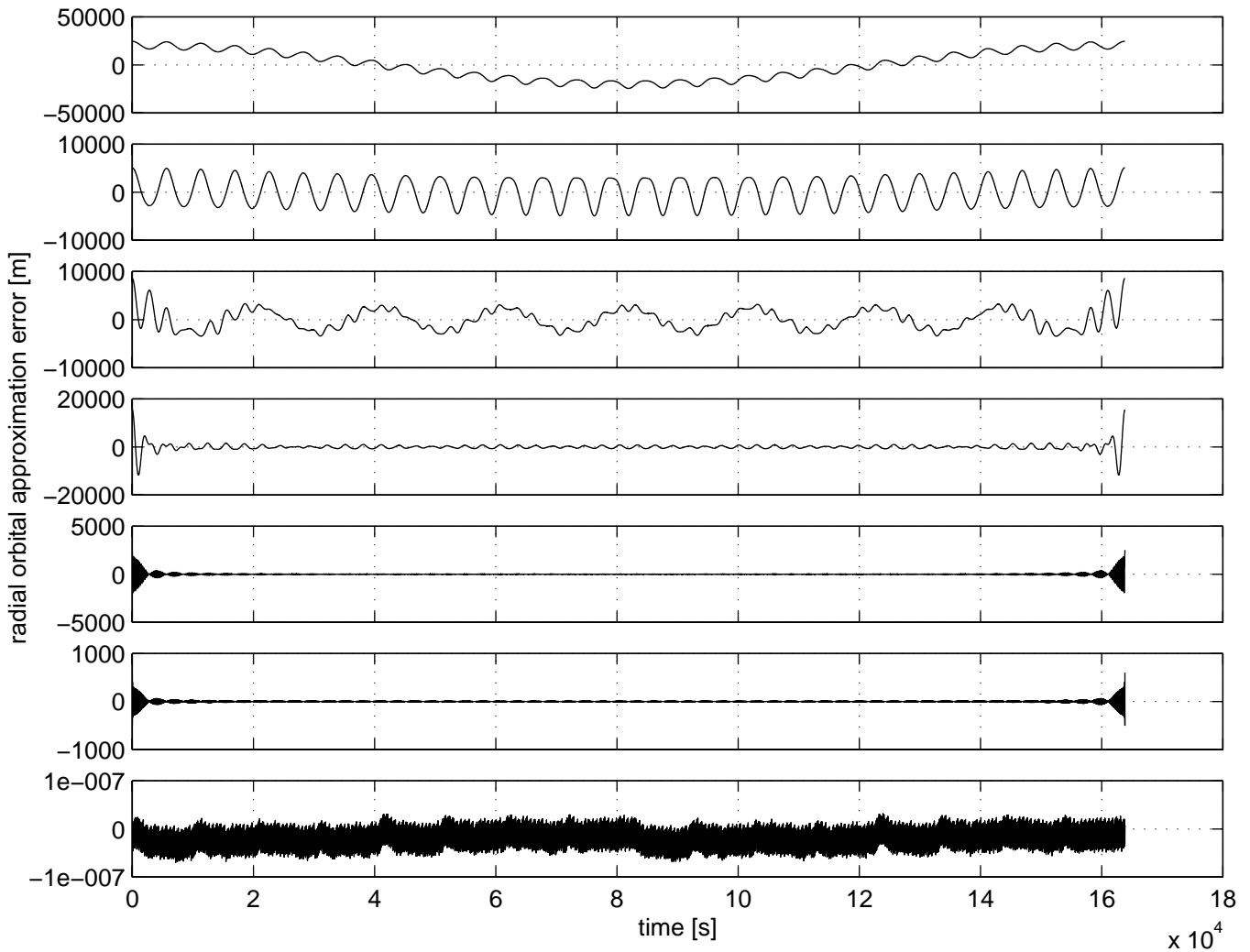
figure 7-5: Difference between original orbit and approximating orbit - radial component
(plots show the cases of table 7-3).

It can be clearly seen that the order of magnitude of the difference between the original orbit and the approximating orbit is decreasing step by step. At the beginning and the end of the arc though an area can be seen where the differences are some orders of magnitude higher than for the rest of the arc. These effects have to be taken into account when an orbit approximation is done using the described method. The arc which can effectively be used is a bit shorter than the original arc. E.g. for the case of 99.999999% of the complete signal power used the maximum difference is around 1000 m. As soon as the first and last 5000 s are cut off, the differences drop below 50 m on a length of the remaining shortened arc of nearly 43 hours.

Regarding the results of this orbit approximation it is clearly seen that even for a rather high percentage of the signal power taken into account, and thus also a high percentage of coefficients, the resulting orbital errors a quite high. The Fourier series representation of orbital position data does not seem to converge rapidly. This effect will be discussed in the following chapter.

7-4 3rd to 6th step: Spectral analysis for orbital sensitivity analysis

As already stated, the aim of the orbit sensitivity analysis is to get an idea on how the orbit of a satellite is influenced by the contribution of certain gravitational model coefficients. Thus gravitational data has to be analyzed. Since in general the coefficients of higher degree and order are of major interest, the gravitational data to be analyzed will be the perturbations resulting as difference between a 'real' orbit and a nominal orbit. The perturbations are computed simply by subtraction. For the following computations the perturbation data results from the difference of the accelerations acting on a satellite for the simulated orbit up to degree & order 90 of EGM96 and a $\bar{c}_{2,0}$ perturbed orbit, i.e. a precessing Kepler ellipse.

7-4.1 Fourier analysis of gravitational acceleration perturbation data

The Fourier analysis method already presented for the approximation of orbit synthesis is applied to the perturbations of the gravitational acceleration vector. This yields the spectrum given in table 7-4 up to 99% of the complete signal power and the adoption levels given in table 7-5.

index	p [sec/rev.]		f [rev./sec]	% of complete signal power	(cumulative)
29	$5.649655172\ 10^3$	(0d 01h 34m 10s)	$1.770019531\ 10^{-4}$	71.8674636	(71.8674636)
28	$5.851428571\ 10^3$	(0d 01h 37m 31s)	$1.708984375\ 10^{-4}$	8.1063910	(79.9738545)
30	$5.461333333\ 10^3$	(0d 01h 31m 01s)	$1.831054688\ 10^{-4}$	7.8165025	(87.7903570)
27	$6.068148148\ 10^3$	(0d 01h 41m 08s)	$1.647949219\ 10^{-4}$	1.9012128	(89.6915698)
31	$5.285161290\ 10^3$	(0d 01h 28m 05s)	$1.892089844\ 10^{-4}$	1.8813341	(91.5729039)
33	$4.964848485\ 10^3$	(0d 01h 22m 45s)	$2.014160156\ 10^{-4}$	0.9137090	(92.4866129)
58	$2.824827586\ 10^3$	(0d 00h 47m 05s)	$3.540039062\ 10^{-4}$	0.8893998	(93.3760128)
26	$6.301538462\ 10^3$	(0d 01h 45m 02s)	$1.586914063\ 10^{-4}$	0.8387752	(94.2147880)
32	$5.120000000\ 10^3$	(0d 01h 25m 20s)	$1.953125000\ 10^{-4}$	0.8385996	(95.0533878)
25	$6.553600000\ 10^3$	(0d 01h 49m 14s)	$1.525878906\ 10^{-4}$	0.7014572	(95.7548449)
34	$4.818823529\ 10^3$	(0d 01h 20m 19s)	$2.075195312\ 10^{-4}$	0.3708957	(96.1257406)
24	$6.826666667\ 10^3$	(0d 01h 53m 47s)	$1.464843750\ 10^{-4}$	0.3322948	(96.4580354)
35	$4.681142857\ 10^3$	(0d 01h 18m 01s)	$2.136230469\ 10^{-4}$	0.2568048	(96.7148401)
23	$7.123478261\ 10^3$	(0d 01h 58m 43s)	$1.403808594\ 10^{-4}$	0.2287677	(96.9436078)
57	$2.874385965\ 10^3$	(0d 00h 47m 54s)	$3.479003906\ 10^{-4}$	0.2071372	(97.1507450)
56	$2.925714286\ 10^3$	(0d 00h 48m 46s)	$3.417968750\ 10^{-4}$	0.1933233	(97.3440682)
36	$4.551111111\ 10^3$	(0d 01h 15m 51s)	$2.197265625\ 10^{-4}$	0.1880527	(97.5321209)
22	$7.447272727\ 10^3$	(0d 02h 04m 07s)	$1.342773438\ 10^{-4}$	0.1658684	(97.6979893)
37	$4.428108108\ 10^3$	(0d 01h 13m 48s)	$2.258300781\ 10^{-4}$	0.1512364	(97.8492257)
21	$7.801904762\ 10^3$	(0d 02h 10m 02s)	$1.281738281\ 10^{-4}$	0.1272137	(97.9764394)
38	$4.311578947\ 10^3$	(0d 01h 11m 52s)	$2.319335937\ 10^{-4}$	0.1194223	(98.0958616)
20	$8.192000000\ 10^3$	(0d 02h 16m 32s)	$1.220703125\ 10^{-4}$	0.1001830	(98.1960446)
39	$4.201025641\ 10^3$	(0d 01h 10m 01s)	$2.380371094\ 10^{-4}$	0.0937256	(98.2897702)
19	$8.623157895\ 10^3$	(0d 02h 23m 43s)	$1.159667969\ 10^{-4}$	0.0801701	(98.3699403)
40	$4.096000000\ 10^3$	(0d 01h 08m 16s)	$2.441406250\ 10^{-4}$	0.0784684	(98.4484087)
54	$3.034074074\ 10^3$	(0d 00h 50m 34s)	$3.295898438\ 10^{-4}$	0.0778766	(98.5262853)
41	$3.996097561\ 10^3$	(0d 01h 06m 36s)	$2.502441406\ 10^{-4}$	0.0741899	(98.6004752)
59	$2.776949153\ 10^3$	(0d 00h 46m 17s)	$3.601074219\ 10^{-4}$	0.0665124	(98.6669876)
18	$9.102222222\ 10^3$	(0d 02h 31m 42s)	$1.098632813\ 10^{-4}$	0.0663677	(98.7333553)
42	$3.900952381\ 10^3$	(0d 01h 05m 01s)	$2.563476563\ 10^{-4}$	0.0613130	(98.7946683)
17	$9.637647059\ 10^3$	(0d 02h 40m 38s)	$1.037597656\ 10^{-4}$	0.0576757	(98.8523440)
55	$2.978909091\ 10^3$	(0d 00h 49m 39s)	$3.356933594\ 10^{-4}$	0.0568556	(98.9091996)
43	$3.810232558\ 10^3$	(0d 01h 03m 30s)	$2.624511719\ 10^{-4}$	0.0538272	(98.9630269)
44	$3.723636364\ 10^3$	(0d 01h 02m 04s)	$2.685546875\ 10^{-4}$	0.0516685	(99.0146953)

table 7-4: Fourier coefficients for the gravitational perturbations (EGM96 up to degree & order 90 without spherical and $\bar{c}_{2,0}$ term) along a CHAMP orbit in descending order with respect to their signal power (explanation of columns see text on page 77).

Figure 7-6 shows the differences of the absolute value of the gravitational acceleration vector between the approximating orbits that have been determined by an IFFT and the given 'original' orbit used as input for the Fourier analysis. The different levels of approximation from table 7-5 are presented.

% of complete signal power	number of coefficients	approx. error
99.9000000	127 of 8192	$1.7 \cdot 10^{-4}\ m/s^2$
99.9900000	1218 of 8192	$1.4 \cdot 10^{-5}\ m/s^2$
99.9990000	6116 of 8192	$1.4 \cdot 10^{-6}\ m/s^2$
99.9999000	7973 of 8192	$1.3 \cdot 10^{-6}\ m/s^2$
99.9999900	8171 of 8192	$1.0 \cdot 10^{-6}\ m/s^2$
99.9999990	8190 of 8192	$6.4 \cdot 10^{-7}\ m/s^2$
99.9999999	8192 0f 8192	$1.8 \cdot 10^{-16}\ m/s^2$
100.0000000	8192 of 8192	$1.8 \cdot 10^{-16}\ m/s^2$

table 7-5: Adoption levels and order of magnitude of approximation error
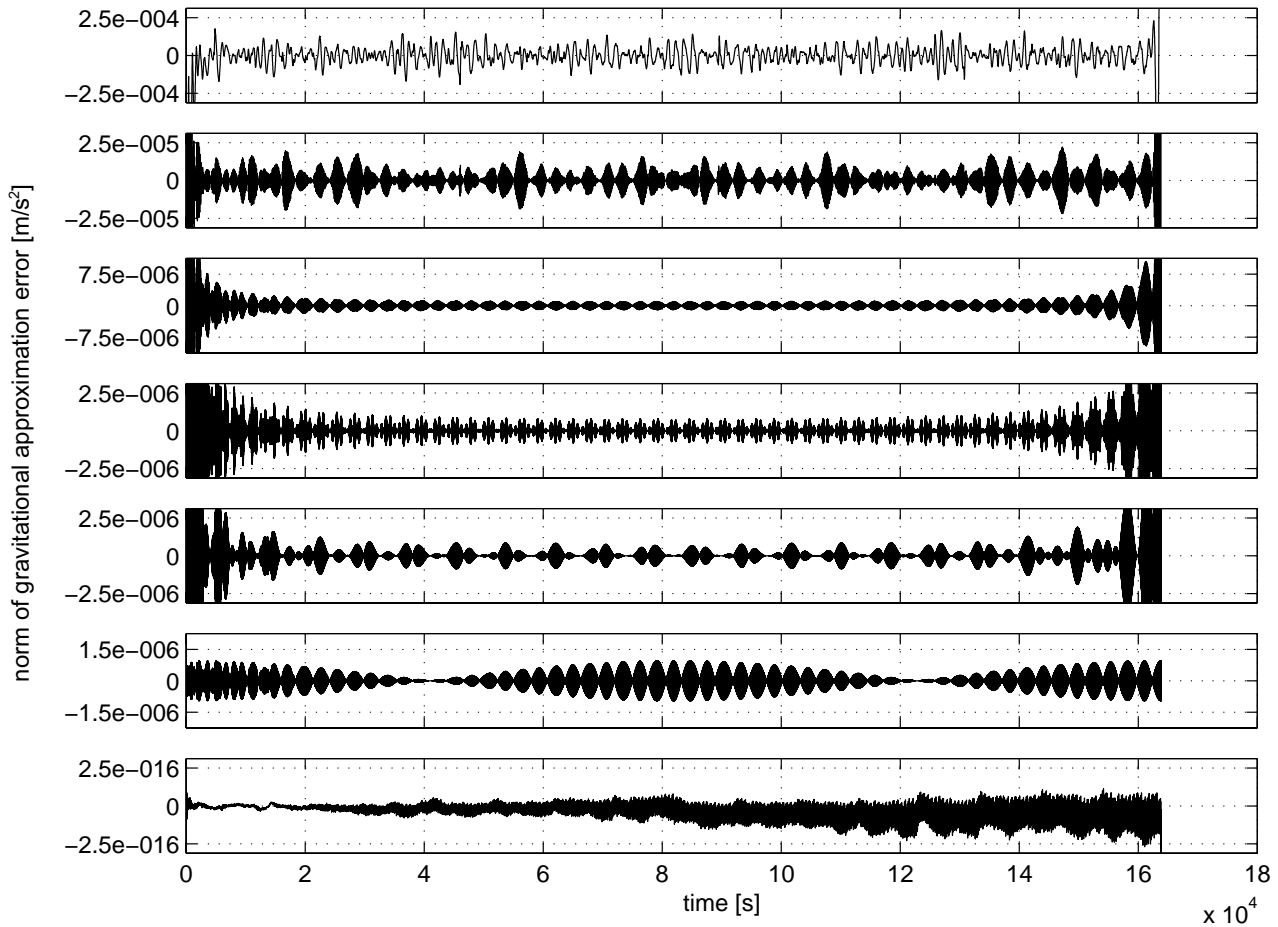
figure 7-6: Differences between real gravitational acceleration and approximated values
(plots show the cases of table 7-5).

As for the approximation of the orbital position vectors by means of a frequency representation (page 78) the convergence of the gravitational acceleration's frequency representation shows the same behaviour. For an approximation equal to or better than $0.1\ mgal = 10^{-6}\ m/s^2$ at least 99.7% of the coefficients have to be taken into account.

7-4.2   Computation of respective lumped coefficients

The respective lumped coefficients for the dominant frequencies that have been determined in the previous subsection 7-4.1 are computed by means of the equations presented in tables 4-6 or 4-7 and 4-8 respectively. Computing the lumped coefficients, i.e. the addends of the infinite sum which are the (surface) spherical harmonics coefficients multiplied by their weights, yields the result presented in table 7-6 and table 7-7. There the degree and order of the most important addends are given in descending order with respect to the contribution they provide for the lumped coefficient $\mathbf{a}_{29}$ and $\mathbf{a}_{28}$ respectively.

It is important to mention that for the selection of the (surface) spherical harmonics gravitational coefficients which have the strongest influence within the lumped coefficient, the complete product of the weight and the (surface) spherical harmonics coefficient itself has to be taken into account (see equations (7-1) and (7-2)). The

weight only does not give a correct impression on the contribution the respective term provides for the lumped coefficient. To make this contribution more evident, tables 7-6 and 7-7 contain a column '%' which gives the percentage of contribution of the respective addend to the analyzed lumped coefficient.

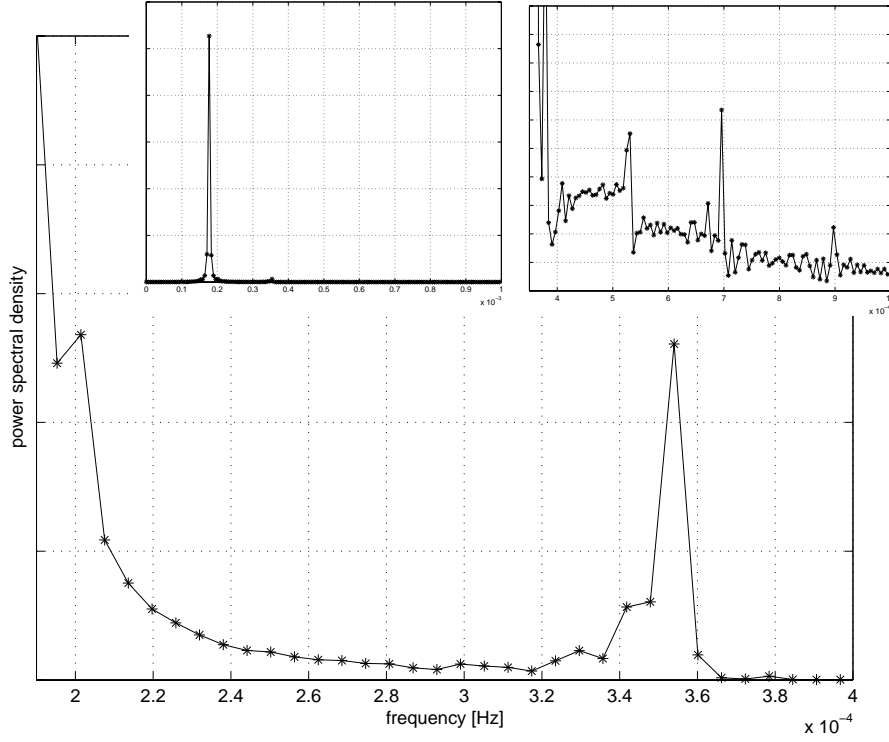**figure 7-7**: Power spectral density for gravitational acceleration on CHAMP from EGM96 up to degree & order 90, Kepler and $\bar{c}_{2,0}$ term removed.
(complete graph on the left side on top, details in the two other graphs)

$$\mathbf{a}_{29} = \sum_{n=0}^{\infty} \sum_{m=0}^{n} [\underbrace{\frac{2\,GM}{t_n - t_0}\,R_{\oplus}^n\,\bar{n}_{n,m}\,\mathbf{a}_{\mathbf{29},n,m}^{\bar{c}}\,\bar{c}_{n,m}}_{\text{left part table 7-6}} + \underbrace{\frac{2\,GM}{t_n - t_0}\,R_{\oplus}^n\,\bar{n}_{n,m}\,\mathbf{a}_{\mathbf{29},n,m}^{\bar{s}}\,\bar{s}_{n,m}}_{\text{right part table 7-6}}] \qquad (7\text{-}1)$$

degree	order	value	%	degree	order	value	%
3	1	$2.479542 \cdot 10^{-2}$	16.1309420	4	1	$4.254515 \cdot 10^{-3}$	4.0597107
7	1	$7.639412 \cdot 10^{-3}$	4.9699065	10	1	$2.710001 \cdot 10^{-3}$	2.5859169
5	2	$6.967329 \cdot 10^{-3}$	4.5326752	13	3	$2.550612 \cdot 10^{-3}$	2.4338256
7	2	$6.831107 \cdot 10^{-3}$	4.4440543	3	1	$2.354793 \cdot 10^{-3}$	2.2469729
9	1	$4.632176 \cdot 10^{-3}$	3.0135149	11	3	$2.327452 \cdot 10^{-3}$	2.2208853
3	2	$3.487451 \cdot 10^{-3}$	2.2688008	21	1	$1.720419 \cdot 10^{-3}$	1.6416451
13	2	$2.399841 \cdot 10^{-3}$	1.5612439	6	2	$1.702388 \cdot 10^{-3}$	1.6244402
3	0	$1.885885 \cdot 10^{-3}$	1.2268842	4	2	$1.479059 \cdot 10^{-3}$	1.4113360
9	3	$1.704665 \cdot 10^{-3}$	1.1089889	21	3	$1.466612 \cdot 10^{-3}$	1.3994597
13	1	$1.564532 \cdot 10^{-3}$	1.0178238	7	1	$1.271645 \cdot 10^{-3}$	1.2134197
27	7	$1.311747 \cdot 10^{-3}$	0.8533721	27	5	$1.246752 \cdot 10^{-3}$	1.1896664
5	1	$1.273502 \cdot 10^{-3}$	0.8284911	5	1	$1.241720 \cdot 10^{-3}$	1.1848643
7	3	$1.242401 \cdot 10^{-3}$	0.8082580	23	3	$1.074653 \cdot 10^{-3}$	1.0254473
30	13	$1.226886 \cdot 10^{-3}$	0.7981644	23	1	$1.071130 \cdot 10^{-3}$	1.0220856
29	10	$1.181745 \cdot 10^{-3}$	0.7687974	7	3	$1.036574 \cdot 10^{-3}$	0.9891122
27	5	$1.166459 \cdot 10^{-3}$	0.7588530	8	1	$9.859688 \cdot 10^{-4}$	0.9408236
26	3	$1.112554 \cdot 10^{-3}$	0.7237849	27	3	$8.931896 \cdot 10^{-4}$	0.8522926
28	9	$1.067151 \cdot 10^{-3}$	0.6942474	21	4	$8.421215 \cdot 10^{-4}$	0.8035628

table 7-6: Lumped coefficient $\mathbf{a}_{29}$.
(the first three columns refer to $\bar{c}_{n,m}$, the last three to $\bar{s}_{n,m}$)

$$\mathbf{a_{28}} = \frac{2\,GM}{t_n - t_0} \sum_{n=0}^{\infty} R_\oplus^n \sum_{m=0}^{n} \bar{n}_{n,m}\, [\ \underbrace{\mathbf{a}_{\mathbf{28},n,m}^{\bar{c}}\ \bar{c}_{n,m}}_{\text{left part table 7-7}}\ +\ \underbrace{\mathbf{a}_{\mathbf{28},n,m}^{\bar{s}}\ \bar{s}_{n,m}}_{\text{right part table 7-7}}\ ] \tag{7-2}$$

degree	order	value	%	degree	order	value	%
26	4	$3.203376 \cdot 10^{-3}$	2.5369466	20	3	$2.350448 \cdot 10^{-3}$	2.3652446
4	0	$2.734021 \cdot 10^{-3}$	2.1652359	4	2	$1.943572 \cdot 10^{-3}$	1.9558074
10	2	$2.611609 \cdot 10^{-3}$	2.0682905	18	1	$1.900493 \cdot 10^{-3}$	1.9124570
10	1	$2.401799 \cdot 10^{-3}$	1.9021289	10	1	$1.889493 \cdot 10^{-3}$	1.9013874
4	2	$2.259310 \cdot 10^{-3}$	1.7892836	16	2	$1.492694 \cdot 10^{-3}$	1.5020914
3	1	$2.044851 \cdot 10^{-3}$	1.6194407	16	1	$1.428929 \cdot 10^{-3}$	1.4379245
18	4	$1.966368 \cdot 10^{-3}$	1.5572855	3	1	$1.199932 \cdot 10^{-3}$	1.2074856
26	6	$1.964815 \cdot 10^{-3}$	1.5560550	12	1	$1.166249 \cdot 10^{-3}$	1.1735904
6	1	$1.922213 \cdot 10^{-3}$	1.5223159	14	1	$1.162455 \cdot 10^{-3}$	1.1697734
8	2	$1.843557 \cdot 10^{-3}$	1.4600241	10	2	$1.121700 \cdot 10^{-3}$	1.1287618
3	0	$1.784475 \cdot 10^{-3}$	1.4132333	24	2	$1.118220 \cdot 10^{-3}$	1.1252594
6	0	$1.287181 \cdot 10^{-3}$	1.0193964	16	3	$1.052452 \cdot 10^{-3}$	1.0590777
27	7	$1.254453 \cdot 10^{-3}$	0.9934770	28	6	$1.040619 \cdot 10^{-3}$	1.0471699
12	1	$1.220923 \cdot 10^{-3}$	0.9669224	16	4	$9.971466 \cdot 10^{-4}$	1.0034239
14	2	$1.138616 \cdot 10^{-3}$	0.9017384	8	2	$9.741486 \cdot 10^{-4}$	0.9802811
20	0	$1.117855 \cdot 10^{-3}$	0.8852966	12	2	$9.644801 \cdot 10^{-4}$	0.9705518
28	2	$1.059424 \cdot 10^{-3}$	0.8390217	20	2	$9.410128 \cdot 10^{-4}$	0.9469368
10	0	$1.025246 \cdot 10^{-3}$	0.8119542	8	3	$8.765847 \cdot 10^{-4}$	0.8821031

table 7-7: Lumped coefficient $\mathbf{a}_{28}$.
(the first three columns refer to $\bar{c}_{n,m}$, the last three to $\bar{s}_{n,m}$)

Figures 7-8 and 7-9 show the contents of tables 7-6 and 7-7 respectively. On the x-axis the combinations of degree and order for the respective (surface) spherical harmonics gravitational coefficients $\bar{c}_{n,m}$ (left column of figures) and $\bar{s}_{n,m}$ (right column of figures) are given in the order $(2,1)$, $(2,2)$, $(3,0)$, $(3,1)$, $\ldots$, $(90,90)$ (the parts for $(0,0)$ and $(2,0)$ have been removed in order to obain the perturbations). The y-axis gives the value of

$$2\,GM \cdot (t_n - t_0)^{-1} \cdot R_\oplus^n \cdot \bar{n}_{n,m} \cdot \bar{c}_{n,m} \cdot \parallel \mathbf{a}_{\mathbf{k},n,m}^{\bar{c}} \parallel\quad,$$
$$2\,GM \cdot (t_n - t_0)^{-1} \cdot R_\oplus^n \cdot \bar{n}_{n,m} \cdot \bar{s}_{n,m} \cdot \parallel \mathbf{a}_{\mathbf{k},n,m}^{\bar{s}} \parallel\quad,$$
$$2\,GM \cdot (t_n - t_0)^{-1} \cdot R_\oplus^n \cdot \bar{n}_{n,m} \cdot \bar{c}_{n,m} \cdot \parallel \mathbf{b}_{\mathbf{k},n,m}^{\bar{c}} \parallel\quad\text{and}$$
$$2\,GM \cdot (t_n - t_0)^{-1} \cdot R_\oplus^n \cdot \bar{n}_{n,m} \cdot \bar{s}_{n,m} \cdot \parallel \mathbf{b}_{\mathbf{k},n,m}^{\bar{s}} \parallel$$

according to table 7-8 in logarithmic scaling. This analysis procedure now yields a set of degree and order combinations for which the (surface) spherical harmonics coefficients of the gravitational field model are candidates for being the coefficients with the strongest influence on the satellite's orbit. In a further step this set has to be examined more closely, e.g. by means of a simulated adjustment method. Aim of this procedure is to finally determine a rather small set of coefficients the specific orbit is sensitive to.

7-5   Discussion of the results

Looking at the results of the sensitivity analysis two main points arise, the results of the frequency analysis of orbital data along a satellite's trajectory and the internal structure of the lumped coefficients. The following subsections will summarise the observations and try to explain them.

7-5.1   Fourier frequency analysis of orbital data

Aim of the Fourier frequency analysis of orbital data along a satellite's trajectory is to find the main influences that yield the perturbations of the real with respect to a nominal trajectory. The result of this analysis will mainly be governed by the behaviour of the perturbing accelerations acting on the satellite.

For the LEO mission CHAMP the spectrum of frequencies of orbital data is rather broad. Although a few frequencies seem to govern the whole signal, the Fourier series itself converges rather slowly. I.e. that the main part of the coefficients and frequencies is necessary to represent the original signal with sufficient accuracy. Resonant effects which are well-known from previous satellite missions for gravitational field determination are not visible in the data.

The reason for this observations are the specific attributes of LEO missions. The dominant feature of LEO missions is the low orbital height. Due to that a lot of higher frequency parts of the Earth's gravitational field have an effect on the orbit than for high flying satellites where these detailed features fade away. In addition the low orbit brings the satellite down into the atmosphere where the aerodynamic perturbations drag and lift play an important role. Especially the drag has a considerable effect on the satellite's orbit. Dominant features in the orbital spectrum - resonances - are caused by the condition of commensurability. Commensurability exists if the number of revolutions of a satellite around the Earth per day approximates an integer value. In that case the satellite crosses the same features in the Earth's field regularly in a way that the effects add up with each resolution. The consequence is a certain frequency becomes dominant in the spectrum. The number of revolutions per day in that case approximates the order of the gravitational coefficients causing this resonant perturbation. Due to the strong influence of the non-gravitational perturbations on the trajectory of a LEO, the satellite will not remain in the condition of commensurability for long which means that the effects are not able to add up. Thus they will vanish in the spectrum of the higher frequency impacts on the orbit caused by the low orbital height.

7-5.2 Lumped coefficients

The results of the computations of the lumped coefficients for CHAMP data clearly show that a one-to-one relationship between a frequency and certain (surface) spherical harmonics coefficients does not exist. Despite the fact that there may arise a few coefficients that may have a higher impact on a lumped coefficient than others, no clear dominance of a certain coefficient or a limited set of coefficients is visible.

This result is confirmed by the frequency analysis of the (surface) spherical harmonics themselves. A spectrum of a (surface) spherical harmonic contains nearly all frequencies without any clearly dominant features.

$\bar{c}_{2,1} \cdots$ $\cdots \bar{c}_{90,90}$ $\bar{s}_{2,1} \cdots$ $\cdots \bar{s}_{90,90}$

figure 7-8: Contribution of the addends for $\bar{c}_{n,m}$ (left column) and $\bar{s}_{n,m}$ (right column) to the lumped coefficients $\mathbf{a_{29}}$ (top line) and $\mathbf{b_{29}}$ (bottom line).

$\bar{c}_{2,1} \ldots$ $\ldots \bar{c}_{90,90}$ $\bar{s}_{2,1} \ldots$ $\ldots \bar{s}_{90,90}$
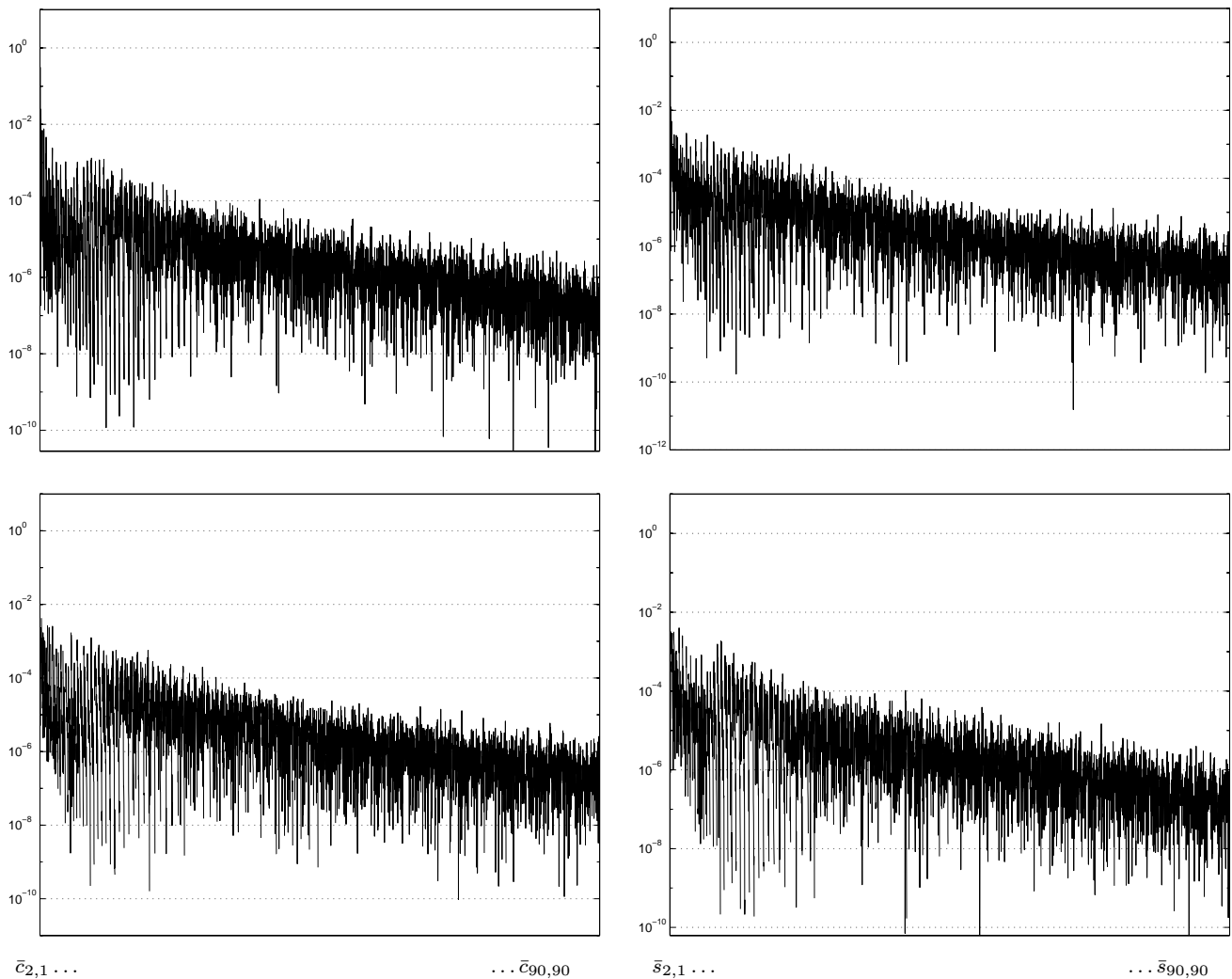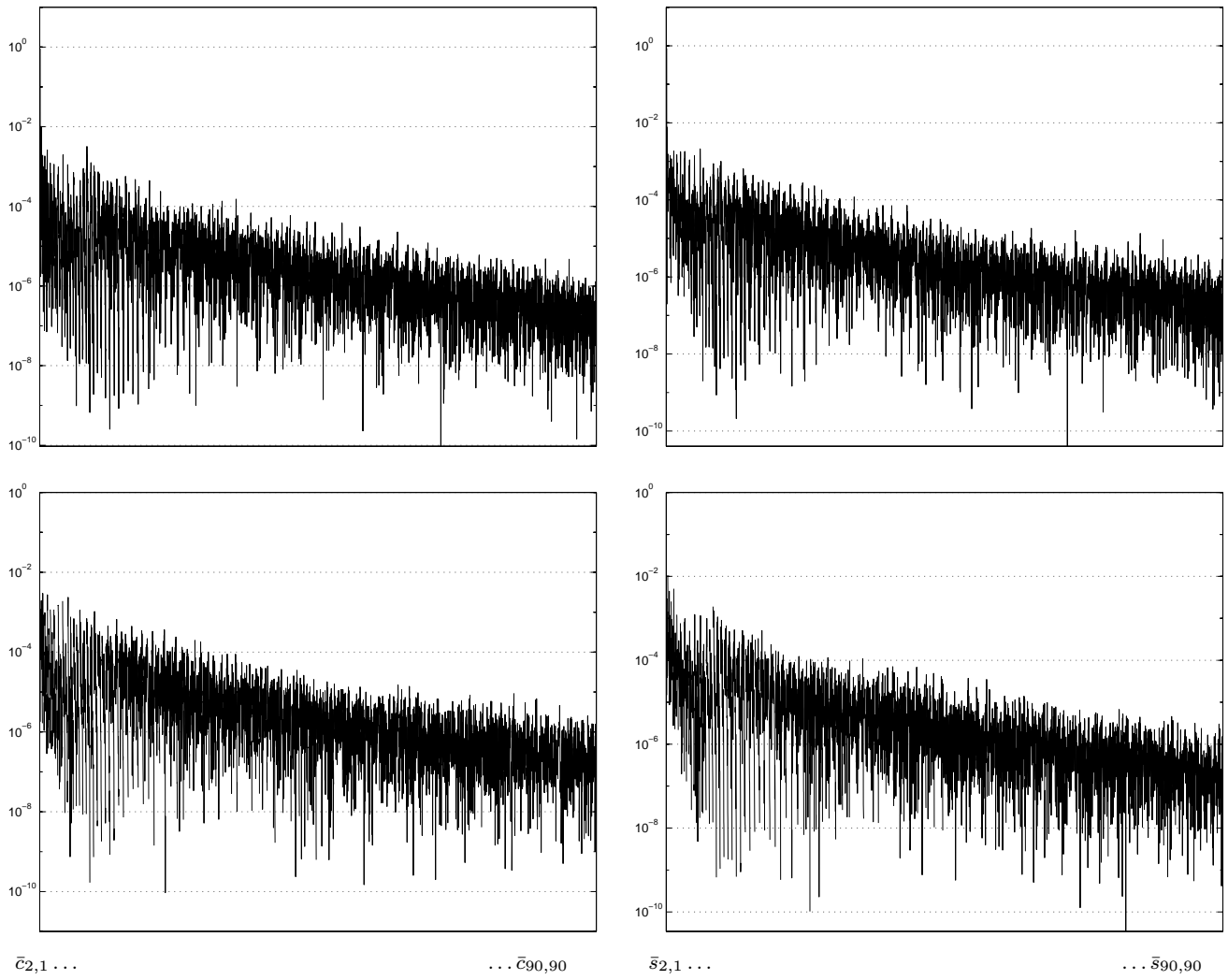
figure 7-9: Contribution of the addends for $\bar{c}_{n,m}$ (left column) and $\bar{s}_{n,m}$ (right column) to the lumped coefficients $\mathbf{a_{28}}$ (top line) and $\mathbf{b_{28}}$ (bottom line).

Chapter 8

Conclusions

8-1 Summary of the presented method and its applications

In this thesis a method for the sensitivity analysis of the orbits and mission layout of low Earth orbiting (LEO) satellites has been presented. The satellites are assumed to be tracked by GPS.

The method itself consists of several parts. First of all, the representation of the gravitational field of the Earth is transformed to the use of Cartesian co-ordinates as they are provided by GPS's geocentric quasi-Earth-fixed reference system WGS84. This representation is kept up for the whole process of the method and thus enables a direct introduction of the tracking data into the algorithms. The **Cartesian representation of the gravitational field and satellite's orbit** is a canonical representation and thus avoids eventual singularities as may arise e.g. with Kepler elements. By only transforming the base functions of the representation into Cartesian co-ordinates, the gravitational model's coefficients remain unaltered. This is a key prerequisite for satellite orbit analyses for the determination and improvement of the existing Earth gravitation models.

A second part of the method considers the problem of obtaining gravitational field values, in that case gravitational acceleration vectors, from the orbit data position and velocity vectors provided by GPS. This is done by application of a **non-linear time-discrete Extended Kalman Filter (dEKF)**. To apply the filter a non-linear state space representation for the system 'satellite trajectory' is set up. For the computations of this thesis only gravitational effects on the satellite are considered. Non-conservative and tidal orbit perturbations are not taken into account, although the filtering method can be extended to take into account these perturbations as well as it is a suitable tool for the determination of (geophysical) parameters describing these and other effects on the satellite. This remains a point to be considered in further investigations.

The core part of the method is the **analytical computation of the lumped coefficients from a gravitational (surface) spherical harmonics model of the Earth** and the Fourier frequency analysis of the gravitational orbit data. The numerical analysis yields the frequencies on the gravitational signal. From this spectrum the most important frequencies (= frequencies with the strongest influence on the satellite's orbit) can be selected. Selection criterion is the contribution of each frequency to the complete signal's signal power. By means of the analytical Fourier representation the connection between the Fourier coefficient (= lumped coefficient) and the gravitational (surface) spherical harmonics coefficients is determined.

Two **applications** are given as an example for the presented analysis method.

First *a given orbit is approximated* by a Fourier series expansion. Thus the number of necessary coefficients to represent the orbit is reduced as well as the computational efforts for the reconstruction of the orbit from the representation coefficients. Depending on the accuracy of approximation needed for a certain application this may yield a considerable reduction of the amount of data to be kept. In addition the existing Fast Fourier Transformation algorithms guarantee an efficient computation of the orbital data. A drawback of this method is that the length of the orbit has to be cut off to avoid boundary effects and reach the necessary level of approximation. Nevertheless it may provide a suitable means for orbit reconstruction within limited computational environments. Consider e.g. a satellite which needs to know its orbit with some accuracy for attitude and pointing purposes. A ground-based orbit prediction for a longer period could be performed. The result is represented as Fourier series, a selection of the coefficients is made with respect to the required orbit accuracy and the thus reduced set of coefficients is up-linked to the satellite together with the initial orbit values. The on-board computer is now able to reconstruct the orbit data, which has been determined by the much more capable computers in the ground stations, in a rather short computational time period using the efficient FFT algorithms. The advantages are reduced data rates for uplink and storage, reduced computational time requirements on board and reduced hardware requirements on board using the more powerful computers on ground. Nevertheless there is a disadvantage of this method regarding to interpretation of the orbit representation. The representation of the orbit by means of a Fourier representation differs from the representations used for e.g. the equations of motion in chapter 2. There each physical effect which influences the satellite's movement is

introduced into the equations by means of a (geo-)physical model. The parameters of these models directly contain a physical meaning. Thus the representation of the satellite's trajectory is done by means of physical parameters. The coefficients of the Fourier representation of the trajectory on the other hand, do not have a direct physical meaning. In the first place they are mere mathematical parameters like e.g. parameters of an exponential series expansion. They can be assigned a sort of indirect physical meaning. They represent the amplitudes of the frequencies within the trajectory of the satellite. They do not describe the (geo-)physical reasons for the movement of the satellite. By means of the lumped coefficients a connection between mathematical description and physical interpretation is found.

The second application is the *orbit sensitivity analysis*. The connection between the (surface) spherical harmonics' coefficients and the Fourier coefficients given by means of the lumped coefficients allows to gain a first idea on the sensitivity of an analyzed orbit on certain parts of the gravitational field. As selection criterion the contribution of the complete summand, i.e. the weight multiplied by the respective gravitational (surface) spherical harmonics coefficient, to the complete value of the lumped coefficient is used. Although some computational efforts have to be performed, the method provides a suitable procedure and helps to reduce the number of unknown coefficients that have to be introduced into the further course of the orbit analysis.

8-2   Comparison and evaluation of analysis methods

In section 1-3 several existing methods for orbit sensitivity analysis have been presented. The advantages and disadvantages of the different methods are compared with the proposed method of this thesis and presented in table 8-1 in a concise way. An explanation of the three other methods for sensitivity analysis is not to be given in the following again; refer to section 1-3 for that.

All methods for sensitivity analysis, including the one presented here, are based on the general assumption, that perturbations that have a high impact on the orbital data signal can also be determined best by an orbit analysis. This assumption implies two main statements.

- To end up with a clear statement on the sensitivity with respect to certain perturbations a clear distinction between dominant and neglectable impacts on the satellite's orbit is desirable.

- The accuracy of determination that can be reached by an orbit analysis is directly linked to the amplitude of the dominant perturbation effect that is determined.

The previous investigations on CHAMP data have shown, that these two statements are not generally valid. In the case of LEO missions with continuous coverage of tracking data for the whole orbit the determination of the impacts on the orbit does not yield a clearly differentiated result. Although there are certain frequencies that play a somewhat dominant role, the vast majority of the non-dominant frequencies is not at all neglectable (see e.g. page 82). For the situation before GPS tracking of satellite missions - high-flying satellites with, in terms of gravitational analysis, poor ground-based tracking coverage - the separation of the spectrum in a dominant and a neglectable part is much more clear. Only for this case the second statement does hold. The dominant (resonant) perturbation effects on the orbit have been the only effects that could be clearly determined from the frequency analysis of orbital data, thus they have automatically been the effect to be determined best. In fact the statement that spectrum contributions with high amplitude are also likely to be determined best is misleading. The accuracy that can be reached for the determination is not improving with the size of the value to be determined. This is a general observation and does not come up with LEO missions only.

These two general considerations hold for all the analysis methods mentioned in this thesis and compared here with respect to the presented method.

The advantage of the method presented here (*'Fourier'*) is, that it tries to avoid the disadvantages of the methods already existing. It includes all frequencies into the investigation and thus does not restrict itself to a few dominating frequencies as it is done for a resonance analysis. Especially in the case of LEO satellites the resonances are not found that clearly in the spectrum. Resonance effects still occur but due to the low orbital height of LEOs the effects of the other frequencies in the perturbation spectrum are that strong, that the resonant frequencies do not dominate the spectra anymore. Analyzing only the resonance frequencies in the course of an orbit sensitivity analysis of a LEO mission would be too strong a restriction.

The modified understanding of the definition of the lumped coefficients works without any linearisation as it is performed for the 'classical' definition of the lumped coefficients. Linearisation errors are thus avoided.

With respect to the parametrisation used the Cartesian co-ordinates form a set of parameters that may not be as geometrically descriptive as the Kepler elements are, but there are no singularities to be expected for any special cases. Additionally, the result of the tracking process by GPS, the position and velocity vectors, are given with respect to the same Cartesian geocentric Earth-fixed reference system, WGS84.

As far as the necessary computing time of the presented method is concerned, a general answer is not at hand and a closer look has to be taken at that. As a matter of fact, the computation of the lumped coefficients by means of a Fourier analysis of a (surface) spherical harmonics series expansion for a gravitational model will be

rather demanding. The evaluation of the various integrations and summations takes quite some time. Despite that, the necessary effort seems to be less than for method three based on a reference orbit. Only the lumped coefficients for the frequencies selected in the previous step will be determined. Rather little computation time will be required for the frequency analysis of the orbit data since rather effective and powerful tools like the fast Fourier transformation (FFT) are available. The same usually holds for the computation of the gravitational acceleration vectors from the GPS orbit data, although the final computation time requirements strongly depend on the numerical methods chosen for the implementation of the proposed discrete extended Kalman filter.

---

table 8-1: <u>Sensitivity analysis methods</u>

'resonance': based on dominant parts of the orbit spectrum

⊖ not really applicable for LEO mission layouts
⊗ gives a rough idea on what to expect from the sensitivity analysis

'Kaula': based on representation of disturbing potential in Keplerian elements

⊕ analytically derived formulae
⊖ high analytical efforts necessary to derive formulae
⊖ formulation based on Keplerian elements (singularities, not in compliance with GPS)

'reference': based on differences between reference orbit and orbit computed with perturbed coefficients

⊖ high computing time requirements
⊖ preinformation needed to reduce computing time requirements
⊗ does not depend on parametrisation (Cartesian possible)

'Fourier': based on comparison of gravitational model and orbital gravitation spectrae

⊕ Cartesian parametrisation (no singularities, in compliance with GPS)
⊗ computation time requirements:
  → high: Fourier analysis of gravitational model for computation of lumped coefficients
  → low: Fourier analysis of orbital gravitation data
  → depends: determination of gravitational vectors from orbit data

(⊖ ... disadvantage, ⊕ ... advantage, ⊗ ... neutral)

8-3   Further applications and investigations

The main field of application for the orbit sensitivity analysis is the preparation of the evaluation of the data of gravitational field missions. On the one hand, a sensitivity analysis should provide information on the capabilities of the mission itself and thus give an important hint on which gravitational coefficients should be fixed and which should be introduced as unknowns to the evaluation. On the other hand, it provides a suitable tool to set up the optimal layout of future gravitational field missions by choosing the orbit in such a way that it is sensitive for the coefficients that are of interest. The prerequisite for these applications is the setup of a sensitivity analysis method that is suited for LEO missions also.

One of the further investigations to be performed has already been mentioned before: The extension of the state space description of the system 'satellite trajectory' to all perturbative effects that act on the satellite in reality. This encloses especially tidal forces and the most important non-conservative accelerations. For LEO satellites this will be aerodynamical influences like drag and lift in the first place. The filter itself can be optimised with respect to the noise and covariance models which are chosen. The linearisation which is necessary for the prediction of the covariances still remains as a major point of concern. Investigations and efforts to set up an alternative method called *unscented filter* for application within satellite geodesy and especially to improve the proposed time-discrete extended Kalman filter are made by S. Julier of the Naval Research Laboratory and the author. These investigations will hopefully come to a successful end in near future.

The orbit sensitivity analysis in the proposed way will yield a rather big and unstructured set of possible candidates for the sensitive gravitational coefficients. These results could maybe be further selected by a simulated gravitational analysis process that yields detailed information on the actual accuracies with which the coefficients can be determined from an orbit analysis.

The application of orbit approximation by means of a Fourier representation is not restricted to the Fourier representation itself. Also other sets of base functions could be used and may provide better results and behaviour.

Annexes

A   Legendre functions

Several different definitions of the Legendre polynomials and functions can be given which yield different definitions of the spherical harmonics. Due to the importance of these functions for the representation of the Earth's gravitational field and to avoid misunderstandings the definitions underlying this thesis will be given in the following overview without proof and derivation. This overview is mainly based on Knickmeyer (1989) and Wenzel (1990).

Definition of the Legendre polynomials

The Legendre polynomials are defined as solutions of the Legendre differential equation, an ordinary second order differential equation

$$\left[(t^2 - 1)\ g'(t)\right]' - n\ (n+1)\ g(t)\ =\ 0\quad. \tag{A-1}$$

The parameterization is by means of the spherical latitude ϕ with respect to an Earth-fixed geocentric equatorial system. The parameter t stands for the sine of the latitude having domain $-\pi/2 \leq \phi \leq +\pi/2$ and range $-1 \leq \sin\phi \leq +1$.
From the differential equation (A-1) the definition of the associated Legendre functions yields as either

$$P_n(t) = \frac{1}{2^n\ n!}\ \frac{d^n}{dt^n}\ (t^2 - 1)^n \qquad (|t| \leq 1)\quad, \tag{A-2}$$

Rodriguez' formula, or the recursive Bonnet's formula

$$(n + 1)\ )P_{n+1}(t) - (2n + 1)\ t\ P_n(t) + n\ P_{n-1}(t) = 0 \tag{A-3}$$

using $t = \sin\phi$ and the initial values for recursion $P_0 = 1$ and $P_1(t) = t$.

First-order derivative of the Legendre polynomials

The first-order derivatives of the Legendre polynomials can easily be computed from the associated Legendre functions following the algorithm set up by equations (A-10) and (A-11).

Definition of the associated Legendre functions

The associated Legendre functions are defined by the ordinary second order differential equation

$$g''(t) - \tan(t)\ g'(t) + \left[n\ (n+1) - \frac{m^2}{\cos^2(t)}\right] g(t)\ =\ 0\quad. \tag{A-4}$$

The parameterization is by means of the spherical latitude ϕ with respect to an Earth-fixed geocentric equatorial system. The parameter t stands for the sine of the latitude having domain $-\pi/2 \leq \phi \leq +\pi/2$ and range $-1 \leq \sin\phi \leq +1$.
From the differential equation (A-4) the definition of the associated Legendre functions yields as

$$P_{n,m}(t) = \frac{1}{2^n\ n!}\ (1 - t^2)^{m/2}\ \frac{d^{n+m}}{dt^{n+m}}\ (t^2 - 1)^n \qquad (|t| \leq 1\ ,\quad 0 \leq |m| \leq n)\quad, \tag{A-5}$$

using $t = \sin\phi$. Alternatively the associated Legendre functions can be represented by means of a series expansion with upper boundary $K \leq (n - m)/2$ being an integer.

$$P_{n,m}(t) = \frac{1}{2^n}\ (1 - t^2)^{m/2}\ \sum_{k=0}^{K}\ (-1)^k\ \frac{(2\ n - 2\ k)!}{k!\ (n - k)!\ (n - m - 2\ k)!}\ t^{n-m-2\ k} \tag{A-6}$$

For the effective computation of higher degrees and orders recursive formulae can be set up. In the following two possible forms of recursion are given avoiding the explicit computation of the binomial coefficients and thus the computation of faculties. Further possibilities can be found in Knickmeyer (1989).

$$P_{n+1,m}(t)\ =\ \frac{1}{(n - m + 1)}\ [(2\ n + 1)\ t\ P_{n,m}(t) - (n + m)\ P_{n-1,m}(t)] \tag{A-7}$$

$$P_{n,m+1}(t)\ =\ 2\ m\ \tan(\phi)\ P_{n,m}(t) - (n + m)\ (n - m + 1)\ P_{n,m-1}(t) \tag{A-8}$$

The Legendre polynomials as well as the associated Legendre functions provide an orthogonal and complete set of base functions by fulfilling the orthogonalisation constraint

$$< P_{n,m}(t), P_{l,m}(t) >= \int_{-1}^{+1} P_{n,m}(t)\ P_{l,m}(t)\ dt = \frac{2}{2n + 1}\ \frac{(n + m)!}{(n - m)!}\ \delta_{n,l}\quad. \tag{A-9}$$

Note that despite orthogonality exists for degrees $n \neq l$, orthonormality does not hold for $n = l$.

First-order derivative of the associated Legendre functions

For the first-order derivative of the associated Legendre functions with respect to the spherical latitude ϕ a recursive formula can be given, too.

$$\frac{dP_{n,m}}{d\phi} = \frac{1}{2} \left[P_{n,m+1}(\sin\phi) - (n+m)(n-m+1) P_{n,m-1}(\sin\phi) \right] \tag{A-10}$$

$$= \frac{1}{(2n+1)\cos\phi} \left[(n+1)(n+m) P_{n-1,m}(\sin\phi) - n(n-m+1) P_{n+1,m}(\sin\phi) \right] \tag{A-11}$$

Definition of the normalized Legendre functions

To fulfill the orthonormalisation constraint (A-9) of the associated Legendre functions the functions have to be devided by

$$\sqrt{\frac{(2n+1)}{2} \cdot \frac{(n-m)!}{(n+m)!}}$$

each. This yields the definition of the normalised Legendre functions.

$$\widetilde{P}_{n,m}(t) = \underbrace{\sqrt{\frac{(2n+1)}{2} \cdot \frac{(n-m)!}{(n+m)!}}}_{=:\widetilde{n}_{n,m}} P_{n,m}(t) \tag{A-12}$$

Definition of the fully normalized Legendre functions

The fully normalized Legendre functions can also be derived from the associated functions by means of multiplication with a normalization factor. In contrast to the normalised Legendre functions the fully normalised Legendre functions already also guarantee orthonormalisation for the (surface) spherical harmonics, which will be introduced in annex B.

$$\bar{P}_{n,m}(t) = \underbrace{\left[(2 - \delta_{0,m})(2n+1)\frac{(n-m)!}{(n+m)!} \right]^{1/2}}_{=:\bar{n}_{n,m}} P_{n,m}(t) \tag{A-13}$$

A series expansion for the fully normalized Legendre functions can be found in the same way using (A-6). With (A-7) and the definition (A-13) of the fully normalized Legendre functions recursive formulae for higher degree and order can be found.

$$\bar{P}_{n,m}(t) = \frac{\bar{n}_{n,m}}{2^n} (1-t^2)^{m/2} \sum_{k=0}^{K} (-1)^k \frac{(2n-2k)!}{k!\,(n-k)!\,(n-m-2k)!} t^{n-m-2k} \tag{A-14}$$

$$\bar{P}_{n+1,m}(t) = \frac{1}{(n-m+1)} \left[(2n+1) t\, \bar{P}_{n,m}(t) - (n+m)\, \bar{P}_{n-1,m}(t) \right] \tag{A-15}$$

$$\bar{P}_{n,m+1}(t) = 2m\,\tan(\phi)\, \bar{P}_{n,m}(t) - (n+m)(n-m+1)\, \bar{P}_{n,m-1}(t) \tag{A-16}$$

First order derivative of the fully normalized Legendre functions

A recursive formula can also be given for the first-order derivative of the fully normalized Legendre functions with respect to ϕ.

$$\frac{d\bar{P}_{n,m}}{d\phi} = \frac{-1}{\sin\phi} \left[(1 - \frac{\delta_{1,m}}{2})^{-1/2} \left[(2n+1)(n+m)(n+m-1)/(2n-1) \right]^{1/2} \bar{P}_{n-1,m-1}(\sin\phi) \right.$$
$$\left. -n\,\cos(\phi)\, \bar{P}_{n,m}(\sin\phi) - \frac{m}{\cos\phi} \bar{P}_{n,m}(\sin\phi) \right] \tag{A-17}$$

B   Scalar-, vector- and tensor-valued surface spherical harmonics

Definition of the scalar-valued surface spherical harmonics

Surface spherical harmonics are created by transforming the Legendre functions onto a unit sphere or the spherical model Earth, respectively. Thus they are defined as

$$Y_n^m(\lambda, \phi) = \left\{ \begin{array}{c} \cos(m\lambda) \\ \sin(m\lambda) \end{array} \right\} P_{n,m}(\sin \phi) \quad . \tag{B-1}$$

For a thorough treatment of the definition and computation as well as graphical visualization of Legendre functions as well as surface spherical harmonics refer to Rabel (1997).

For the estimation of the resolution of (surface) spherical harmonics models of a field value over a sphere (gravitational values, topography/height values) it is necessary to know the behaviour of the oscillation of the harmonics. According to the choice of degree and order three cases have to be considered.

Zonal harmonics having order $m = 0$ divide the sphere by means of n parallels (circles of constant latitude) into $n + 1$ zones where the harmonics either run over or under the surface of the sphere. From the same degree and order $n = m$ the sectoral harmonics result. They divide the sphere into $2n$ sectors by means of $2n$ meridians. The general case of $n \neq m \neq 0$ yields the tesseral harmonics and divides the sphere along the meridians and lines of constant latitude into a chessboard pattern of $4m$ spherical triangles and $2m$ $(n - m - 1)$ spherical squares. For illustration refer to figure B-1, which has been created using the programs from Rabel (1997).
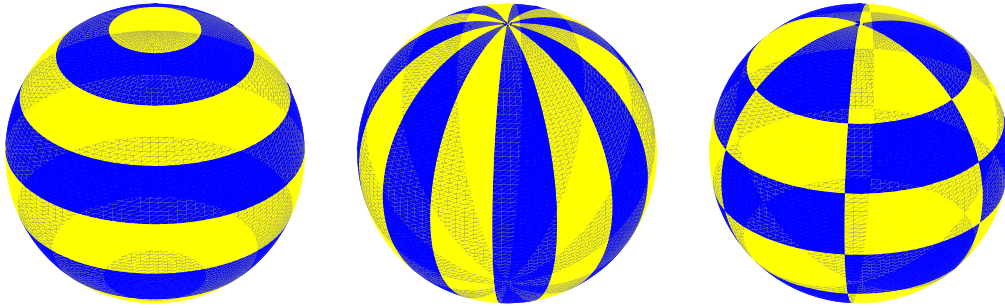

figure B-1: Zonal, sectoral and tesseral surface spherical harmonics Y_7^0, Y_7^7, Y_7^3
(dark area is negative and light positive w.r.t. the surface of the sphere)

Definition of the normalized scalar-valued surface spherical harmonics

The area of definition of the spherical harmonics is the unit sphere and for that area they form a complete system of orthonormal base functions. They are defined by means of the partial second-order differential equation

$$\frac{\partial^2 e(\lambda, \phi)}{\partial \phi^2} - \tan(\phi) \, \frac{\partial e(\lambda, \phi)}{\partial \phi} + \frac{1}{\cos^2(\phi)} \, \frac{\partial^2 e(\lambda, \phi)}{\partial \lambda^2} + n \, (n+1) \, e(\lambda, \phi) = 0 \tag{B-2}$$

in spherical longitude λ and spherical latitude ϕ with respect to a Earth-fixed geocentric reference system. Thus the real scalar spherical harmonics based on the definition of the fully normalized Legendre functions (A-13) are

$$e_{n,m}(\lambda, \phi) = \left\{ \begin{array}{c} \cos m\lambda \\ \sin |m| \lambda \end{array} \right\} \bar{P}_{n,|m|}(\sin \phi) \qquad \left\{ \begin{array}{l} \text{for } m \geq 0 \\ \text{for } m < 0 \end{array} \right. \quad . \tag{B-3}$$

Derivatives of the normalized scalar-valued surface spherical harmonics

In the following the derivatives of the scalar-valued surface spherical harmonics with respect to the spherical co-ordinates λ, ϕ and r are given.

$$
\begin{aligned}
\frac{\partial}{\partial \lambda} e_{n,m}(\lambda, \phi) &= \left\{ \begin{array}{c} -m \, \sin m\lambda \\ |m| \, \cos |m| \lambda \end{array} \right\} \bar{P}_{n,|m|}(\sin \phi) && \left\{ \begin{array}{l} \text{for } m \geq 0 \\ \text{for } m < 0 \end{array} \right. \\[2ex]
\frac{\partial}{\partial \phi} e_{n,m}(\lambda, \phi) &= \left\{ \begin{array}{c} \cos m\lambda \\ \sin |m| \lambda \end{array} \right\} \frac{\partial}{\partial \phi} \bar{P}_{n,|m|}(\sin \phi) && \left\{ \begin{array}{l} \text{for } m \geq 0 \\ \text{for } m < 0 \end{array} \right.
\end{aligned}
\tag{B-4}
$$

Definition of the vector-valued surface spherical harmonics

Using the definition of the scalar-valued surface spherical harmonics the vector-valued spherical harmonics are defined as

$$\mathbf{R}_{n,m}(\lambda, \phi) = e_{n,m}(\lambda, \phi) \, \mathbf{e}_r \tag{B-5}$$

$$\mathbf{S}_{n,m}(\lambda, \phi) = \frac{r}{\sqrt{n(n+1)}} \, grad \, e_{n,m}(\lambda, \phi) \tag{B-6}$$

$$= \frac{1}{\sqrt{n(n+1)}} \left(\frac{1}{\cos\phi} \frac{\partial}{\partial\lambda} e_{n,m}(\lambda, \phi) \, \mathbf{e}_\lambda + \frac{\partial}{\partial\phi} e_{n,m}(\lambda, \phi) \, \mathbf{e}_\phi \right) \tag{B-7}$$

$$\mathbf{T}_{n,m}(\lambda, \phi) = \frac{1}{\sqrt{n(n+1)}} \left(\frac{\partial}{\partial\phi} e_{n,m}(\lambda, \phi) \, \mathbf{e}_\lambda - \frac{1}{\cos\phi} \frac{\partial}{\partial\lambda} e_{n,m}(\lambda, \phi) \, \mathbf{e}_\phi \right) \tag{B-8}$$

and

$$\mathbf{T}_{n,m}(\lambda, \phi) = -\mathbf{e}_r \times \mathbf{S}_{n,m}(\lambda, \phi) \qquad\qquad \mathbf{S}_{n,m}(\lambda, \phi) = \mathbf{e}_r \times \mathbf{T}_{n,m}(\lambda, \phi) \tag{B-9}$$

Definition of the tensor-valued surface spherical harmonics

The tensor-valued spherical harmonics come up when the gradient of the gravitational acceleration vector is to be computed. Technically they are created by applying the gradient operator to the gravitational vector also. There are nine different tensor-valued spherical surface harmonics that can be devided into different types and that are defined as follows. For the definitions $\wedge$ denotes the antisymmetric product $\mathbf{a} \wedge \mathbf{b} := \mathbf{a} \otimes \mathbf{b} - \mathbf{b} \otimes \mathbf{a}$ and $\vee$ the symmetric product $\mathbf{a} \vee \mathbf{b} := \mathbf{a} \otimes \mathbf{b} + \mathbf{b} \otimes \mathbf{a}$ with $\otimes$ marking the non-commutative dyadic product of two vectors $\mathbf{a}$ and $\mathbf{b}$ creating a tensor of second order.

Antisymmetric tensor-valued surface spherical harmonics:

$$\mathbf{T}_{n,m}^R = \frac{1}{\sqrt{2}} \, \mathbf{e}_\lambda \wedge \mathbf{e}_\phi \, e_{n,m}(\lambda, \phi) \qquad (n \geq 0)$$

$$\mathbf{T}_{n,m}^S = -\frac{1}{\sqrt{2}} \, \mathbf{e}_r \wedge \mathbf{T}_{n,m} \qquad (n \geq 1) \tag{B-10}$$

$$\mathbf{T}_{n,m}^T = -\frac{1}{\sqrt{2}} \, \mathbf{e}_r \wedge \mathbf{S}_{n,m} \qquad (n \geq 1)$$

Symmetric tangential tensor-valued surface spherical harmonics with vanishing trace ($n \geq 2$):

$$\mathbf{T}_{n,m}^{E2} = \left[(\mathbf{e}_\phi \otimes \mathbf{e}_\phi - \mathbf{e}_\lambda \otimes \mathbf{e}_\lambda) \left(\frac{\partial^2}{\partial\phi^2} + \tan\phi \frac{\partial}{\partial\phi} - \frac{1}{cos2\phi} \frac{\partial^2}{\partial\lambda 2} \right) + 2 \, \mathbf{e}_\phi \vee \mathbf{e}_\lambda \frac{\partial}{\partial\phi} \left(\frac{1}{\cos\phi} \frac{\partial}{\partial\lambda} \right) \right]$$
$$\frac{e_{n,m}(\lambda, \phi)}{\sqrt{2 \, (n+2) \, (n+1) \, n \, (n-1)}}$$

$$\mathbf{T}_{n,m}^{B2} = -\left[2 \, (\mathbf{e}_\phi \otimes \mathbf{e}_\phi - \mathbf{e}_\lambda \otimes \mathbf{e}_\lambda) \frac{\partial}{\partial\phi} \left(\frac{1}{\cos\phi} \frac{\partial}{\partial\lambda} \right) - \mathbf{e}_\phi \vee \mathbf{e}_\lambda \left(\frac{\partial^2}{\partial\phi^2} + \tan\phi \frac{\partial}{\partial\phi} - \frac{1}{cos^2\phi} \frac{\partial^2}{\partial\lambda^2} \right) \right]$$
$$\frac{1}{\sqrt{2 \, (n+2) \, (n+1) \, n \, (n-1)}} \tag{B-11}$$

Symmetric mixed tensor-valued surface spherical harmonics:

$$\mathbf{T}_{n,m}^{L0} = \mathbf{e}_r \otimes \mathbf{e}_r \, e_{n,m}(\lambda, \phi) \qquad (n \geq 0)$$

$$\mathbf{T}_{n,m}^{T0} = \frac{1}{\sqrt{2}} \, (\mathbf{e}_\phi \otimes \mathbf{e}_\phi + \mathbf{e}_\lambda \otimes \mathbf{e}_\lambda) \, e_{n,m}(\lambda, \phi) \qquad (n \geq 1)$$

$$\mathbf{T}_{n,m}^{E1} = -\mathbf{e}_r \vee \mathbf{S}_{n,m} \cdot \frac{1}{\sqrt{2}} \qquad (n \geq 1) \tag{B-12}$$

$$\mathbf{T}_{n,m}^{B1} = -\mathbf{e}_r \vee \mathbf{T}_{n,m} \cdot \frac{1}{\sqrt{2}} \qquad (n \geq 1)$$

Spherical harmonics series expansion of a function

A 2π-periodic function given in spherical co-ordinates can be given as series expansion with respect to spherical harmonics.

$$f(\lambda, \phi, r) = \sum_{n=0}^{\infty} \sum_{m=0}^{n} \bar{f}_{n,m}(\lambda, \phi, r) \, (\bar{c}_{n,m} \, \cos m\lambda + \bar{s}_{n,m} \, \sin m\lambda) \, \bar{P}_{n,m}(\sin\phi) \qquad , \tag{B-13}$$

with $\bar{c}_{n,m}$ and $\bar{s}_{n,m}$ being scalar expansion co-efficients not depending on the co-ordinates. $\bar{f}_{n,m}(\lambda, \phi, r)$ is a co-ordinate dependent factor.

C   The dedicated gravity field mission CHAMP

The dedicated gravity and magnetic field mission CHAMP ('***Cha****llenging* ***M****ini-Satellite* ***P****ayload for Geophysical Research and Application*') is a German mini-satellite project that has been launched successfully on Juli 15th 2000 from Plesetsk cosmodrome. Under the lead of the Geoforschungszentrum Potsdam (GFZ), the German geophysical research centre, and with contributions by NASA's JET Propulsion Laboratory (JPL), the French Centre National d'Études Spatiales (CNES) and several other research institutions as well as companies, the mission aims at

- measuring the gravity field of the Earth,

- measuring the magnetic field of the Earth,

- sounding the atmosphere and

- flying a GPS-based passive altimetry experiment.

Mission instrumentation

To achieve the aims mentioned above, the satellite system CHAMP combines a variety of different scientific instruments. For the first time a wide range of scientific data will be collected and fixed with respect to space continuously over a period of five years combined on a low-Earth-orbiting platform. The observables are (DFG 1997)

- precise satellite-to-satellite high-low distance measurements between GPS satellites and CHAMP (positioning),

- three axial acceleration measurements (non-conservative surface accelerations, satellite attitude control manoeuvres),

- star sensor measurements (satellite orientation),

- occultation measurements between CHAMP and GPS satellites rising or descending, respectively, with respect to the Earth (atmospheric and ionospheric sounding),

- measuring scalar and vectorial magnetic forces (Earth's magnetic field),

- ion-drift-meter measurements (electric field),

- satellite laser ranging measurements (positioning) and

- GPS based altimetry measurements using a nadir oriented GPS receiver antenna (height of satellite over ice and ocean areas).

Mission characteristics

The CHAMP mission is set up for a duration of five years starting at a maximum and ending near a minimum of solar activity and flux. Since CHAMP, as a low orbiter, is flying in the atmosphere of the Earth, this aim requires an orbit manoeuvre to reach the proposed lifetime. Depending on the solar activity, more precisely the extend of the solar flux maximum, either a 30 km descend manoeuvre after two years (case of low solar maximum) or a 30 km ascend manoeuvre after four years (case of high solar maximum) will be performed. The general orbit characteristics to be achieved are

- a nearly circular orbit, eccentricity near to zero ($e < 0,005$),

- nearly polar orbit with a high inclination of 87° and

- an initial orbit height of 470 km decreasing to 300 km during the five years of its lifetime.

The plot of a simulated CHAMP orbit is given in figure 7-1 in table 7-1.

Gravity field measurements with CHAMP

The determination of the gravity field by means of the CHAMP mission is based on a precise orbit determination (POD) using the tracking data provided by the POD GPS receiver. POD in this context stands for cm-accurate, quasi-continuous determination of full three-dimensional position and velocity vectors of the satellite.

The scientific requirements with respect to POD, that have to be fulfilled to guarantee the wanted accuracy of gravity field recovery, can be met with an estimated measurement bandwidth for the orbit perturbations ranging from $(1/revolution)^{-1}$ up to $(1/200\ revolution)^{-1}$. This equals a frequency range from $2 \cdot 10^{-4}\ Hz$ to $4 \cdot 10^{-2}\ Hz$.

The main part within the POD will be taken by a 12 channel GPS TurboRogue Space Receiver (JPL) with an accuracy better than 0.2 cm in phase and 30 cm in range measurements at a sampling rate of 0.1 Hz. The GPS-POD solution will be supported by satellite laser ranging (SLR) measurements to the 4 prism laser reflector attached to the Earth pointing side of CHAMP, which enables a determination of the range between CHAMP and the SLR ground station with an accuracy of $1 \ldots 2$ cm without any ambiguities. Naturally the coverage of the SLR data is limited to the availability of ground stations and thus will not be quasi-continuous and global neither w.r.t time nor location. The result of the POD will be a time series of position and velocity vectors of CHAMP with a sampling rate of 1 minute (all numbers given are preliminary numbers based on Reigber et al. (1996) and private communication).

Non-conservative forces acting on the satellite will be taken into account by means of a three-axial accelerometer at the center of gravity (CoG) of CHAMP. The accelerations measured include atmospheric drag, solar radiation pressure and satellite's attitude manoeuvres. For a correct interpretation of the accelerometer data the accelerometer is linked with two star sensors to provide an absolute orientation in space. The accelerometer provides a measurement range of $\pm 10^{-4}\ ms^{-2}$ with a resolution of less than $5 \cdot 10^{-9}\ ms^{-2}$ and a frequency range from 0.1 to 0.0001 Hz and provides preprocessed and calibrated acceleration data at a temporal resolution of 1 Hz (for the calibration of the accelerometer refer to Pérosanz et al. (1999)). A discussion of the accelerometer's contribution to the determination of the gravitational field can already be found in 1-1-2 due to its importance.
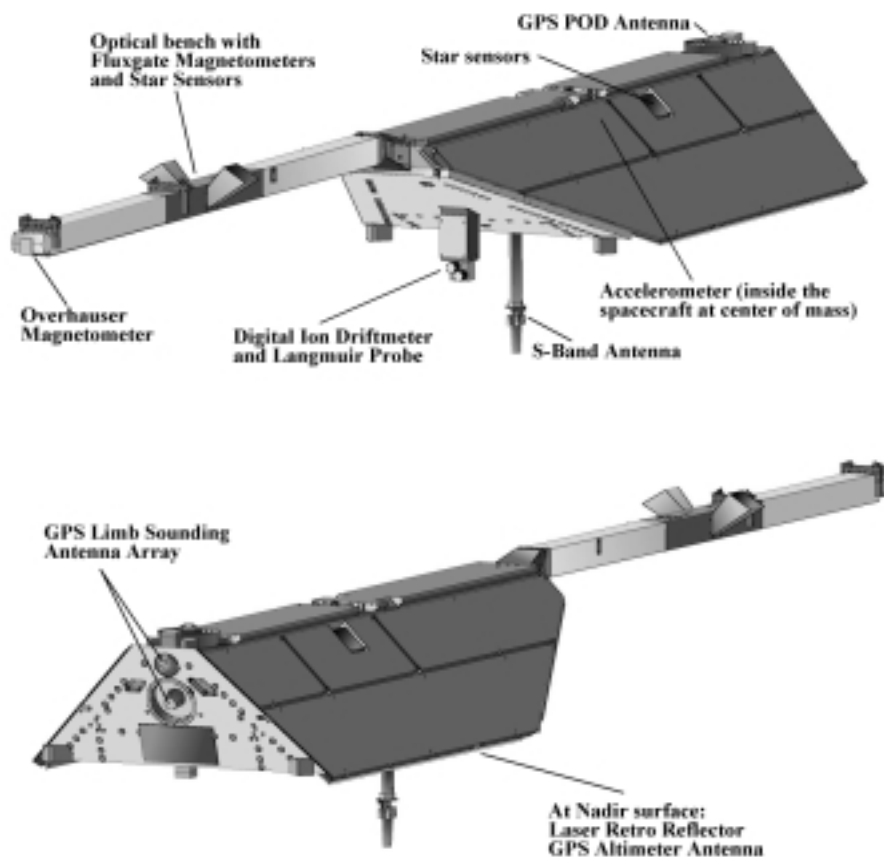

figure 8-1: Overview sketch for CHAMP and its instrumentation
(*GFZ, CHAMP project site, http://op.gfz-potsdam.de/champ/*)
(web address valid at September 22, 2000)

D   Numerical integration methods applied

For the integration of the second-order ordinary vector-valued differential equation Newton's equation of motion (2-1)

$$\ddot{\mathbf{x}}(t) = \frac{1}{m_{sat.}} \, \mathbf{F}(t, \mathbf{x}, \dot{\mathbf{x}}) \tag{D-1}$$

two numerical integration methods are applied. The well-known theoretical background can be found in any textbook on numerical methods and shall be given here as an overview following mainly Schwarz (1986) and Isaacson and Keller (1966).

Starting from (D-1) the second-order differential equation can be transformed into a system of first-order ordinary vector-valued differential equations (D-2).

$$
\begin{aligned}
\dot{\mathbf{y}}(t) &:= \mathbf{x}(t) \\
\frac{d}{dt} \, \dot{\mathbf{y}}(t) &= \ddot{\mathbf{y}}(t) \\
\frac{d}{dt} \, \ddot{\mathbf{y}}(t) &= \frac{1}{m_{sat.}} \, \mathbf{F}(t, \mathbf{x}, \dot{\mathbf{x}})
\end{aligned}
\tag{D-2}
$$

Since each differential equation of order higher than 1 can be transformed into a system of first-order differential equations, the following discussion will be based on a first-order ordinary vector-valued differential equation and its equivalent integral equation (D-3) and can be applied analogously.

$$\dot{\mathbf{y}}(t) = \mathbf{f}(t, \mathbf{y}(t)) \qquad \Longleftrightarrow \qquad \mathbf{y}(t_{k+1}) = \mathbf{y}(t_k) + \int\limits_{t_k}^{t_{k+1}} \mathbf{f}(t', \mathbf{y}(t')) \, dt' \tag{D-3}$$

The principle of numerical integration is based upon an approximation representation $\mathbf{Y}_j$ of $\mathbf{y}(t_j)$ at discrete points of time $t_j \in [t_k, t_{k+1}]$. The approximation $\mathbf{Y}_{k+1}$ for $\mathbf{y}(t_{k+1})$ is computed by adding an approximation of the integral to the approximation $\mathbf{Y}_k$ for $\mathbf{y}(t_k)$. Based on the method chosen for approximating the integral different methods of numerical integration can be set up.

Equation (D-4) gives a general description of a numerical integration method. m is the number of approximations used to compute $\mathbf{Y}_{k+1}$ with coefficient α_0 usually set to 1, h denotes the time step width of the approximation.

$$\sum_{j=0}^{m} \alpha_j \, \mathbf{Y}_{k+1-j} = h \, \mathbf{F}(t_{k+1}, \mathbf{Y}_{k+1-m}, \dots, \mathbf{Y}_{k+1}, h) \tag{D-4}$$

For $m = 1$ so-called *single-step methods* are defined, for $m > 1$ and $\mathbf{F}$ a linear polynomial with coefficients β *linear multi-step methods* are defined:

- single-step methods taking into account only the previous value $\mathbf{Y}_k$ for the computation of $\mathbf{Y}_{k+1}$ as given in (D-5),

- multi-step methods taking into account m previous values $\mathbf{Y}_{k+1-m}$, $\mathbf{Y}_{k+1-m+1}$, $\dots, \mathbf{Y}_k$ as given in (D-6).

$$\mathbf{Y}_{k+1} = \mathbf{Y}_k + h \, \mathbf{F}(t_k, \mathbf{Y}_k, \mathbf{Y}_{k+1}) \tag{D-5}$$

$$\mathbf{Y}_{k+1} = \sum_{i=1}^{m} \alpha_j \, \mathbf{Y}_{k+1-j} + h \sum_{j=0}^{m} \beta_j \, \mathbf{f}(t_{k+1-j}, \mathbf{Y}_{k+1-j}) \tag{D-6}$$

If $\mathbf{F}$ and $\mathbf{f}$ respectively depend on $\mathbf{Y}_{k+1}$ the method is called implicit, if not it is called explicit.

Within the single- and multi-step methods the *predictor-corrector* methods form a special set of numerical integration methods. For predictor-corrector methods the two different methods are combined, an explicit method only using previous values for the determination of $\mathbf{Y}_{k+1}$ (thus called *predictor*) and an implicit method using an estimation of $\mathbf{Y}_{k+1}$ in addition to previous values to obtain a better estimation of $\mathbf{Y}_{k+1}$ (thus called *corrector*). The predictor serves for the determination of the initial estimation of $\mathbf{Y}_{k+1}$ which will be improved by the corrector. In general the order of the truncation error of the corrector is one higher than the error order of the predictor.

For the definition of a numerical integration method a suitable function $\mathbf{F}$ has to be defined in close connection with the differential equation's inhomogeneity $\mathbf{f}$. For the integration of the satellite's equation of motion (2-1) two different types of numerical methods are used: the Runge-Kutta method, a single-step method, and the Adams-Moulton / Adams-Bashforth multistep predictor-corrector method.

A comparison of the two numerical integration methods presented here has been performed for the integration of a Kepler orbit for 35 revolutions. The closing error of the orbital ellipse after each revolution gives an idea of the integration error which has to be taken into account when choosing an appropriate method. The results of this comparison are given in figure 7-2.

Numerical integration by means of a 6th order Runge-Kutta method

For the class of the explicit single-step Runge-Kutta methods the right-hand function $\mathbf{F}$ of (D-5) is defined as the following sum

$$\mathbf{F}(t, \mathbf{Y}, h) = \sum_{i=1}^{\mu} c_i \, \mathbf{K}_i(t, \mathbf{Y}, h) \tag{D-7}$$

with

$$\mathbf{K}_1(t, \mathbf{Y}, h) \;\; = \;\; \mathbf{f}(t, \mathbf{Y})$$

$$\mathbf{K}_i(t, \mathbf{Y}, h) \;\; = \;\; \mathbf{f}(t + a_i \, h, \mathbf{Y} + h \sum_{l=1}^{i-1} b_{il} \, \mathbf{K}_l(t, \mathbf{Y}, h)) \;\;\; .$$

The 6th order Runge-Kutta methods is defined as

$$\mathbf{x}(t_{k+1}) = \mathbf{x}(t_k) + \frac{t_{k+1} - t_k}{336} \, (14 \, \mathbf{K}_1 + 35 \, \mathbf{K}_4 + 162 \, \mathbf{K}_5 + 125 \, \mathbf{K}_6) \tag{D-8}$$

with

$$\mathbf{K}_1 \;\; = \;\; \mathbf{f}\left(t_k, \mathbf{x}(t_k)\right)$$

$$\mathbf{K}_2 \;\; = \;\; \mathbf{f}\left(t_k + \frac{t_{k+1} - t_k}{2}, \mathbf{x}(t_k) + \frac{t_{k+1} - t_k}{2} \, \mathbf{K}_1\right)$$

$$\mathbf{K}_3 \;\; = \;\; \mathbf{f}\left(t_k + \frac{t_{k+1} - t_k}{2}, \mathbf{x}(t_k) + \frac{t_{k+1} - t_k}{2} \, \mathbf{K}_2\right)$$

$$\mathbf{K}_4 \;\; = \;\; \mathbf{f}\left(t_k + (t_{k+1} - t_k), \mathbf{x}(t_k) + (t_{k+1} - t_k) \, \mathbf{K}_3\right)$$

$$\mathbf{K}_5 \;\; = \;\; \mathbf{f}\left(t_k + \frac{2}{3} \, (t_{k+1} - t_k), \mathbf{x}(t_k) + \frac{t_{k+1} - t_k}{27} \, (7 \, \mathbf{K}_1 + 10 \, \mathbf{K}_2 + \mathbf{K}_4)\right)$$

$$\mathbf{K}_6 \;\; = \;\; \mathbf{f}\left(t_k + \frac{1}{5} \, (t_{k+1} - t_k), \mathbf{x}(t_k) + \frac{t_{k+1} - t_k}{625} \, (28 \, \mathbf{K}_1 - 125 \, \mathbf{K}_2 + 546 \, \mathbf{K}_3 + 54 \, \mathbf{K}_4 - 378 \, \mathbf{K}_5)\right)$$

The determination of the coefficients a_i, b_{il} and c_i is based on a set of condition equations drawn from the Taylor expansion in powers of h of the representation (D-9) of the local truncation error of the Runge-Kutta method.

$$\mathbf{d}_{k+1} = \mathbf{y}(t_{k+1}) - y(t_k) - h \sum_{i=1}^{\mu} c_i \, \mathbf{K}_i(t, \mathbf{y}(t_k), h) \tag{D-9}$$

The truncation error is computed as difference between the true value $\mathbf{y}(t_{k+1})$ at t_{k+1} and the estimated approximation value $\mathbf{Y}(t_{k+1})$ computed from the Runge-Kutta method's equations (D-7) at $\mathbf{Y} = \mathbf{y}(t_k)$.
The Taylor expansion yields generally written

$$\mathbf{d}_{k+1} = \mathbf{D}_1 \, h + \mathbf{D}_2 \, h^2 + \mathbf{D}_3 \, h^3 + \mathbf{D}_4 \, h^4 + \ldots \tag{D-10}$$

with coefficients $\mathbf{D}_i$ depending, amongst others, on a_i, b_{il} and c_i.
The overall number of coefficients to be determined is computed as

$$
\left.
\begin{array}{lll}
a_i : & (i = 2, \ldots, \mu) & \mu - 1 \\
b_{il} : & (i = 1, \ldots, \mu), \; (l = 1, \ldots, i - 1) & \sum_{j=1}^{\mu} (j - 1) \\
c_i : & (i = 1, \ldots, \mu) & \mu
\end{array}
\right\} \implies n = 2\mu - 1 + \frac{\mu(\mu - 1)}{2} \quad , \tag{D-11}
$$

which have to fulfil (D-12) in order to guarantee that certain predictor values for the differential equation $\mathbf{y}' = \mathbf{1}$ are exact.

$$a_k = \sum_{j=1}^{k-1} b_{kj} \tag{D-12}$$

To guarantee a certain error order all the $\mathbf{D}_i$ belonging to the addends below this order have to vanish. This yields condition equations for the determination of a_i, b_{il} and c_i. A detailed example for the determination of the coefficients for a third-order Runge-Kutta method is given in Schwarz (1993), section 9.1.4.
For the temporal prediction step (6-18) of the discrete Extended Kalman-Bucy filter (dEKF) a 6th order Runge-Kutta numerical integration method as shown in equation (D-8) has been chosen (Engeln-Müllges and Reutter (1988), section 17.3.4). The order of the local truncation error of the 6th order Runge-Kutta method is $q_l = 6$, the order of the global truncation error $q_g = q_l - 1 = 5$ (Engeln-Müllges and Reutter (1988), section 17.3.4.1).

Numerical integration by means of an Adams-Moulton / Adams-Bashforth method

The 12th order Adams-Moulton / Adams-Bashforth multistep method with local discretization error $\mid d \mid \leq h^{13}$ has been chosen from the class of predictor-corrector methods (Stiefel and Scheifele (1971), Scheinert (1996), Engeln-Müllges and Reutter (1988)). It is a method to solve a first-order differential equation,thus computes the position based on the solution for the velocity.

Methods of the Adams type are constructed by substituting the right-handed function $\mathbf{f}$ of (D-6) by means of a Lagrangian polynomial of order μ (D-13). The coefficients α_j are set to $\alpha_1 = -1$ and $\alpha_2 = \alpha_3 = \ldots = 0$. The β_j are computed from the Lagrangian polynomial itself (Stiefel and Scheifele (1971)).

$$\mathbf{I}_\mu(t) = \sum_{i=0}^{\mu} \mathbf{y}(t_i)\, L_i(t) \tag{D-13}$$

$$\text{with} \qquad L_i(t) = \frac{(t - t_0)\ldots(t - t_{i-1})(t - t_{i+1})\ldots(t - t_\mu)}{(t_i - t_0)\ldots(t_i - t_{i-1})(t_i - t_{i+1})\ldots(t_i - t_\mu)}$$

which yields with the coefficients

i	b_i (vel.)	b_i (pos.)	$b_i^\star$ (vel.)	$b_i^\star$ (pos.)
0	1	$\dfrac{1}{2}$	1	$\dfrac{1}{2}$
1	$\dfrac{1}{2}$	$\dfrac{1}{6}$	$-\dfrac{1}{2}$	$-\dfrac{1}{3}$
2	$\dfrac{5}{12}$	$\dfrac{1}{8}$	$-\dfrac{1}{12}$	$-\dfrac{1}{24}$
3	$\dfrac{3}{8}$	$\dfrac{19}{180}$	$-\dfrac{1}{24}$	$-\dfrac{7}{360}$
4	$\dfrac{251}{720}$	$\dfrac{3}{32}$	$-\dfrac{19}{720}$	$-\dfrac{17}{1440}$
5	$\dfrac{95}{288}$	$\dfrac{863}{10080}$	$-\dfrac{27}{1440}$	$-\dfrac{41}{5040}$
6	$\dfrac{19087}{60480}$	$\dfrac{275}{3456}$	$-\dfrac{863}{60480}$	$-\dfrac{731}{120960}$
7	$\dfrac{36799}{120960}$	$\dfrac{33959}{453600}$	$-\dfrac{1375}{120960}$	$-\dfrac{8563}{1814400}$
8	$\dfrac{1070017}{3628800}$	$\dfrac{400967}{5644800}$	$-\dfrac{33953}{3628800}$	$-\dfrac{27719}{7257600}$
9	$\dfrac{2082753}{7357600}$	$\dfrac{325043}{47900160}$	$-\dfrac{57281}{7257600}$	$-\dfrac{190073}{59875200}$
10	$\dfrac{134211265}{479001600}$	$\dfrac{359667}{5519360}$	$-\dfrac{3250433}{479001600}$	$-\dfrac{516149}{191600640}$
11	$\dfrac{262747265}{958003200}$	$\dfrac{13695779093}{217945728000}$	$-\dfrac{5675265}{958003200}$	$-\dfrac{1013143139}{435891456000}$
12	$\dfrac{703604254357}{2615348736000}$	$\dfrac{28915048019}{47551795200}$	$-\dfrac{13695779093}{2615348736000}$	$-\dfrac{1519024289}{74724249600}$

The advantage of the predictor-corrector methods with respect to Runge-Kutta methods is that only two more evaluations of the function to be integrated are necessary for each step and thus the methods are more economical. More advantages of predictor-corrector methods with respect to explicit single-step methods are the higher order of truncation error and the better stability.

The 12th order Adams-Moulton / Adams-Bashforth multistep method is defined as shown below. The coefficients are determined from the Lagrangian interpolation polynomial approximating the right-handed side of the differential equation to be integrated. Thus different sets of coefficients are formed for the determination of

the position and the velocity from Newton's equation of motion (2-1).

$$\textbf{Predictor:} \qquad \bar{\mathbf{X}}(t_{k+1}) \quad = \quad \mathbf{X}(t_k) + dt \sum_{i=0}^{m} b_i \, \mathbf{f}_{k-i}$$

(Adams-Bashforth)

$$\textbf{Evaluation I:} \qquad \bar{\mathbf{f}}_{k+1} \quad = \quad \mathbf{f}(t_{k+1}, \bar{\mathbf{X}}(t_{k+1}))$$

$$\textbf{Corrector:} \qquad \mathbf{X}(t_{k+1}) \quad = \quad \mathbf{X}(t_k) + dt \left[b_0^\star \, \bar{\mathbf{f}}_{k+1} + \sum_{i=1}^{m} b_i^\star \, \mathbf{f}_{k+1-i} \right]$$

(Adams-Moulton)

$$\textbf{Evaluation II:} \qquad \mathbf{f}_{k+1} \quad = \quad \mathbf{f}(t_{k+1}, \mathbf{X}(t_{k+1}))$$

(D-14)

Since both steps of the Adams-Moulton / Adams-Bashforth method are multi-step methods the necessary number of initial / previous values have to be known. For their determination e.g. single-step methods can be used (another possibility would be the use of self-starting multi-step methods like the Cowell method instead of the Adams-Moulton / Adams-Bashforth methods).

E Integral representation of Newton's equation of motion

In this annex the determination of an integral representation of Newton's equation of motion is presented. It provides the prove for the equivalences shown in table 2-6 and 2-7.

Integration of Newton's equation of motion

The acceleration is the second derivative of the position with respect to time, thus Newton's equation of motion (2-1)

$$\frac{d^2}{dt^2}\,\mathbf{x}(t) = \frac{1}{m_{sat.}}\,\mathbf{F}(t)$$

can be transformed into an integral equation for the satellite's position vector by means of two integration steps. First integration step:

$$\int_{t_A}^{t_i} \ddot{\mathbf{x}}(t')\,dt' \;=\; \frac{1}{m_{Sat.}}\int_{t_A}^{t_i} \mathbf{F}(t')\,dt' \tag{E-1}$$

$$\dot{\mathbf{x}}(t_i) \;=\; \frac{1}{m_{Sat.}}\int_{t_A}^{t_i} \mathbf{F}(t')\,dt' + \mathbf{C} \tag{E-2}$$

Second integration step:

$$\mathbf{x}(t_i) = \frac{1}{m_{Sat.}}\int_{t''=t_A}^{t_i}\int_{t'=t_A}^{t''} \mathbf{F}(t')\,dt'\,dt'' + \mathbf{C}\int_{t_A}^{t_i} dt'' + \mathbf{D} \tag{E-3}$$

The double integral can be transformed into a single integral by means of the relation determined in the last subsection of this annex.

$$\dot{\mathbf{x}}(t_i) \;=\; \frac{1}{m_{Sat.}}\int_{t'=t_A}^{t_i} \mathbf{F}(t')\,dt' + \mathbf{C} \tag{E-4}$$

$$\mathbf{x}(t_i) \;=\; \frac{1}{m_{Sat.}}\int_{t'=t_A}^{t_i} \mathbf{F}(t')\,(t_i - t')\,dt' + \mathbf{C}\,(t_i - t_0) + \mathbf{D} \tag{E-5}$$

The constants of integration C and D can be determined either from initial values or from boundary values. In the first case the initial value problem of orbit integration is represented, in the second case the boundary value problem of orbit analysis.

Determination of the constants of integration

The determination of the *initial value problem* of orbit integration is performed by means of the two initial values $\mathbf{x}(t_A) = \mathbf{x}_A$ and $\dot{\mathbf{x}}(t_A) = \dot{\mathbf{x}}_A$ over the time interval $[t_A = t_0, t_l]$ with t_l being the point of time of evaluation. (E-4) and (E-5) yield

$$\mathbf{C} \;=\; \dot{\mathbf{x}}_A \tag{E-6}$$

$$\mathbf{D} \;=\; \mathbf{x}_A \tag{E-7}$$

The determination of the *boundary value problem* of orbit analysis over the time interval $[t_A = t_0, t_E]$ is performed by means of the two boundary values $\mathbf{x}(t_A) = \mathbf{x}_A$ und $\mathbf{x}(t_E) = \mathbf{x}_E$. For the constants of integration (E-5) yields

$$\mathbf{C} \;=\; \frac{1}{t_E - t_A}\left(\mathbf{x}_E - \mathbf{x}_A - \frac{1}{m_{Sat.}}\int_{t'=t_A}^{t_E} \mathbf{F}(t')\,(t_E - t')\,dt'\right) \tag{E-8}$$

$$\mathbf{D} \;=\; \mathbf{x}_A \quad . \tag{E-9}$$

Inserting these constants into (E-4) and (E-5) yields the integral representations (2-5) and (2-7) equivalent to Newton's equation of motion.

Transformation of a double integral into a single integral

Starting from the double integral over $\mathbf{f}(s)$ continuous on the interval of integration $[a, s]$

$$I = \int\limits_{s_2=a}^{s} \int\limits_{s_1=a}^{s_2} \mathbf{f}(s_1) \; ds_1 \; ds_2 \qquad (\text{E-10})$$

and using the Heaviside function as Green's function for the inverse differential operator (= integral operator) of the temporal derivative (Roach (1968))

$$H(x) = \begin{cases} 1 & \text{for} \quad x \geq 0 \\ 0 & \text{for} \quad x < 0 \end{cases} \qquad (\text{E-11})$$

with

$$\int H(x) \; dx = x \cdot H(x) \qquad (\text{E-12})$$

yields with the limits of integration $a \leq s_1 \leq s_2$ and $a \leq s_2 \leq s$, i.e. $a \leq s_1 \leq s_2 \leq s$ and thus $H(s_2 - s_1) = 1$ always,

$$\int\limits_{s_2=a}^{s} \int\limits_{s_1=a}^{s_2} \mathbf{f}(s_1) \; ds_1 \; ds_2 \;=\; \int\limits_{s_1=a}^{s} \mathbf{f}(s_1) \int\limits_{s_2=a}^{s_1} H(s_2 - s_1) \; ds_2 \; ds_1$$

$$=\; \int\limits_{s_1=a}^{s} \mathbf{f}(s_1) \; [(s_2 - s_1) \cdot H(s_2 - s_1)]_{s_2=a}^{s_1} \; ds_1$$

$$=\; \int\limits_{s_1=a}^{s} \mathbf{f}(s_1) \; [(s - s_1) \cdot \underbrace{H(s - s_1)}_{=\,1} - (a - s_1) \cdot \underbrace{H(a - s_1)}_{=\,0}] \; ds_1$$

$$\int\limits_{s_2=a}^{s} \int\limits_{s_1=a}^{s_2} \mathbf{f}(s_1) \; ds_1 \; ds_2 \;=\; \int\limits_{s_1=a}^{s} \mathbf{f}(s_1) \; (s - s_1) \; ds_1 \qquad . \qquad (\text{E-13})$$

The change of the order of integration is possible if the integrand is continuous over the whole interval of integration (Bronstein and Semedjajew (1989), section 3.1.9.2).

The transformation of a double integral into a single integral can thus be performed for the case of this thesis as

$$\int\limits_{t''=t_0}^{t_i} \int\limits_{t'=t_0}^{t''} \mathbf{F}(t') \; dt' \; dt'' = \int\limits_{t'=t_0}^{t_i} \mathbf{F}(t') \; (t_i - t') \; dt' \qquad (\text{E-14})$$

initial value problem of orbit computation (table orbit analysis (table

Literature references

Abbreviations   (web addresses valid at September 22, 2000)

ASR: *Advances in Space Research, COSPAR*

BMBW FB: *Forschungsbericht des Bundesministeriums für Bildung und Wissenschaft (research report of the German federal ministry for education and science)*

CSR-TM: *Technical memorandum, Centre for Space Research, University of Texas at Austin* web address: *http://www.csr.utexas.edu*

DFG: *Deutsche Forschungsgemeinschaft (German Research Council / Foundation)* web address: *http://www.dfg.de*

DGK A: *Deutsche Geodätische Kommission, Reihe A (Theoretische Geodäsie), München / Munich (Germany) (German Geodectic Commission, publications on theoretical geodesy)* web address: *http://www.dgfi.badw.de/dgfi/DGK/dgk_d.html*

DGK C: *Deutsche Geodätische Kommission, Reihe C (Dissertationen), München / Munich (Germany) (German Geodectic Commission, dissertations)* web address: *http://www.dgfi.badw.de/dgfi/DGK/dgk_d.html*

GFZ STR: *Scientific Technical Report des Geoforschungszentrums Potsdam, Potsdam (Germany) (scientific technical report of the geoscience research centre Potsdam)* web address: *http://www.gfz-potsdam.de*

GIS: *Geodätisches Institut der Universität Stuttgart (Germany) (Geodetic Institute of the University of Stuttgart)* web address: *http://www.uni-stuttgart.de/gi*

GIS TR: *Technical report of the Geodetic Institute of the University of Stuttgart* web address: *http://www.uni-stuttgart.de/gi*

IEEE: *The Institute of Electrical and Electronics Engineers, Inc.* web address: *http://www.ieee.org*

JGR: *Journal of Geophysical Research* web address: *http://www.agu.org/pubs/agu_jour.html*

JoG: *Journal of Geodesy, Springer Verlag, Berlin-Heidelberg* web address: *http://link.springer-ny.com/link/service/journals/00190/*

NASA GSFC Report: *Report, NASA Goddard Space Flight Center, Greenbelt (Maryland, USA)* web address: *http://www.gsfc.nasa.gov*

NASA TM: *Technical memorandum, NASA*

OSU-DGS Report: *Report, Department of Geodetic Science at Ohio State University, Columbus (Ohio, USA)* web address: *http://geodesy.eng.ohio-state.edu/index.html*

Delft Report: *Reports of the Department of Mathematical and Physical Geodesy, Faculty of Geodesy, Delft University of Technology* web address: *http://www.geo.tudelft.nl/*

ZfV: *Zeitschrift für Vermessungswesen*

References

Abramowitz A., Stegun I.A. (eds.) (1965): *Handbook of Mathematical Functions*,
Dover Publications Inc., New York 1965

Ardalan A.A. (1996): *Spheroidal co-ordinates and spheroidal eigenspace of the Earth gravity field*,
MSc. thesis, GIS, Stuttgart 1996

Arfa-Kaboodvand K. (1997): *Zur präziesen Berechnung der Oberflächenkräfte eines erdgebundenen Satelliten auf Basis der Hill-Variablen*,
DGK C Heft Nr. 476, München 1997

Bayer M., Beth S., Maier T. (1998): *Wavelet modelling of vectorial components in gravitational field determination*,
in: Freeden W. (ed.), *Progress in geodetic science*, Shaker Verlag, Aachen 1998, 208-216

Bettadpur S., Schutz B.E., Lundberg J.B. (1992): *Spherical harmonic synthesis and least squares computations in satellite gravity gradiometry*,
bulletin géodésique 66:1992

Brammer K., Siffling G. (1985): *Kalman-Bucy-Filter*,
R. Oldenbourg Verlag, München-Wien 1985

Bronstein I.N., Semedjajew K.A. (1989): *Taschenbuch der Mathematik*,
Verlag Harri Deutsch, Thun-Frankfurt/Main 1989

Cappelari J.O., Velez C.E., Fuchs A.J. (1976): *Mathematical Theory of the Goddard Trajectory Determination System*,
NASA GSFC Report X-582-76-77, Greenbelt (Maryland) 1976

Chauvineau B., Métris G. (1994): *Planar nondissipative spin-orbit coupling*,
ICARUS **109**, pp. 191-203, 1994

Chui Ch. (1990): *Die Bewegung künstlicher Satelliten im anisotropen Gravitationsfeld einer gleichmässig rotierenden starren Modellerde*,
DGK C Heft Nr. 357, München 1990

Chui Ch. (1997): *Satellite orbit integration based on canonical transformations with special regard to the resonance and coupling effects*,
DGK A Heft Nr. 112, München 1997

Chui Ch., Mareyen M. (1992): *Gauss' equations of motion in term of Hill variables and first application to numerical integration of satellite orbits*,
manuscripta geodaetica, **17**, pp. 155-163, 1992

Chui Ch., Lelgemann D., Mai E. (1997): *Über die Hillgleichungen und Gaussgleichungen*,
presentation at Geodetic Week 1997, Berlin, 1997

Chui C.K., Chen G. (1989): *Linear systems and optimal control*,
Springer-Verlag, Berlin-Heidelberg-New York 1989

Colombo O.L. (1981): *Numerical methods for harmonic analysis on the sphere*,
OSU-DGS Report No. 310, Columbus, 1981

DFG (1997): *Forschungsvorhaben 'Geowissenschaftliche Nutzung zukünftiger Satellitenmissionen'*,
Application presented to the DFG, co-ordination K.H. Ilk, University of Bonn, 1997

Engeln-Müllges G., Reutter F. (1988): *Numerische Mathematik für Ingenieure*,
BI Wissenschaftsverlag, Mannheim-Wien-Zürich 1988

Escobal P.R. (1975): *Methods of Orbit Determination*,
Robert E. Krieger Publishing Comp., Malabar (Florida) 1975

Feltens J. (1991): *Nichtgravitative Störeinflüsse bei der Modellierung von GPS-Erdumlaufbahnen*,
DGK C Heft Nr. 371, München 1991

Freeden W. (1999): *Multiscale modelling of spaceborne geodata,*
B. G. Teubner, Stuttgart 1999

Freeden W., Gervens T., Schreiner M. (1998): *Constructive approximation on the sphere (with applications to geomathematics),*
Oxford Science Publication, Clarendon Press, Oxford 1998

Freeden W., Michel V. (1999): *Constructive approximation and numerical methods in geodetic research today - an attempt to a categorization based on an uncertainty principle,*
JoG (1999) 73:452-465

Freeden W., Schreiner M. (1995): *New wavelet methods for approximating harmonic functions,*
in: Sanso F. (ed.), *IAG Symposia, No. 114,*
Springer, Berlin-Heidelberg-New York 1995, 112-121

Freeden W., Windheuser U. (1997): *Combined Spherical Harmonic and Wavelet Expansion,*
Applied and Computational Harmonic Analysis (ACHA), 4, 1997, 1-37

Goodwin G.C., Payne R.L. (1977): *Dynamic system identification,*
Academic Press Inc., New York-London 1977

Grafarend E.W. (1979): *Space-time geodesy,*
Bolletino di geodesia e scienze affini, <u>XXXVIII</u> n° 2, 1979, 305-343

Grafarend E.W., Schaffrin B., Pachelski W., Middel B., Thong N.C. (1990): *Review of algorithms for the synthesis of gravitational functionals,*
Observations of artificial satellites of the Earth, No. 27, pp. 343-360, Warszawa (Warsaw) 1990

Grafarend E.W. (1999): *Introductory lectures to geodesy,*
vol. 1, GIS, Stuttgart 1999

Grafarend E.W., Engels J., Varga P. (1998): *Cartesian moments of the mass density: The complete McCullagh formulae,*
publication draft, Stuttgart 1998

Grewal M.S., Andews A.P. (1993): *Kalman filtering - Theory and practice,*
Prentice Hall, Inc., Englewood Cliffs 1993

Guthmann A. (1994): *Einführung in die Himmelsmechanik und Ephemeridenrechnung,*
BI Wissenschaftsverlag, Mannheim-Wien-Zürich 1994

Hofsommer D.J., Potters M.L. (1960): *Table of Fourier coefficients of associated Legendre functions,*
in: Proceedings of the KNAW, series A, Mathematical Sciences, vol. 63, no. 5, pp. 460-466, Amsterdam 1960

Ilk K.H. (1972): *Zur vorläufigen Bahnbestimmung künstlicher Erdsatelliten,*
BMBW-FB W 72-16, München 1972

Isaacson E., Keller H.B. (1966): *Analysis of numerical methods,*
Dover Publications Inc., New York 1966

Isermann R. (1988): *Identifikation dynamischer Systeme,* Band I + II,
Springer Verlag, Berlin-Heidelberg 1988

Jarosch M. (1984): *Darstellung des Gravitationspotentials der Erde in kartesischen Basisfunktionen,*
DGK C Heft Nr. 100, München 1984

Jazwinski A.H. (1970): *Stochastic processes and filtering theory,*
Academic Press, New York-London 1970

Johannsen B. (1998): *Berechnung des Einflusses der Erdalbedo auf eine Satellitenbahn,*
study report, GIS, Stuttgart 1998

Julier S., Uhlmann J.K. (1994a): *A general method for approximating nonlinear transformations of probability distributions,*
WWW-Publication, 1994
can be downloaded from http://www.robots.ox.ac.uk/~siju, web-address valid at September 22, 2000

Julier S., Uhlmann J.K. (1994b): *A new extension of the Kalman filter to nonlinear systems,*
in: The Proceedings of AeroSense: The 11th International Symposium on Aerospace/Defense Sensing, Simulation and Controls, Orlando (Florida)
can be downloaded from http://www.robots.ox.ac.uk/ siju, web-address valid at September 22, 2000

Julier S., Uhlmann J.K. (1996): *A general method for approximating nonlinear transformations of probability distributions,*
WWW-Publication, Robotics Research Group, Dept. of Engineering Science, University of Oxford, Oxford 1996
can be downloaded from http://www.robots.ox.ac.uk/ siju, web-address valid at September 22, 2000

Kalman R.E. (1960): *A new approach to linear filtering and prediciton problems,*
Transaction of the ASME, Journal of Basic Engineering, **82**:34-45, March 1960

Kaula W. (1966): *Theory of satellite geodesy,*
Blaisdell Publishing Company, Waltham (Mass.) 1966

King-Hele D. (1987): *Satellite Orbits in an Atmosphere, Theory and Applications,*
Blackie and Son Ltd., Glasgow-London 1987

König R., Bode A., Chen Z., Grunwaldt L., Neubert R., Reigber Ch., Schwintzer P. (1996): *The GFZ-1 Mission: Design, Operations and First Results,*
GFZ STR96/09, Potsdam 1996

Kleusberg A. (1983): *Diagnose und Therapie von geodätischen Satellitennetzen vom Typ Doppler,*
DGK C Heft Nr. 293, München 1983

Klokočník J. (1982): *A review of methods of comparison of 'resonant' lumped geopotential coefficients,*
Bull. Astron. Inst. Czechosl. **33** (1982) 89-104

Klosko S.M., Wagner C.A. (1977): *Gravitational harmonics from shallow resonant orbits,*
Celestial mechanics 16 (1977) 143-163

Klosko S.M., Wagner C.A. (1982): *Spherical harmonic representation of the gravity field from dynamic satellite data,*
Planet. Space Science, Vol. 30, No. 1, pp. 5-28, 1982

Knocke P., Ries J. (1987): *Earth radiation pressure effects on satellites,*
CSR-TM-87-01, Austin (Texas) 1987

Koop R., Stelpstra D. (1989): *On the computation of the gravitational potential and its first and second order derivatives,*
manuscripta geodaetica (1989) 14: 373-382

Krauss S. (1998): *Wirkung der Atmosphärenreibung auf Satelliten,*
study report, GIS, Stuttgart 1998

Krebs V. (1980): *Nichtlineare Filterung,*
R. Oldenbourg Verlag, München-Wien 1980

Lemoine F.G. , Kenyon S.C, Trimmer R., Factor J., Pavlis N.K., Klosko S.M., Chinn D.S., Torrence M.H., Williamson R.G., Cox C.M., Wang Y.M., Luthcke S.B., Pavlis E.C., Rapp R.H., Olson T.R. (1998): *EGM96: The NASA GSFC and NIMA joint geopotential model,*
NASA TM (*in preparation*), 1998

Lerch F.J. , Wagner C.A., Putney B.G., Sandson M.L., Brownd J.E., Richardson J.A., Taylor W.A. (1972b): *Gravitational field models GEM3 and 4,*
NASA GSFC Report X-592-72-476, 1972

Lerch F.J. , Wagner C.A., Richardson J.A., Brownd J.E. (1974): *Goddard Earth models (5 and 6),*
NASA GSFC Report X-921-74-145, 1974

Maybeck P.S. (1979): *Stochastic models, estimation and control* Vol. 1-3,
Academic Press Inc., New York-London 1979

Milani A., Nobili, A.M., Farinella P. (1987): *Non-gravitational perturbations and satellite geodesy,*
Adam Hilger Publishing Company, Bristol 1987

Minkler G., Minkler J. (1993): *Theory and application of Kalman filtering,*
Magellan Book Company, Palm Bay (FL) 1993

Montenbruck O. (1991): *Ephemeridenrechnung und Bahnbestimmung geostationärer Satelliten mit Hilfe der Taylorreihenintegration,*
DGK C Heft Nr. 384, München 1991

Moon P., Spencer D. (1961): *Field theory handbook,*
Springer Verlag, Berlin-Göttingen-Heidelberg 1961

Moritz H., Mueller I. (1988): *Earth rotation - Theory and observation,*
The Ungar Publishing Company, New York 1988

Nagel E. (1976): *Bezugssysteme der Satellitengeodäsie,*
DGK C Heft Nr. 223, München 1976

Pérosanz F., Loyer S., Biancale R. (1999): *Star accelerometer in-flight dynamic calibration in the frame of the CHAMP geodetic mission,*
poster presentation at the IUGG99 general assembly, Birmingham 1999

Petersen I.R., Savkin A.V. (1999): *Robust Kalman filtering for signals and systems with large uncertainties,*
Birkhäuser, Boston-Basel-Berlin 1999

Pfister Ch.A.G. (1998): *Gravitative Einflüsse anderer Himmelskörper auf Satellitenbahnen,*
study report, GIS, Stuttgart 1998

Piehler J., Zschiesche H.-U. (1990): *Simulationsmethoden,*
BSB B.G. Teubner Verlagsgesellschaft, Leipzig 1976

Press W.H., Teukolsky S.A., Vetterling W.T., Flannery B.P. (1992): *Numerical Recipes in C,*
Cambridge University Press, Cambridge 1992

Rabel D. (1997): *Kugelfunktionsentwicklungen des Gravitationspotentials am Beispiel des OSU91A,*
study report, GIS, Stuttgart 1997

Rapp R.H. (1981): *The Earth's gravity field to degree and order 180 using Seasat altimeter data, terrestrial gravity data and other data,*
OSU-DGS report no. 322, 1981

Rapp R.H., Wang Y.M., Pavlis N.K. (1991): *The Ohio State 1991 Geopotential and Sea Surface Topography Harmonic Coefficent Models,*
OSU-DGS report no. 410, 1991

Reigber Ch. (1989): *Gravity field recovery from satellite tracking data,*
in: Sanso F., Rummel R. (eds.), *Theory of satellite geodesy and gravity field determination,*
Springer Verlag, Berlin-Heidelberg-New York 1989, 197-234

Reigber Ch., Balmino G., Moynot B., Mueller H. (1983a): *The GRIM3 Earth gravity field model,*
manuscripta geodaetica (1983) 8: 93-138

Reigber Ch., Rizos C., Bosch W., Balmino G., Moynot B. (1983b): *An improved GRIM3 Earth gravity field (GRIM3B),*
presentation at the XVIII IUGG/IAG general assembly, Hamburg 1983

Reigber Ch. , Bock R., Förste Ch., Grunwaldt L., Jankowski N., Lühr H., Schwintzer P., Tilgner C. (1996): *CHAMP Phase B Executive Summary,*
GFZ STR96/13, Potsdam 1996

Ricardi L.J., Burrows M.L. (1972): *A recurrence technique for expanding a function in spherical harmonics,*
IEEE Transactions on Computers, p. 583-585, 1972

Richter B. (1986): *Entwurf eines nichtrelativistischen geodätisch - astronomischen Bezugssystems,*
DGK C Heft Nr. 322, München 1986

Richter B. (1994): *Die Grundlagen der geodätischen Astronomie,*
GIS, Stuttgart 1994

Roach G.F. (1982): *Green's Functions*,
Cambridge University Press, Cambridge 1982

Rummel R. (1997): *Spherical spectral properties of the Earth's gravitational potential and its first and second derivatives*,
in: Sanso F., Rummel R. (eds.), *Geodetic boundary value problems in view of the one centimeter geoid*,
Springer Verlag, Berlin-Heidelberg-New York 1997, 357-404

Sanz-Serna J.M. (1992): *Numerical ordinary differential equations vs. dynamical systems*,
in: Broomhead D.S., Iserles A. (eds.), *The dynamics of numerics and the numerics of dynamics*,
Clarendon Press, Oxford, 1992

Schäfer Ch. (1997): *Satellitenbahnanalyse und -synthese auf der Basis einer integralen Darstellung der Bewegungsgleichung*,
presentation at Geodetic Week 1997, Berlin, 1997

Schäfer Ch. (1998a): *A concept for satellite orbit sensitivity analysis*,
presentation at the IVth Hotine-Marussi Symposium on Mathematical Geodesy (proceedings in preparation), Trento, 1998

Schäfer Ch., Krauss S., Sayda F., Grafarend E.W. (1998b): *Aufbau einer Programmsammlung zur Berechnung von Störeinflüssen auf Satellitenbahnen*,
in: Freeden W. (ed.), *Progress in Geodetic Science*, proceedings of the Geodetic Week 1998 at Kaiserslautern, Shaker Verlag, Aachen, 1998

Schaffrin B. (1991): *Generating robustified Kalman filters for the integration of GPS and INS*,
GIS TR no.15, Stuttgart, 1991

Schaffrin B. (1992): *New filter designs for a hybrid GPS/INS navigation and surveying system*,
internal report SFB 228, Stuttgart, 1992

Scheinert M. (1996): *Zur Bahndynamik niedrigfliegender Satelliten*,
DGK C Heft Nr. 435, München 1996

Sayda F. (1997): *Direkter Solardruck als Störeinflusse auf Satellitenbahnen*,
study report, GIS, Stuttgart 1997

Schmutzer E. (1989): *Grundlagen der Theoretischen Physik I, II*,
BI Wissenschaftsverlag, Mannheim-Wien-Zürich 1989

Schneider M. (1968): *Zur dynamischen Nutzung der Bahnen künstlicher Satelliten*,
BMBW-FB W 68-55, München 1968

Schneider M. (1972a): *Determinierung von Bewegungsproblemen durch zeitliche Randwerte*,
BMBW-FB W 72-17, München 1972

Schneider M. (1972b): *Über die Lösung von Anfangswertproblemen der Punktmechanik mit Hilfe von Randwertproblemen*,
BMBW-FB W 72-23, München 1972

Schneider M. (1981): *Himmelsmechanik*,
BI Wissenschaftsverlag, Mannheim 1981

Schneider M. (1988): *Satellitengeodäsie - Grundlagen*,
BI Wissenschaftsverlag, Mannheim 1988

Schrama E.J.O. (1986): *Estimability of potential coefficients from orbit perturbations*,
Delft Report no. 86.I, August 1986

Schrama E.J.O. (1991): *Gravity field error analysis: Applications of Global Positioning System receivers and gradiometers on low orbiting platforms*,
JGR, Vol. 96, No. B12, pp. 20041-20051, November 1991

Schrama E.J.O. (1992): *A systematic approach to satellite geodesy*,
February 1992

Schrick K.-W. (1977): *Anwendungen der Kalman-Filter-Technik*,
R. Oldenbourg Verlag, München-Wien 1970

Schwarz H.R. (1986): *Numerische Mathematik*,
B.G. Teubner, Stuttgart 1986

Schwintzer P. (1999): private communication, GFZ Potsdam

Schwintzer P. , Reigber C., Barth W., Massmann F.-H., Raimondo J., Gerstl M., Bode A., Li H., Biancale R., Balmino G., Moynot B., Lemoine J., Marty J., Barlier F., Boudon Y. (1992): *GRIM4 - Globale Erdschwerefeldmodelle*,
ZfV, Heft 4, pp. 227-247, 1992.

Schwintzer P. , Reigber C., Bode A., Kang Z., Zhu S., Massmann F.-H., Raimondo J., Biancale R., Balmino G., Lemoine J., Moynot B., Marty J., Barlier F., Boudon Y. (1997): *Long-wavelength global gravity field models: GRIM4-S4, GRIM4-C4*,
JoG (1997) 71: 189-208

Sedgewick R. (1988): *Algorithms*,
Series in Computer science, Addison-Wesley, Reading (Massachusetts) 1988

Seeber G. (1989): *Satellitengeodäsie, Grundlagen, Methoden und Anwendungen*,
Walter de Gruyter, Berlin und New York 1989

Sigl R., Schneider M., Reigber Ch., Ludwig H. (1970): *Anwendung der Hammersteinschen Methode der unendlich vielen Variablen auf Probleme der Satellitengeodäsie und Himmelsmechanik*,
BMBW-FB W 70-33, München 1970

Sneeuw N.J. (1992): *Representation coefficients and their use in satellite geodesy*,
manuscripta geodaetica (1992) 17: 117-123

Sneeuw N.J., Bun R. (1996): *Global spherical harmonic computation by two-dimensional fourier methods*,
JoG (1996) 70:224-232

Stephens G.L., Campbell G.G., Vonder Haar T.H. (1981): *Earth radiation budgets*,
JGR, Vol. 86, No. C10, pp. 9739-9760, 1981

Stiefel E.L., Scheifele G. (1971): *Linear and regular celestial mechanics*,
Springer Verlag, Berlin 1971

Stumpff K. (1974): *Himmelsmechanik*,
VEB Deutscher Verlag der Wissenschaften, Berlin 1979

Tapley B. , Watkins J., Ries J., Davis G., Eanes R., Poole S., Rim H., Schutz B., Shum C., Nerem R., Lerch F., Marshall J., Klosko S., Pavlis N., Williamson R. (1996): *The Joint Gravity Model 3*,
JGR, Vol. 101, No. C12, pp. 28029-28049, 1996

Thalhammer M. (1995): *Regionale Gravitationsfeldbestimmung mit zukünftigen Satellitenmissionen (SST und Gradiometrie)*,
DGK C Heft Nr. 437, München 1995

Thong N.C. (1993): *Untersuchungen zur Lösung der fixen gravimetrischen Randwertprobleme mittels sphäroidaler und Greenscher Funktionen*,
DGK C Heft Nr. 399, München 1993

Überhuber Ch. (1995): *Computernumerik 1, 2*,
Springer Verlag, Berlin-Heidelberg 1995

Wahr J. (1995): *Earth tides*,
in: *Global Earth physics*, AGU Reference Shelf 1, 1995, pp. 40-45

Welch G., Bishop G. (1996): *An introduction to the Kalman filter*,
WWW-Publication, Dept. of Computer Science, University of North Carolina, Chapel Hill 1996
can be downloaded from http://www., web-address valid at September 22, 2000

Wenzel G. (1998a): *Ultra hoch auflösende Kugelfunktionsmodelle GPM98A und GPM98B des Erdschwere-felds*,
WWW-Publication, extended abstract for the presentation at the Geodetic Week 1998, Kaiserslautern 1998

Wenzel G. (1998b): *Spherical harmonic models*,
WWW-Publication, Hannover 1998

Wiejak W., Schrama E.J.O., Rummel R. (1991): *Spectral representation of the satellite-to-satellite tracking observables*,
ASR, Vol. 11, No. 6, pp. (6)197-(6)224, 1991

Wong C.W. (1994): *Mathematische Physik: Konzepte, Methoden, Übungen*,
Spektrum Akademischer Verlag GmbH, Heidelberg-Berlin-Oxford 1994

Yoder C.F. (1995): *Astrometric and geodetic properties of Earth and solar system*,
in: *Global Earth physics*, AGU Reference Shelf 1, 1995, pp. 1-27

You R.-J. (1995): *Zur analytischen Bahnberechnung künstlicher Erdsatelliten mittels konformer Transformationen*,
DGK C Heft Nr. 440, München 1995

Satellite missions in the WWW

last update September 22, 2000

Missions' links *http://ilrs.gsfc.nasa.gov/satellitelinks.html*
list of links to satellite missions provided by the NASA GSFC

CHAMP: *http://op.gfz-potsdam.de/champ/*
GFZ Potsdam (geophysical research centre Potsdam) (Germany)

GOCE: *http://www.estec.esa.nl/vrwww/explorer/GRAVITY.html*
ESA (European Space Agency)

GPB: *http://www.onr.navy.mil/02/c0241e/GPB.htm*
NASA, Stanford University (both USA)

GRACE: *http://www.csr.utexas.edu/grace/*
NASA (USA), GFZ Potsdam (Germany)

ICESat: *http://icesat.gsfc.nasa.gov/index.htm*
NASA GSFC (USA)

Jason: *http://sirius-ci.cst.cnes.fr:8090/HTML/information/frames/missions/jason_uk.html*
NASA (USA), CNES (France)

Ørsted: *http://web.dmi.dk/projects/oersted/*
DMI (Danish Meteorological Institute) (Denmark)

SAC-C: *http://www.conae.gov.ar/sac-c/folleto.html*
NASA (USA), CONAE (Comisión Nacional de Actividades Espaciales) (Argentina)

SUNSAT: *http://sunsat.ee.sun.ac.za/index.html*
ESL (Electronic Systems Laboratory, University of Stellenbosch) (South Africa)

VCL: *http://essp.gsfc.nasa.gov/vcl/*
University of Maryland, NASA GSFC et al. (USA)